Investigation of Force, Kinetochores, and Tension in the Saccharomyces Cerevisiae Mitotic Spindle

Investigation of force, kinetochores, and tension in the *Saccharomyces cerevisiae* mitotic spindle

A dissertation presented

by

Natalie Jo Nannas

to

The Department of Molecular and Cellular Biology

in partial fulfillment of the requirements
for the degree of
Doctor of Philosophy
in the subject of

Biology

Harvard University
Cambridge, Massachusetts

May 2013

Advisor's Name: Professor Andrew W. Murray **Natalie J. Nannas**

Investigation of force, kinetochores, and tension in the *Saccharomyces cerevisiae* mitotic spindle

ABSTRACT

Cells must faithfully segregate their chromosomes at division; errors in this process causes cells to inherit an incorrect number of chromosomes, a hallmark of birth defects and cancer. The machinery required to segregate chromosomes is called the spindle, a bipolar array of microtubules that attach to chromosomes through the kinetochore. Replicated chromosomes contain two sister chromatids whose kinetochores must attach to microtubules from opposite poles to ensure correct inheritance of chromosomes. The spindle checkpoint monitors the attachment to the spindle and prevents cell division until all chromatids are attached to opposite poles. Both the spindle and the checkpoint are critical for correct segregation, and we sought to understand the regulation of these two components.

The spindle is assembled to a characteristic metaphase length, but it is unknown what determines this length. It has been proposed that spindle length could be regulated a balance of two forces: one generated by interaction between microtubules that elongates the spindle and a second due to interactions between kinetochores and microtubules that shortens the spindle. We tested this force-balance model which predicts that altering the number of kinetochores will alter spindle length. We manipulated the number of kinetochores and found that spindle length scales with the number of kinetochores; introducing extra kinetochores produces shorter spindles and inhibiting kinetochores produces longer spindles. Our results suggest that attachment of

chromosomes to the spindle via kinetochores produces an inward force that opposes outward force. We also found that the number of microtubules in the spindle varied with the number of kinetochores.

In addition to establishing a spindle, cells must also guarantee that chromosomes are correctly attached to it. Correct attachment generates tension as the chromatids are pulled toward opposite poles but held together by cohesin until anaphase. The spindle checkpoint monitors this tension which causes stretching of chromatin and kinetochores. Lack of tension on activates the checkpoint, but is unknown if the checkpoint measures stretch between kinetochores (inter-kinetochore stretch) or within kinetochores (intra-kinetochore). We tethered sister chromatids together to inhibit inter-kinetochore stretch and found that the checkpoint was not activated. Our results negate inter-kinetochore models and support intra-kinetochore models.

Table of Contents

List of Figures

List of Tables

Acknowledgments

There are many people who have helped me develop as a scientist and supported my graduate school endeavors. First, I would like to thank my advisor, Andrew Murray for his guidance, his humor, his coaching (and cheerleading), and his patience. Andrew has been a deeply influential mentor, providing guidance when things seemed bleak and pushing me to think independently, even when it was not comfortable. Thank you for appreciating my dreams and helping me reach for them. A big thanks to all of the members of Murray lab for your help and encouragement over the years. Thanks to Quincey Justman who demystified microscopy and to Liedewij Laan who spent hours discussing biophysics. Thanks to both Mary Wahl and Melanie Müller who helped write the Java and Matlab code used to analyze my microscopy images. Thanks to Lori Huberman for being a true friend from the first day of graduate school. I would also owe a big thank you to our collaborators at the University of Colorado, Mark Winey, Eileen O'Toole, and Tom Giddings, Jr. for performing the electron tomography presented in this thesis. I would also like to thank the MCB Department for funding in my first year and the National Science Foundation for funding in my third, fourth and fifth year that helped make this research possible. Thanks to the Harvard MCB Department and the FAS Center for Systems Biology for being an intellectual community that always kept me on my toes.

I owe many thanks to the people who supported me outside of lab. My parents have always supported my dreams, encouraged learning and education, and believed in me, even when I had doubts. They probably knew that I would still be in school twenty-two years after my first day of first grade. Thank you to my grandparents who showed me the value and joy of life-long learning. Thank you to my in-laws for welcoming me as family and supporting me during the difficult times. I had the opportunity to live and work with over sixty Harvard College freshmen

as a Proctor during my time in graduate school. While I was there to mentor them, I owe them thanks for their enthusiasm and energy that kept me going. Thanks to the Freshmen Deans Office for their support during the highs and lows of proctoring. Last, I want to thank my husband John. You were there for me every step of the way; I would not have been able to do it without you.

Chapter One:

Introduction

ABSTRACT

Accurate segregation of chromosomes is essential for producing genetically identical daughter cells. Errors in this process lead to many human diseases and disorders. Chromosomes are segregated in mitosis by the spindle, a dynamic system of microtubules that attach to chromosomes through the kinetochore. Replicated chromosomes consist of two sister chromatids held together by cohesin rings until anaphase; kinetochores on sister chromatids must attach to opposite poles of the spindle to ensure equal segregation of chromosomes. Cells do not divide until all chromosomes are properly attached to the spindle. The mechanism monitoring accurate attachment, the spindle checkpoint, utilizes a kinase called Ipl1/Aurora B to sense tension on chromosomes as an indicator of correct attachment. Tensionless attachments and unattached kinetochores activate the spindle checkpoint, which prevents the metaphase to anaphase transition by inhibiting the anaphase-promoting complex (APC) and its co-activator Cdc20. Once all chromosomes are correctly attached to the spindle, cells proceed into anaphase, cleaving the cohesin rings and pulling sister chromatids to each pole. This chapter will summarize the current body of literature surrounding chromosome segregation, focusing on the machinery of segregation, the spindle, and on the spindle checkpoint mechanism. The components of the spindle, how the spindle achieves its characteristic length, and how the spindle checkpoint monitors proper attachment of chromosomes to the spindle will be discussed.

INTRODUCTION

The importance of chromosome segregation

The faithful segregation of genetic material is essential for an organism's viability and reproduction. Most organisms package their genetic material into chromosomes and segregate these chromosomes equally between their daughter cells during cell division. If mistakes occur during this division process, daughter cells can inherit an incorrect number of chromosomes, a condition called aneuploidy. If chromosome missegregation occurs during meiosis or early development, the resulting aneuploidy is often lethal or causes severe birth defects. Detrimental effects of aneuploidy on development have been observed and characterized in all major multi-cellular model organisms (*Drosophila*, *C.elegans*, and mice) (Siegel and Amon 2012). In humans, at least 5% of all pregnancies terminate *in utero* due to aneuploidy of the embryo, making chromosome missegregation the leading cause of miscarriage (Hassold et al. 2007). Aneuploidy is also the leading cause of congenital birth defects in humans; chromosomal abnormalities occur 1 out 160 live births, and they cause a range of disorders depending on identity of the missing or extra chromosome (Driscoll and Gross 2009). Down's syndrome is caused by the presence of an extra copy of chromosome 21 and occurs in approximately 1 of 800 births. An extra copy, or partial copy, of chromosome 18 causes Edwards syndrome, which occurs in 1 of 6,000 births (Driscoll and Gross 2009). A missing copy of the X chromosome in females is the only viable chromosomal loss condition, and it results in Turner syndrome (Siegel and Amon 2012).

Aneuploidy is also linked to cancer development and progression, although the relationship is not as clearly causative as it is for birth defects. While it has been documented that

75% of blood cancers and 90% of solid tumors have abnormal chromosome numbers, there is much debate about whether aneuploidy initiates tumorigenesis or is a result of unstable chromosome segregation (Siegel and Amon 2012; Weaver and Cleveland 2006). Genes, such as those encoding kinetochore proteins (CENP-E), spindle checkpoint proteins (BUB1, BUBR1, BUB3, MAD1, MAD2), whose function ensure correct segregation of chromosomes are frequently mutated or misregulated in cancers (Weaver and Cleveland 2006; Weaver et al. 2007). To date, nearly all tested tumors isolated from the pancreas, colon, T-cells, head and neck are impaired in the mechanisms that prevent chromosome missegregation, as are half of the tumors isolated from the breast, liver, lungs, throat and thyroid (Weaver and Cleveland 2006). The presence of abnormal chromosome numbers and impaired segregation mechanisms in mature tumors does not prove that aneuploidy is the driver of tumorigenesis. Aneuploidy has been found in human pre-cancerous cells of the cervix (Duensing and Munger 2004; Ried et al. 1999), bone marrow (Amiel et al. 2005), colon (Ried et al. 1999, Matsuura et al. 2006), oesophagus (Doak et al. 2004), and head and neck (Ai et al. 2001), as well as in pre-malignant mouse breast cells (Medina 2002) and marsupial skin cells (Dooley et al. 1993). When aneuploidy is induced in mice, there is a 3 fold increase in lung tumor occurrence and 10% of test animals developed lymphomas of the spleen while none were observed in wild-type (Weaver et al. 2007). However in this same study, Weaver et al. observed a 50% decrease in spontaneous liver tumors in animals with induced aneuploidy compared to wild-type animals, suggesting that in some cellular contexts, aneuploidy can inhibit tumorigenesis (2007). Individuals with an extra copy of chromosome 21 (Down's syndrome) have lower incidence of solid tumors such as breast, liver and bladder cancer, but young children with Down's syndrome are most likely to develop leukemia than their non-aneuploid counterparts (Hasle et al. 2000; Satgé et al 2003; Fonatsch

2010). While the role of aneuploidy in tumor progression is still being explored, missegregation of chromosomes is clearly correlated with cancer.

The effects of incorrectly segregating chromosomes can be devastating to health and reproduction, thus understanding how this process works is essential. In my thesis research, I sought to better understand two aspects of chromosome segregation: how cells establish the segregation machinery, and how they monitor the attachment of their chromosomes to the spindle. Cells assemble the spindle every division to pull chromosomes apart, and it is always built to the same length. We wanted to understand what regulates the length of the metaphase spindle. Additionally, chromosomes must correctly attach to the spindle, and we investigated how cells use tension to sense incorrect attachments. We addressed these questions using the eukaryotic model organism budding yeast, *Saccharomyces cerevisiae*. The simplicity of *S.cerevisiae* and the power of its genetic tools allowed us to directly manipulate the underpinnings of chromosome segregation, and yet the yeast proteins that regulate and execute chromosome segregation have a high degree of homology with their mammalian counterparts (Lampson and Cheeseman 2011). Through the approaches described in Chapter 2 and Chapter 3, I sought to investigate the mechanisms of chromosome segregation and contribute to understanding this fundamental process.

S.cerevisiae **mitotic spindle: components and assembly**

Chromatids and cohesin

Most organisms store their genetic material on chromosomes, highly compacted structures consisting of DNA and proteins. The number of chromosomes an organisms possesses is species-dependent; haploid human cells have 23 chromosomes and haploid *S.cerevisiae* cells have 16 chromosomes. Cells can either divide through a process called mitosis that maintains the number of chromosomes, or cells can go through two successive divisions called meiosis that reduces the ploidy, typically from diploid (2 copies of each chromosome) to haploid (1 copy). Meiosis is often used to generate gametes, such as sperm or eggs, that will fuse in sexual reproduction to form a genetically distinct offspring. This literature review will focus on the mechanism of mitosis; readers interested in meiosis should refer to Marston and Amon's comprehensive review (2004).

To faithfully segregate its chromosomes, a cell must progress through a series of controlled steps collectively called the cell cycle. In *S. cerevisiae*, the cell cycle begins in G1 and progresses into S phase once cellular size requirements have been satisfied (**Figure 1-1A**) (Rupeš 2002). Chromosomes are duplicated in S phase, and the two identical copies are called sister chromatids (**Figure 1-1B**). Chromatids are held together by cohesin, ring-shaped complexes made up of four proteins Smc1, Smc3, Scc3 and Scc1 (also called Mcd1p) (Nasmyth 2005; Guacci et al. 1997). The cohesin ring has a diameter of approximately 30-35nm and is thought to encircle the sister chromatids packaged into 10nm chromatin fibers (Haering et al. 2008). Cohesin is loaded at specific sites along chromatids by the Scc2/Scc4 protein complex in G1 (Ciosk et al. 2000) and is thought to translocate along chromatin, possibly pushed by transcriptional machinery. Chromatin immunoprecipitation studies have shown that cohesin

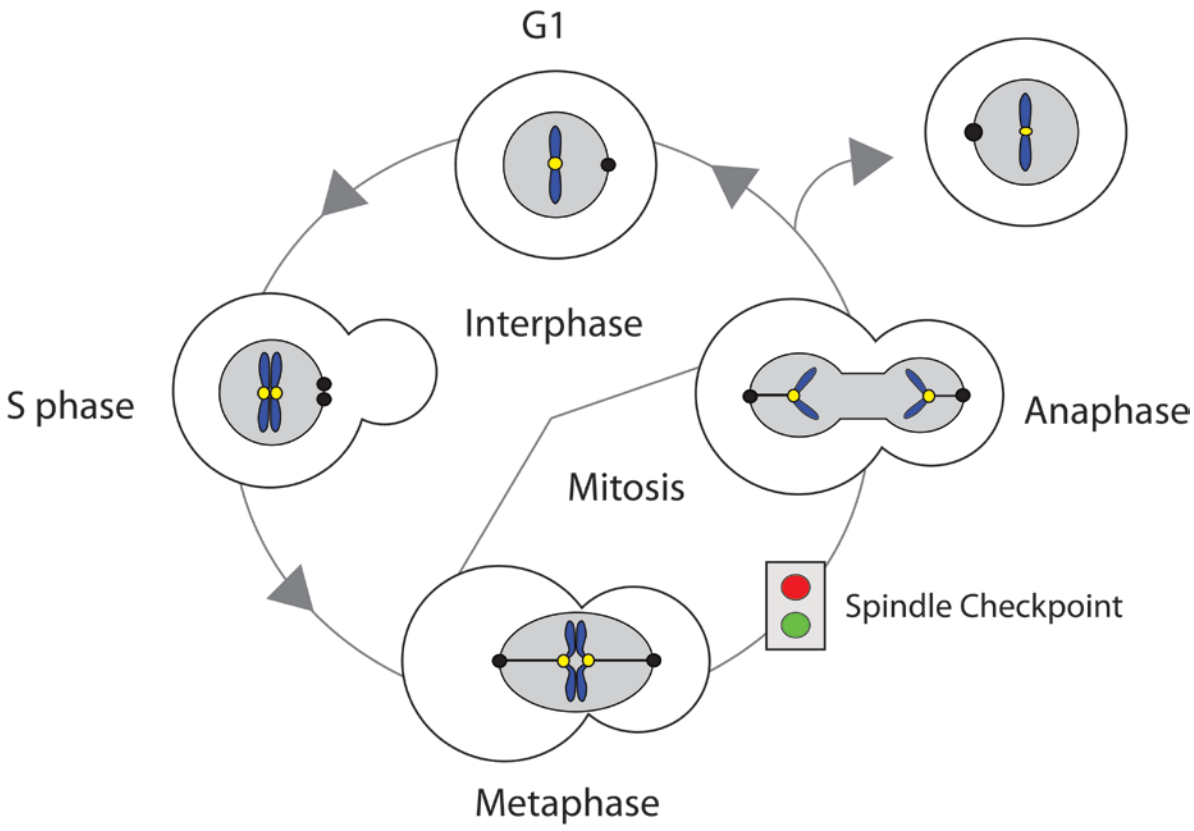

Figure 1-1A. The *Saccharomyces cerevisiae* cell cycle. The cell cycle begins in G1 where cells have a single copy of every chromosome (blue) and a single spindle pole body (black dot). In S phase, DNA is replicated and the spindle pole body is duplicated; cells now contain two spindle poles and two copies of every chromosome. These two copies are called sister chromatids and they are held together until anaphase. After G1 the cells begin budding a new daughter cell that can be seen in S phase. When the cells enter mitosis, the must attach the kinetochores (yellow dot) to microtubules (black line) from spindle poles that have migrated to opposite sides. More specifics on the metaphase attachment of chromosomes is found in part (**B**). In *S.cerevisiae*, spindle pole bodies are embedded in the nuclear envelope, and mitosis takes place within the nucleus (gray). Cells cannot leave metaphase unless chromatids are attached to opposite poles. This attachment is monitored by the spindle checkpoint which delays the entry to anaphase until all chromosomes are correctly attached. Once the checkpoint is satisfied, cells enter anaphase and the two chromatids are pulled apart into the two resulting cells. The nucleus and cell walls divide, and now both cells are at the beginning of the cell cycle in G1.

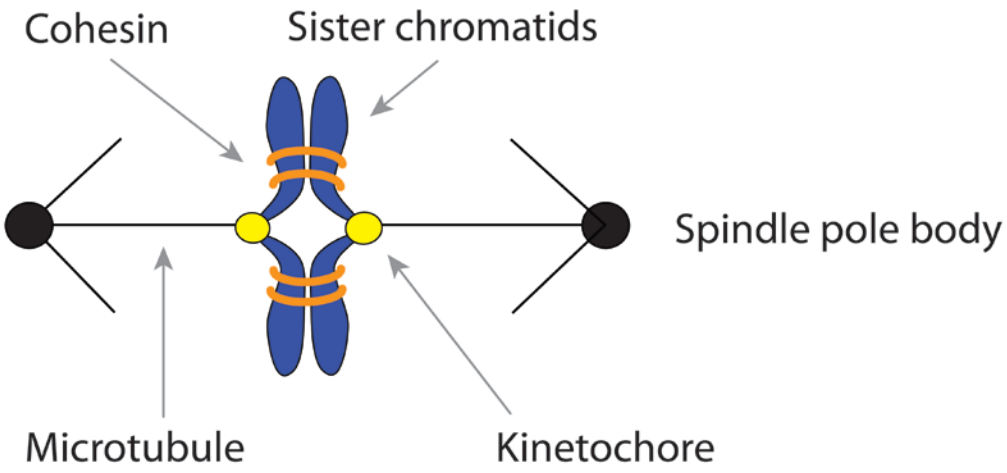

Figure 1-1B (Cell cycle continued). Attachment of chromosomes to the mitotic spindle. Cells must correctly attach their chromosomes to the segregation machinery, the mitotic spindle, in metaphase. The spindle is comprised of two spindle pole bodies that nucleate microtubules. Chromosomes attach to microtubules in the spindle through the kinetochore, a protein complex binds centromeres on chromosomes and attaches to microtubules. In order to be correctly attached to the spindle, the two chromatids of a chromosome must attach to microtubules from opposite spindle pole bodies, a state referred to as bi-orientation. Bi-oriented chromosomes experience tension as the microtubules attempt to pull the two chromatids apart but are resisted by cohesin rings. Cohesin tethers the sister chromatids together until anaphase, when the rings are cleaved and the sisters are pulled apart.

located along silenced genes will be pushed to sites of transcriptional convergence within 30 minutes of gene activation (Lengronne et al. 2004). Cohesin is highly enriched in the 50kb region around the kinetochore, the protein complex that connects the chromosome to microtubules, as compared to other locations on the chromosome arms (Weber et al. 2004). Given the size of its components, it is possible for yeast replication machinery to pass through the 35nm cohesin ring while duplicating DNA (D. Jeruzalmi, personal communication). However, it is unknown if the replication machinery passes through cohesin rings, or if rings must be transiently broken and re-deposited behind the replication machinery. The proteins Ctf4, Ctf18 and Eco1 are required to establish cohesin during replication. They may either hold the replication machinery in a tight configuration allowing it to pass through cohesin rings or they may transfer the cohesin behind the replication fork (Lengronne et al. 2006). Cohesin rings hold the two sister chromatids and prevent sister separation until anaphase. At anaphase, the newly liberated protease separase (Esp1 in *S.cerevisiae*) cleaves cohesin and chromatids are pulled apart (Uhlmann et al 2000). Separase is inhibited prior to anaphase by securin (Pds1 in *S.cerevisiae*) until the Anapahse Promoting Complex (APC) ubiquitinates securin, targeting it for degradation (see below for more on the action of separase, securin and the APC) (Musacchio and Salmon 2007).

Microtubules and spindle pole bodies

After DNA replication, cells progress into mitosis and assemble the spindle, a dynamic system of microtubules that segregates chromosomes. Microtubules are nucleated from organizing centers, called spindle pole bodies in *S.cerevisiae*. The yeast spindle pole is duplicated in late G1/early S phase so a bipolar spindle can be established in mitosis (O'Toole

and Winey 2001). Unlike higher eukaryotes that break down their nuclear envelope, *S. cerevisiae* and other fungi undergo a "closed mitosis" where mitosis proceeds within an intact nucleus (De Souza and Osmani 2007) (**Figure 1-1A**). Spindle pole bodies are embedded in the nuclear envelope and nucleate microtubules in both directions, inward into the nucleoplasm and outward to the cytoplasm. Astral microtubules in the cytoplasm help position the nucleus in the bud neck, the site of division between mother cell and daughter cell (Markus et al. 2012). Within the nucleus, each spindle pole body nucleates approximately 20 microtubules. These 40 microtubules make up the 2.0 µm long *S.cerevisiae* mitotic spindle. There are two distinct populations of microtubules classified by their lengths; of the 40 microtubules, 32 are needed to attach to the two sister chromatids of the 16 yeast chromosomes. These "kinetochore microtubules" are short, averaging only 0.3µm (Winey et al. 1995). The remaining 8 microtubules or interpolar microtubules form the "core bundle" and span the spindle with an average length of 1.5µm (Winey et al. 1995) (**Figure 1-2A and B**). The number of microtubules in the *S. cerevisiae* mitotic spindle strongly suggests that each kinetochore attaches to a single microtubule, as there are 32 chromatids and 36 ± 7 kinetochore microtubules.

Unlike other species with electron dense kinetochores (McEwen and Dong 2010), yeast kinetochores cannot be seen *in vivo* by electron microscopy. It is thought that stable microtubule-kinetochore interactions are end-on attachments (the end of the microtubule is bound by the kinetochore) because this type of attachment is preferred by cells. Lateral attachments (the kinetochore interact with the side of microtubule) are converted to end-on attachments, and end-on attachments allow more processive pulling of chromatids (Tanaka et al. 2007). If stable kinetochore-microtubule interactions are end-on interactions, this necessitates that there is one microtubule per kinetochore. Thus, because the number of short microtubules (36 ± 7) closely

A)

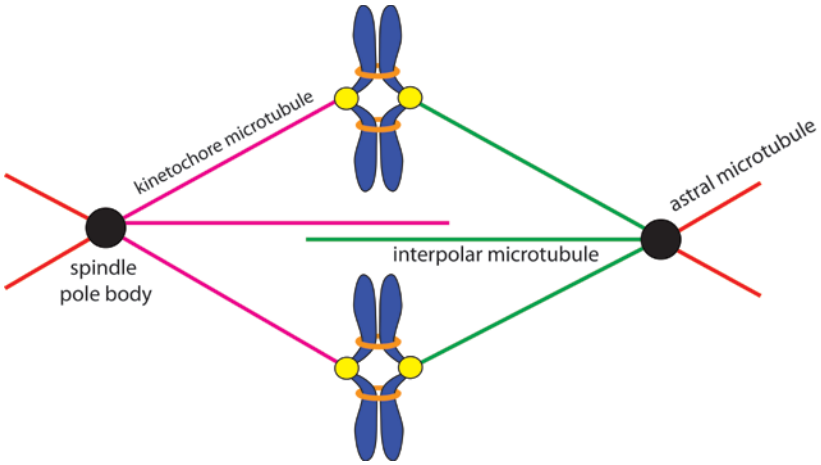

B)

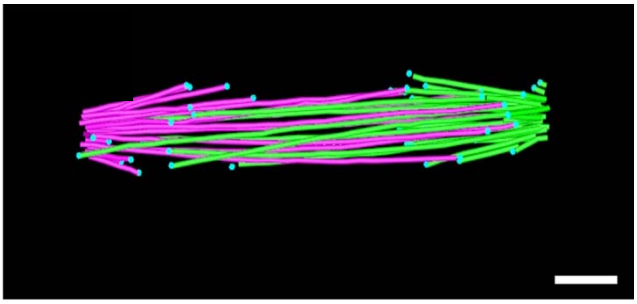

Figure 1-2. Microtubules in the *S.cerevisiae* mitotic spindle. Within the mitotic spindle, *S.cerevisiae* have kinetochore microtubules that attach to kinetochore and interpolar microtubules that reach into the mid-zone of the spine and are cross-linked by motor proteins. Outside of spindle are astral microtubules (red) that reach into the cytoplasm and position the nucleus. Microtubules within the spindle are labeled pink and green, pink if they are nucleated from one spindle pole body and green from the other (**A**). *S.cerevisiae* have approximately 32 short kinetochore microtubules to attach to the 32 kinetochores on 16 chromosomes and 8 interpolar microtubules; these microtubules are densely packed in the 2µm spindle (**B**). This image is a three-dimensional reconstruction of a *S.cerevisiae* spindle acquired by electron tomography. Many of the kinetochore microtubules in the spindle are quite short, only ~30-100nm long; this demonstrates how the spindle cartoon in part (A) is not to scale. In reality, the chromatids are stretched nearly to the spindle poles (up to 1µm of chromatin stretch in a 2µm spindle). The white scale bar represents 100nm.

C)

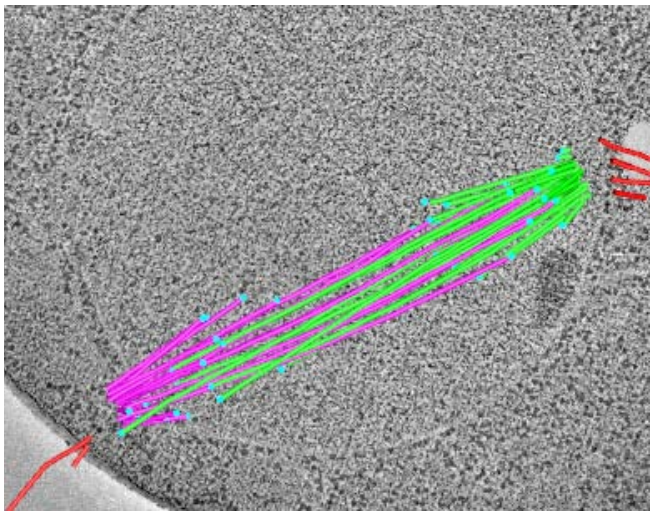

D)

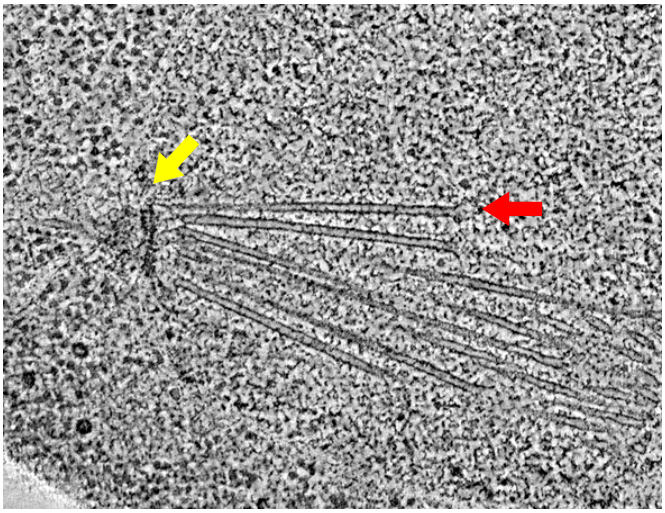

Figure 1-2 (continued). Microtubules in the *S.cerevisiae* mitotic spindle. The reconstructed spindle from (B) is over-layed on the original electron microscopy image in (**C**). The red lines are astral microtubules that are outside the nucleus. In the image, the edge of the nucleus is visible. Many sections of electron microscopy images were taken and synthesized to produce the reconstruction in (**C**). In part (D) the image is zoomed in on the spindle pole body (yellow arrow) and kinetochore microtubules. The end of the kinetochore microtubule (red arrow) appears to end in nothing, but because there are the same number of kinetochore microtubules as kinetochores, and kinetochores have been shown to attach end-on to microtubules, it is believed that these microtubules are attached to kinetochores.

matches the number of kinetochores (32), it is thought that these microtubules terminate in kinetochores (**Figure 1-2C**) (Winey et al. 1995; Müller-Reichert et al. 2003).

Kinetochores and centromeres

Kinetochores are large protein complexes that mediate attachment of chromosomes to microtubules. Many aspects of the kinetochore, including specific proteins, general structure, activity and regulation are highly conserved across eukaryotic organisms (McIntosh et al. 2013; Welburn and Cheeseman 2008). The yeast kinetochore is composed of over 65 proteins organized into sub-complexes within the larger kinetochore structure (Westermann et al. 2007). The sub-complexes are classified into layers based on early electron microscopy that described kinetochores as three-layer discs (Bazett-Jones and Ottensmeyer 1981; Bazett-Jones et al. 1988). These layers are a DNA-binding layer, a microtubule-binding layer, and a linker layer (Westermann et al. 2007) (**Figure 1-3**). The DNA-binding layer of the kinetochore interacts with centromeres, the genetic loci where kinetochores assemble. In *S.cerevisiae* the centromere is only a 125bp long sequence with a conserved organization and AT content found on all 16 chromosomes. This sequence is organized into three elements, CDEI, II, and III, which bind specific kinetochore proteins (Bloom and Carbon 1982). These small "point" centromeres are all that is necessary to assemble a functional kinetochore and segregate a chromosome (Clarke and Carbon 1980). In most species, centromeres extend over kilo- and megabase pair regions with repeating sequence motifs. The location of kinetochore binding within these regions is thought to be controlled in part by epigenetics (Mehta et al. 2010).

In *S.cerevisiae*, the 125bp centromere wraps around a single nucleosome containing a kinetochore-specific histone Cse4 (CENP-A in other species); Cse4 depletion leads to impaired

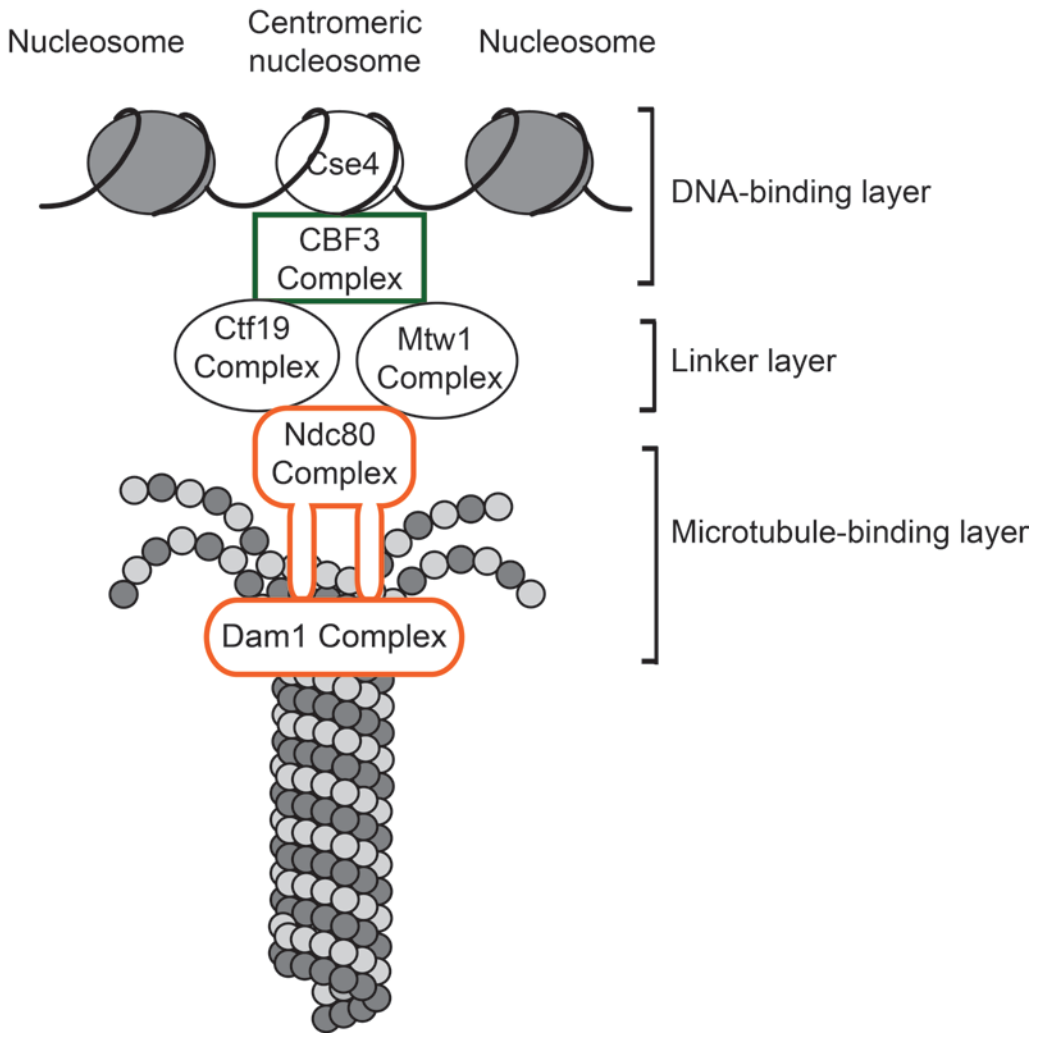

Figure 1-3. *S.cerevisiae* kinetochore structure. The *S.cerevisiae* is made up of over 65 proteins organized into three layers. The DNA-binding layer of the kinetochore binds the ~125bp centromere. A centromeric nucleosome wraps around the centromere and contains a kinetochore-specific histone Cse4. The CBF3 complex (consisting of Cep3, Cft13, Ndc10, and Skp1) also binds the centromere and interacts with components of the linker layer. The Ctf19 and Mtw1 complexes make up the linker layer and their functions are not well understood. The microtubule-binding layer connects the rest of the kinetochore to microtubules. The Ndc80 complex is highly conserved across species; more specifics on the interaction of Ndc80 with microtubules is found in Figure 1-4. The Dam1 complex not conserved in higher eukaryotes and is thought to be unique to species with point centromeres. Dam1 forms a ring around microtubules and can harness the power of depolymerizing microtubules to pull chromosomes during anaphase segregation.

recruitment of other kinetochore proteins (Collins et al. 2005). The CBF3 complex is another major component of the DNA-binding layer; it is composed of Cep3, Ctf13, Ndc10, and Skp1 (Westermann et al. 2007). All other kinetochore proteins depend on the presence of the CBF3 complex to associate with the centromere, including Cse4 (Ortiz et al. 1999; Westermann et al. 2007); depletion of Cep3p or Ndc10p inhibits kinetochore function (Strunnikov et al. 1995; Jiang et al. 1993; Goh et al. 1993). The CBF3 complex binds the CDEIII element with Cep3 providing the most essential contact through sequence-specific binding of its zinc-finger domain (Espelin et al. 1997). *In vitro* studies have shown that Ndc10 also makes important contacts with the CDEII element (Espelin et al. 2003). The CBF3 complex is unique to species with point centromeres (Meraldi et al. 2006).

The DNA-binding layer of the kinetochore recruits the linker and microtubule-binding layer of the kinetochore. The linker layer is composed of three complexes: the Mtw1, Spc105, and Ctf19 complexes. Immunoprecipitation studies of these complexes have identified many of the subunits and their respective stoichometries (Cheeseman et al. 2002; De Wulf et al. 2003; Nekrasov et al. 2003; Westermann et al. 2003). Deletion and depletion of the complexes yield defects in chromosome attachment and segregation (Ghosh et al. 2001; Nekrasov et al. 2003; Pinsky et al. 2003). The Spc105 and Mtw1 complexes are conserved in higher eukaryotes, including *C.elegans* and humans (Cheeseman et al. 2004; Kline et al. 2006), and the Cse4-positioning function of the Ctf19 complex appears to be conserved in humans (Okada et al. 2006; Mythreye and Bloom 2003).

The microtubule-binding layer is composed of the Ndc80 complex and the Dam1 complex. The Ndc80 complex is one of the best studied kinetochore complexes and the only one with a 3D cryo-electron microscopy structure and crystal structure (Wilson-Kubalek et al. 2008;

Ciferri et al. 2008). The Ndc80 complex is a 4 protein complex with a highly conserved dumbbell-shaped structure; its subunits are Ndc80p, Nuf2p, Spc24p, and Spc25p (**Figure 1-4A**) (Wei et al. 2005). All four proteins are essential in *S.cerevisiae*; temperature-sensitive alleles show defects in chromosome segregation and *ndc80-1* strains at the restrictive temperature show detachment of chromosomes from the spindle (Wigge and Kilmartin 2001). Ndc80 and Nuf2 form a dimer that contacts microtubules through their globular head domains, specifically at a calponin-homology domain found on the head of Ndc80p (**Figure 1-4B**) (Wei et al. 2005; Wei et al. 2007; Wilson-Kubalek et al. 2008). Structural studies performed with purified Ndc80 from higher eukaryotes show that the Ndc80 calponin-homology domain contacts and binds microtubules at the interface between α/β tubulin dimers (Wilson-Kubalek et al. 2008). The Spc42 and Spc25 dimer have similar globular head domains that are thought to contact the inner kinetochore (Wei et al. 2005). Together the complex forms a 570Å long dumbbell with the shaft consisting of the two dimers wrapping into an α-helical coiled-coils that are linked to each other through the C-termini of Ndc80/Nuf2 and the N-termini of Spc24/Spc25 (Wei et al. 2005).

Another important feature of the complex is the unstructured, positively charged N-terminal tail of Ndc80. The basic N-terminal tail promotes a tight interaction between Ndc80 and acidic, negatively-charged microtubules; deletion of the 80 amino acid N-terminal tail in human Ndc80 produces 100x weaker binding interaction (Ciferri et al. 2008) and deletion of the 110 amino acid N-terminal tail in yeast causes 10x lower affinity for microtubules (Wei et al. 2007) (**Figure 1-4C**). The charge of the N-terminal tail can be modified by phosphorylations on serines and threonines that reduce the affinity of the complex for microtubules; in humans 9 sites have been identified that reduce affinity (Ciferri et al 2008; DeLuca et al. 2006; Cheeseman et al. 2006) and 7 sites have been identified in *S.cerevisiae* (Akiyoshi et al. 2009; Cheeseman et al.

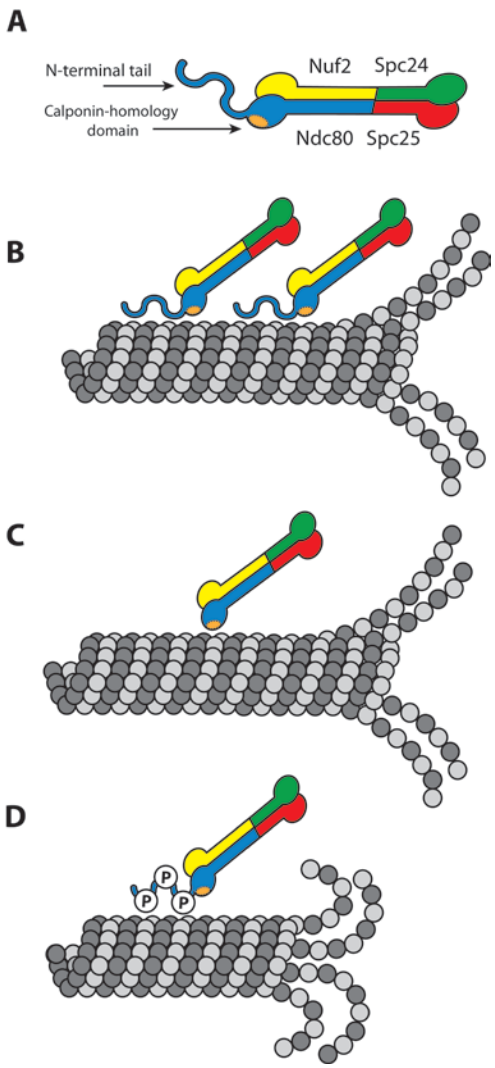

Figure 1-4. Structure of the Ndc80 complex and its interaction with microtubules. The Ndc80 complex is comprised of 4 subunits: Ndc80, Nuf2, Spc24, and Spc25 (**A**). Ndc80 and Nuf2 form a dimer with a globular head that contacts microtubules. Spc24 and Spc25 also form a dimer with a globular head; the two dimers interact to form a dumbell-shaped structure. Ndc80 has an unstructured N-terminal tail and a calponin-homology domain that are important for binding microtubules. They contact microtubules at the interface between α/β tubulin dimers (dark and light gray subunits with the microtubule) (**B**). Deletion of the N-terminal tail causes a reduction in Ndc80's binding affinity for microtubules (10x reduction in yeast, 100x reduction in humans) (**C**). The N-terminal tail of Ndc80 has several sites that are phosphorylated by the Ipl1/Aurora B kinase in response to lack of tension (**D**). Phosphorylation of these sites not only reduces the complex's affinity for microtubules, but it also inhibits its ability to rescue depolymerizing microtubules. Depolymerizing microtubules bound by phosphorylated Ndc80 have a tighter curling back of protofilaments than microtubules bound by non-phosphorylated forms of Ndc80. (Figure from Nannas and Murray 2012).

2002) (**Figure 1-4D**). None of the seven identified phosphorylation sites (T21, T54, T71, T74, S37, S95, and S100) has more impact on binding than the others, leading to the interpretation that it is the cumulative charge rather than one particular residue that is responsible for altered affinities (Akiyoshi et al. 2009). Ndc80's N-terminal tail is phosphorylated by the Ipl1/Aurora B kinase which monitors the correct attachment of microtubules to kinetochores (Akiyoshi et al. 2009; Cheeseman et al. 2002). Surveillance mechanisms will be discussed in detail in the section on the spindle checkpoint. It is thought that the Ipl1 phosphorylation of the Ndc80 tail causes incorrect kinetochore attachments to be released (Pinsky and Biggins 2005).

The phosphorylation of the Ndc80 tail also affects how the complex is able to alter microtubule dynamics. The Ndc80 complex can bind and track on the end of disassembling microtubules. As microtubules depolymerize, the 13 protofilaments that make up the microtubule curl outward (seen in Figure 1-3). Ndc80 is able to bind disassembling microtubule ends and promote a straighter geometry of the protofilaments (**Figure 1-4 B,C**). Holding the protofilaments in a straighter geometry promotes microtubule rescue, conversion from shrinking to growing microtubules (Umbreit et al. 2012). Phospho-mimetic mutations in the tail of Ndc80 reduces the complex's affinity for microtubules (similar to deletion of the tail) and also abolishes the ability of the Ndc80 complex to hold protofilaments in a straighter geometry. With these phospho-mimetic mutants, disassembling microtubule are tightly curled in the same geometry as microtubules devoid of Ndc80 complex (**Figure 1-4D**) (Umbreit et al. 2012) (Figure 4 from Nannas and Murray 2012). Thus, when the N-terminal tail of Ndc80 is phosphorylated, the complex has reduced binding affinity for microtubules, is unable to promote the straighter geometry of protofilaments, and cannot rescue microtubules.

The Dam1 complex is another major component of the microtubule-binding layer of the kinetochore. This complex has a structure thought to be unique to *S.cerevisiae* and other organisms with point centromeres; electron microscopy of *in vitro* Dam1 reconstitution shows a 32nm ring that can assemble around the 24nm diameter of a microtubule (Miranda et al. 2005; Westermann et al. 2005). The diameter of the Dam1 ring complex is nearly optimal for encircling microtubules and acting as a force coupler, transmitting the energy of depolymerizing microtubules to pulling force on chromosomes (Mahadevan and Mitchison 2005). Whole yeast kinetochores purified and observed by electron microscopy reveal a ring assembled around microtubules, suggesting that the Dam1 ring seen *in vitro* is not an artifact of reconstitution with purified proteins (Gonen et al. 2012). As microtubules depolymerize, their protofilaments curl outward (**Figure 1-3**) trapping the Dam1 complex and forcing it to slide along the microtubule ahead of the depolymerizing end. *In vitro* studies have visualized the translocation of Dam1 complexes on microtubules; Dam1 is able to track the ends of depolymerizing microtubules and exert a force up to 3pN (Asbury et al. 2006; Westermann et al. 2006). Unlike many other species, *S.cerevisiae* kinetochores attach to a single microtubule (Winey et al. 1995); mammals have 10-30 microtubules attaching to each kinetochore (McEwen and Dong 2010) and even the fission yeast, *Schizosaccharomyces pombe,* has 2-4 microtubules attached to each kinetochore (Ding et al. 1993). Studies suggest that the Dam1 ring may be essential to maintain attachment to a single microtubule. Dam1 is not essential in *S.pombe*, with its 2-4 microtubules/kinetochore (Sachez-Perez et al. 2005), but it is essential in both *S.cerevisiae* (Cheeseman et al. 2001) and *C.albicans* (Burrack et al. 2011), two fungi with 1 microtubule per kinetochore. Interestingly, over-expressing the centromeric histone, CENP-A, in *C.albicans* (Cse4 in *S.cerevisisae*) increases the number of microtubules attached to the kinetochore, and this increased microtubule/kinetochore

ratio partially rescues *dam1* depletion mutants. Based on fluorescent microscopy of tubulin-GFP, Burrack et al. estimated approximately 60% of kinetochores had 2 microtubules attached when CENP-A was overexpressed, and in cells depeleted for Dam1, 36% had normal chromosome segregation compared to 6% without CENP-A overexpression (2011).

The Ipl1 complex, also known as the chromosomal passenger complex, is another complex involved in kinetochore function, but its location in or around kinetochores is still under investigation. The Ipl1 complex is responsible for making sure only correct attachments are maintained. The functions of Ipl1 will be discussed below in the section on the spindle checkpoint. The 4 subunits of the complex, Ipl1 (a protein kinase), Sli15, Bir1, and Nbl1 are highly conserved; in humans and other higher eukaryotes they are called Aurora B kinase, INCENP, Survivin, and Borealin, respectively (Ruchaud et al. 2007; Nakajima et al. 2009). Ipl1p/Aurora B is a serine/threonine kinase responsible for turning over incorrect chromosomal attachments, and the other three components help localize and activate the kinase (Ruchaud et al. 2007).

Synthetic kinetochores can recapitulate most kinetochore functions. Lacefield et al. have shown that kinetochore function can be achieved by tethering multiple copies of a single component of the Dam1 complex to DNA (Lacefield et al. 2009). Fusing Ask1 to the lactose-repressor protein (LacI) and allowing it to bind the lactose operator (LacO) creates a "synthetic kinetchore" that can accurately segregate an acentric chromosome (**Figure 1-5**). Ask1-LacI recruits other kinetochore components to build the synthetic kinetochore; its ability to bind microtubules and segregate chromosomes requires components of the linker layer and microtubule-binding layer, but not the DNA binding components Ctf13 and Ndc10 (Lacefield et al. 2009). Synthetic kinetochores are able to confer nearly all kinetochore functions: they align

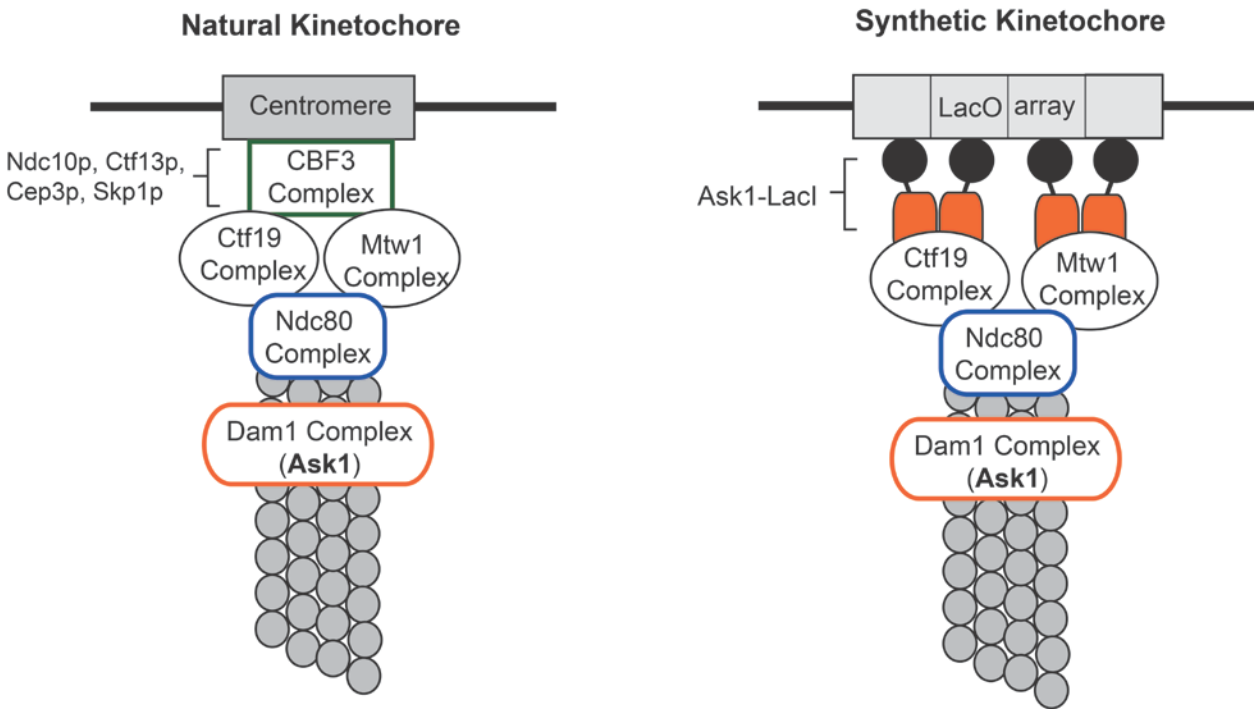

Figure 1-5. Natural kinetochore and synthetic kinetochore structure. Natural kinetochores bind chromatin at the centromere. The CBF3 complex is the primary structure that links chromatin to the rest of the kinetochore proteins. A synthetic kinetochore can be created by introducing Lac operator arrays into chromatin and expressing a fusion of Ask and the Lac repressor. Ask1 is a component of the Dam1 complex. The synthetic kinetochore does not require CBF3 complex members Ndc10 and Ctf13, but it does require components of the Ctf19, Mtw1, and Dam1 complex. The actual architecture of the synthetic kinetochore is unknown as well as how Ask1 recruits these other complexes.

and bi-orient chromosomes, detect and correct mono-oriented chromosomes, and segregate acentric plasmids and chromosomes. However, the synthetic kinetochore did not activate the spindle checkpoint in response to unattached kinetochores (A.W. Murray, personal communication). While inferior to natural kinetochores in strength and precision of attachment, synthetic kinetochores are a powerful tool offering the ability to control when, where, and how pieces of DNA are conferred segregation ability. In Chapter 2, I discuss how synthetic kinetochores were used to probe the role of kinetochores and length-dependent forces in setting the length of the metaphase spindle.

Metaphase spindle length

All of the components discussed above must come together to form the mitotic spindle; microtubules nucleated from spindle pole bodies reach out and attach to kinetochores on sister chromatids while interpolar microtubules span the length of the spindle providing structural support. The *S.cerevisiae* mitotic spindle assembles to a characteristic length of 1.8µm (Winey et al. 1995; Straight et al. 1998). The spindles of other species have highly characteristic lengths as well (Goshima and Scholey 2010). Spindles across all species are made of similar, highly dynamic components, and yet their lengths are quite variable. **Table 1-1** demonstrates the range of spindle lengths found in different organisms, from the 2.0µm of *S.cerevisiae* to the 60µm spindle in *Xenopus* embryos. How do cells decide how large to build the spindle? There are three general categories of spindle length control models: molecular rulers, chemical gradients, and mechanical balance of forces (**Figure 1-6**). In my thesis, I investigated how *S.cerevisiae* determines its 2.0 µm metaphase length, specifically testing predictions of the balance of force model.

Table 1-1. Spindle lengths in different organisms and cell types.

Organism/Cell type	**Spindle length**	**Reference**
S.cerevisiae	2.0µm	Winey et al. 1995
S.pombe	2.5µm	Nabeshima et al. 1998
Drosophila embryo	11.8µm	Brust-Mascher et al. 2009
HeLa	14.0µm	Cai et al. 2009
Sea urchin	20.0µm	Foe and von Dassow 2008
Newt fibroblast	34.0µm	Taylor 1995
Newt lung	44.3µm	Rieder 1977
Xenopus embryo	60.0µm	Wühr et al. 2008

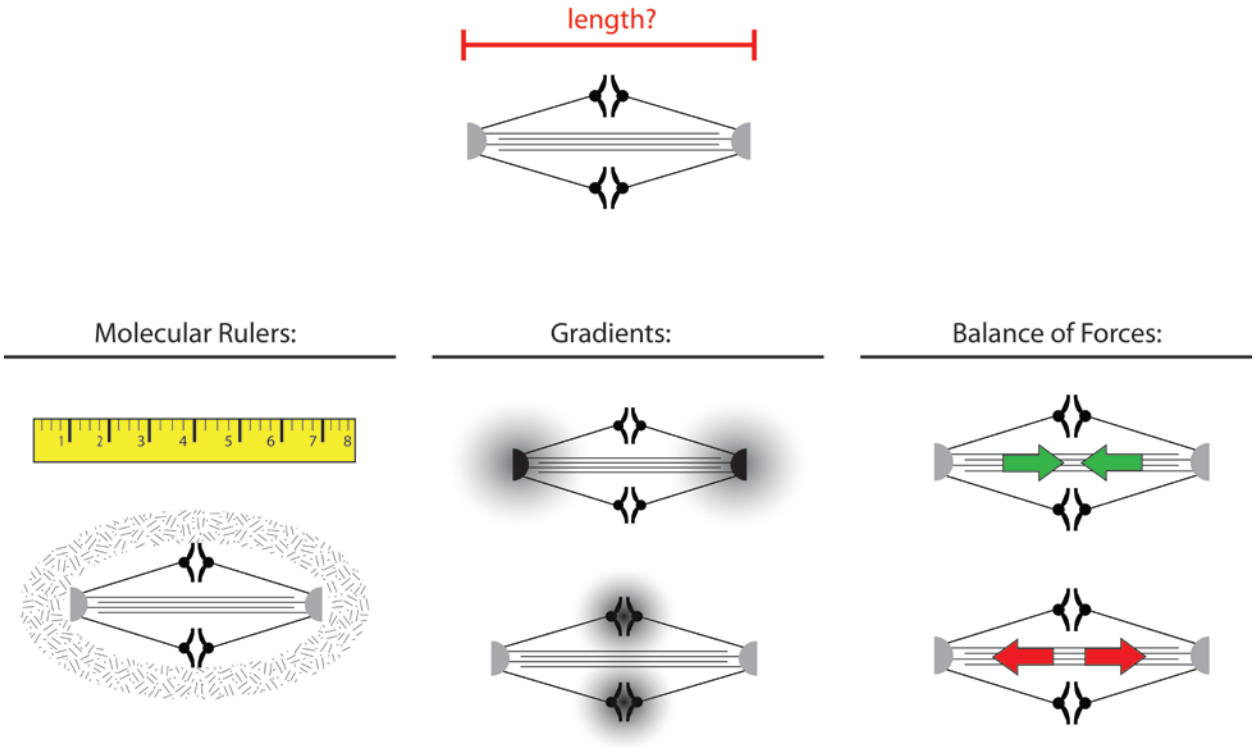

Figure 1-6. Models of spindle length regulation. There are many models of spindle length regulation, but they can grouped by mechanism into three general categories. Spindle length has been proposed to be regulated by molecular rulers, gradients or a balance of forces. Molecular ruler models posit that spindle length is determined by a spindle matrix that surrounds the spindle and provides a physical restraint on the elongation of the metaphase spindle. Gradient models propose that spindle length is governed by gradients emanating from either the poles (centrosomes in the species where evidence has been found), or from chromatin. The Ran-GTP gradient is established around chromatin in some species and causes the nucleation of microtubules near chromosomes. The third type of spindle length regulation is based on a balance of forces generated in the spindle. There are many sources of force-generation and different models place emphasis on certain forces; in all models, spindle length is the resulting equilibrium of these two forces.

Molecular rulers are structures by which cells measure how large to build other structures (**Figure 1-6**). For example, the tails of lambda bacteriophage could assemble to any length, but they have a highly specified length (Marshall 2004). Tail length is regulated by the molecular ruler gpH, a single protein that stretches during assembly and dictates the length of the assembling tail. The gpH ruler interacts with and protects the end of the growing bacteriophage tail. As soon as the tail has grown longer than the gpH protein, it is exposed to the inhibitory protein gpU and assembly is terminated (Katsura 1987, 1990). In spindle assembly, it has been proposed that the spindle matrix, an elastic hydrogel, could provide a ruler by which the cell determines spindle length (Johansen et al. 2011). When microtubules are depolymerized in sea urchins (Kane and Forer 1965; Rebhun and Palazzo 1998) and *Drosophila* (Yao et al. 2012), a hydrogel of nuclear envelope proteins that encased the spindle is left behind. This matrix has been best studied in *Drosophila,* where 4 nuclear proteins have been identifed as components of the matrix: Megator, Skeletor, Chromator and EAST (Qi et al. 2004, 2005; Rath et al. 2004). Megator is found in nuclear pore complexes (Zimowska et al. 1997) and could provide structure to a spindle matrix with its large N-terminal coiled-coil. It has been proposed that the spindle matrix could act as a ruler, providing a physical barrier that prohibits the spindle from elongating further (Goshima and Scholey 2010; Johansen et al. 2011). Disruption or depletion of different spindle matrix components such as nuclear pore components and nuclear lamins has been shown to alter spindle length in *Drosophila* (Civelekoglu-Scholey et al. 2010, Kramer and Hawley 2003) and spindle organization in *Xenopus* (Ma et al. 2009, Tsai et al. 2006) and in HeLa cells (Liu and Zheng 2009). However, when *Xenopus* meiotic spindles were probed with needles, the resulting movements suggested that the matrix does not provide strong mechanical resistance to force and may only weakly provide structural support for the spindle (Gatlin et al. 2010)

The second general mechanism proposed to set spindle length is chemical gradients (**Figure 1-6**). The most well studied gradient associated with spindle assembly is the RanGTP gradient (Kalab and Heald 2008, Bastiaens et al. 2006). Ran is a GTP binding protein that cycles between a GTP- and GDP-bound state, and helps bring materials in and out of the nucleus. Ran releases cargoes when converted from the GDP bound to the GTP bound state (Ström and Weis 2001). Ran's guanine nucleotide exchange factor RCC1 (regulator of chromatin condensation) binds to chromatin and promotes the release of cargoes near chromosomes. This activity is required to assemble spindles; in mitotic *Xenopus* extracts, spindles assemble around chromatin-coated beads in the presence of RCC1 (Heald et al. 1996), but failed to assemble in extracts where RCC1 activity was inhibited (Carazo-Salas et al. 1999). RCC1 alone without chromatin is sufficient to induce assembly of a bipolar spindle (Halpin et al. 2011). RCC1 establishes a gradient of RanGTP around chromosomes; RanGTP directly promotes microtubule nucleation and stabilization, as well as stimulating deposition of spindle assembly factors that stabilize microtubules (Carazo-Salas et al. 2001; Wilde et al. 2001; Caudron et al. 2005; Bastiaens et al. 2006). The spatial patterning of this microtubule-stabilizing gradient could determine spindle length; altering the size of the RanGTP gradient has been shown to disrupt spindle assembly, causing randomly oriented microtubule structures, loss of bipolarity, and a decrease in microtubule-kinetochore attachments (Caudron et al. 2005).

Another molecular gradient has been shown to directly modulate spindle length in *C.elegans* embryos. It had been previously shown that in *Xenopus*, spindle length scales with cell size (Wühr et al. 2008). How the size of the cell might influence spindle length was unknown until it was shown in *C.elegans* embryos that spindle length scales with the size of centrosomes (Greenan et al. 2010) and in turn centrosome size scales with cell size (Decker et al. 2011).

Greenan et al. discovered a gradient of the protein TPXL-1 emanating from centrosomes (2010). TPXL-1 is the *C.elegans* homolog of the vertebrate protein TPX2; these proteins bind the Aurora A kinase and localize it to the spindle and centrosomes (Özlü et al. 2005). Like its paralog Aurora B, the Aurora A kinase is involved in cell division control and is responsible for maturation of centrosomes (Hannak et al. 2001). Greenan et al. showed that spindle length correlates with centrosome size during *C.elegans* development and reducing the size of the centrosome through molecular perturbation shortens the TPXL-1 gradient and causes a shortening of the spindle (2010).

The third general mechanism of spindle length regulation posits that spindle length is the result of opposing mechanical forces (**Figure 1-6**). There are many documented sources of force generation in the mitotic spindle and the relative importance of each of these forces in setting spindle length may vary across different species (Goshima and Scholey 2010). Some of these forces arise from microtubule polymerization and depolymerization (Inoué and Salmon 1995; Laan et al. 2008), sliding of microtubules (Brust-Mascher et al. 2009), astral microtubules (Adames and Cooper 2000), motor proteins (Saunders et al. 1992, 1997; Straight et al. 1998), and the spring-properties of chromatin (Goshima et al. 1999; Bouck and Bloom 2007). Quantitative models seek to understand the contributions of these different forces (Gardner et al. 2006, 2008; Dumont and Mitchison 2009; Loughlin et al. 2011; Stephens et al. 2013), but the underlying unifying concept is that spindle length is a steady-state equilibrium between pushing and pulling forces. In order to achieve stable steady-state lengths, at least one of these spindle forces must have some length-dependency. The magnitude of the force must vary depending on the length of the polymer along which force is generated.

An example of the different sources of force contribution comes from *Xenopus*. In the *Xenopus* family, spindle are longer in *X.laevis* than in and *X.tropicalis*; it was shown that a higher rate of microtubule depolymerization caused by the protein katanin led to shorter spindles in *X.tropicalis* (Loughlin et al. 2011). Katanin in *X.laevis* is inhibited by phosphorylation at the p60 catalytic subunit, but katanin in *X.tropicalis* is non-phosphorylatable which results in a higher level of microtubule severing and depolymerization (Loughlin et al. 2011). However, katanin is not the only sources of microtubule destabilization in *X.laevis*; developmental regulation of kif2a, a kinesin-13 microtubule-destabilizing motor alters spindle length as well (Wilbur and Heald 2013). Different models of spindle length regulation weigh the contributions of these sources of force, and it is likely that the most significant source of force and mechanism of spindle length regulation varies between species.

The metaphase spindle length of yeast is thought to be governed by a balance of length-dependent forces. *S. cerevisiae* spindles are a simple system compared to higher eukaryotes, and the force contributors are better understood and more easily manipulated (**Figure 1-7**). The outward pushing forces are thought to come from kinesin-5 family of (+) end directed microtubule, motors Cin8 and Kip1. These two motors have redundant functions; deletion of either causes the spindle to shorten (Straight et al. 1998). Likewise, increasing the concentration of Cin8 causes the spindle to elongate (Saunders et al. 1997). This outward pushing is resisted by inward forces from other motor proteins like Kar3 a member of the kinesin-14 family of (-) end directed motors. Over-expression of Kar3 in *S.cerevisiae* causes a shortening of the spindle (Saunders et al. 1997), and deletion of the Kar3 homolog in *S.pombe* causes an elongation of the spindle (Troxell et al. 2001). Motor proteins that promote microtubule depolymerization also create inward force; deletion of the microtubule-destabilizing motor Kip3 causes the spindle to

elongate (Straight et al. 1998). In this simple model of force balance (**Figure 1-7**), outward pushing forces are also resisted by chromatids attached to the spindle and held together by cohesin; disrupting attachment or cohesin should extend the spindle. This has been observed in *S.pombe* where mutations in kinetochore proteins Mis6 and Mis12 causes a 35-60% extension of the spindle (Goshima et al. 1999). Disrupting cohesin (Stephens et al. 2011) and loosening the packing of chromatin (Bouck and Bloom 2007) has been shown to elongate the *S.cerevisiae* spindle. These studies support a balance of force model of yeast spindle length, but no studies to date have demonstrated the length-dependency of forces.

In my thesis, I sought to understand which of these three general mechanisms regulates spindle length in *Saccharomyces cerevisiae*. Balance of length-dependent forces is thought to be main regulator of spindle length in *S.cerevisiae,* and so I specifically tested predictions of this model in Chapter 2. We found that spindle length is set by the number of chromosomal attachments; we manipulated the number of functional kinetochores and found that spindles were shorter with more kinetochores and longer with fewer kinetochore. Our results support the force-balance model of spindle length regulation.

The Spindle Checkpoint

Attaching chromosomes to the spindle: distinguishing correct and incorrect attachments

All chromosomes must correctly attach to the spindle in metaphase. A correct attachment is generated when microtubules from opposite spindle pole bodies attach to kinetochores on sister chromatids (amphitelic attachment); a chromosome in this configuration is said to be "bi-oriented" (**Figure 1-8A**). Aneuploidy would result if cells divide with incorrect or "mono-oriented" chromosomes such as both sister kinetochores attaching to the same pole (syntelic attachment) (**Figure 1-8B**) , or only one of the two sister kinetochores attaching to a microtubule

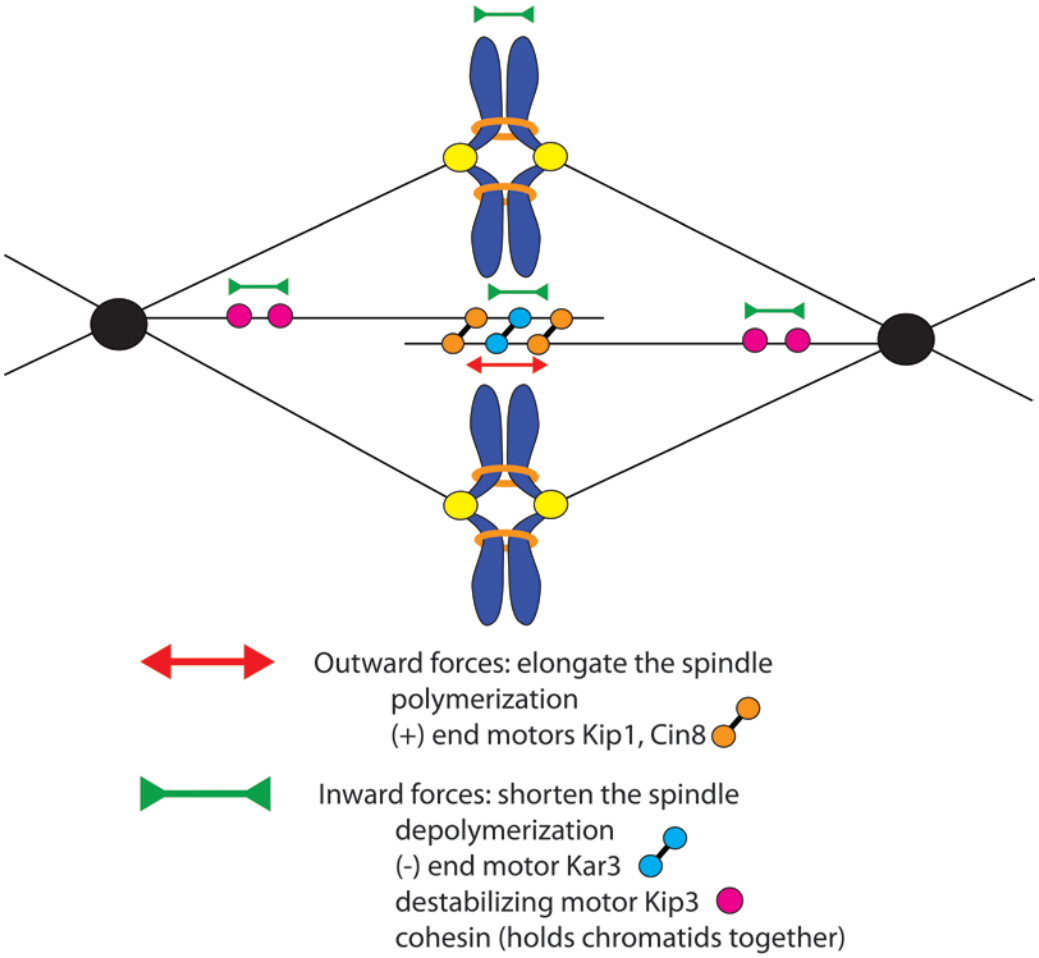

Figure 1-7. Forces in the *S.cerevisiae* spindle. There are many sources of force in the *S.cerevisiae*. Outward forces are generated by microtubule polymerization that drives poles apart and by (+) end directed motor proteins Kip1 and Cin8. Inward forces are thought to come from microtubule depolymerization, the (-) end directed motor Kar3, the microtubule-destabilizing motor Kip3, and by cohesin that resists the pulling generated by depolymerizing microtubules. The relative contribute and importance of these forces in setting spindle length is still under investigation. It is also unknown if the attachment of chromosomes to the spindle is an important contributor of force in setting spindle length.

(monotelic attachment) (**Figure 1-8C**). A merotelic attachment is another incorrect attachment where a single kinetochore attaches to microtubules from opposite poles (**Figure 1-8D**); this type of error cannot occur in *S.cerevisiae* since its kinetochores attach to only a single microtubule (Winey et al. 1995). To avoid aneuploidy, all chromosomes must be bi-oriented before the cell enters anaphase. Mono-oriented attachments are selectively destabilized and turned over, providing the kinetochore another chance to make a correct attachment (Cheeseman et al. 2002; Biggins and Murray 2001).

How do cells distinguish bi-oriented and mono-oriented chromosomes? Correct attachments generate tension across the sister chromatids; if kinetochores are attached to opposite poles, poleward forces attempt to pull the sisters apart but are resisted by cohesin rings that hold the two chromatids together (**Figure 1-8A**). This configuration generates tension which can be visualized by pre-anaphase stretching of the chromatin around the centromere. Chromatin can be fluorescently labeled by introducing a Lac operator array at a desired location and expressing GFP fused to the Lac repressor (Straight et al. 1997). In yeast cells where the LacO array is placed within 4kb of the centromere, two GFP dots representing the pericentric chromatin can be resolved up to 0.8-1.0 μm apart before anaphase, approximately half the length of the 2.0μm metaphase spindle (**Figure 1-9**) (Goshima et al. 2000). A single GFP dot represents chromosomes that are mono-oriented or bi-oriented but not stretched far enough apart to be resolved by light microscopy (**Figure 1-9**).

Mono-oriented chromosomes are not under tension; either they have only one kinetochore attached or both kinetochores are attached to same pole. Ipl1, the founding member of the Aurora serine/threonine kinase family (Chan and Botstein 1993), is responsible for sensing this tension; attachments that do not generate tension are destabilized, and without Ipl1 incorrect

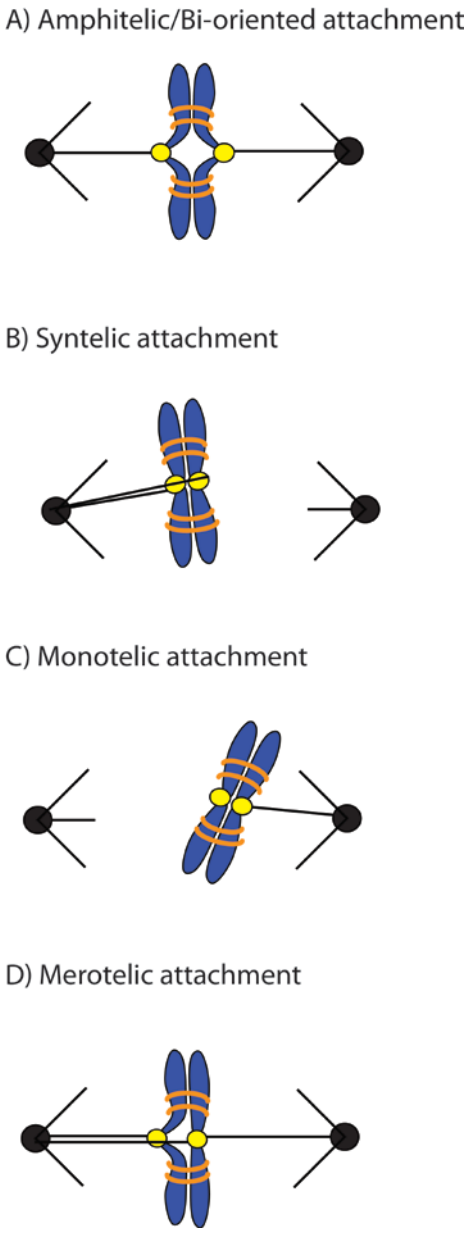

Figure 1-8. Different types of chromosomal attachment. Chromosomal attachments must be bi-oriented (amphitelic) to ensure correct segregation and satisfy the spindle checkpoint (**A**). All other attachments are incorrect and will activate the spindle checkpoint. Syntelic attachments occur with both kinetochores on sister chromatids attach to the same pole (**B**). Monotelic attachments occur when only one of the kinetochores is attached and the other is unattached (**C**). Merotelic attachment do not occur in *S.cerevisiae* because only one microtubule attaches per kinetochore, but in other organisms where kinetochore attach to multiple microtubules, merotelic attachments can occur where one kinetochore is attached to both poles (**D**).

attachments persist (Biggins et al. 1999; Biggins and Murray 2001; Tanaka et al. 2002). Ipl1 phosphorylates seven different serine and threonine sites on the Ndc80p N-terminal tail which causes a decrease in kinetochore affinity for the microtubule affinities (Cheeseman et al. 2002; Akiyoshi et al. 2009). In addition to destabilizing incorrect attachments, Ipl1 also buys additional time for the cell to make a correct attachment; it activates the spindle assembly checkpoint which delays the cell cycle until all chromosomes are correctly attached (Biggins et al. 1999; Biggins and Murray 2001).

In addition to an Ipl1-based mechanism of distinguishing correct and incorrect attachments, tension itself can act as a mechanism to selectively stabilize attachments. Yeast kinetochores purified and reconstituted *in vitro* remained attached to microtubules at a higher frequency if under tension (Akiyoshi et al. 2010). Beads coated with reconstituted kinetochores were placed under tension using a laser trap; kinetochores with 5pN of force placed on them (physiological spindle force) remained attached to microtubules twice as long as kinetochore under only 1pN of force. This stabilization of attachment did not dependent on Ipl1 or Ipl1-induced phosphorylations as neither the kinase nor ATP was present in the system. These results suggest that tension itself provides a direct mechanical stabilization of kinetochore-microtubule attachments (Akiyoshi et al. 2010).

Checkpoint activation by lack of tension or unattached kinetochores

The spindle checkpoint is a surveillance mechanism activated by unattached kinetochores and mono-oriented attachments that delays the cell cycle in metaphase until all chromosomes are bi-oriented (**Figure1-10**). The checkpoint is activated by Ipl1 in response to tensionless attachments (Stern and Murray 2001), but the checkpoint can be activated without Ipl1. Treating cells with microtubule-depolymerizing drugs, such as nocodazole and benomyl, causes a cell

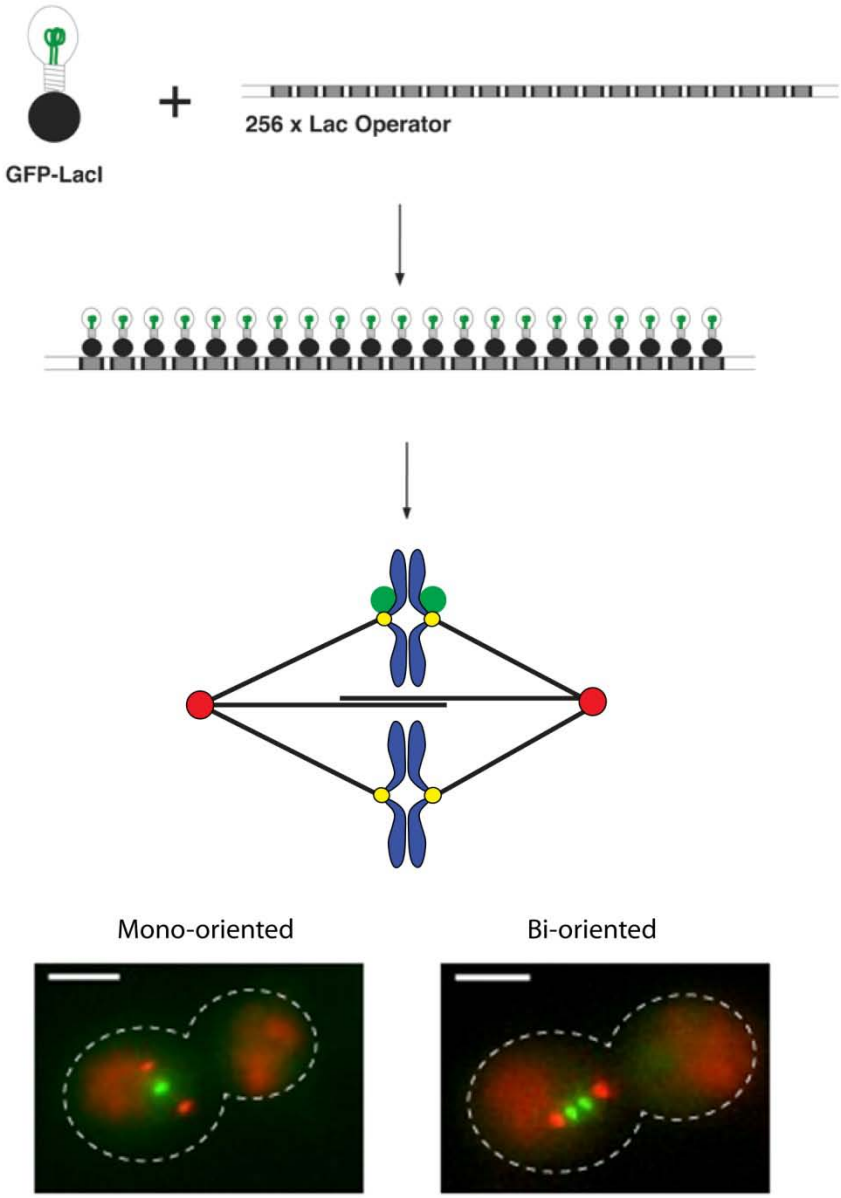

Figure 1-9. Visualizing *S.cerevisiae* chromosomes by fluorescent microscopy. A single chromosome can be visualized by introducing a 256 repeat Lac operator into the chromatin near a centromere. Expression of GFP-LacI causes the single chromosome containing the LacO array to be tagged with GFP. A mono-oriented chromosome (or a chromosome not stretching far enough apart to be resolved as 2 dots) appears a single GFP dot and a bi-oriented chromosomes appears as two. Spindle pole bodies are labeled red (Spc42-mCherry). The white bar denotes 3µm.

cycle arrest in metaphase (Li and Murray 1991), even in cells lacking Ipl1 (Biggins et al. 2001). Microtubule-depolymerizing drugs create empty, unattached kinetochores, and for many years, the field has contested whether the spindle checkpoint is activated solely by unattached kinetochores or by both unattached kinetochores and by lack of tension (Pinsky and Biggins 2005). In PtK1 cells, an unattached kinetochore will cause a delay in metaphase; laser-ablation of the kinetochore induces immediate entry to anaphase (Rieder et al. 1995). The authors argue that the chromosome with a laser-ablated kinetochore still does not experience tension, but the checkpoint is satisfied. Further support for an empty kinetochore activation of the checkpoint is Ipl1's mechanism of action. Ipl1 phosphorylates components of the kinetochore and destabilizes kinetochore attachment (Cheeseman et al 2002); it is thought that Ipl1 activates the checkpoint indirectly by creating an unattached kinetochore. The kinase is required to re-orient or change the attachment state of a chromosome (Tanaka et al. 2002) and fluorescent studies have shown that Ipl1 will cause the release of microtubules from kinetochore mutants that cannot generate tension (Pinsky et al. 2006). However, these Ipl1 studies do not rigorously rule out the possibility that the kinase both creates unattached kinetochores and directly activates the checkpoint.

Localization studies have shown that the checkpoint maybe differentially activated under different conditions; checkpoint proteins Mad2 and Mad1 localize to the kinetochore when unattached, and a phosphorylated form of Mad3 localizes to the kinetochore when treated with taxol (attached kinetochore but reduced tension). Introducing unphosphorylatable Mad3 abolishes the tension-sensing checkpoint but does not affect cells ability to respond to microtubule poisons (King et al. 2007). Additionally, Ipl1 will activate the spindle checkpoint in cells with no cohesin (no tension because no resistance to separation) and in cells that have not replicated their chromosomes (no tension because no pairing partner) but fluorescent microscopy

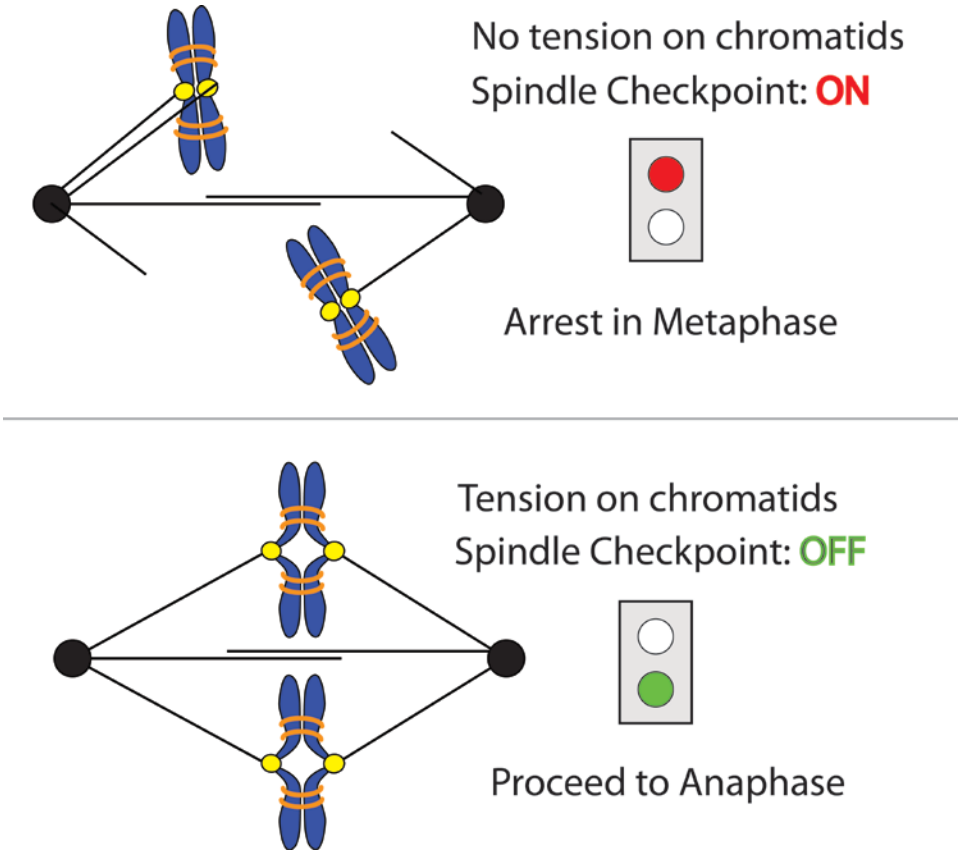

Figure 1-10. The spindle checkpoint monitors tension on chromatids. The spindle checkpoint ensures that chromosomes are properly segregated. The checkpoint monitors both attachment of kinetochores by microtubules and the tension generated across a correctly attached chromosomes. An unattached kinetochore or a chromosome with both kinetochores attached to the same pole activates the checkpoint and causes cells to arrest in metaphase. Once all chromosomes are bi-oriented and under tension, the spindle checkpoint is satisfied and turns off, allowing cells to proceed into anaphase.

indicates that most of the chromosomes are still attached to microtubules (Stern and Murray 2001).

A recent study performed in both *S.cerevisiae* and human cells provides support for the dual function of the Ipl1/Aurora B kinase, both creating unattached kinetochores and directly activating the checkpoint. Matson et al. showed that components of the inner kinetochore COMA complex (yeast proteins Chl4, Cft3 and Ctf19 and their human homologs CENP-H/I/N) are not required for checkpoint-induced arrest if cells are treated with paclitaxel, but are required if cells are treated with nocodazole and do not have a functional Ipl1/Aurora B kinase (2012). Paclitaxel is the generic form of taxol which stabilizes microtubules and causes a reduction of tension on kinetochores due to the inhibition of microtubule depolymerization; this reduction in kinetochore stretching by taxol activates the spindle checkpoint (Maresca and Salmon 2009). Matson et al. showed that a subset of yeast and human COMA proteins are not required for this tension-based arrest, but are essential for arrest in response to unattached kinetochores created by nocodazole if cells do not have functional Ipl1/Aurora B. Cells that have a functional kinase are able to arrest in response to nocodazole and do not require the COMA proteins. These findings suggest that there are two separable pathways to spindle checkpoint activation: an Ipl1-dependent pathway and an Ipl1-independent pathway, which would mean that Ipl1/Aurora B directly activates the checkpoint in addition to destabilizing microtubules.

The most famous and elegant studies supporting a tension-sensing mechanism in the spindle checkpoint come from Bruce Nicklas' studies of meiotic mantid spermatocytes. Nicklas pioneered the ability to exert force on chromosomes with a glass needle (Nicklas 1983). In mantid spermatocytes, the sex chromosome is a trivalent with one Y chromosomes paired with two X chromosomes and in 10% of meioses one of the X chromosomes fails to pair and is left

tensionless without a partner (Li and Nicklas 1995). Nicklas showed that the presence of this tensionless X chromosome causes a 5 hour delay in metaphase I and eventual cell death. Applying a glass needle and pulling on the unpaired chromosome creates tension, and the cells entered anaphase within 55 minutes (Li and Nicklas 1995). Nicklas also showed that the kinetochores are reversibly phosphorylated depending on their tension state; kinetochores of tensionless chromosomes are phosphorylated presumably by the spindle checkpoint, and applying tension leads to their de-phosphorylation. Relaxing the applied tension causes re-phosphorylation (Li and Nicklas 1997).

Regardless of exactly how the Ipl1/Aurora B kinase activates the spindle checkpoint, the kinase does activate the checkpoint in response to tensionless attachments. One major outstanding questions is where the kinase senses tension. Two different locations have been proposed, either tension is sensed within the kinetochore (intra-kinetochore stretch) (**Figure 1-11A**) or between the sister kinetochores (inter-kinetochore stretch) (**Figure 1-11B**). The intra-kinetochore stretch model suggests that the Ipl1/Aurora B kinase monitors the separation within a kinetochore, activating the checkpoint when the kinteochore is compressed but silencing it when the kinetochore is elongated by tension (Uchida et al. 2009; Maresca and Salmon 2009). Uchida et al. showed that treating HeLa cells with low amounts of nocodazole or depleting condesin (loosening the packing of chromatids) lead to a compression of the kinetochore but had no effect on inter-kinetochore stretch; compression of the kinetochore activated the checkpoint (2009). Uchida et al. also found that mono-oriented chromosomes that still maintained intra-kinetochore stretch but no inter-kinetochore stretch, did not activate the checkpoint. Maresca and Salmon similarly showed that treating *Drosophila* S2 cells with a certain amount of taxol, a

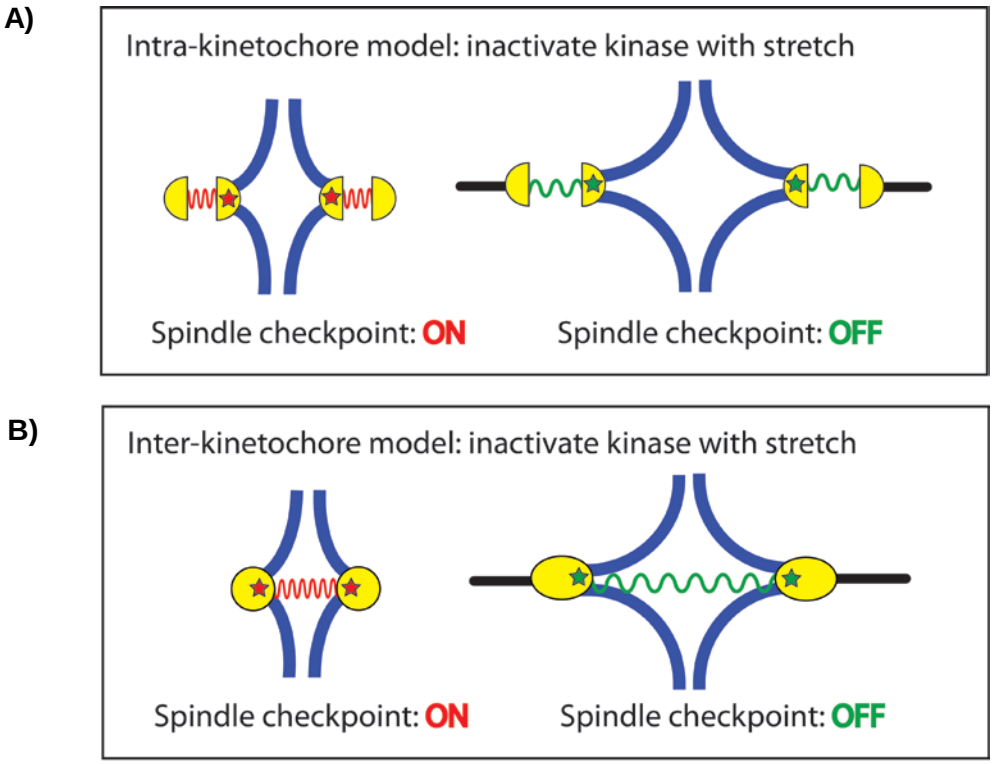

Figure 1-11. Deactivation of the Ipl1 kinase with tension: inter- and intra-kinetochore models. Tension on bi-oriented chromosomes could either be sensed within kinetochores (intra-kinetochore) or between them (inter-kinetochore). In this version of the intra-kinetochore model (**A**), lack of tension within the kinetochore activates the kinase (red star= active kinase), which then destabilizes microtubules and activates the checkpoint. Stretch within the kinetochore deactivates the kinase (green star) and spindle checkpoint is turned off. In the inter-kinetochore model (B), lack of tension between kinetochores activates the kinase which turns on the spindle checkpoint. When chromatids are stretched, the kinase is deactivated and no longer turns on the spindle checkpoint.

drug that stabilizes microtubules and inhibits their dynamic disassembly (Schiff et al. 1979), caused a reduction in inter-kinetochore stretch but not intra-kinetochore stretch, and these cells did not activation the checkpoint. Application of a larger dose of taxol caused a reduction in both intra- and inter-kinetochore stretch and cells then activated the checkpoint (2009).

The second model (**Figure 1-11B**) posits that the Ipl1/Aurora B kinase measures the distance between sister kinetochores. Kinetochores separate by up to 1 µm during metaphase due to dynamically unstable microtubules attempingt to pull the two chromatids apart despite the cohesins that hold them together (He et al. 2000). The opposition of these forces causes the chromatin around the centromere to behave like a spring and stretch to 7nm, beads on a string chromatin fiber conformation (Goshima et al. 2000; Bloom and Yeh 2010). PICH, a protein identified in HeLa has been proposed as a potential sensor of inter-kinetochore stretch due to its unique localization between kinetochores (Tanaka 2008); PICH can be seen as a long thread connecting separating kinetochore in metaphase and anaphase (Baumann et al. 2007; Wang et al. 2008). An additional argument for measurement of the inter-kinetochore distance is the dynamic instability of microtubules. During metaphase, bi-oriented chromatids undergo "breathing", cycles of stretching and retracting as microtubules polymerize and depolymerize. GFP-labeled centromeres can be visualized splitting into two dots and coalescing into a single dot every few minutes (He et al. 2000). The intra-kinetochore models do not explain how intra-kinetochore stretch is maintained during breathing; microtubule polymerization at both sister kinetochores should reduce the tension on kinetochores and the intra-kinetochore distance. If inter-kinetochore distance is measured, there may be some minimum distance threshold that is not crossed during breathing.

Variations of both models exist to explain how Ipl1 measures tension. The kinase may either be de-activated by tension within or between kinetochores, or it may be constitutively active but be spatially separated from its critical substrates when kinetochores are stretched. In the intra-kinetochore stretch model, it has been proposed that the Ipl1p binding partners Sli15p and Bir1p could be a spring that becomes stretched within the kinetochore and deactivates Ipl1p (Sandall et al. 2006). The PICH protein visualized between kinetochores has been proposed to play a similar role de-activating the kinase in inter-kinetochore stretch models (Tanaka 2008; Baumann et al. 2007; Wang L.H. et al. 2008).

Ipl1p activity may also be silenced by separating the kinase from its targets, thus the kinase is always active but cannot reach its targets when stretched (**Figure 1-12**). In an elegant study of Aurora B activity, Liu et al. created a FRET based sensor that reported Aurora B activity and could be placed at varying locations within the centromere and kinetochore. Liu et al. showed that a kinase substrate placed in the inner centromere (densely packaged centromere chromatin) near the Aurora B kinase is phosphorylated even on bi-oriented chromosomes (2009). When the substrate was placed further away from the kinase, in the middle or outer kinetochore, it was not phosphorylated. This suggests that the Aurora B kinase remains active even on bi-oriented chromosomes, but cannot reach its targets at the microtubule-kinetochore interface when the chromatids are stretched (**Figure 1-12A**). Liu et al. also demonstrated that repositioning the kinase close to its substrates causes constitutive target phosphorylation, destabilization of correct attachments, and metaphase arrest due to activation of the checkpoint (2009).

It may be possible to spatially separate Ipl1 from its targets given an intra-kinetochore stretch model. Yeast kinetochores elongate under tension; inner and outer kinetochore

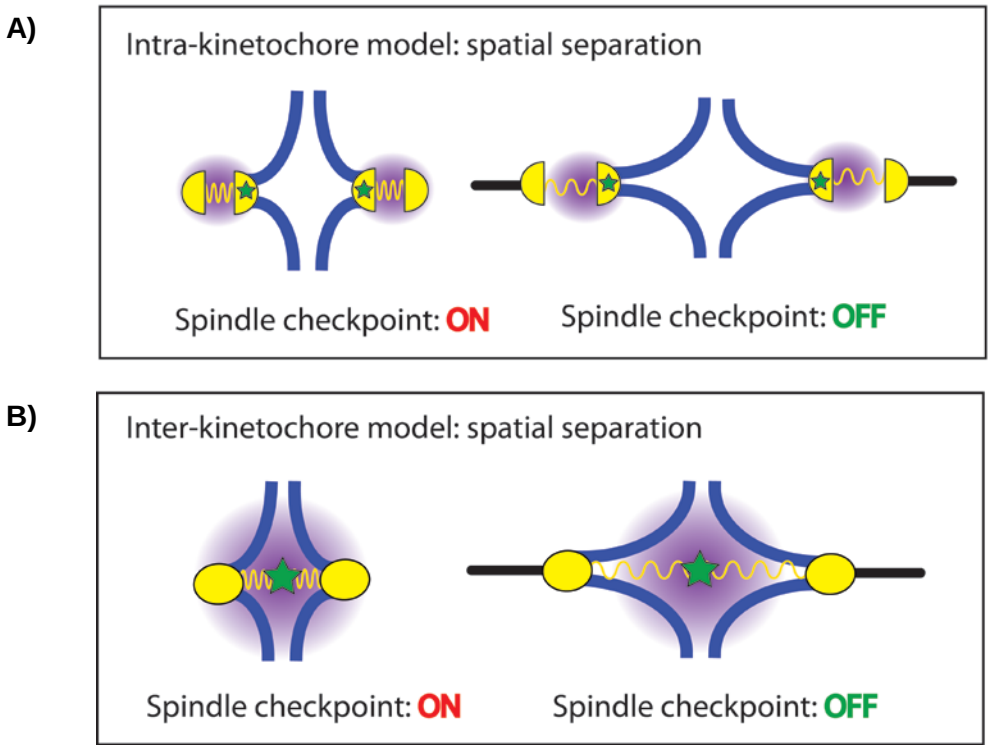

Figure 1-12. Spatial separation of the kinase from its targets: intra- and inter-kinetochore models. Tension on bi-oriented chromosomes is either measured between or within kinetochores; in this spatial separation version of the two models, the kinase (green star) is constitutively active and the microtubule-kinetochore interface must stretch beyond the range of kinase activity (purple region). In the spatial separation version of intra-kinetochore model (**A**), the kinase is located within the inner kinetochore and when there is no tension, targets at the interface are phosphorylated and the spindle checkpoint is turned on. When the chromatid is under tension, the kinetochore elongates and the microtubule-kinetochore interface is pulled out beyond the range of kinase activity. In the spatial separation version of inter-kinetochore model (B), the kinase is located between sister chromatids. Without tension, the chromatin is not stretched and the kinase is able to reach its targets; when tension is generated, chromatin stretches and the kinetochore-microtubule is separated from the kinase and the spindle checkpoint is turned off.

components can be visually resolved (Uchida et al. 2009; Maresca and Salmon 2009). The Ndc80 complex has a long coiled-coil domain that contains a flexible elbow-like hinge that is thought to straighten out under tension (Wang H.W. et al 2008). Straightening of the Ndc80 complex under tension may create enough distance in the kinetochore to separate an internally localized Ipl1p from the microtubule-kinetochore interface.

In support of spatial kinase separation in the inter-kinetochore model (**Figure 1-12B**), studies in *Xenopus* showed that Aurora B localizes to chromatin between the two kinetochores; when the chromatids are stretched, Aurora B remains in between the kinetochores while kinase targets like MCAK are stretched away. Treatment with nocodazole or taxol cause the Aurora B and MCAK to co-localize again (Andrews et al. 2004). In *Saccharomyces cerevisiae*, the localization of Ipl1p at metaphase is controversial, with five different results being reported: in between stretched kinetochores (Shimogawa et al. 2009), diffusely in the spindle (Tanaka et al. 2002), to the spindle and spindle poles (Kang et al. 2001; Kim et al. 1999; Huh et al.2003), co-localized with kinetochore proteins (Makrontoni and Stark 2009), and heterogeneous localization, depending on the cell (Buvelot et al. 2003).

In my thesis work, I investigated where the Ipl1 kinase monitors tension, either between kinetochores or within them. My findings on this question are discussed in Chapter 3; we found that the spindle checkpoint is not activated by inhibition of inter-kinetochore stretching. I also investigated a novel mechanism of Ipl1 tension sensation; this work, which was largely inconclusive, is presented in Appendix 1.

Spindle checkpoint mechanism

Once activated by a mono-oriented chromosome, either a tensionless attachment or an empty kinetochore, the spindle checkpoint delays anaphase until all chromosomes are bi-oriented. To prevent the metaphase to anaphase transition, checkpoint proteins block the ability of the Anaphase Promoting Complex (APC) to target proteins for destruction. In an error-free mitosis, the APC with its co-activator Cdc20 (Yu 2007) will ubiquitinate proteins that hold the cell in metaphase, targeting them for destruction and allowing the cell to enter anaphase (**Figure 1-12A**) (Musacchio and Salmon 2007). The APC^{Cdc20} has two main targets: cyclin B and Pds1. Destroying cyclin B inactivates Cdk1, the driver of the cell cycle, and allows the cells to begin the biochemical transition out of mitosis and back to G1 (Hershko 1999). Securin (Pds1in *S.cerevisiae*) is an inhibitor of a protease called separase (Esp1); when securin is destroyed, separase is released and it cleaves the Scc1 subunit of cohesin (Cohen-Fix et al. 1996; Cohen-Fix and Koshland 1997; Ciosk et al. 1998) . Cleavage of cohesin triggers anaphase; sister chromatids are released and move toward the poles of the spindle (Uhlmann 1999, 2000).

When the spindle checkpoint has been activated, the APC^{Cdc20} is inhibited, preventing separase from cleaving the cohesin rings and arresting the cell biochemically in metaphase (**Figure 1-12B**). The checkpoint inhibits the APC^{Cdc20} by sequestering its activator Cdc20. Checkpoint proteins Mad2, Mad3, and Bub3 bind Cdc20 preventing its interaction with the APC (Hwang et al. 1998), creating what is known as the "mitotic checkpoint complex" or MCC (Sudkain et al. 2001). Mutations can be in made in Cdc20 that are resistant to the spindle checkpoint and these forms of Cdc20 are not bound by the Mad proteins (Hwang et al. 1998). Other checkpoint proteins include Mad1and the kinases Bub1 and Mps1; these proteins amplify

activation of the checkpoint and increase the rate of MCC complex formation (Hardwick et al. 1996; Weiss and Winey 1996; Abrieu et al. 2001; Morrow et al. 2005).

While there has been extensive work devoted to the checkpoint, the exact mechanisms of action and signaling, as well as the roles and hierarchical interactions of proteins and complexes are still unclear. The predominant molecular model for spindle checkpoint function is based on checkpoint proteins localizing to empty kinetochores. The kinetochore acts as a scaffold to bring together MCC components which can then act as diffusible templates for further MCC formation (Musacchio and Salmon 2007). This model is based on a large body of work on protein localization, recruitment and dynamics performed in a range of model systems. In *Xenopus*, treatment with microtubule-depolymerizing drugs induces localization of Xmad2 (*Xenopus* homolog of Mad2) to unattached kinetochores. This localization diminishes 50-100 fold as the kinetochore becomes attached (Chen et al. 1996; Waters et al. 1998). Xmad2 localization to unattached kinetochores is dependent on Xmad1, without which Xmad2 cannot bind kinetochores and the checkpoint is inactivated (Chen et al. 1998). Further support for the model come from studies that show that MCC constituents cycle on and off kinetochores; MCC complexes are only transiently localized to kinetochores, supporting the interpretation that they are formed at kinetochores but become diffusible complexes (Howell et al. 2000, 2004).

Mad2 exists in two different conformations, open and closed. Open Mad2 becomes closed upon binding to Mad1 or Cdc20 (Luo et al. 2002). If open-Mad2 binds Mad1, it becomes closed-Mad2 and is tethered at the kinetochore (Chen et al. 1998; Howell et al. 2000; 2004). This tethered closed-Mad2 is capable of dimerizing with open-Mad2 , which promotes its conversion to closed-Mad2 and interaction with Cdc20. Thus closed-Mad2 at the kinetochore is thought to act as a template, transiently binding open-Mad2 , converting it to closed-Mad2, helping it bind

Cdc20 and releasing the newly assembled MCC complex (Chung and Chen 2002; De Antoni et al. 2005). The diffusible MCC complex is thought to serve as a positive feeback loop and by stimulating more C-MAD2-Cdc20 formation away from the kinetochore (Musacchio and Salmon 2007). Ultimately, all Cdc20 is bound and sequestered by Mad2 and other spindle checkpoint proteins in the MCC complex. Without active Cdc20, cells arrest in metaphase until the checkpoint is satisfied and silenced by the bi-orientation of all chromosomes on the spindle.

Closing Remarks

The faithful segregation of chromosomes is essential for life, and cells have evolved elaborate mechanisms to ensure the process proceeds correctly. We know that cells assemble the spindle to pull sister chromatids apart, but we do not know how cells determine how long to build the metaphase spindle. We have discovered that cells use a surveillance mechanism, the spindle checkpoint, to monitor attachment of chromosomes to the spindle. The checkpoint measures the tension on chromatids to distinguish correct and incorrect attachments, but we do not know where or how the checkpoint monitors tension. In Chapter 2, I will discuss an investigation of spindle length regulation and evidence supporting a balance of length-dependent forces model. In Chapter 3, I will present data that supports measurement of tension within kinetochores, and in the Appendix I will describe experiments that disprove one model of Ipl1 tension-sensation. Chapter 4 describes new questions, experiments and future directions to of chromosome segregation research.

References

Abrieu A., Magnaghi-Jaulin L., Kahana J.A., Peter M., Castro A., Vigneron S., Lorca T., Cleveland D.W. and J.C. Labbé. 2001. Mps1 is a kinetochore-associated kinase essential for the vertebrate mitotic checkpoint. *Cell* 106: 83-93.

Adames N.R. and J.A. Cooper. 2000. Microtubule interactions with the cell cortex causing nuclear movements in *Saccharomyces cerevisiae*. *J Cell Biol* 149: 863-874.

Amiel A., Gronich N., Yukla M., Suliman S., Josef G., Gaber E., Drori G., Fejgin M.D., and M Lisher. Random aneuploidy in neoplastic and pre-neoplastic diseases, multiple myeloma, and monoclonal gammopathy. *Cancer Genet Cytogenet* 162: 78-81.

Ai H., Barrera J.E., Meyers A.D., Shroyer K.R., and M. Varella-Garcia. 2001. Chromosomal aneuploidy precedes morphological changes and supports multifocality in head and neck lesions. *Laryngoscope* 111: 1853-1858.

Akiyoshi B., Nelson C.R., Ranish J.A., and S. Biggins. 2009. Analysis of Ipl1-mediated phosphorylation of the Ndc80 kinetochore protein in *Saccharomyces cerevisiae*. *Genet* 183: 1591-1595.

Akiyoshi B., Sarangapani K., Powers A.F., Nelson C.R., Reichow S.L., Arellano-Santoyo H., Gonen T., Ranish J.A., Asbury C.L. and S. Biggins. 2010. Tension directly stabilizes reconstituted kinetochore-microtubule attachments. *Nature* 468: 576-579.

Asbury C.L., Gestaut D.R., Powers A.F., Franck A.D., and T.N. Davis. 2006. The Dam1 kinetochore complex harnesses microtubule dynamics to produce force and movement. *Proc Natl Acad Sci USA* 103: 9873-9878.

Baumann C., Kömer R., Hofmann K., and E.A. Nigg. 2007. PICH, a Centromere-Associated SNF2 Family ATPase, Is Regulated by Plk1 and Required for the Spindle Checkpoint. *Cell* 128: 101-114.

Bastiaens P. M. Caudron, P. Niethammer, E. Karsenti. 2006. Gradients in the self-organization of the mitotic spindle. *Trends Cell Biol* 16: 125-134.

Bazett-Jones D.P. and F.P. Ottensmeyer. 1981. Phosphorous distrubution in the nucleosome. *Science* 211: 169-170.

Bazett-Jones D.P., Locklear L. and J.B. Rattner. 1988. Electron spectroscopic imaging of DNA. *J Ultrastruct Mol Struct Res* 99: 48-58.

Biggins B., Severin F.F., Bhalla N., Sassoon I., Hyman A. and A.W. Murray. 1999. The conserved protein kinase Ipl1 regulates microtubule binding to kinetochore in budding yeast. *Gene Dev* 13: 532-544.

Biggins S. and A.W. Murray. 2001. The budding yeast protein kinase Ipl1/Aurora allows the absence of tension to activate the spindle checkpoint. *Genes Dev.* 15: 3118-29.

Bloom K.S. and J. Carbon. 1982. Yeast centromere DNA is in a unique and highly ordered structure in chromosomes and small circular minichromosomes. *Cell* 29: 305-317.

Bouck D.C. and K. Bloom. 2007. Pericentric chromatin is an elastic component of the mitotic spindle. *Curr Biol* 17: 741-748.

Brust-Mascher I., Sommi P., Cheerambathur D.K., and J.M. Scholey. 2009. Kinesin-5-dependent poleward flux and spindle length control in *Drosophila* embryo mitosis. *Mol Biol Cell* 20: 1749-1762.

Burrack L.S., Applen S.E., and J. Berman. 2011. The requirement for the Dam1 complex is dependent upon the number of kinetochore proteins and microtubules. *Curr Biol* 21: 889-896.

Buvelot S., Tatsutani S.Y., Vermaak D., and S. Biggins. 2003. The budding yeast Ipl1/Aurora protein kinase regulates mitotic spindle disassembly. *J Cell Biol* 160: 329-339.

Cai S., Weaver L.N., Ems-ChClung S.C., and C.D. Walczak. 2009. Kinesin-14 family proteins HSET/XCTK2 control spindle length by cross-linking and sliding microtubules. *Mol Biol Cell* 20: 1348-1359.

Carazo-Salas R.E., Guarguaglini G., Gruss O.J., Segreg A., Karsenti E. and I.W. Mattaj. 1999. Generation of GTP-bound Ran by RCC1 is required for chromatin-induced mitotic spindle formation. *Nature* 400: 178-181.

Carazo-Salas R.E., Gruss O.J., Mattaj I.W. and E. Karsenti. 2001. Ran-GTP coordinates regulation of microtubule nucleation and dynamics during mitotic-spindle assembly. *Nat Cell Biol* 3: 228-234.

Caudron M., G. Bunt, P. Bastiaens, E. Karsenti.. 2005. Spatial coordination of spindle asssembly by chromosome-mediated signaling gradients. *Science* 309: 1373-1376.

Chan C.S. and D. Botstein. 1993. Isolation and characterization of chromosome-gain and increase-in-ploidy mutants in yeast. *Genetics*, 135: 677-91.

Cheeseman I.M. Enquist-Newman T., Müller-Reichert, Drubin D.G. and G.Barnes. 2001. Mitotic spindle integrity and kinetochore function linked by the Duo1p/Dam1p complex. *J Cell Biol* 152: 197-212.

Cheeseman I.M., Anderson S., Jwa M., Green E.M., Kang J.S., Yates J.R. III, Chan C.S., Drubin D.G. and G. Barnes. 2002. Phospho-regulation of kinetochore-microtubule attachments by the Aurora kinase Ipl1p. *Cell* 111: 163-172.

Cheeseman I.M., Niessen S., Anderson S., Hyndman F. and J.R. Yates. 2004. A conserved protein network controls assembly of the outer kinetochore's ability to sustain tension. *Genes Dev* 18: 2255-2268.

Cheeseman I.M., Chappie J.S., Wilson-Kubalek E.M., and A. Desai. 2006. The conserved KMN network constitutes the core microtubule-binding site of the kinetochore. *Cell* 127: 983-997.

Chen R.H., Waters J.C., Salmon E.D. and A.W. Murray. 1996. Association of spindle assembly checkpoint component XMAD2 with unattached kinetochores. *Science* 274: 242-246.

Chen R.H., Shevchenko A., Mann M., and A.W. Murray. 1998. Spindle checkpoint protein Xmad1 recruits Mad2 to unattached kinetochores. *J Cell Biol* 143: 283-295.

Chung E., and R.H. Chen. 2002. Spindle checkpoint requires Mad1-bound and Mad1-free Mad2. *Mol Bio Cell* 13: 1501-1511.

Ciferri, C., Pasqualato S., Screpanti E., Varetti G., Santaguida S., Dos Reis G., Maiolica A., Polka J., De Luca J.G., De Wulf P., Salek M., Rappsilber J., Moores C.A., Salmon E.D., and A. Musacchio. 2008. Implications for kinetochore-microtubule attachment from the structure of an engineered Ndc80 complex. *Cell* 133: 427-439.

Ciosk R., Zachariae W., Michaelis C., Shevchenko A., Mann M., and K. Nasmyth. 1998. An ESP1/PDS1 complex regulates loss of sister chromatid cohesion at the metaphase to anaphase transition in yeast. *Cell* 93: 1067-1076.

Ciosk R., Shirayama M., Shevchenko A., Tanaka T., Toth A., Shevchenko A., and K. Nasmyth. 2000. Cohesin's binding to chromosomes depends on a separate complex consisting of Scc2 and Scc4 proteins. *Mol Cell* 5: 243-254.

Civelekoglu-Scholey G., L. Tao, R. Wollman, I. Brust-Mascher, P. Sommi, A. Mogilner, J.M. Scholey. 2010. Prometaphase spindle maintenance by an antagonistic motor-dependent force-balance made robust by a disassembling lamin B envelope. *J Cell Biol* 188: 49-68.

Clark L. and J. Carbon. 1980. Isolation of yeast centromere and construction of functional circular chromosomes. *Nature* 287: 504-509.

Cohen-Fix O., Peters J.M., Kirschner M.W., and D. Koshland. 1996. Anaphase initiation in *Saccharomyces cerevisiae* is controlled by the APC-dependent degradation of the anaphase inhibitor Pds1p. *Genes Dev* 10: 3081-3093.

Cohen-Fix O. and D. Koshland. 1997. The anaphase inhibitor of *Saccharomyces cerevisiae* Pds1p is a target of the DNA damage checkpoint pathway. *Proc Natl Acad Sci USA* 94: 14361-14366.

Collins K.A., Castillo A.R., Tatsutani S.Y. and S. Biggins. 2005. De novo kinetochore assembly requires the centromeric histone H3 variant. *Mol Biol Cell* 16: 5649-5660.

De Antoni A., Pearson C.G., Cimini D., Canman J.C., Sala V., Nezi L., Mapelli M., Sironi L., Faretta M., Salmon E.D. and A. Musacchio. 2005. The Mad1/Mad2 complex as a template for Mad2 activation in the spindle assembly checkpoint. *Curr Biol* 15: 214-225.

Decker M., Jaensch S., Pozniakovsky A., Zinke A., O'Connell K.F., Zachariae W., Myers E., and A.A. Hyman. 2011. Limiting amounts of centrosome material set centromere size in *C.elegans* embryos. *Curr Biol*. 21: 1259-1267.

DeLuca J.G., Gall W.E., Ciferri C., Cimini D., Musacchio A., and E.D. Salmon. 2006. Kinetochore microtubule dynamics and attachment stability are regulated by Hec1. *Cell* 127: 969-982.

DeSouza C.P.C and S.A. Osmani. 2007. Mitosis, not just open or closed. *Eukaryot Cell* 6: 1521-1527.

DeWulf P., McAinsh A.D. and P.K. Sorger. 2003. Hierarchial assembly of the budding yeast kinetochore from multiple subcomplexes. *Genes Dev* 17: 2901-2921.

Doak S.H., Jenkins G.J., Parry E.M., Griffiths A.P., Baxter J.N., and J.M. Parry. 2004. Differential expression of the MAD2, BUB1, and HSP27 genes in Barrett's oesophagus-their association with aneuploidy and neoplastic progression. *Mutat Res* 547: 133-144.

Dooley T.P., Mattern V.L., Moore C.M., Porter P.A., Robinson E.S., and J.L. VandeBerg. 1993. Cell lines derived from ultraviolet radiation-induced benign melanocytic nevi in Monodelphis domestica. *Cancer Genet Cytogenet* 71: 55-66.

Driscoll D.A. and S.G. Gross. 2009. Prenatal screening for aneuploidy. *N Eng J Med* 360: 2556-2562.

Duensing S. and K. Munger. 2004. Mechanisms of genomic instability in human cancer: insights from studies with human papillomavirus oncoproteins. *Int J Cancer* 109: 157-162.

Dumont S. and T.J. Mitchison. 2009. Force and length in the mitotic spindle. *Curr Biol* 19: R749-R761.

Espelin C.W., Kaplan K.B. and P.K. Sorger. 1997. Probing the architecture of a simple kinetochore using DNA-protein crosslinking. *J Cell Biol* 139: 1383-1396.

Espelin C.W. Simons K.T., Harrison S.C. and P.K. Sorger. 2003. Binding of the essential *Saccharomyces cerevisiae* kinetochore protein Ndc10p to CDEII. *Mol Biol Cell* 14: 4557-4568.

Foe V.S. and G. von Dassow. 2008. Stable and dynamic microtubules coordinately shape the myosin activation zone during cytokinetic furrow formation. *J Cell Biol*183: 457-470.

Fonatsch, C. 2010. Role of Chromosome 21 in Hematology and Oncology. *Genes Chromosomes Cancer* 49: 497-508.

Gardner M.K. and D.J. Odde. 2006. Modeling of chromosome motility during mitosis. *Curr Opin Cell Biol* 18: 639-647.

Gardner M.K., Bouck D.C., Paliulis L.V., Meehl J.B., O'Toole E.T. Haase J., Soubry A, Joglekar A.P., Winey M., Salmon E.D., Bloom K., and D.J. Odde. 2008. Chromosome congression by kinesin-5-motor-mediated disassembly of longer kinetochore microtubules. *Cell* 125: 894-906.

Gatlin J.C., Matov A., Danuser G., Mitchison T.J. and E.D. Salmon. 2010. Directly probing the mechanical properties of the spindle and its matrix. *J Cell Biol* 188: 481-489.

Ghosh S.K., Poddar A., Hajra S., Sanyal K., and P. Sinha. 2001. The IML3/MCM19 gene of *Saccharomyces cerevisiae* is required for a kinetochore-related process during chromosome segregation. *Mol Genet Genomics* 265: 249-257.

Goh P.Y. and J.V. Kilmartin. 1993. NDC10: a gene involved in chromosome segregation in *Saccharomyces cerevisiae*. *J Cell Biol* 121: 503-512.

Gonen S., Akiyoshi B., Iadanza M.G., Shi D., Duggan N., Biggins S. and T. Gonen. 2012. The structure of purified kinetochores reveals multiple microtubule attachment sites. *Nat Struct Mol Biol* 19: 925-929.

Goshima G., Saitoh S. and M. Yanagida. 1999. Proper metaphase spindle length is determined by centromere proteins Mis12 and Mis6 required for faithful chromosome segregation. *Genes Dev* 13: 1664-1677.

Goshima G and M Yanagida. 2000. Establishing biorientation occurs with precocious separation of the sister kinetochores, but not the arms, in the early spindle of budding yeast. *Cell*, 100: 619-33.

Goshima G., Wollman R., Stuurman N., Scholey J.M. and R.D.Vale. 2005. Length control of the metaphase spindle length. *Curr Biol* 15: 1979-1988.

Goshima G. and J. Scholey. 2010. Control of mitotic spindle length. *Annu Rev Cell Dev Biol* 26: 21-57.

Greenan G. C.P. Brangwynne, S. Jaensch, J. Gharakhani, F. Julicher, A.A. Hyman. 2010. Centrosome size sets mitotic spindle length in *Caenorhabditis elegans* embryos. *Curr Biol* 20: 353-358.

Guacci V., Koshland D., and A. Strunnikov. 1997. A direct link between sister chromatid cohesion and chromosome condensation revealed through the analysis of *MCD1* in *S.cerevisiae*. *Cell* 91: 47-57.

Haering C.H., Farcas A.M., Arumugam P., Metson J., and K. Nasmyth. 2008. The cohesin ring concatenates sister DNA molecules. *Nature* 454: 297-301.

Halpin D., Kalab P., Wang J., Weis K., and R. Heald. 2011. Mitotic spindle assembly around RCC1-coated beads in *Xenopus* egg extracts. *PLoS Biol* 9: e1001225.

Hannak E., Kirkham M., Hyman A.A. and K. Oegema. 2001. Aurora-A kinase is required for centrosome maturation in *Caenorhabditis elegans*. *J Cell Biol* 155: 1109-1116.

Hardwick K.G., Weiss E., Luca F.C., Winey M. and A.W. Murray. 1996. Activation of the budding yeast spindle assembly checkpoint without mitotic spindle disruption. *Science* 16: 953-956.

Hasle H., Clemmensen I.H., and M. Mikkelsen. 2000. Risks of leukemia and solid tumours in individuals with Down's syndrome. *Lancet* 355: 165-169.

Hassold T., Hall H., and P. Hunt. 2007. The origin of human aneuploidy: where we have been, where we are going?. *Hum Mol Genet*. 15: R203-8.

He X, Asthana S and PK Sorger. 2000. Transient sister chromatid separation and elastic deformation of chromosomes during mitosis in budding yeast. *Cell*, 101: 763-775.

Heald R., Tournebize R., Blank T., Sandaltzopoulos R., Becker P., Hyman A.A. and E., Karsenti. 1996. Self-organization of microtubules into bipolar spindles around artificial chromosomes in *Xenopus* egg extracts. *Nature* 382: 420-425.

Hershko A. 1999. Mechanisms and regulation of the degradation of cyclin B. *Philos Trans R Soc Lond B Biol Sci* 29: 1571-1576.

Howell B.J., Hoffman D.B., Fang G., Murray A.W. and E.D. Salmon. 2000. Visualization of Mad2 dynamics at kinetochores, along spindle fibers, and at spindle poles in living cells. *J Cell Biol* 150: 1233-1250.

Howell B.J., Moree B., Farrar E.M., Stewart S., Fang G., and E.D. Salmon. 2004. Spindle checkpoint protein dynamics at kinetochores in living cells. *Curr Biol* 14: 953-964.

Huh W.-K., Falvo J.V., Gerke L.C., Carroll A.S., Howson R.W., Weissam J.S. and E.K. O'Shea. 2003. Global analysis of protein localization in budding yeast. *Nature* 425: 686-691.

Hwang L.H., Lau L.F., Smith D.L., Mistrot C.A., Hardwick K.G., Hwang E.S., Amon A. and A.W. Murray. 1998. Budding yeast Cdc20: a target of the spindle checkpoint. *Science* 279: 1041-1044.

Inoué S. and E.D. Salmon. 1995. Force generation by microtubule assembly/disassembly in mitosis and related movements. *Mol Biol Cell* 6: 1619-1640.

Jiang W., Lechner J. and J. Carbon. 1993. Isolation and characterization of a gene (CBF2) specifying a protein component of the budding yeast kinetochore. *J Cell Biol* 121: 513-519.

Johansen, K.M., A. Forger, C. Yao, J. Girton, J. Johansen. 2011. Do nuclear envelope and intranuclear proteins reorganize during mitosis to form an elastic, hydrogel-like spindle matrix? *Chromosome Res*. 19: 345-365.

Kalab P. and R. Heald. 2008. The RanGTP gradient- a GPS for the mitotic spindle. *J Cell Sci* 121: 1577-1586.

Kane R.E. and A. Forer. 1965. The mitotic apparatus. Structural changes after isolation. *J Cell Biol* 25: 31-39.

Kang J., Cheeseman I.M., Kallstrom G., Velmurugan S., Barnes G. and C.S.M. Chan. 2001. Functional cooperation of Dam1, Ipl1, and the inner centromere protein (INCENP)-related protein Sli15 during chromosome segregation. *J Cell Biol* 155: 763-774.

Katsura I. 1987. Determination of bacteriophage lambda tail length by a protein ruler. *Nature* 327: 73-75.

Katsura I. 1990. Mechanism of length determination in bacteriophage lambda tails. *Adv Biophys* 26: 1-18.

Kiermaier E., Woehrer S., Peng Y., Mechtler K. and S. Westermann. 2009. A Dam1-based artificial kinetochore is sufficient to promote chromosome segregation in budding yeast. *Nat Cell Biol* 11: 1109-1115.

Kim J.H., Kang J.S. and C.S.M. Chan. 1999. Sli15 associates with the Ipl1 protein kinase to promote proper chromosome segregation in *Saccharomycs cerevisiae*. *J Cell Biol* 145: 1381-1394.

King E.M.J, Rachidi N., Morrice N., Hardwick K.G., and M.J.R. Stark. 2007. Ipl1p-dependent phosphorylation of Mad3p is required for the spindle checkpoint response to lack of tension at kinetochores. *Genes Dev* 21: 1163-1168.

Kline S.L., Cheeseman I.M., Hori T., Fukagawa T., and A. Desai. 2006. The human Mis12 complex is required for kinetochore assembly and proper chromosome segregation. *J Cell Biol* 173: 9-17.

Kramer J. and R.S. Hawley. 2003. The spindle-associated transmembrane protein Axs identifies a membranous structure ensheathing the meiotic spindle. *Nat Cell Biol* 5: 261-263.

Laan L., Husson J., Munteanu E.L., Kerssemakers J.W.J. and M. Dogterom. 2008. Force-generation and dynamic instability of microtubule bundles. *Proc Natl Acad Sci USA* 105: 8920-8925.

Lacefield S., Lau D.T.C. and A.W. Murray. 2009. Recruiting a microtubule-binding complex to DNA directs chromosome segregation in budding yeast. *Nat Cell Biol* 11: 1116-1120.

Lampson M.A. and I.M. Cheeseman. (2011). Sensing centromere tension: Aurora B and the regulation of kinetochore function. *Trends Cell Biol* 21: 133-140.

Lengronne A., Katou Y., Saori M., Yokobayashi S., Kelly G.P., Itoh T., Watanabe Y., Shirahige K, and F. Ulhmann. 2004. Cohesin relocates from sites of chromosomal loading to places of convergent transcription. *Nature* 430: 573-78.

Lengronne A., McIntyre J., Katou Y., Kanoh Y., Hopfner K.P., Shiraghige K., and F. Uhlmann. 2006. Establishment of sister chromatid cohesion at the *S.cerevisiae* replication fork. *Mol Cell* 23: 787-799.

Li R. and A.W. Murray. 1991. Feedback control of mitosis in budding yeast. *Cell* 66: 519-531.

Li X. and R.B. Nicklas. 1995. Mitotic forces control a cell-cycle checkpoint. *Nature* 16: 630-632.

Li X. and R.B. Nicklas. 1997. Tension-sensitive kinetochore phosphorylation and the chromosome distribution checkpoint in praying mantid spermatyocytes. *J Cell Sci* 110: 537-545.

Liu D., Vader G., Vromans M.J., Lampson M.A. and S.M. Lens. 2009. Sensing chromsome bi-orientation by spatial separation of aurora B kinase from kinetochore substrates. *Science* 323: 1350-1353.

Liu Z. and Y. Zheng. 2009. A requirement for epsin in mitotic membrane and spindle organization. *J Cell Biol* 186: 473-480.

Loughlin R., Wilbur J.D., McNally F.J., Nédélec, and R. Heald. 2011. Katanin contributes to interspecies spindle length scaling in *Xenopus*. *Cell* 147: 1397-1407.

Luo X., Tang Z., Rizo J. and H. Yu. 2002. The Mad2 spindle checkpoint rptein undergoes similar major conformational changes upon binding to either Mad1 or Cdc20. *Mol Cell* 9: 59-71.

Kramer J. and R.S. Hawley. 2003. The spindle-associated transmembrane protein Axs identifies a membranous structure ensheathing the meiotic spindle. *Nat Cell Biol* 5: 261-263.

Mahadevan L. and T.J. Mitchison. 2005. Cell biology: powerful curves. *Nature* 435: 895-897.

Makrantoni V. and M.J.R. Stark. 2009. Efficient chromosome biorientation and the tension checkpoint in *Saccharomycs cerevisiae* both require Bir1. *Mol Cell Biol* 29: 455-4562.

Maresa T.J. and E.D. Salmon. 2009. Intrakinetochore stretch is associated with changes in kinetochore phosphorylation and spindle assembly checkpoint activity. *J Cell Biol* 184: 373-381.

Markus S.M., Kalutkiewicz K.A., and W. Lee. 2012. Astral microtubule asymmetry provides directional cues for spindle positioning in budding yeast. *Exp Cell Res* 318: 1400-1406.

Marshall W.F. 2004. Cellular length control systems. *Annu Rev Cell Dev Biol* 20: 677-693.

Marston A.L. and A. Amon. 2004. Meiosis: cell-cycle control shuffle and deal. *Nat Rev Mol Cell Biol* 5: 983-997.

Matson D.R., Demirel P.B., Stukenberg P.T., and D.J. Burke. 2012. A conserved role for COMA/CENP-H/I/N kinetochore proteins in the spindle checkpoint. *Genes Dev*. 26: 542-547.

Matsuura S., Matsumoto Y., Morishima K., Izumi H., Matsumoto H., Ito E., Tsutsui K., Kobayashi J., Tauchi H., Kajiwara Y., Hama S., Kurisu K., Tahara H., Oshimura M., Komatsu K., Ikeuchi T., and T Kajii. Monoallelic BUB1B mutations and defective mitotic-spindle checkpoint in seven families with premature chromatid separation (PCS) syndrome. *Am J Med Genet A* 140: 358-67.

McEwen B.F. and Y. Dong. 2010. Contrasting models for kinetochore microtubule attachment in mammalian cells. *Cell Mol Life Sci* 67: 2163-2172.

McIntosh J.R, O'Toole E., Zhudenkov K., Morphew M., Schwartz C., Ataullakhanov F.I., and E.L. Grishchuk. 2013. Conserved and divergent features of kinetochores and spindle microtubules ends from five species. *J Cell Biol* 200: 459-474.

Medina D. 2002. Biological and molecular characteristics of the premalignant mouse mammary gland. *Bichim Biophys Acta* 1603: 1-9.

Mehta G.D., Agarwal M.P. and S.K. Ghosh. 2010. Centromere identity: a challenge to be faced. *Mol Genet Genomics* 284: 75-94.

Meraldi P., McAnish A.D., Rheinbay E. and P.K. Sorger. 2006. Phylogenetic and structural analysis of centromeric DNA and kinetochore proteins. *Genome Biol* 7: R23.

Miranda J.J., De Wulf P., Sorger P.K. and S.C. Harrison. 2005. The yeast DASH complex forms closed rings on microtubules. *Nat Struct Mol Biol* 12: 138-143.

Morrow C.J., Tighe A., Johnson V.L., Scott M.I., Ditchfield C. and S.S. Taylor. 2005. Bub1 and aurora B cooperate to maintain BubR1-mediated inhibition of APC/C-Cdc20. *J Cell Sci* 118: 3639-3652.

Musacchio A. and E.D. Salmon. 2007. The spindle-assembly checkpoint in space and time. *Nat Rev* 8: 379-393.

Müller-Reichert T., Sassoon I., O'Toole E., Romao M., Ashford A.J., Hyman A.A. and C. Antony. 2003. Analysis of the distribution of the kinetochore protein Ndc10p in *Saccharomyces cerevisiae* using 3-D modeling of mitotic spindles. *Chromosoma* 111: 417-428.

Mythreye K. and K.S. Bloom. 2003. Differential kinetochore protein requirements for establishment versus propagation of centromere activity in *Saccharomyces cerevisiae*. 160: 833-843.

Nabeshima K., Nakagawa T., Straight A.F., Murray A.W., Chikashige Y., Yamashita Y.M., Hiraoka Y., and M. Yanagida. 1998. Dynamics of centromeres during metaphase-anaphase transition in fission yeast: Dis1 is implicated in force balance in metaphase bipolar spindle. *Mol Biol Cell* 9: 3211-3225.

Nakajima Y., Tyers R.G., Wong C.C., Yates J.R. III, Drubin D.G. and G. Barnes. 2009. Nbl1p: a Borealin/Dasra/CSC-1-like protein essential for Aurora/Ipl1 complex function and integrity in *Saccharomyces cerevisiae*. *Mol Biol Cell* 20: 1772-1784.

Nannas N.J. and A.W. Murray. 2012. Complications dawn for kinetochore regulation by Aurora. *Proc Natl Acad Sci USA* 109: 15972-15973.

Nasmyth K. 2005. How might cohesin hold sister chromatids together? *Phil Trans R Soc B* 360: 483-496.

Nekrasov V.S., Smith M.A., Peak-Chew S. and J.V. Kilmartin. 2003. Interactions between centromere complexes in *Saccharomyces cerevisiae*. *Mol Biol Cell* 14: 4931-4946.

Nicklas R.B. 1983. Measurements of the force produced by the mitotic spindle in anaphase. *J Cell Biol* 97: 542-548.

Okada M, Chesseman I.M., Hori T., Okawa K., McLeod I.X. Yates III J.R., Desai A., and T. Fukagawa. 2006. The CENP-H-I complex is required for the efficient incorporation of newly synthesized CENP-A into centromeres. *Nat Cell Biol* 8: 446-457.

Ortiz J., Stemmann O., Rank S., and J. Lechner. 1999. A putative protein complex consisting of Ctf19, Mcm21, and Okp1 represents a missing link in the budding yeast kinetochore. *Genes Dev* 13: 1140-1155.

O'Toole E. and M. Winey. 2001. The spindle cycle in budding yeast. *Nat Cell Biol* 3: E23-27.

Özlü N., Srayko M., Kinoshita K., Habermann B., O'Toole E., Müller-Reichert T., Schmalz N., Desai A., and A.A. Human. 2005. An essential function of the *C.elegans* ortholog of TPX2 is to localize activated Aurora A kinase to mitotic spindles. *Dev Cell* 9: 237-248.

Pinsky, B.A., Tatsutani S.Y., Collins K.A. and S. Biggins. 2003. An Mtw1 complex promotes kinetochore biorientation that is monitored by the Ipl1/Aurora protein kinase. *Dev Cell* 5: 735-745.

Pinsky B.A. and S. Biggins. 2005. The spindle checkpoint: tension versus attachment. *Trends Cell Biol* 15: 486-493.

Pinsky, B.A., Kung C., Shokat K.M., and S. Biggins. 2006. The Ipl1-Aurora kinase activates the spindle checkpoint by creating unattached kinetochores. *Nat Cell Biol* 8: 78-83.

Qi H, Rath U., Wang D., Xu Y.Z., Ding Y., Zhang W., Blacketer M.J., Paddy M.R., Girton J., Johansen J. and K.M. Johansen. 2004. Megator, an essential coiled-coil protein that localizes to the putative spindle matrix during mitosis in *Drosophila*. *Mol Biol Cell* 15: 4854-4865.

Qi H., Rath U., Ding Y., Ji Y., Blacketer M.J., Girton J., Johansen J. and K.M. Johansen. 2005. EAST interacts with Megator and localizes to the putative spindle matrix during mitosis in *Drosophila*. *J Cell Biochem* 95: 1284-1291.

Rath U., Wang D., Ding Y., Xu Y.Z., Qi H., Blacketer M.J., Girton J., Johansen J. and K.M. Johansen. 2004. Chromator, a novel and essential chromodomain protein interacts directlly with the putative spindle matrix protein skeletor. *J Cell Biochem* 15: 1033-1047.

Rebhun L.I. and R.E. Palazzo. 1988. In vitro reactivation of anaphase B in isolated spindles of sea urchin egg. *Cell Motil Cytoskel* 10: 197-209.

Ried T., Heselmeyer-Haddad K., Blegen H., Schrock E., and G. Auer. 1999. Genomic changes defining the genesis, progression and malignancy potential in solid human tumors: a phenotype/genotype correlation. *Genes Chromos Cancer* 25: 195-204.

Rieder C.L. 1977. *An in-vitro light and electron microscopy study of anaphase chromosome movements in normal and temperature elecated Taricha lung cells*. Ph.D. thesis. Univ. Oregon, Eugene, 294pp.

Ruchaud S., Carmena M., and W.C. Earnshaw. 2007. Chromosomal passengers: conducting cell division. *Nat Rev Mol Cell Biol* 8: 798-812.

Rupeš, I. 2002. Checking cell size in yeast. *Trends Genet* 18: 479-485.

Sanchez-Perez I., Renwick S.J., Crawley K., Karig I., Buck V., Meadows J.C., Franco-Sanchez A., Fleig U., Toda T., and J.B. Millar. 2005. The DASH complex and Klp5/Klp6 kinesin coordinate bipolar chromosome attachment in fission yeast. *EMBO J* 24: 2931-2943.

Sandall S., Severin F., McLeod I.X., Yates J.R. III, Oegema K., Hyman A. and A. Desai. 2006. A complex of Bir1-Sli15 (Survivin-INCENP) connects centromeres to microtubules and is the likely tension sensor controlling Aurora B activation. *Cell* 127: 1179-1191.

Satgé D., Sasco A.J., and B. Lacour. 2003. Are solid tumors different in children with Down's syndrome? *Int J Cancer* 106: 297-98.

Saunders W.S. and M.A. Hoyt. 1992. Kinesin-related proteins required for structural integrity of the mitotic spindle. *Cell* 70: 451-458.

Saunders W.S., Lengyel V. and M.A. Hoyt. Mitotic spindle function in *Saccharomyces cerevisiae* requires a balance between different types of kinesin-related motors. *Mol Biol Cell* 8: 1025-1033.

Schiff P., Fant J., and S.B. Horowitz. 1979. Promotion of microtubule assembly *in vitro* by taxol. *Nature* 277: 665-667.

Shimogawa M.M., Widlund P.O., Riffle M., Ess M., and T.N. Davis. 2009. Bir1 is required for the tension checkpoint. *Mol Biol Cell* 20: 915-923.

Siegel J.J. and A. Amon. 2012. New insights into the troubles of aneuploidy. *Annu Rev Cell Dev Biol* 28: 189-214.

Stephens A.D., Haase J., Vicci L., Taylor R.M. II., and K. Bloom. 2011. Cohesin, condensin, and the intramolecular centromere loop together generate the mitotic chromatin spring. *J Cell Biol* 193: 1167-1180.

Stephens A.D., Haggerty R.A., Vasqueez P.A., Vicci L., Snider C.E., Shih F., Quammen C., Mullins C., Haase J., Taylor II R.M., Veraasdonk J.S., Falvo M.R., Jin Y., Forest M.G. and K. Bloom. 2013. Pericentric chromatin loops function as a nonliner spring in mitotic force balance. 200: epub ahead of print.

Stern B. and A.W. Murray. 2001. Lack of tension at kinetochores activates the spindle checkpoint in budding yeast. *Curr Biol* 11: 1462-1467.

Straight A.F., Marshall W.F., Sedat J.W. and A.W. Murray. 1997. Mitosis in living budding yeast: anaphase A but no metaphase plate. *Science* 277: 574-578.

Straight A.F., Sedat J.W., and A.W. Murray 1998. Time-lapse microscopy reveals unique roles for kinesins during anaphase in budding yeast. *J Cell Biol* 143: 687-694.

Ström A.C. and K. Weis. 2001. Importin-beta-like nuclear transport receptors. *Genome Biol* 2: 3008.1-3008.9

Strunnikov A.V., Kingsbury J., and D. Koshland. 1995. CEP3 encodes a centromere protein of *Saccharomyces cerevisiae*. *J Cell Biol* 128: 740-760.

Sudakin V., Chan G.K., and T.J. Yen. 2001. Checkpoint inhibition of the APC/C in HeLa cells is mediated by a complex of BUBR1, BUB3, CDC20, and MAD2. *J Cell Biol* 154: 925-936.

Tanaka T., Rachidi N., Janke C., Pereira G., Galova M., Schiebel E., Stark M.J.R., and K. Nasmyth. 2002. Evidence that the Ipl1-Sli15 (Aurora Kinase-INCENP) complex promotes chromosome bi-orientation by altering kinetochore-spindle pole connections. *Cell* 108: 317-329.

Tanaka K., Kitamura E., Kitamura Y., and T.Tanaka. 2007. Molecular mechanisms of microtubule-dependent kinetochore transport toward spindle poles. *J Cell Biol* 178: 269-281.

Tanaka T. 2008. Bi-orienting chromosomes: acrobatics on the mitotic spindle. *Chromosoma* 117: 521-533.

Taylor E.W. 1959. Dynamics of spindle formation and its inhibition by chemicals. *J Biophys Biochem Cytol* 6:193-196.

Tsai, M.Y., S. Wang, J.M. Heidinger, D.K. Shumaker, S.A. Adam, R.D. Goldman, Y. Zheng. 2006. A Mitotic Lamin B Matrix Induced by RanGTP Required for Spindle Assembly. *Science* 311: 1887-1893.

Uchida K.S.K., Takagaki K., Kumada K., Hirayama Y., Noda T. and T. Hirota. 2009. Kinetochore stretching inactivates the spindle assembly checkpoint. *J Cell Biol* 184: 383-390.

Uhlmann F., Lottspeich F. and K. Nasmyth. 1999. Sister-chromatid separation at anaphase onset is promoted by cleavage of the cohesin subunit Scc1. *Nature* 400: 37-42.

Uhlmann F., Wernic D., Poupart M.A., Koonin E.V., and K. Nasmyth. 2000. Cleavage of cohesin by the CD clan protease separin triggers anaphase in yeast. *Cell* 103: 375-386.

Umbreit N.T., Gestaut D.R., Tien J.F., Vollmar B.S., Gonen T., Asbury C.L. and T.N. Davis. 2012. The Ndc80 kinetochore complex directly modulates microtubule dynamics. *Proc Natl Acad Sci USA* 109: 16113-16118.

Wang H.W., Long S., Ciferri C., Westermann S., Drubin D., Barnes G., and E. Nogales. 2008. Architecture and flexibility of the yeast Ndc80 kinetochore complex. *J Mol Biol* 383: 894-903.

Wang L .H., Schwarzbraun T., Speicher M.R., and E.A. Nigg. 2008. Persistence of DNA threads in human anaphase cells suggests late completion of sister chromatid decatenation. *Chromosoma* 117: 123-35.

Weaver B.A.A. and D.W. Cleveland. 2006. Does aneuploidy cause cancer? *Curr Opin Cell Biol* 18: 658-667.

Weaver B.A.A., Silk A.D., Montagna C., Verdier-Pinard P., and and D.W. Cleveland. 2007. Aneuploidy acts both oncogenically and as a tumer suppressor. *Cancer Cell* 11: 25-36.

Weber S.A., Gerton J., Polancic J., DeRisi J., Koshland D., and P. Megee. 2004. The kinetochore is an enhancer of pericentric cohesin binding. *PLoS Bio* 2: E260.

Wei R.R., Sorger P.K. and S.C. Harrison. 2005. Molecular organization of the Ndc80 complex, an essential kinetochore component. *Proc Natl Acad Sci USA* 102: 5363-5367.

Wei R.R., Al-Bassam J., and S.C. Harrison. 2007. The Ndc80/HEC1 complex is a contact point for kinetochore-microtubule attachment. *Nat Struct Mol Biol* 14: 54-59.

Weiss E. and M.Winey. 1996. The *Saccharomyces cerevisiae* spindle pole body duplication gene MPS1 is part of a mitotic checkpoint. *J Cell Biol* 132: 111-123.

Welburn J.P.I and I.M. Cheeseman. 2008. Towards a molecular structure of the eukaryotic kinetochore. *Dev Cell* 15: 645-655.

Westermann S., Cheeseman I.M., Anderson S., Yates J.R. III, Drubin D.G. and G.Barnes. 2003. Architecture of the budding yeast kinetochore reveals a conserved molecular core. *J Cell Biol* 163: 215-22.

Westermann S., Avila-Sakar A., Wang H.W., Niederstrasser H., Wong J., Drubin D.G., Nogales E., and G. Barnes. 2005. Formation of a dynamic kinetochore-microtubule interface through assembly of the Dam1 ring complex. *Mol Cell* 17: 277-290.

Westermann. S, Wang H.W., Avila-Sakar A., Drubin D.G., Nogales E., and G. Barnes. 2006. The Dam1 kinetochore ring complex moves processively on depolymerizing microtubule ends. *Nature* 440: 565-569.

Westermann S., Drubin D.G, and G. Barnes. 2007. Structures and functions of the yeast kinetochore complexes. *Annu Rev Biochem* 76: 563-559.

Wigge P.A. and J.V. Kilmartin. 2001.The Ndc80p complex from *Saccharomyces cerevisiae* contains conserved centromere components and has a function in chromosome segregation. *J Cell Biol* 152: 349-360.

Wilbur J.D. and R.Heald. 2013. Mitotic spindle scaling during *Xenopus* develeopment by kif2a and importin α. *Elife*. 2e00290.

Wilde A., Lizarraga S.B., Zhang L., Wiese C., Gliksman N.R., Walczak C.E. and Y. Zheng. 2001. Ran stimulates spindle assembly by altering microtubule dynamics and the balance of motor activities. *Nat Cell Biol* 3: 221-227.

Wilson-Kubalek E., Cheeseman I.M., Yoskioka C., Desai A., and R.A. Milligan. 2008. Orientation and structure of the Ndc80 complex on the microtubule lattice. *J Cell Biol* 182: 1055-1061.

Winey, M. Mamay C.L., O'Toole E.T., Mastronarde D.N. Giddings Jr T.H., McDonald K.L. and J.R. McIntosh. 1995. Three-dimensional ultrastructural analysis of the *Saccharomyces cereivisiae* mitotic spindle. *J Cell Biol* 129: 1601-1615.

Wühr M., Chen Y., Dumont S., Groen A.C., Needleman D.J., Salic A., and T.J. Mitchison. 2008. Evidence for an upper limit to mitotic spindle length. *Curr Biol* 18: 1256-1261.

Yao, C. U. Rath, H. Maiato, D. Sharp, J. Girton, K.M. Johansen and J. Johansen. 2012. A nuclear-derived proteinaceous matrix embeds the microtubules spindle apparatus during mitosis. *Mol Biol Cell*. 18: 3532-3541.

Yu H. 2007. Cdc20: a WD40 activator for a cell cycle degradation machine. *Mol Cell* 27: 3-16.

Zimowska G., Aris J.P, and M.R. Paddy. 1997. A *Drosophila* Tpr homolog is localized both in the extrachromosomal channel network and to the nuclear pore complexes. *J Cell Sci* 110: 927-944.

Chapter Two:

Chromosomal attachments set spindle length and regulate microtubule number in the Saccharomyces cerevisiae mitotic spindle

ABSTRACT

The mitotic spindle is a dynamic structure, which has a characteristic steady-state length that varies between different cell types. One model for spindle length regulation appeals to a balance between two forces. One, due to microtubules that attach to the chromosomes at their kinetochores, would shorten the spindle, while the other, due to interaction between microtubules, would elongate the spindle. This model predicts that altering the number of kinetochores will alter spindle length. We manipulated the number of functional kinetochores in the budding yeast, *Saccharomyces cerevisiae*, and found that spindle length scales with the number of kinetochores. Spindles are longer in cells whose kinetochores have been inactivated by the *ndc10-1* mutant, but the spindle shortens with the addition of synthetic kinetochores. Introducing multiple, extra kinetochores into otherwise normal cells led to spindles shorter than those of wild-type cells. The simplest interpretation of these results is that kinetochore-microtubule interactions generate an inward force that balances forces that would otherwise elongate the spindle. Electron microscopy of cells revealed that two different manipulations of kinetochore number altered the number of spindle microtubules: adding multiple additional kinetochores increases the number of spindle microtubules above normal levels, and adding synthetic kinetochores to cells whose normal kinetochores have been inactivated raises the number of spindle microtubules towards wild type levels.

INTRODUCTION

Cells must make decisions about how large to build their internal structures; without proper size regulation, cellular structures may be unable to fulfill their functions. The mitotic spindle is a cellular structure with a certain length that must be recreated every cell division. It is a dynamic structure comprised of microtubules, motor proteins, and other microtubule-associated proteins organized into a bipolar array whose function is to faithfully segregate chromosomes (Bloom and Joglekar 2010). Microtubules attach to chromosomes through kinetochores, large protein complexes that assemble on the centromeres of chromosomes (Westermann et al. 2006). Chromosomes must correctly attach to the spindle, with sister chromatids attaching to microtubules from opposite poles but held together by cohesin rings, a state called bi-orientation (**Figure 2-1A**). Once all chromosomes are bi-oriented, the spindle checkpoint that monitors and ensures correct attachment is satisfied, allowing cells to progress from metaphase to anaphase; cohesin is cleaved and chromatids are pulled to opposite poles (Tanaka 2008). While there is much variation between species and cell types, from the ~2µm *S.cerevisiae* spindle (Winey et al. 1995; Straight et al. 1997) to the 90µm spindle of a single-cell *Xenopus* embryo (Wühr et al. 2008), the mitotic metaphase spindle of a given cell type has a characteristic steady-state length (Goshima and Scholey 2010).

What sets the length of the mitotic metaphase spindle? Proposed mechanisms can be grouped into three general categories: 1) molecular rulers 2) gradients and 3) balance of opposing forces. Molecular rulers are physical structures or proteins that dictate the length of another structure. For example, the lambda bacteriophage tail is built to a highly specified length determined by the gpH protein (Katsura 1987, 1990). A proposed molecular ruler of spindle length is the spindle matrix, which may provide a physical restraint to spindle elongation,

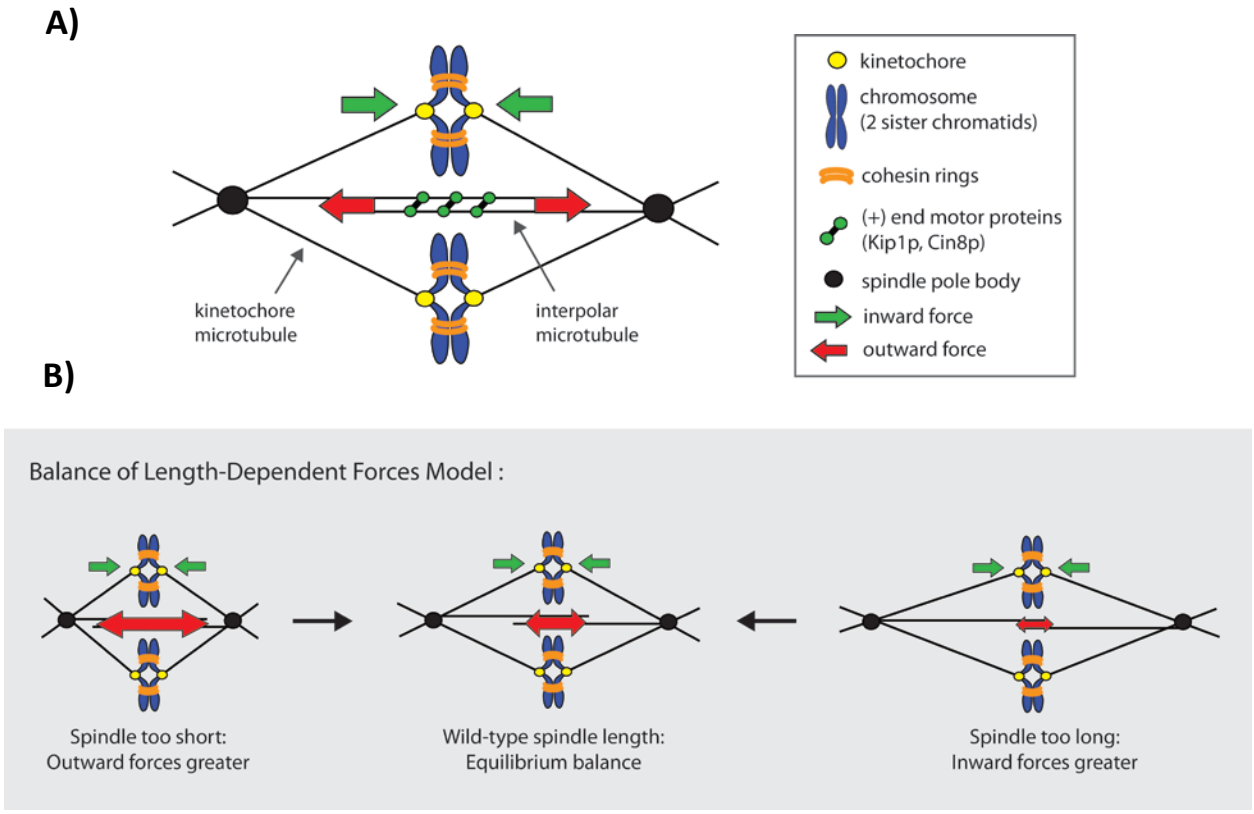

Figure 2-1 (A) *S.cerevisiae* spindle: components and forces. The sister chromatids of a replicated chromosome attach to the spindle via kinetochore, which bind kinetochore microtubules emanating from opposite spindle pole bodies (bi-orientation). Interpolar microtubules reach into the spindle midzone and are bound by motor proteins. While there are many potential sources of force, our investigation focuses the known contribution of outward forces (red arrows) contributed by the kinesin-5 (+) end motor proteins Cin8 and Kip1, and possible contribution of inward force by chromosomal attachments (green arrows). The motor proteins cross-link interpolar microtubules and push spindle pole bodies outward; chromatids that held together by cohesin and attached to the spindle may create an inward resistive force.

(**B**) **Balance of length-dependent forces model:** In order for the spindle to maintain a robust length at an equilibrium balance point, the magnitude of forces must be length-dependent. If the spindle is too short, outward forces are greater than inward forces, and the spindle elongates. As the spindle elongates, the magnitude of outward force decreases. If the spindle becomes too long, inward force is greater than outward force and the spindle shortens back to the equilibrium length.

C)

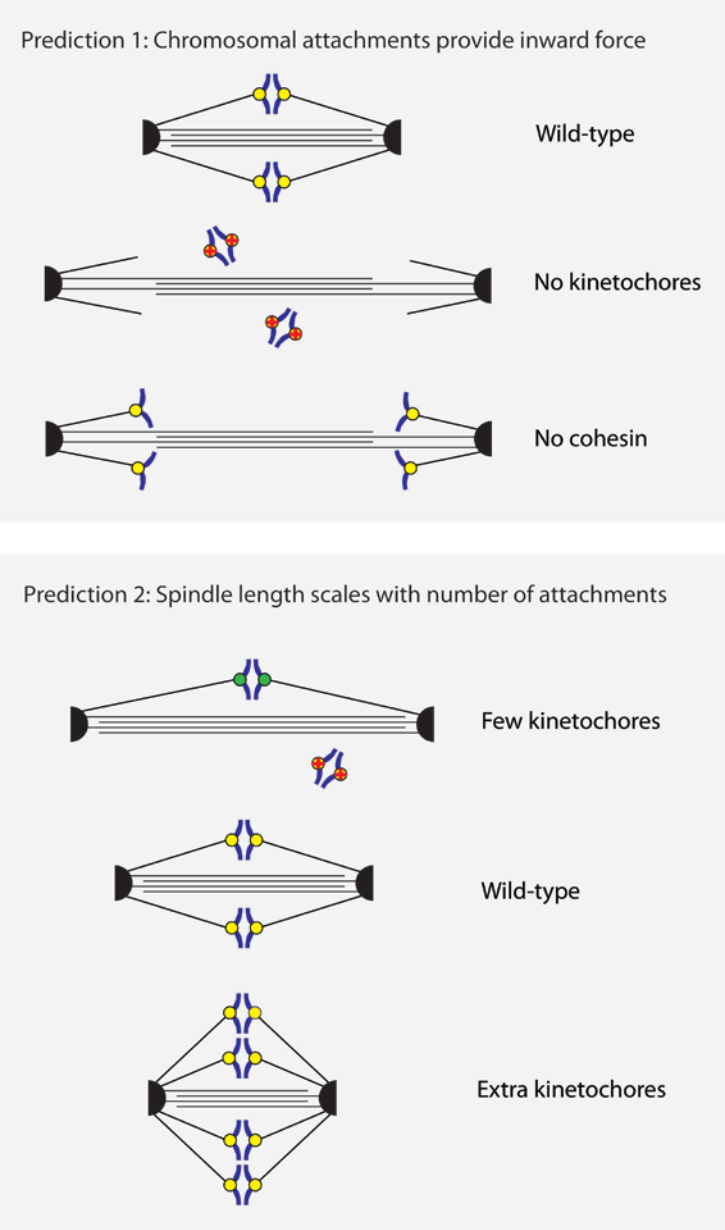

Figure 2-1 (continued) (C) Predictions of force-balance model. The model makes two main predictions: 1) Chromosomal attachment provide an inward resistive force to outward forces. If kinetochores are inhibited (red-crossed dots), the spindle should elongate. Similar elongation should occur if cohesion between sister chromatids is inhibited. 2) Spindle length scales with number of chromosomal attachments. Each attachment contributes inward force and altering the number of attachments will shift the equilibrium spindle length. Limiting attachment to a few kinetochores should elongate the spindle compared to wild-type, and introducing extra kinetochores should cause the spindle to shorten.

however it is unclear what sets the length of the matrix (Johansen et al 2011). When microtubules are depolymerized in *Drosophila* (Yao et al. 2012) and sea urchins (Kane and Forer 1965; Rebhun and Palazzo 1998), a hydrogel matrix of nuclear envelope proteins is left behind. Disruption of matrix components has been shown to alter spindle length in *Drosophila* (Civelekoglu-Scholey 2010, Kramer and Hawley 2003) and spindle organization in *Xenopus* (Ma et al. 2009, Tsai et al. 2006) and in HeLa cells (Liu and Zheng 2009). The second category of models for spindle length regulation is based on gradients; the most studied gradient associated with spindle assembly is the RanGTP gradient (reviewed in Kalab and Heald 2008, Bastiaens et al. 2006). Ran's guanine nucleotide exchange factor RCC1 (regulator of chromatin condensation) binds chromatin and promotes the release of Ran cargoes, including microtubule regulators, near chromosomes. In *Xenopus* extracts, beads coated with RCC1 are sufficient to induce the assembly of a bipolar spindle (Heald et al. 1996; Halpin D et al. 2011). A gradient of microtubule stabilization and nucleation forms around chromatin due to local activation of spindle assembly factors (Carazo-Salas et al. 2001; Caudron et al. 2005), and this gradient could affect the length of a stable spindle. Indeed, another spindle gradient has been shown to directly modulate spindle length in *C.elegans* embryos. Greenan et al. have shown that a centrosome-based gradient of the Aurora A binding protein TPXL-1 scales with spindle length; reduction of centrosome size causes a shortening of the spindle (Greenan et al. 2010).

The third type of mechanism proposed to regulate spindle length is based on balancing of opposing forces. There are many sources of force that act on the spindle and are known to modulate spindle length, such as microtubule polymerization and depolymerization (Inoué and Salmon 1995; Laan et al. 2008), microtubule sliding (Brust-Mascher et al. 2009), astral microtubules (Adames and Cooper 2000), motor proteins (Saunders et al. 1992, 1997; Straight et

al. 1998; Sharp et al. 2000), bi-oriented chromatids and their compaction (Goshima et al. 1999; Bouck and Bloom 2007; Stephens et al. 2011) (Reviewed in Goshima and Scholey 2010). Different models seek to understand the contributions of these complex forces (Goshima et al. 2005; Gardner et al. 2006, 2008; Dumont and Mitchison 2009; Loughlin et al. 2011; Stephens et al. 2013), but generally balance of force models posit that spindle length is a steady-state equilibrium of forces. At its simplest, spindle length can be thought of as a result of outward pushing forces generated by (+) end directed motor proteins associated with microtubules that overlap from the two halves of the spindle, which are opposed by forces that pull the kinetochores towards the spindle poles: because the sister chromatids are held together by cohesin rings, the net effect of these forces is to pull the two poles towards each other (**Figure 2-1**). In budding yeast, increasing the concentration of Cin8, an outward pushing motor of the kinesin-5 class, causes the spindle to elongate (Saunders et al. 1997), whereas removing Cin8 or its paralog Kip1 causes the spindle to shorten (Straight et al. 1998). Inhibiting the cohesin that binds sister chromatids causes spindles to elongate in both budding yeast (Stephens et al. 2011) and in fission yeast (Goshima 1999).

This general mechanism of spindle length regulation by force balance makes two predictions: 1) Attachment of chromosomes to the spindle is important for setting spindle length because they provide inward force; inhibiting attachments should make spindles longer. 2) Forces in the spindle must be length-dependent. For example, the outwards force exerted by kinesins acting on overlapping microtubules might fall as the distance between the poles fell. Without length-dependence, spindles would elongate or collapse with fluctuations in force. If length-dependent forces play a role in setting spindle length, spindle length should vary with the number of chromosomal attachments as they reach new steady-state equilibriums (See **Figure 2-**

1C for predictions). Based on our current knowledge of molecular rulers and spindle gradients, neither of these mechanisms predict changes in spindle length with varying chromosomal attachment.

We sought to test these two predictions of spindle length regulation by a balance of forces in *Saccharomyces cerevisiae*, common baker's yeast. To test the first prediction, we inhibited the attachment of all chromosomes to the spindle using kinetochore mutants and measured the resulting metaphase spindle length. In all kinetochore mutants tested (*ndc10-1*, *ctf13-30, cep3-2*), metaphase spindles were longer than wild-type. This elongated phenotype could be suppressed by deleting Kip1, supporting the first prediction that attachment provides an inward force that opposes outward directed forces. To test the prediction of length-dependent forces, we varied the number of attachments to the spindle. In strains with no kinetochores, we introduced one, two, or three synthetic kinetochores. Synthetic kinetochores are made by tethering a component of the Dam1 complex to the chromosome via the interaction between the Lac repressor and its operator (Lacefield et al. 2009). Introduction of a synthetic kinetochore reduced spindle length in the kinetochore mutant *ndc10-1*, and additional synthetic kinetochores further shortened spindle length. The trend was further tested by adding extra kinetochores to a wild-type spindle. Extra kinetochores were introduced by transforming centromeric plasmids and selecting for varying numbers of plasmids. Metaphase spindle length varied with the number of kinetochores; spindles were shorter in strains with more centromeric plasmids, supporting the second prediction of force balance.

In the process of testing the force balance model, we created haploid *S.cerevisiae* strains with more than 30 centromeric plasmids, twice number of endogenous centromeres. Previous electron microscopy of haploid yeast cells showed that spindles contain an average of 40

microtubules (Winey et al. 1995); our cells with an average of 23 centromeric plasmids had an increase in the number of microtubules to 78 microtubules, similar to the number needed to attach one microtubule to each kinetochore. Cells with inhibited kinetochores (*ndc10-1*) had reduced numbers of microtubules and asymmetric spindles, similar to previous studies (Romao et al. 2008). Introducing synthetic kinetochores promoted an increase in microtubule number and a symmetric distribution of microtubule number from the two spindle poles. These results suggest that the kinetochores increase the number of microtubules, and that the *S.cerevisiae* spindle maybe more adaptable than previously thought, capable of nucleating more microtubules to meet cellular demands.

RESULTS

Temperature sensitive mutant ndc10-1 eliminates kinetochores but is still capable of nucleating a bipolar spindle.

We sought to test two predictions of the hypothesis that a balance of forces regulates spindle length in *S.cerevisiae*: 1) attachment of chromosomes to the spindle provides an inward force that pulls the poles towards each other and 2) at least one force is length-dependent allowing the number of chromosomal attachments to regulate the length of the spindle (**Figure 2-1C**). Eliminating chromosomal attachments should make the spindle longer, and adding attachments should make it shorter. To test these predictions, we manipulated the number of functional kinetochores.

Temperature sensitive kinetochore mutants were used to detach chromosomes from the spindle. In subsequent experiments, we introduced synthetic kinetochores to add back controlled

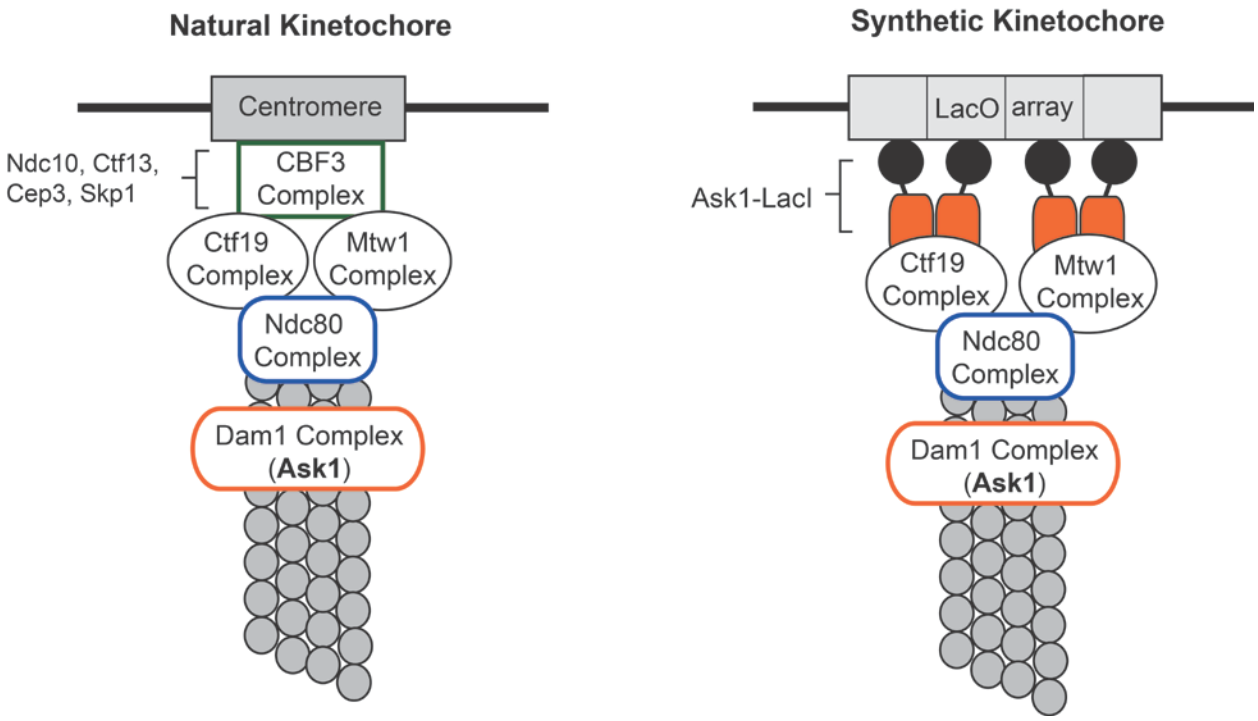

Figure 2-2. Natural and synthetic kinetochores. *S.cerevisiae* kinetochores contain over 65 proteins organized into multiple complexes and bind to the ~125bp conserved centromere sequence. The CBF3 complex, consisting of proteins Ndc10p, Ctf13p, Cep3p, and Skp1p, contacts the centromere and provides most of the DNA-binding properties of kinetochores. The synthetic kinetochore confers chromosome segregation function; it is generated by fusing Ask1p, a component of the Dam1 complex, to the lac repressor and introducing a lac operator array as a binding site. Tethered Ask1-LacI recruits other kinetochore components, however the architecture of the synthetic kinetochore is unknown. The synthetic requires components of the Ctf19, Mtw1, Ndc80 and Dam1 complexes, but it does not require Ndc10p and Ctf13p and is thought to bypass the need for the DNA-binding CBF3 complex.

numbers of attachments (**Figure 2-2**), making it necessary to deplete kinetochore proteins not required by the synthetic kinetochore. Synthetic kinetochores are created by tethering the kinetochore protein Ask1 to chromatin via the binding of the Lac repressor to its operator. The architecture of the synthetic kinetochore is not well understood, but it is known that Ndc10 and Cft13 are not required for synthetic kinetochore function. The synthetic kinetochore may bypass the need for all components of the centromere-binding CBF3 complex (Ndc10, Ctf13, Cep3, and Skp1) (Lacefield et al. 2009). Strains with temperature sensitive alleles of Ndc10 (*ndc10-1* and *ndc10-2*), Ctf13 (*ctf13-30*), and Cep3 (*cep3*-2) were tested for their ability to abolish kinetochore function. If kinetochores are fully eliminated, cells cannot activate the spindle checkpoint in response to microtubule-depolymerizing drugs benomyl and nocodazole (Gardner et al. 2001). Cells were synchronized in G1 with alpha factor and released to the restrictive temperature in the presence of benomyl and nocodazole; activation of the spindle checkpoint causes cells to arrest in mitosis with a large budded morphology (**Figure 2-3A**). Four hours post-release, approximately 90% of wild-type cells were large budded and only 10% of cells deleted for the spindle checkpoint (*mad2*Δ) were arrested (**Figure 2-3B**). Of the kinetochore mutants, only *ndc10-1* showed mitotic progression similar to *mad2*Δ cells. Strains with *ndc10-2, ctf13-30,* or *cep3-2* showed some degree of spindle checkpoint-induced arrest suggesting that they are not true kinetochore nulls, which agrees with previous studies (Gardner et al. 2001) and makes them unsuitable for our experiments.

As the only kinetochore null mutant, *ndc10-1* was chosen over the other mutants for chromosome detachment experiments. One concern with using *ndc10-1* is the disruption of other possible Ndc10 functions. In addition to the kinetochore, Ndc10 localizes to microtubules, the spindle midzone and spindle pole bodies (Goh and Kilmartin 1993; Muller-Reichert et al. 2003;

A)

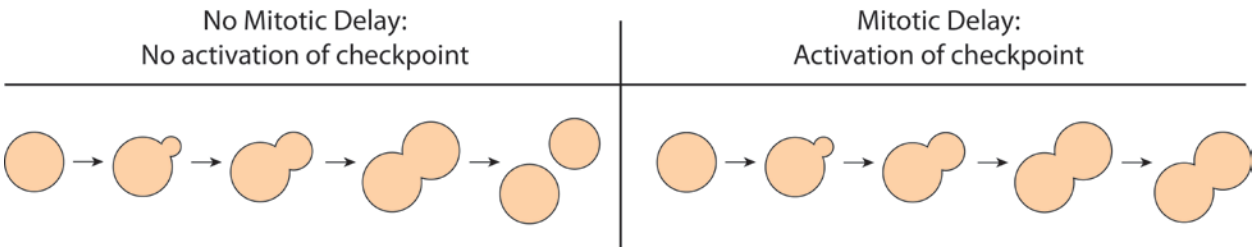

B)

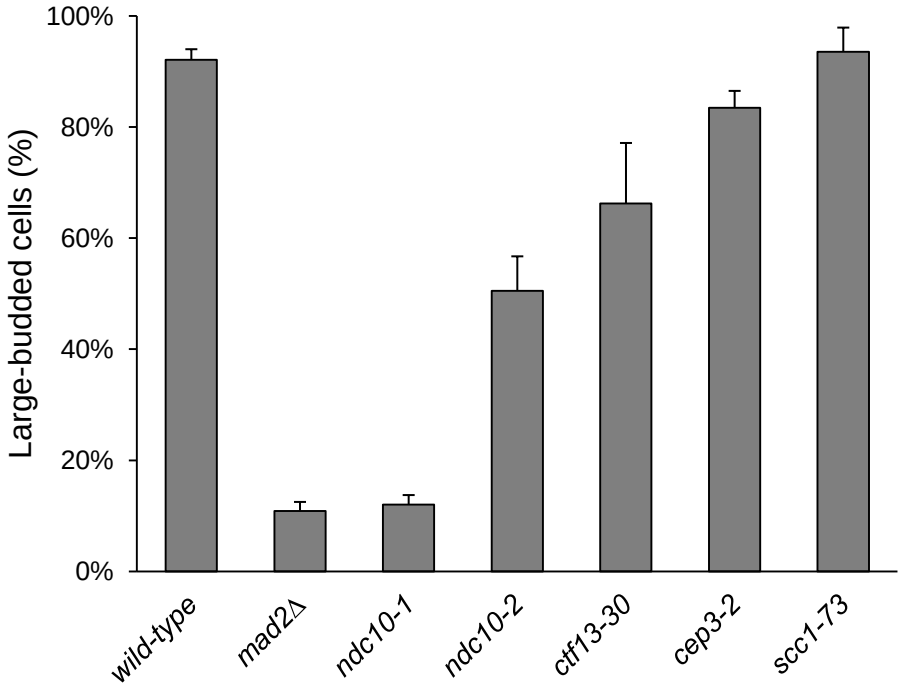

Figure 2-3. Spindle checkpoint activation in response to microtubule-depolymerization. (A) Checkpoint activation can be determined by cell morphology. Activating the checkpoint causes a delay in mitosis and results in an accumulation of large-budded cells. **(B)** Wild-type cells activate the spindle checkpoint in response to microtubule depolymerization and arrest in mitosis as large-budded cells. Cells that do not contain a functional checkpoint (*mad2*Δ) or functional kinetochores escape mitotic arrest; *ndc10-1* escapes arrest at the same frequency as *mad2*Δ suggesting that it does not have functional kinetochores. The *ndc10-2*, *ctf13-30*, and *cep3-2* strains have a higher percentage of large-budded cells than *mad2*Δ and *ndc10-1*, suggesting that kinetochores are not fully abolished. *scc1-73* is a positive control; cohesin is inhibited but kinetochores should be functional and able to activate the spindle checkpoint. The percentage of large-budded cells was determined by light microscopy after 4 hours growth in benomyl and nocodazole. Error bars represent the standard deviation of three independent trials; a minimum of 150 cells were scored for each trial.

Bouck and Bloom 2005). Ndc10 has been proposed to play important post-metaphase roles in maintaining anaphase spindle integrity and directing cytokinesis (Bouck and Bloom 2005). It is also proposed to play a role in spindle pole body maturation; electron microscopy of *ndc10-1* spindles shows a reduction in microtubules. Mutant spindles also have an asymmetric distribution of microtubules with one under-developed spindle pole body nucleating only a few microtubules (Romao et al. 2008). To reduce possible anaphase and cytokinesis defects, synchronized *ndc10-1* cultures were exposed to the restrictive temperature only in G1 through metaphase. The role of Ndc10 in spindle pole body maturation is critical, if *ndc10-1* cells are unable to nucleate microtubules from both spindle pole bodies during metaphase, chromosomal attachments between the two poles cannot be added back.

The asymmetric spindle phenotype seen in *ndc10-1* strains could be due to a defect in spindle pole body maturation or it could be a caused by the absence of kinetochores available to stabilize microtubules nucleated from the new spindle pole body. To determine if both *ndc10-1* spindle pole bodies are functional, electron tomography was performed on spindles from wild-type, *ndc10-1* and *ndc10-1* strains with three synthetic kinetochore pairs (sKT). Each chromosome consists of two chromatids after replication, each chromatid assembles a kinetochore so kinetochores are referred to as "kinetochore pairs" (**Figure 2-1**). Synchronized, metaphase-arrested cells grown at the restrictive temperature were prepared for electron tomography by high pressure freezing and freeze-substitution. Plastic embedded cells were serial-sectioned, visualized by tomography, and three-dimensional reconstructions of spindles were created (see Methods and Materials, and O'Toole et al. 2002).

Wild-type spindles had approximately symmetric microtubule distribution with an average of 26 microtubules from each spindle pole body (**Figure 2-4**, **Table 2-1**). As Romao et

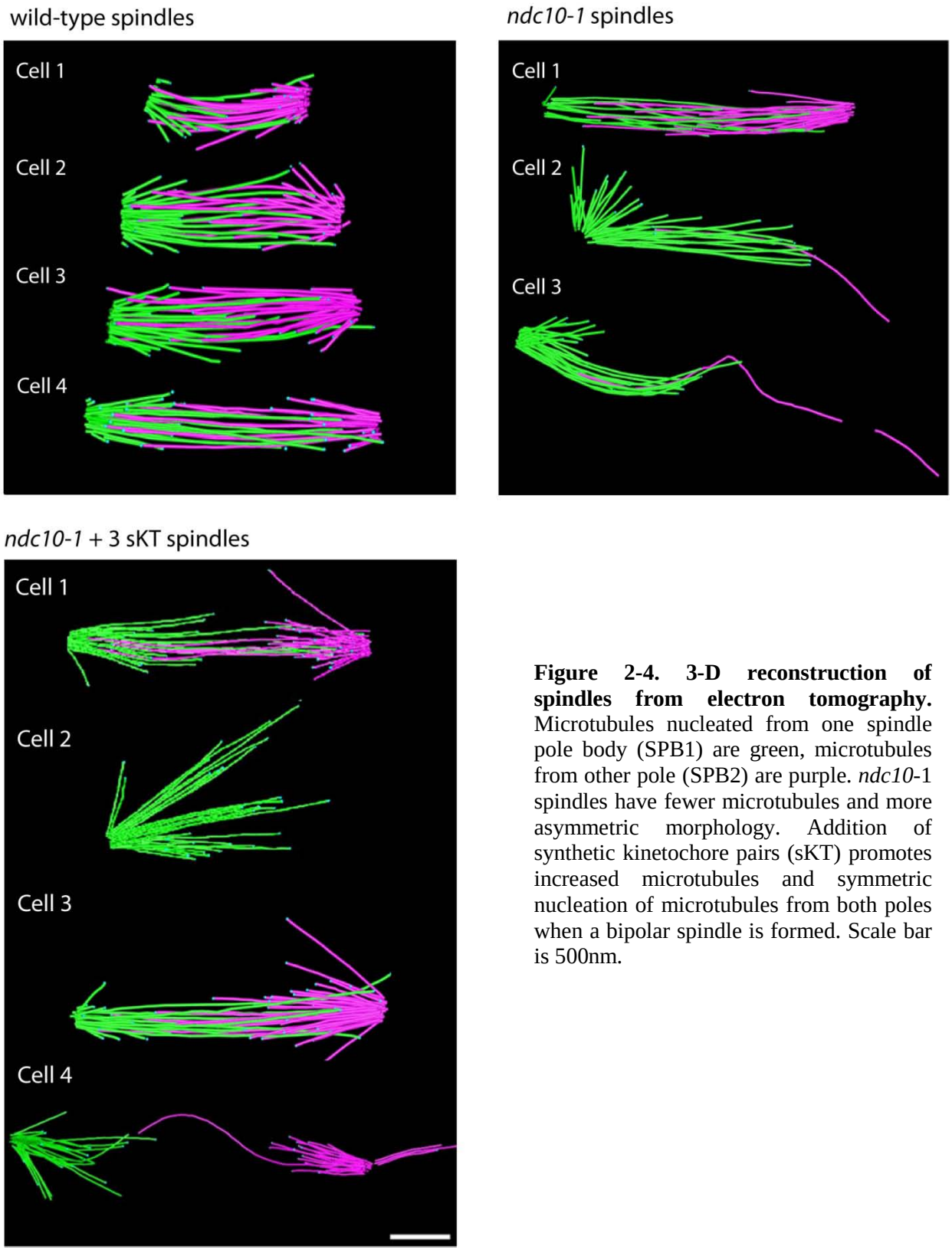

Figure 2-4. 3-D reconstruction of spindles from electron tomography. Microtubules nucleated from one spindle pole body (SPB1) are green, microtubules from other pole (SPB2) are purple. *ndc10*-1 spindles have fewer microtubules and more asymmetric morphology. Addition of synthetic kinetochore pairs (sKT) promotes increased microtubules and symmetric nucleation of microtubules from both poles when a bipolar spindle is formed. Scale bar is 500nm.

Table 2-1. Quantification of *ndc10*-1 spindle reconstructions.

		Spindle Length	Total MTs	SPB 1	SPB 2
wild-type	Cell 1	0.918 µm	50	28	22
	Cell 2	1.298 µm	51	28	23
	Cell 3	1.545 µm	53	27	26
	Cell 4	1.564 µm	51	28	23
ndc10-1	Cell 1	2.668 µm	37	13	24
	Cell 2	1.657 µm	34	33	1
	Cell 3	4.982 µm	26	25	1
ndc10-1+ 3 SK	Cell 1	2.723 µm	57	27	30
	Cell 2	monopolar	34	34	-
	Cell 3	3.430 µm	50	27	23
	Cell 4	2.356 µm	61	21	40

Quantification of spindle lengths, total number of microtubules in the spindle (Total MTs), microtubules from one pole (SPB1) or the other (SPB2) in wild-type cells, *ndc10-1* cells, and *ndc10-1* cells with 3 synthetic kinetochore pairs (sKT). Average number of microtubules decreases in *ndc10-1* spindles compared to wild-type (p-value = 0.02), but increases with the addition of synthetic kinetochores (p-value= 0.05, p-value= 0.006 if monopolar spindle in Cell2 is excluded from analysis).

al. reported, *ndc10-1* spindles had a reduced number of microtubules (average 32.3 microtubules compared to 51.25 in wild-type, p-value= 0.02) and asymmetric spindles. In two out of the three reconstructed *ndc10-1* cells the asymmetry was severe, with one pole attached to only a single microtubule, whereas the other cell showed a roughly 3-fold difference in the number of microtubules emanating from the two poles (**Table 2-1**). When 3 synthetic kinetochore pairs were introduced to *ndc10-1* cells, spindles were still phenotypically different from wild-type with a lack of interpolar microtubules in Cell 4 and a monopolar spindle in Cell 2, but when two spindle pole bodies were present (Cells 1, 3, 4), both were able produce many more microtubules than *ndc10-1* (p-value =0.05 if Cell 2 included in analysis, p-value=0.007 if Cell 2 excluded). The distribution of microtubules shows a more symmetric distribution (*ndc10-1+3 synthetic kinetochore pairs* Cells 1, 3, 4) similar to wild-type. These synthetic kinetochore spindles demonstrate that both spindle pole bodies in *ndc10-1* strains are capable of nucleating microtubules, suggesting that reduced microtubule number in *ndc10-1* cells could be a result of missing stabilization provided by kinetochores rather than under-developed poles.

Chromosomal attachment provides inward resistance to elongation forces

With *ndc10-1* selected as the kinetochore mutant, metaphase spindle length was measured in cells with no chromosomal attachments. Wild-type and *ndc10-1* cells were grown to log phase at the permissive temperature (23°C), synchronized in G1 with alpha-factor, and released into a Cdc20 depletion-induced metaphase arrest at the restrictive temperature (37°C) (**Figure 2-5**). Spindle pole bodies were labeled with a fluorescent protein fused to a spindle pole body component (Spc42-mCherry) and a single chromosome (Chromosome XV) was labeled with GFP by inserting a Lac operator array near CEN15 and expressing GFP-LacI (Straight et al.

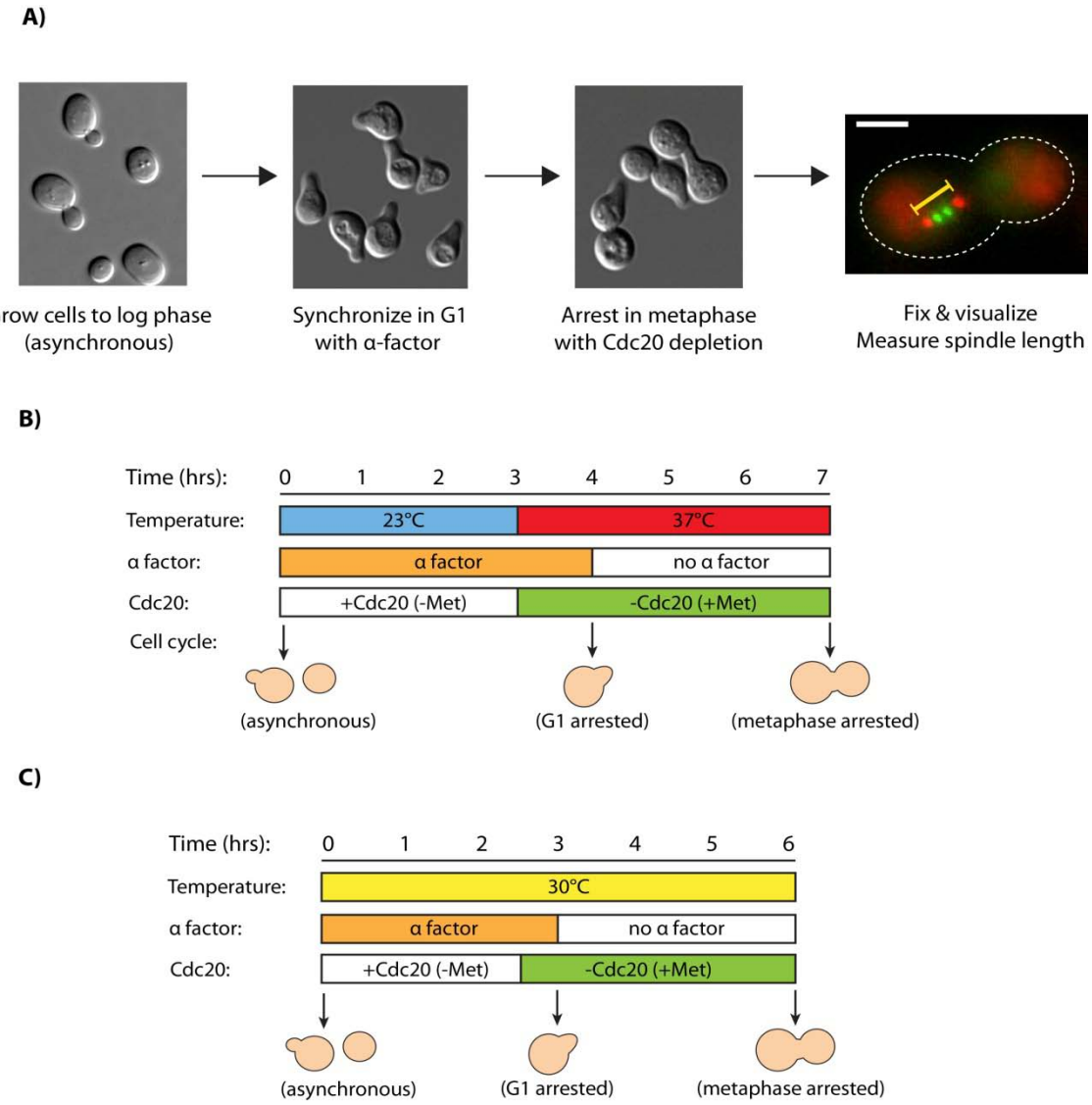

Figure 2-5. Experimental set-up to measure metaphase spindle length. In all spindle length experiments, cells were grown in log phase for 24 hours. Asynchronous populations were treated with α factor to arrest cells in G1. Cells were washed and released from G1 into a metaphase arrest generated by depletion of Cdc20, an essential co-activator of the Anaphase Promoting Complex. After 3 hours post-release from G1, cells were fixed and visualized by fluorescent microscopy. Spindle length (yellow bar) was measured as the distance between labeled spindle pole bodies (Spc42-mCherry; also shown GFP-chromosome III and 2μm scale bar) (**A**). Experiments using temperature sensitive alleles like *ndc10-1* used the protocol shown in (**B**). Cells were arrested at the permissive temperature and raised to the restrictive temperature for the final hour of G1 synchronization. The addition of methionine (Met) repressed Cdc20 expression and arrested cells in metaphase; methionine was added in the last hour of α factor arrest. All other experiments that did not use temperature-sensitive strains used the protocol shown in (**C**). Cells were grown at 30°C for the duration of the experiment; after 2.5 hours in α factor, Met was added to repress Cdc20. Cells were washed and released in metaphase arrest after 3 hours of synchronization.

1996). Spindle length was measured as the three-dimensional distance between poles from analyzing image stacks acquired by fluorescence microscopy on fixed metaphase cells. We report spindle length as the average length of measured spindles (n>100 per trial); error bars represent the standard deviation of average spindle length across all trials. Examples of fluorescent spindles are shown in **Figure 2-6**. The average metaphase spindle length was 1.75 times longer when chromosomal attachments were inhibited; the spindle length of *ndc10-1* cells was 3.82 ± 0.20μm compared to the wild-type spindle length of 2.18 ± 0.02μm (**Figure 2-7**). Spindle lengths in cells with no kinetochores were compared to cells with no cohesin as it has been previously shown that inhibiting cohesin elongates the spindle (Stephens et al. 2011). Removing chromosome attachments and decoupling sister chromatids should equally elongate the spindle because both manipulations eliminate any inward force contributed by chromosomes (**Figure 2-1C**). Cohesin was inhibited by placing the gene encoding one of its subunits, Mcd1, under the *GAL1* galactose promoter (denoted by *GAL*). These cells produce cohesin when grown in galactose but not when grown in glucose. Spindle length in cells grown in galactose (cohesin expressed) was 1.85 ± 0.07μm, but when grown in glucose, spindles were 3.67±0.15μm, similar to the spindle length of *ndc10-1* cells (**Figure 2-7**). *GAL-MCD1* strains were grown at 30°C and *ndc10-1* strains were grown at 37°C, so wild-type spindle length was measured in cells grown at both temperature. Temperature did not significantly impact wild-type spindle length (2.14 ± 0.02μm at 30°C vs. 2.18 ± 0.02μm at 37°C).

In addition to creating longer spindles, inhibiting kinetochores or cohesin also increased the variation in spindle length. In Figure 2-7, error bars represent standard deviation of average spindle length across trials rather than standard deviation of the population's spindle length. The distribution of spindle lengths in a population of wild-type cells has a tight distribution around

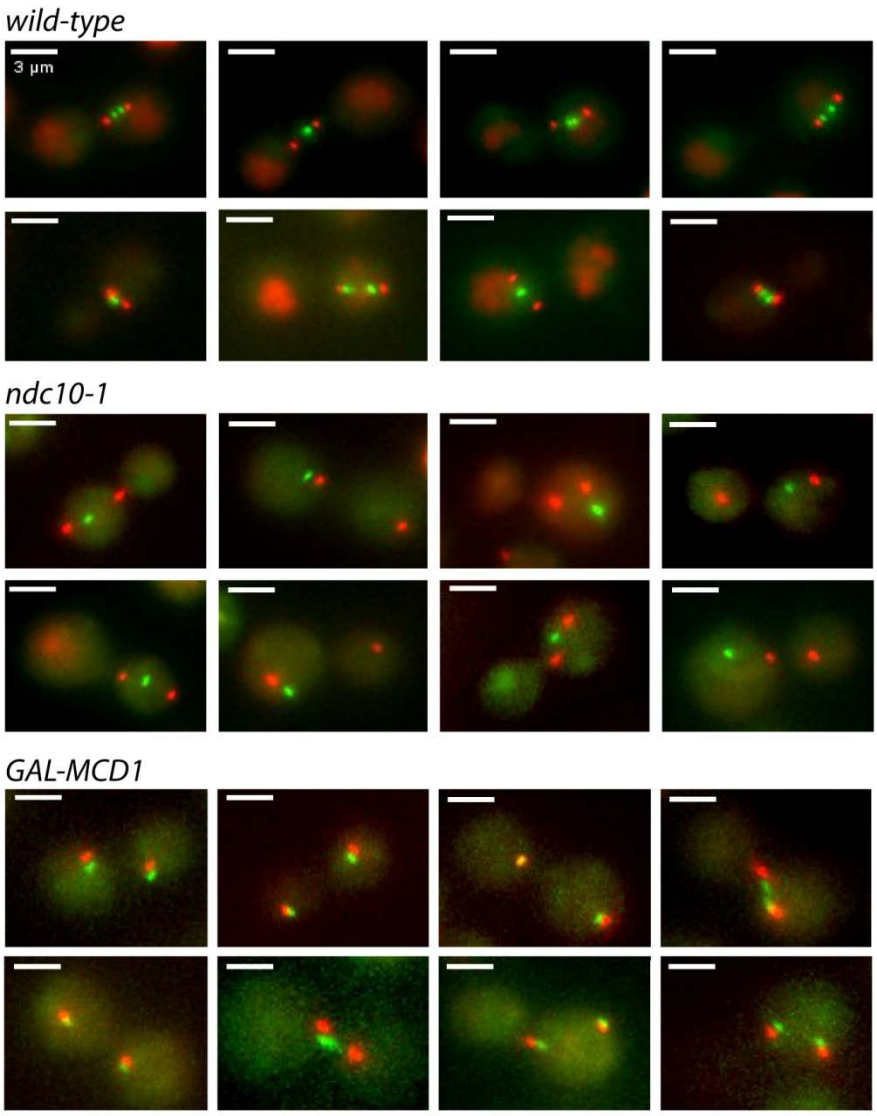

Figure 2-6. Spindles are elongated without kinetochores or cohesin (fluorescent spindle images). Representative fluorescent images of wild-type, *ndc10-1*, and *GAL-MCD1* spindles. Spindle pole bodies (red) are labeled with Spc42-mCherry and Chromosome XV (green) is labeled with GFP by insertion of a lac operator array near CEN15 and GFP-LacI expression. Spindle length is measured as the three dimensional distance between spindle pole bodies. Scale bar is 3µm.

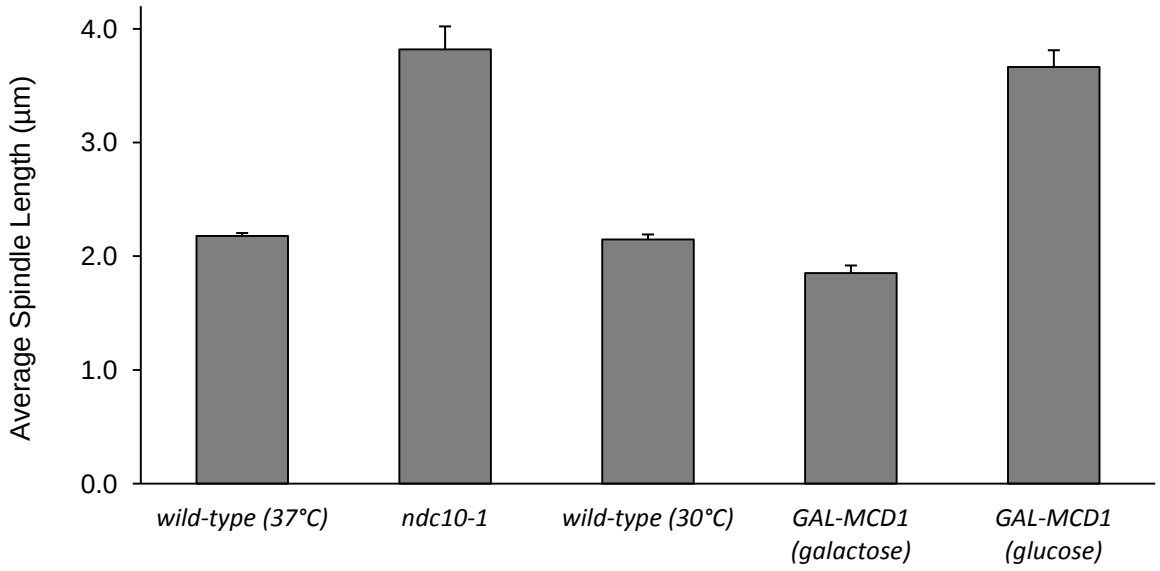

Figure 2-7. Average length of spindles without kinetochores or cohesin. Spindle length was elongated in *ndc10-1* strains and *GAL-MCD1* strains grown in glucose (cohesin inhibited) compared to wild-types grown at either temperature and *GAL-MCD1* strains grown in galactose (cohesin expressed). Elongation was statistically significant (p-values < 0.001). Spindle length was measured as the three-dimensional distance between spindle pole bodies (n>120 cells). Length is reported as the average of these cells; error bar represent standard deviation in average spindle length across a minimum of 3 independent trials.

2µm with a standard deviation of ±0.5µm (**Figure 2-8A**). Eliminating kinetochores with the *ndc10-1* allele creates longer spindles on average, but also a high variation in spindle length. The distribution of spindle lengths in *ndc10-1* cells is broad with a standard deviation of the mean of ±1.4µm (**Figure 2-8B**). *GAL-MCD1* cells grown in glucose to inhibit cohesin had a similarly broad distribution with a standard deviation of ±1.3µm, while cells expressing cohesin had a distribution more similar to wild-type with a standard deviation of ±0.6µm (**Figure 2-8 C and D**). All distributions are plotted in **Figure 2-8E**; spindle length histograms show spindle length data from all cells measured in all biological replicates. The high variation in spindle length in *ndc10-1* and *GAL-MCD1* (Off) suggests that chromosomal attachments, facilitated by kinetochores and cohesin, restrain spindle elongation. Without kinetochores and cohesin to maintain chromosomal attachments, spindles can elongate to any length based on fluctuations of outward pushing forces.

The elongated spindle phenotype was not specific to *ndc10-1*; the other CBF3 mutants *ctf13-30* and *cep3-2* had longer spindles as well (**Figure 2-9**). Both *cep3-2* and *ctf13-30* spindles were longer than wild-type, but shorter than *ndc10-1* spindles, most likely due to incomplete abolishment of kinetochore function as suggested by the checkpoint activation assay (**Figure 2-3B**). This result suggests that the presence of a few functional kinetochores can partially restrain the elongation of the spindle.

To confirm that kinetochores were inactivated in *ndc10-1* cells and cohesin function was eliminated in *GAL-MCD1* cells on glucose, the position of sister chromatids was scored. When a chromosome is bi-oriented, its sister chromatids come under tension as they are pulled toward opposite poles but resisted by cohesin. This pre-anaphase separation of sister kinetochores can be visualized if a Lac operator array is placed near the centromere and GFP-LacI is expressed

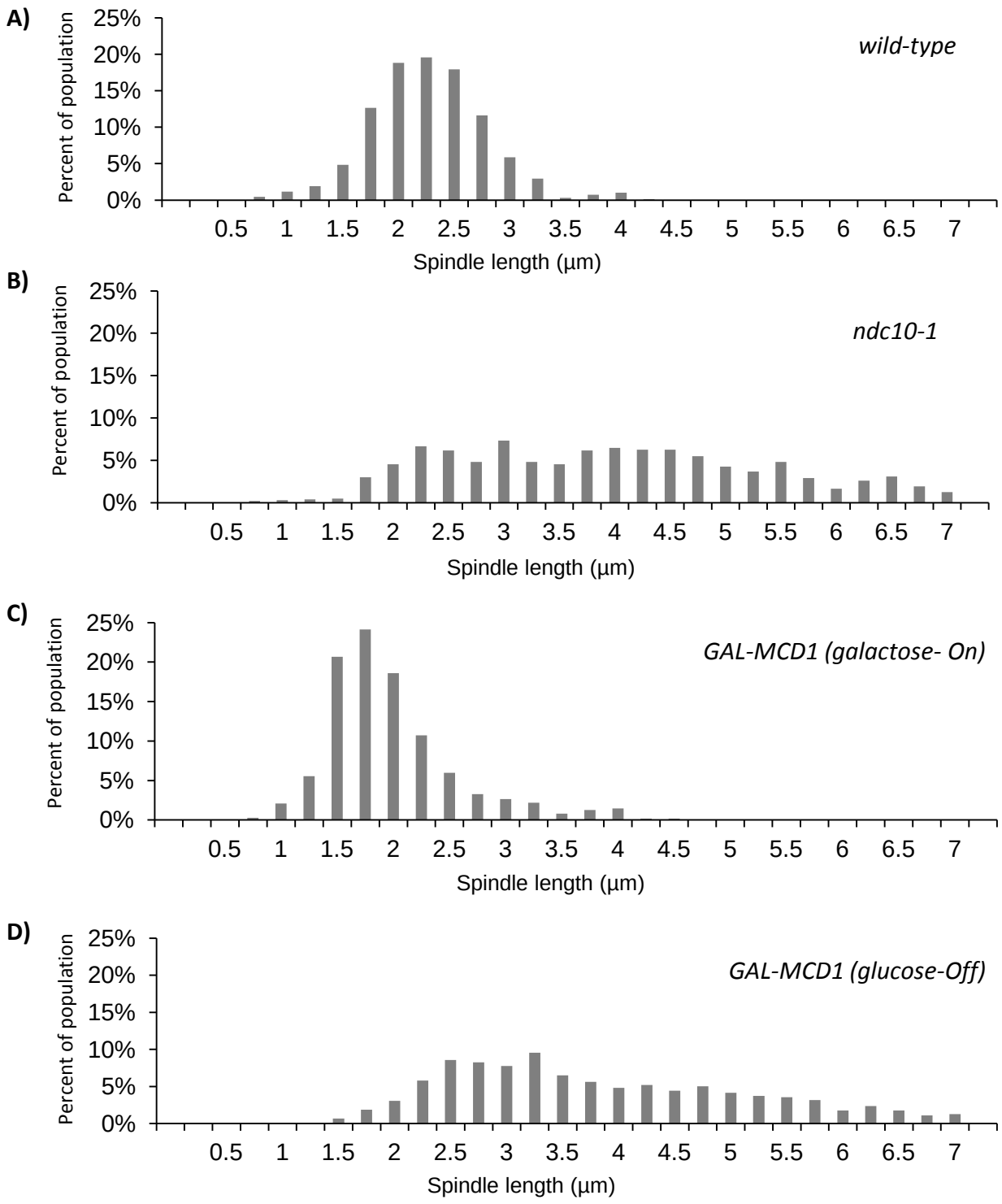

Figure 2-8. Distribution of spindle lengths in wild-type, kinetochore and cohesin inhibited cells: strains plotted individually.

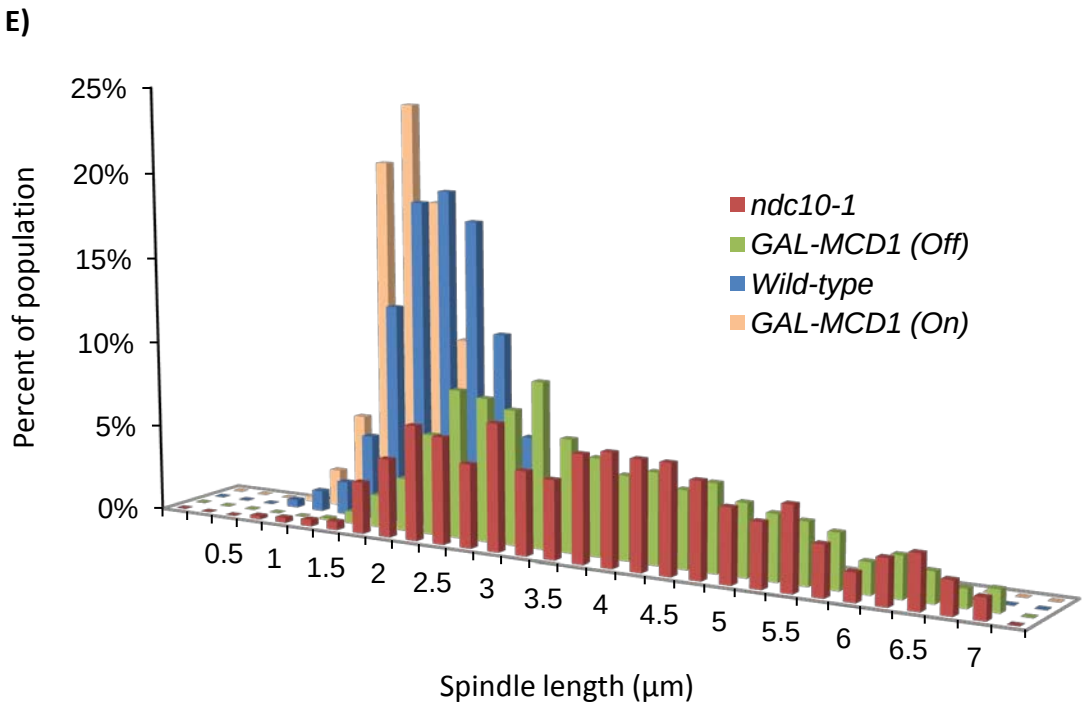

Figure 2-8 (continued). Distribution of spindle lengths in wild-type, kinetochore and cohesin inhibited cells: all strains plotted together. The distribution of spindle lengths of all measured cells is plotted in A-E: wild-type (**A**), *ndc10-1* (**B**), *GAL-MCD1* grown in galactose so cohesin is expressed (**C**), and *GAL-MCD1* grown in glucose so cohesin is repressed (**D**), and all four strains (**E**). Spindle lengths are binned in 0.5µm increments and plotted vs. the percentage of total cells in the population of that length. All cells measured in all biological replicates are represented in the distribution histograms. Wild-type and *GAL-MCD1* (On) have tight distributions while the variation in spindle length in *ndc10-1* and *GAL-MCD1* (Off) is significantly increased. The broad distributions suggest that spindles are no longer restrained and can elongate to any length given fluctuations in outward force.

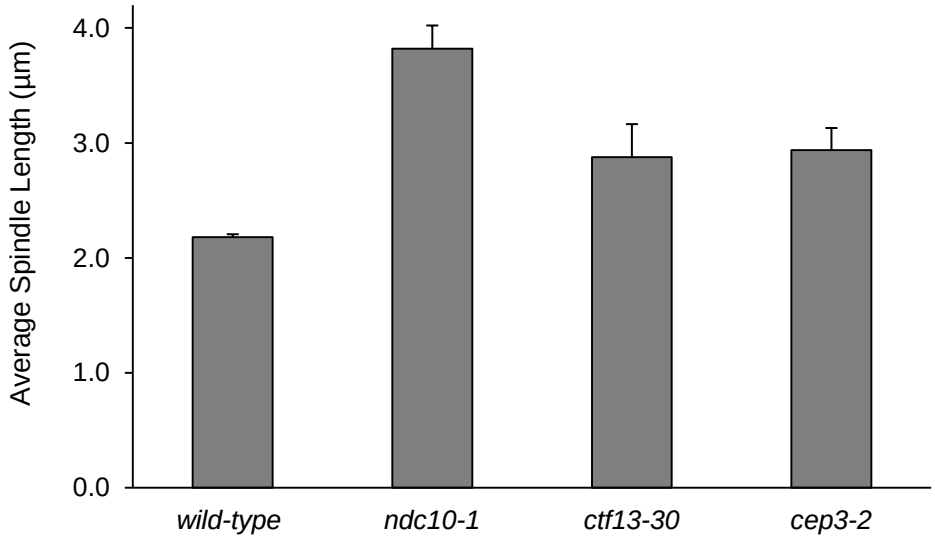

Figure 2-9. Average spindle length in other inner kinetochore mutants. Spindle length was elongated in all three kinetochore mutants of the CBF3 complex, *ndc10-1*, *ctf13-30*, and *cep3-2*, compared to wild-type (p-value <0.001). *ctf13-30* and *cep3-2* spindles were shorter than *ndc10*-1 spindles, most likely due to incomplete inhibition of kinetochore (p-value <0.001). Spindle length was measured as the three-dimensional distance between spindle pole bodies in a minimum of 110 cells. Length is reported as the average of these cells; error bar represent standard deviation in average spindle length across a minimum of 3 independent trials.

(**Figure 2-10A**) (Goshima and Yanagida 2000). The presence of two GFP dots separated by 0.2-1.0μm indicate a bi-oriented chromosome, and a single GFP dot indicates either a bi-oriented chromosome that is not stretched far enough apart to be resolved by light microscopy or a mono-oriented chromosome (**Figure 2-10A**). In wild-type cells with functional kinetochores and functional cohesin, 49.9 ± 1.5% of cells with GFP-labeled Chromosome XV have 2 dots indicating bi-orientation. In *ndc10-1,* only 3.9 ± 3.7% of cells have 2 GFP dots and 95.8% have a single GFP dot suggesting that kinetochores are non-functional (**Figure 2-10B**). Similar to *ndc10-1,* only 13.9 ± 2.6% of *GAL-MCD1* cells have the narrowly separated dots that indicate a bi-oriented chromosome; however unlike *ndc10-1* in which nearly all cells have a single GFP dot, 76.7 ± 2.6% of *GAL-MCD1* cells have two GFP dots localized near either spindle pole body. These dots are further than 1.0μm apart thus are not considered bi-oriented. The presence of two GFP dots at the poles indicates that chromatids were prematurely pulled apart in metaphase, suggesting kinetochores are functional but cohesin is not (**Figure 2-10C**).

The longer spindles seen with detachment of chromosomes or decoupling of sister chromatids supports the prediction that chromosomal attachments provide an inward force that resists outward pushing forces. These outward forces are generated by kinesin-5 (+) end-directed motors Cin8 and Kip1: removing either motor shortens the metaphase spindle and slows the separation of the spindle poles in anaphase (Straight et al. 1998). To demonstrate that chromosomal attachment and (+) end-directed motors create opposing forces, we compared spindle length in *ndc10-1* and *kip1*Δ single mutants and the *ndc10-1 kip1*Δ double mutant. When Kip1 is deleted in cells with functional kinetochores, the average spindle length is 1.39 ± 0.05μm, significantly shorter than the wild-type spindle length of 2.15±0.05μm (p-value<0.001) (**Figure 2-11**). As demonstrated above, knocking out kinetochores creates a longer spindles (3.82

A)

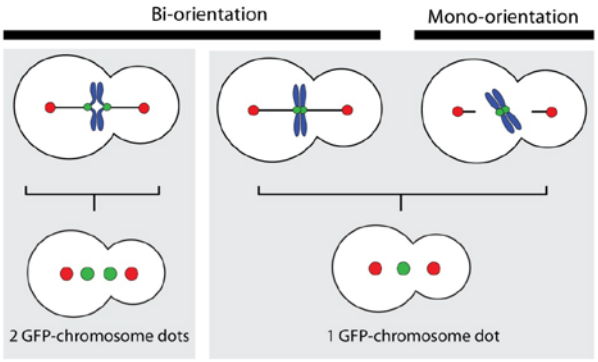

B)

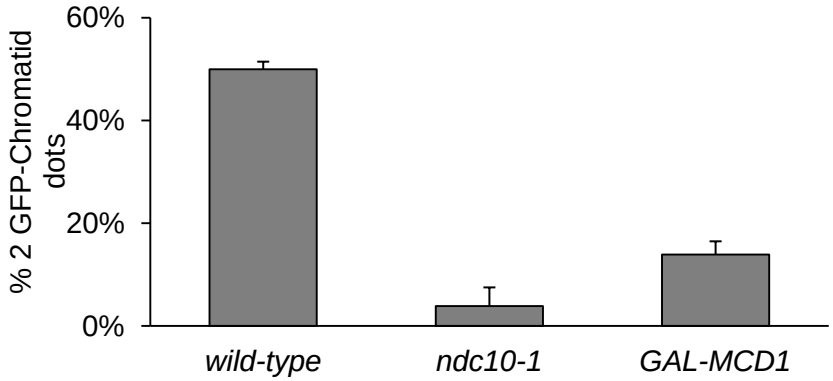

C)

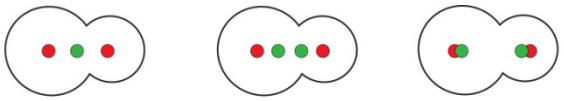

	1 Dot	2 Dots	2 Dots at poles
wild-type	49.6 ± 3.8%	49.9 ±1.5%	2.6 ± 1.3%
ndc10-1	95.8 ± 3.3%	3.9 ± 3.7%	0.3 ± 0.5%
GAL-MCD1	9.4 ± 3.3%	13.9 ± 2.6%	76.7 ± 2.6%

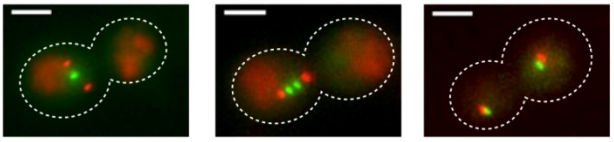

Figure 2-10. Chromosome bi-orientation and position in the spindle. Correct attachment of a chromosome to the spindle results in bi-orientation,visualized as two GFP dots. A single GFP dot can either represent a bi-oriented chromosome not stretched apart or a mono-oriented chromosome not correctly attached to the spindle. Red dots denote spindle pole bodies **(A)**. Percentage of cells with 2 GFP dots signifying correctly attached chromosome XV. Both *ndc10-1* and *GAL-MCD1* strains have few bi-oriented chromosomes compared to wild-type. Cells (n>170) were scored for GFP dots; error bars are standard deviation across 3 independent trials **(B)** Position of chromosomes were scored to distinguish between mono-orientation and pre-mature separation of sister chromatids. Most *ndc10-1* cells contain a single GFP dot while *GAL-MCD1* cells contain two dots pre-maturely segregated to the poles. Percentages calculated from n>170 scored cells, error represents standard deviation across 3 independent trials. Scale bar is 3µm **(C)**.

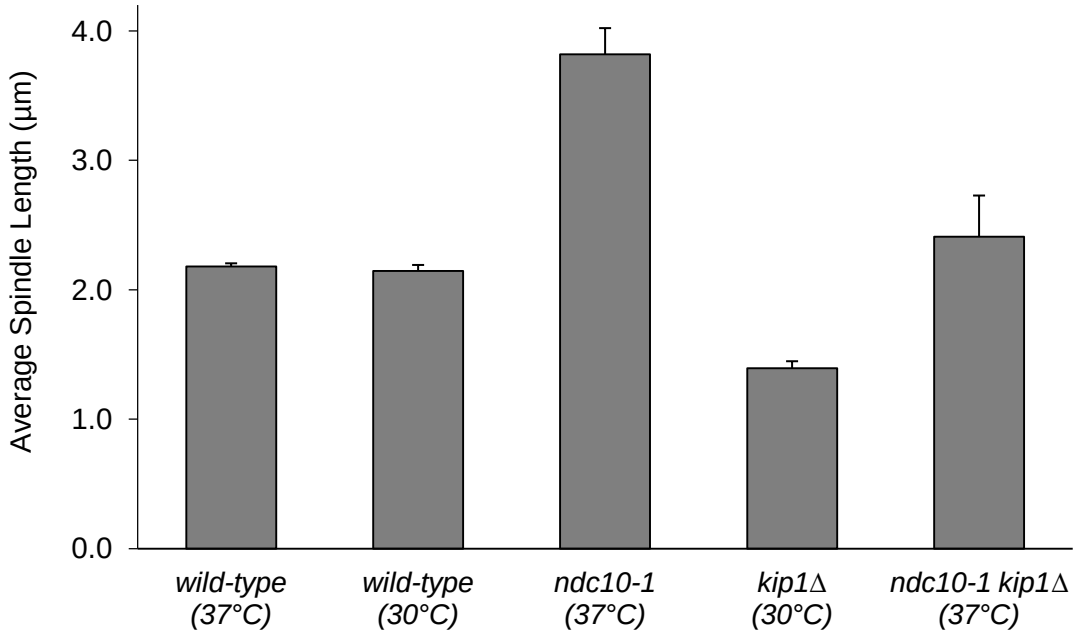

Figure 2-11. Average spindle length in kinetochore and kinesin-5 motor mutants. Deletion of Kip1, a kinesin-5 motor, shortens the spindle and inhibition of Ndc10 elongates the spindle. Eliminating both allows the spindle to approach wild-type length, suggesting that Kip1 and Ndc10 generate opposing forces in the spindle. Spindle length was measured as the three-dimensional distance between spindle pole bodies in a minimum of 150 cells. Length is reported as the average of these cells; error bar represent standard deviation in average spindle length across a minimum of 3 independent trials.

± 0.20μm). When Kip1 is deleted and kinetochores are simultaneously rendered non-functional by *ndc10-1*, the spindle approaches wild-type length at 2.41± 0.3μm suggesting that (+) end directed motors and kinetochores generate opposing forces.

Together, the three results support the force balance model: reducing the ability of kinetochore-pole connections to generate inward forces leads to elongation of the metaphase spindle (**Figure 2-1C**). Spindles elongate when attachments between chromosomes and poles are removed from the spindle by inhibiting kinetochores; spindle length is similarly inhibited when the cohesion that holds sister chromatids together is removed, thus breaking the link that allows forces on the kinetochore to pull the poles together. When the (+) end motor protein Kip1 is deleted, elongation is attenuated.

Spindle length scales with number of kinetochores: support for length-dependent forces

The second prediction of force-balance models asserts that the magnitude of forces in the spindle are length-dependent, which would cause spindle length to scale with the number of attachments to the spindle. As the number of attachments are increased, the amount of inward force is increased and new balance points are reached at shorter spindle lengths (**Figure 2-1C**). We altered the number of chromosomal attachments by manipulating the number of functional kinetochores. We did this in two ways: 1) by knocking out natural kinetochore using *ndc10-1* and introducing a certain number of synthetic kinetochores to reattach a few chromosomes, 2) by introducing extra kinetochores on centromeric plasmids (see below). As mentioned above, it is important to note that after replication, a single chromosome (or plasmid) consists of two chromatids tethered together by cohesin (**Figure 2-1**). Each chromatid has a centromere that recruits a kinetochore, thus a single chromosome has two paired kinetochores that each must attach to a microtubule. In the following experiments, we manipulated the number of functional

kinetochores to alter chromosome attachment and we will refer to the number of kinetochores as "kinetochore pairs" since post replication chromosomes have two kinetochores.

In *ndc10-1* cells, a controlled number of chromosomes were reattached to the spindle using synthetic kinetochores (sKT). Synthetic kinetochores were introduced to *ndc10-1* cells by placing a 256 repeat Lac operator array near the centromere and expressing Ask1-LacI (**Figure 2-2**). Strains were created that contained one, two and three synthetic kinetochores pairs by using strains with LacO arrays placed on Chromosomes XV, III, and VIII. Metaphase spindle length was measured as described above (**Figure 2-5**). Average spindle length decreased with the addition of each synthetic kinetochore pair (**Figure 2-12**); the addition of a single synthetic kinetochore pair decreases the length of the *ndc10-1* spindle from 3.82 ± 0.20μm to 3.46 ± 0.22μm (p-value<0.0001). The presence of two synthetic kinetochore pairs shortened the spindle to 3.21 ± 0.24μm, and a third shortened the spindle to 3.10 ± 0.25μm (p-values<0.04 for each additional synthetic kinetochore pair).

Spindle shortening depends on Ask1-LacI expression. When the Ask1-LacI fusion is placed under the inducible galactose promoter, cells with a single synthetic kinetochore pair grown in galactose at 37°C have an average spindle length of 3.24μm. The same cells grown in glucose at 37°C (repressed expression of Ask-LacI) have 3.49μm spindles, a statistically significant decrease in length (p-value=0.02). Wild-type spindle length is not statistically different in two medias (**Figure 2-13**).

Increasing the number of attachments between chromosomes and the spindle poles above the wild-type number should further shorten the spindle (**Figure 2-1C**). We introduced additional attachments in the form of centromeric plasmids (**Figure 2-14A**); plasmids bearing a

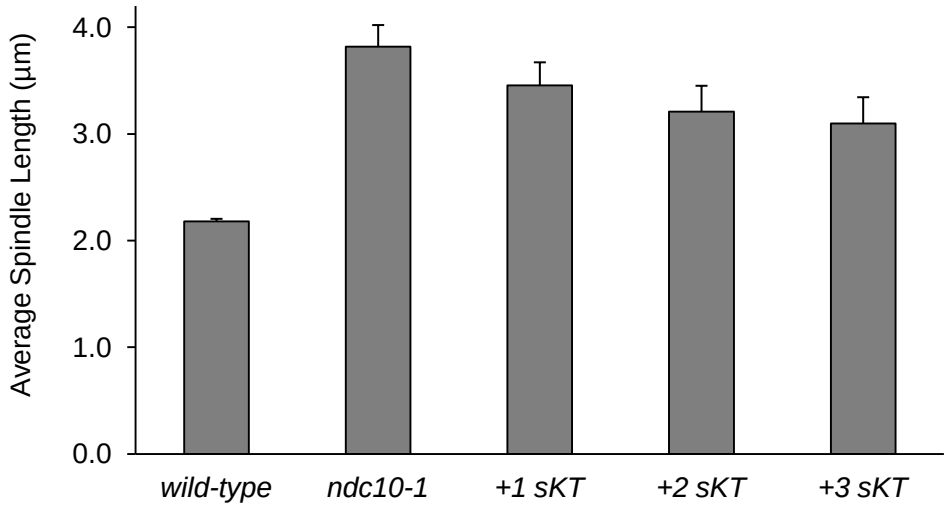

Figure 2-12. Spindle length shortens with addition of synthetic kinetochores. Elongated *ndc10-1* spindles were shortened with the successive addition of synthetic kinetochore pairs (sKT). Decrease in average spindle length with each additional synthetic kinetochore pair was significant (p-value < 0.04). Spindle length was measured as the three-dimensional distance between spindle pole bodies in a minimum of 100 cells. Length is reported as the average of these cells; error bar represent standard deviation in average spindle length across a minimum of 3 independent trials.

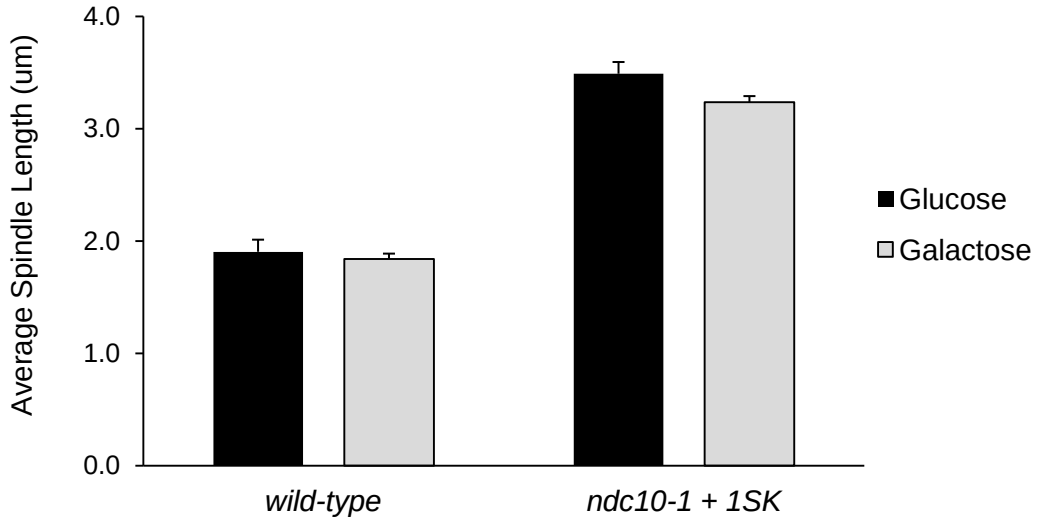

Figure 2-13. Shorter spindle length is dependent on Ask1-LacI expression. The shorter spindle length observed when a single synthetic kinetochore is added to *ndc10-1* spindles is dependent on expression of Ask1-LacI, the protein fusion that creates the synthetic kinetochore. Ask1-LacI was placed on the GAL1 promoter; expression of the fusion protein is induced in galactose and repressed in glucose. Cells were grown in 2% raffinose, synchronized in G1, and released into metaphase arrest in either 2% glucose or 2% galactose containing media. Wild-type cells grown in glucose and galactose had spindles that were the same length (no statistical difference, p-value=0.36), but spindles from *ndc10-1* + 1 synthetic kinetochore cells grown in glucose (Ask1-LacI repressed) were longer than spindles from *ndc10-1* + 1 synthetic kinetochore cells grown in galactose (Ask-LacI expressed) (p-value=0.02). Spindle length was measured as the three-dimensional distance between spindle pole bodies in a minimum of 70 cells. Length is reported as the average of these cells; error bar represent standard deviation in average spindle length across 3 independent trials.

centromeric DNA sequence can assemble a fully functional natural kinetochore (Clarke and Carbon 1980). Like chromosomes, post-replication plasmids have two copies tethered together and thus have two kinetochores (kinetochore pairs) to attach to the spindle (**Figure 2-14A**). Multiple centromeric plasmids can extend the cell cycle (Futcher and Carbon 1986), but this toxicity is abolished with deletion of the spindle checkpoint, so plasmids were introduced to *mad2*Δ strains (Wells and Murray 1996). To create strains with varying numbers of additional kinetochore pairs, we used copper-resistance to provide a graded selection for plasmid copy number (**Figure 2-14B**). The centromeric plasmids carried the only available copy of the *CUP1* gene, both genomic copies (*CUP1-1* and *CUP1-2*) were deleted. *CUP1* encodes metallothionein and confers copy number-dependent copper resistance (Karin et al. 1984); laboratory strains of *S.cerevisiae* with 1-2 copies of *CUP1* can grow in 0.15mM copper sulfate ($CuSO_4$) but industrial strains have been isolated that can grow in 2mM $CuSO_4$ and have up to 10 copies of *CUP1* (Welch et al. 1983). Centromeric plasmids bearing *CUP1* were transformed in Spc42-mCherry *mad2*Δ cells, and transformants were grown initially in 0.01mM $CuSO_4$ and grown subsequently in selectively higher concentrations of copper sulfate to drive up plasmid copy number (**Figure 2-14B**). Strains resistant to 1.0-3.0mM $CuSO_4$ contained on average 20-30 plasmids. The mean number of plasmids present in strains was determined at the beginning of every experiment by quantitative PCR of the centromere sequence relative to ALG9, a house keeping with stable expression (Teste et al. 2009). The number of plasmids will always be reported as the number of plasmids before replication as qPCR was performed on samples synchronized in G1 at the beginning of every experiment. As explained above, a single replicated plasmid recruits two kinetochores after its replication and thus we refer to the number of kinetochore pairs (**Figure 2-**

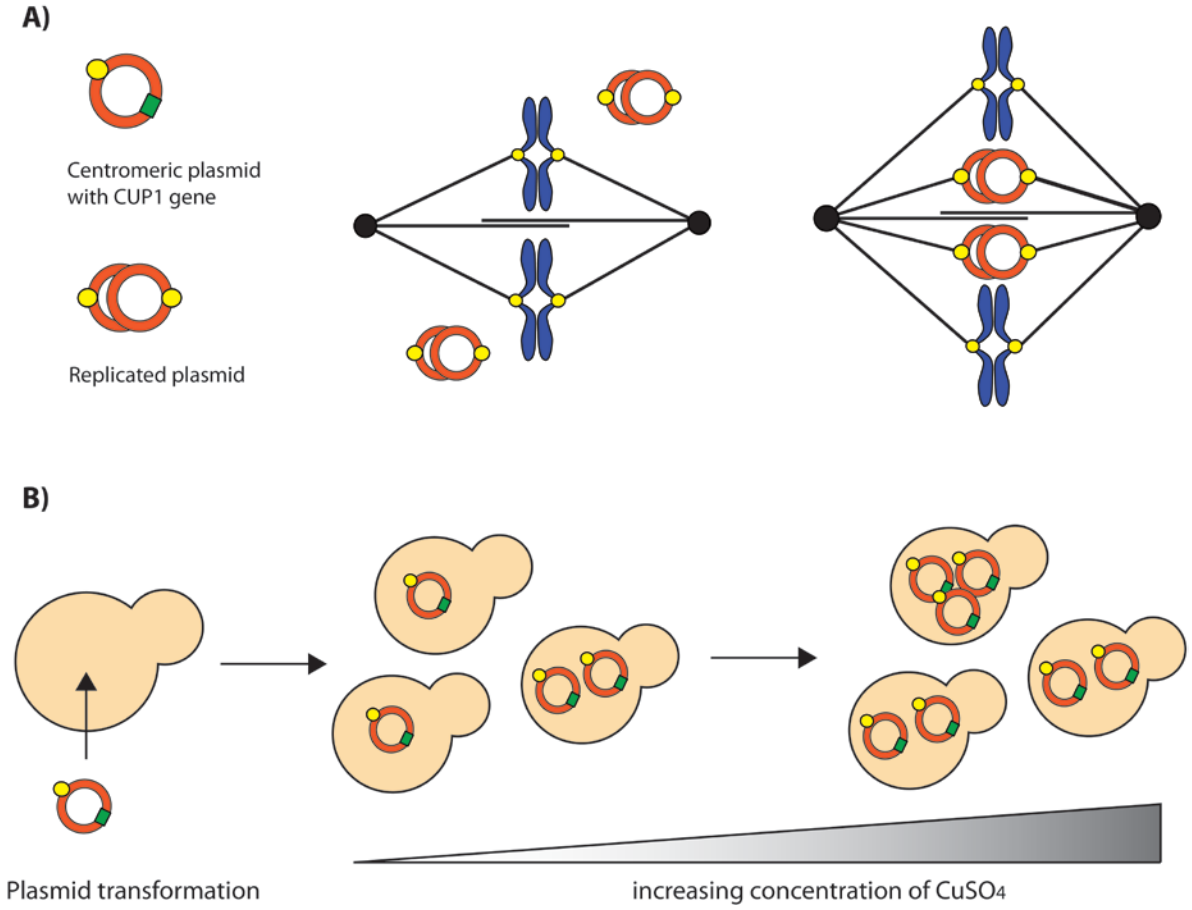

Figure 2-14. Introducing centromeric plasmids as additional attachments to the spindle. Centromeric plasmids can assemble a natural kinetochore (yellow circle) and contain a copy of the *CUP1* copper resistance gene (green box). Replicated plasmids attach to the spindle via kinetochores like endogenous chromosomes; each replicated plasmid has two copies and thus assembles a pair of kinetochores to attach to the spindle (**A**). Plasmids were transformed into cells and grown in increasing concentrations of copper sulfate ($CuSO_4$) to select for cells that acquire multiple copies of the plasmid by non-disjunction events (**B**).

14A). Spindle length was measured in cells with 0- 30 plasmids (0-30 extra kinetochore pairs). Average spindle length scaled with the number kinetochore pairs, shortening with additional kinetochore pairs (**Figure 2-15**). Cells containing an average of 5 plasmids and thus 5 extra kinetochore pairs were ~20% shorter than wild-type (no extra kinetochore pairs) with a spindle length of 1.78 ± 0.20μm compared to 2.00± 0.14μm. Introducing 10 extra kinetochore pairs gave a spindle length of 1.51 ± 0.0.7μm, 20 extra kinetochore pairs gave an average length of 1.38 ± 0.10μm, and 30 extra kinetochore pairs gave an average length of 1.28 ± 0.09μm. Spindles with extra kinetochore pairs were both significantly shorter than wild-type (p-values<0.001) and shorter with each increase in the number of extra kinetochore pairs (p-values<0.001, for each comparison). We probed the minimum spindle length by growing cells in a large range of copper sulfate concentrations to drive up the number of plasmids; the average spindle length plateaued around a length of 1.2μm. The shortest spindles recovered had an average length of 1.07μm and were measured in cells contained an average of 54 plasmids (**Figure 2-16**).

To investigate the effect of the extra kinetochore pairs on the behavior of a cell's chromosomes we tagged the centromere of chromosome III with a LacO array and scored it for bi-orientation (**Figure 2-17A**) as previously described (**Figure 2-10A**). The percentage of cells with stretched chromatids (2 GFP dots) and the distance these chromatids stretched apart quickly decreased with the addition of plasmids. Wild-type cells with 0 plasmids have approximately 50% of chromosomes stretched apart enough to produce two resolvable GFP dots, while the presence of just 1-5 plasmids or extra kinetochore pairs causes a drop to approximately 25% paired dots (**Figure 2-17A**). The percent of cells with two dots does not significantly change with increased numbers of extra kinetochore pairs, for example 22.40% of cells have a stretched chromosome with 5 extra kinetochore pairs present and 22.36% stretched with 25 present.

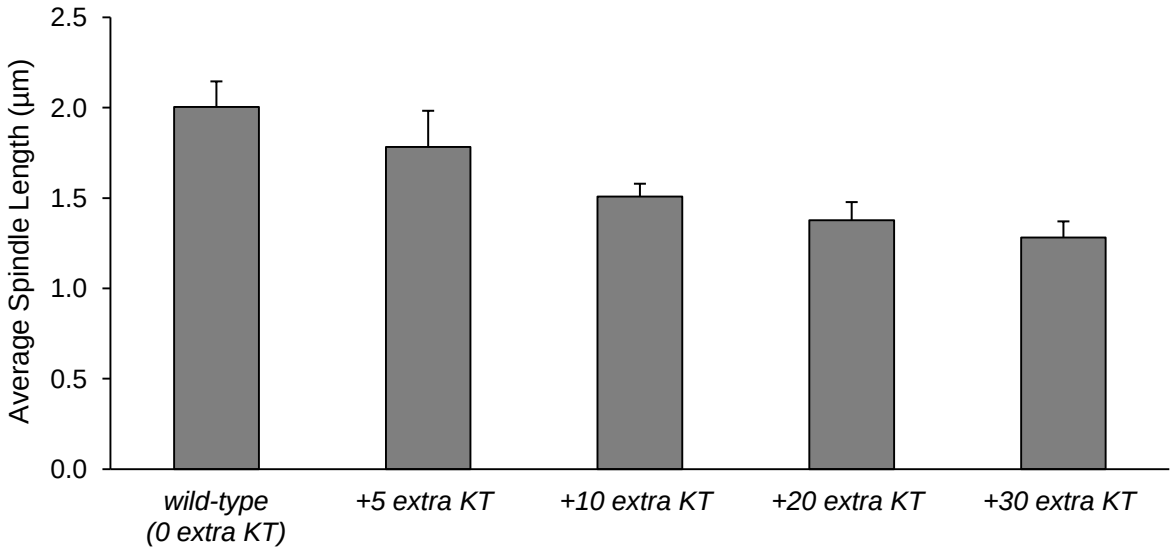

Figure 2-15. Average spindle length shortens with extra kinetochores. Extra kinetochore pairs were introduced by centromeric plasmids. Strains were isolated that contained 5, 10, 20, or 30 copies of the centromeric plasmids. Spindle length shortened compared to wild-type (0 extra kinetochore pairs) and with increasing numbers of kinetochore pairs (p-values<0.001). Spindle length was measured as the three-dimensional distance between spindle pole bodies in a minimum of 100 cells. Length is reported as the average of these cells; error bar represent standard deviation in average spindle length across a 5 independent trials.

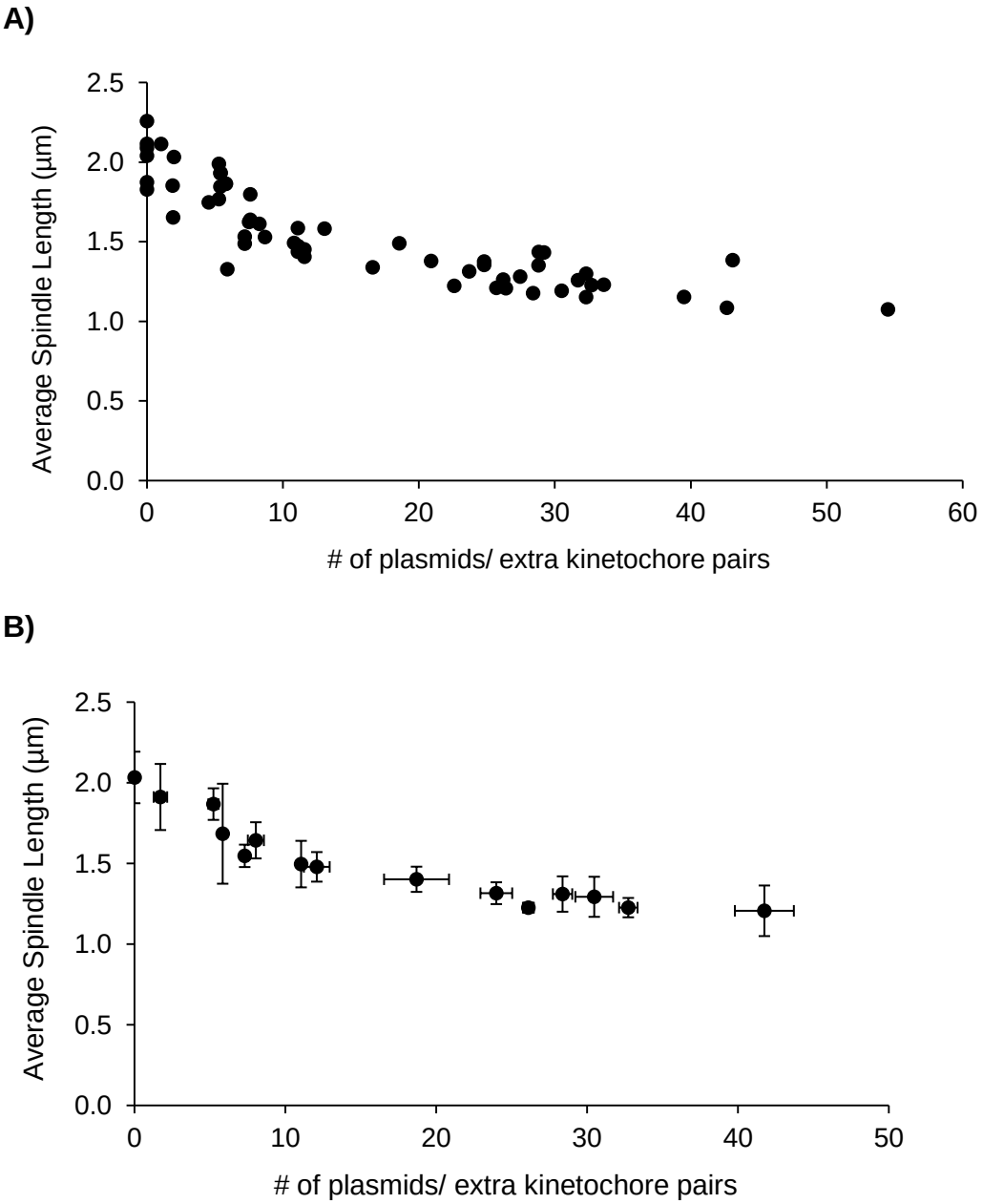

Figure 2-16. Spindle length scales with number of attachments. Cells were grown in a range of copper sulfate concentrations to acquire a range of plasmid numbers. Average spindle length scaled with the number of plasmids; spindle length plateaus around 1.2µm. Each data point represents an independent trial with the average spindle length of at least 100 cells and the number of plasmids determined by qPCR (**A**). 3 independent trials from (**A**) were averaged and plotted in (**B**) to give average spindle length vs. average plasmid number. Error bar represent the standard deviations between trial averages.

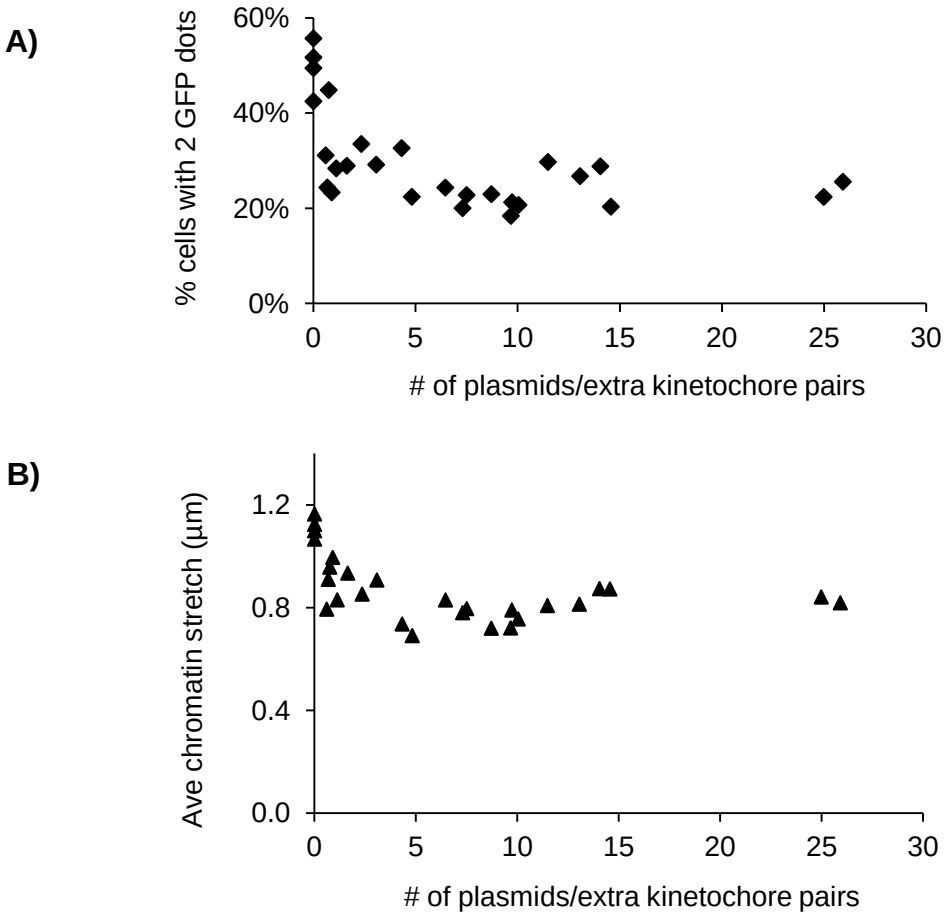

Figure 2-17. Ability to bi-orient a chromosome in the presence of extra attachments. Percentage of cells with 2 GFP dots signifying correctly attached chromosome III in strains containing a range of plasmids (**A**). The percent of stretch chromosomes quickly drops off in the presence of plasmids/ extra pairs of kinetochores but plateaus around 25%. Cells (n>100) were scored for GFP dots; error bars are standard deviation across 3 independent trials The distance sister chromatids stretched was measured in (B). Stretch distance plateaus around 0.8µm. Chromatin stretch was measured as the three-dimensional distance between GPF dots (n>100); error bar represent standard deviation in average spindle length across 4 independent trials.

Likewise, the distance chromatids stretch plateaus around 0.8μm with the presence of just a few extra kinetochore pairs. Wild-type cells with 0 extra kinetochore pairs have an average chromatin stretch of 1.12μm but the presence of 1 extra kinetochore pair yielded an average chromatin of 0.83μm, 4 extra kinetochore pairs gave 0.74μm stretch, and 25 extra kinetochore pairs gave 0.84μm stretch (**Figure 2-17B**). The percentage of stretched chromatids did not approach 0% with increased plasmids, and the average distance between separated GFP dots did not drop below 0.69μm despite our ability to measure individual distances as small as 0.3μm. This result suggests that while the presence of plasmids with their extra kinetochore pairs alters the stretching of chromatids, increasing numbers of plasmids does not prevent attachment and bi-orientation.

In summary, spindle length scales with the number of kinetochore pairs. Introducing a synthetic kinetochore pair to spindles without natural kinetochores shortens the spindle. Subsequent addition of synthetic kinetochore pairs further shortens the spindle. Spindles shorter than wild-type are produced when additional kinetochore pairs are introduced on centromeric plasmids. This scaling relationship between kinetochore number and spindle length is shown in **Figure 2-18**, which contains all spindle length data from synthetic kinetochores and extra kinetochores on centromeric plasmids. Data collected with synthetic kinetochores is denoted in black and data collected with centromeric plasmids is denoted in gray. **Figure 2-18** shows that spindle length shortens with the addition of kinetochore pairs, but we are hesitant to use both data sets together to define a quantitative relationship between kinetochores and spindle length due to the fact that the genotypes are different between strains in these two data sets (Table 2-3) and because synthetic kinetochores are not identical to natural kinetochores (see Chapter 4 for

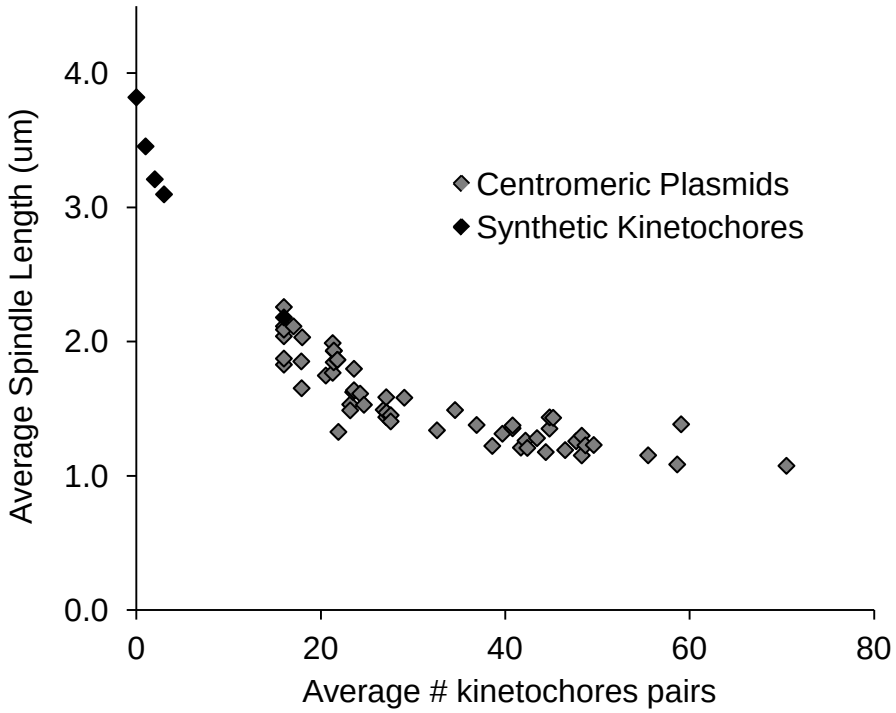

Figure 2-18. All spindle length data: kinetochore number determines spindle length. Spindle length data from Figure 2-12 (synthetic kinetochores in *ndc10-1*) and Figure 2-16A (centromeric plasmids) is plotted together to demonstrate the qualitative relationship between the number of kinetochore pairs and spindle length. Defining a quantitative relationship between kinetochores and spindle length using both data sets would be inappropriate because one set used synthetic kinetochores while the other used natural kinetochores assembled on centromeric plasmids.

further discussion). However, our data does demonstrate qualitatively that spindle length varies with kinetochore number, which supports the second prediction of force balance models because spindle can reach new steady-state lengths with changing numbers of chromosome-to-pole attachments (**Figure 2-1C**). The cells containing many centromeric plasmids are viable and able to bi-orient a labeled chromosome, implying that every chromosome attaches and bi-orients on the spindle.

Extra kinetochores increase microtubule number

Unlike animal and plant spindles where most microtubules do not interact with kinetochores, more than 70% of the budding yeast spindle microtubules are believed to terminate at kinetochores. This observation has led to speculation that the spindle pole bodies have a fixed and limited ability to nucleate microtubules. The strains we created which introduced as many as twice the number of endogenous kinetochores allowed us to test this idea. Previous electron microscopy of haploid yeast spindles has shown that metaphase spindles contain 44±8 microtubules with 36 identified as kinetochore microtubules available to attach the 32 kinetochores (Winey et al. 1995). Our strains would require many more microtubules; for example, cells with 20 plasmids thus 20 extra kinetochore pairs (40 total kinetochores) would require a minimum of 80 microtubules (32 to attach kinetochores on 16 endogenous chromosomes, 40 for the plasmids, and 8 for the interpolar microtubules).

Yeast spindle pole bodies have been argued to be operating at or near their microtubule nucleation capacity based on their surface size and microtubule packing density (Winey and Bloom 2012). Since the cells we created with extra kinetochores show normal growth and fail to produce unusually high frequencies of dead cells, one of the following possibilities must be correct: spindle pole bodies can support many more microtubules than are present in unperturbed

cells, or single microtubules must be able to support the attachment and segregation of multiple kinetochores. To distinguish between these possibilities, we performed electron tomography on cells containing many copies of the centromeric plasmids. Cells were grown in $CuSO_4$ to select for high copy number, synchronized in G1 with alpha factor, released into a metaphase arrest and prepared for imaging by electron tomography (see Methods and Materials). Wild-type cells contained an average of 51.3 ± 1.3 microtubules, within the standard deviation of microtubules previously observed (Winey et al. 1995). Cells containing 23 plasmids, as determined by qPCR, contained more microtubules than wild-type with an average of 73.8 ± 6.9 microtubules, statistically different microtubule numbers from wild-type (p-value=0.006) (**Figure 2-19, Table 2-2**). Because *S.cerevisiae* chromosomes do not condense to a visible structure, we used programs described in Winey et al. 1995 to identify the central, "core bundle" and presumptive kinetochore microtubules. We used a pairing analysis as described in Methods and Materials and in Winey et al., 1995 to identify the microtubules of the central spindle; these are defined as microtubules that are separated by up to 45 nm for lengths of 300 nm and greater. Those microtubules are shown in yellow and form an obvious central spindle. Microtubules that do not fit the pairing criterion are displayed in purple and green and represent the putative kinetochore microtubules. The difference in microtubule number comes from additional kinetochore microtubules, labeled in green and purple in **Figure 2-19** (p-value=0.005). The middle panel of **Figure 2-19** shows only kinetochore microtubules to highlight the difference in number and morphology. Spindles with 23 plasmid have 62.75 ± 7.7 kinetochore microtubules compared to 38 ± 2.4 for wild-type. The number of interpolar microtubules (labeled in yellow in the top panel) is not significantly different between wild-type and plasmid spindles.

In addition to having more kinetochore microtubules, spindles with plasmids also have a "bushy" morphology with more of their microtubules projecting away from the spindle. This morphology can be quantified by measuring the pitch angle of the microtubules from the central spindle axis (**Figure 2-20A**). The average pitch angle of kinetochore microtubules in the four spindles from cells containing an average of 23 extra centromeres is greater than wild-type (p-value=0.05); the average pitch angle in plasmid spindles is 22.9±3.2° compared to 19.5±1.4° in wild-type (**Figure 2-20B**).

The diameter of the spindle pole body central plaque was measured to determine if the spindle pole bodies increased in size with increased plasmid number. Wild type spindle pole bodies had a mean diameter of 106.8 $\pm$ 9.7 nm (n=7). Spindle pole bodies from cells containing 23 extra kinetochore pairs were larger, with an average diameter of 163.4 $\pm$ 32.8 (n=8) (p-value=0.001) (**Figure 2-20C**).

The plasmid spindles show that the number of kinetochore microtubules increases as the number of kinetochores increase. This same pattern was also seen with the *ndc10-1* spindles (**Figure 2-4; Table 2-1**). Inhibiting kinetochores led to an overall decrease in microtubule number (average 32.3 microtubules compared to 51.25 in wild-type, p-value= 0.02), and introducing synthetic kinetochores increased the number of microtubules (p-value=0.007).

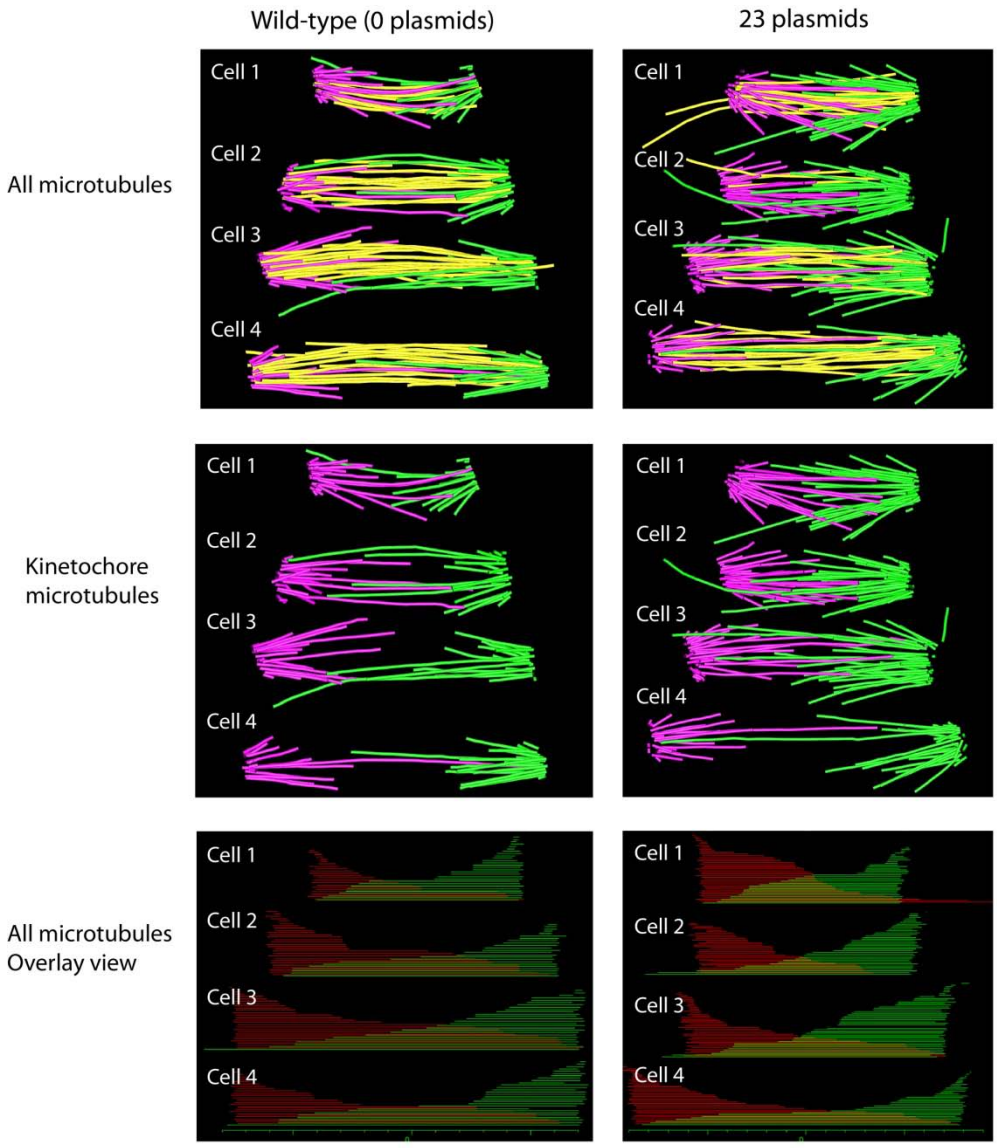

Figure 2-19. 3-D reconstruction of spindles from electron tomography. Microtubules are categorized as kinetochore microtubules or interpolar microtubules based on length and pitch angle from the spindle. Interpolar microtubules are yellow, kinetochore microtubules from one spindle pole body (SPB1) are green, and kinetochore microtubules from other pole (SPB2) are purple. All microtubules are shown in the first row; only kinetochore microtubules are shown in the second row. The third row shows all microtubules displayed in a two-dimesional overlay view. Cells containing 23 plasmids have more microtubules than wild-type (p-value=0.006), specifically more kinetochore microtubules (p-value=0.005) but no statistical different in interpolar microtubule number.

Table 2-2. Quantification of extra plasmid spindles.

		Spindle Length	Total MTs	SPB1	SPB2	Interpolar MTs	Kinetochore MTs
wild-type	Cell 1	0.918 µm	50	28	22	15	36 (20/16)
	Cell 2	1.298 µm	51	28	23	12	39 (21/18)
	Cell 3	1.545 µm	53	27	26	9	41 (23/18)
	Cell 4	1.564 µm	51	28	23	17	36 (19/17)
23 plasmids	Cell 1	1.160 µm	75	41	34	14	63 (33/28)
	Cell 2	1.271 µm	69	33	36	17	52 (27/25)
	Cell 3	1.425 µm	83	44	39	14	70 (37/33)
	Cell 4	1.817 µm	68	38	31	3	66 (37/29)

The total number of microtubules (Total MTs) from spindles in Figure 2-16 was quantified and classified: number of microtubules from one spindle pole body or the other (SPB1 and SPB2), and classified as interpolar microtubules or kinetochore microtubules. Kinetochore microtubules contributed from either spindle pole body is recorded in parentheses.

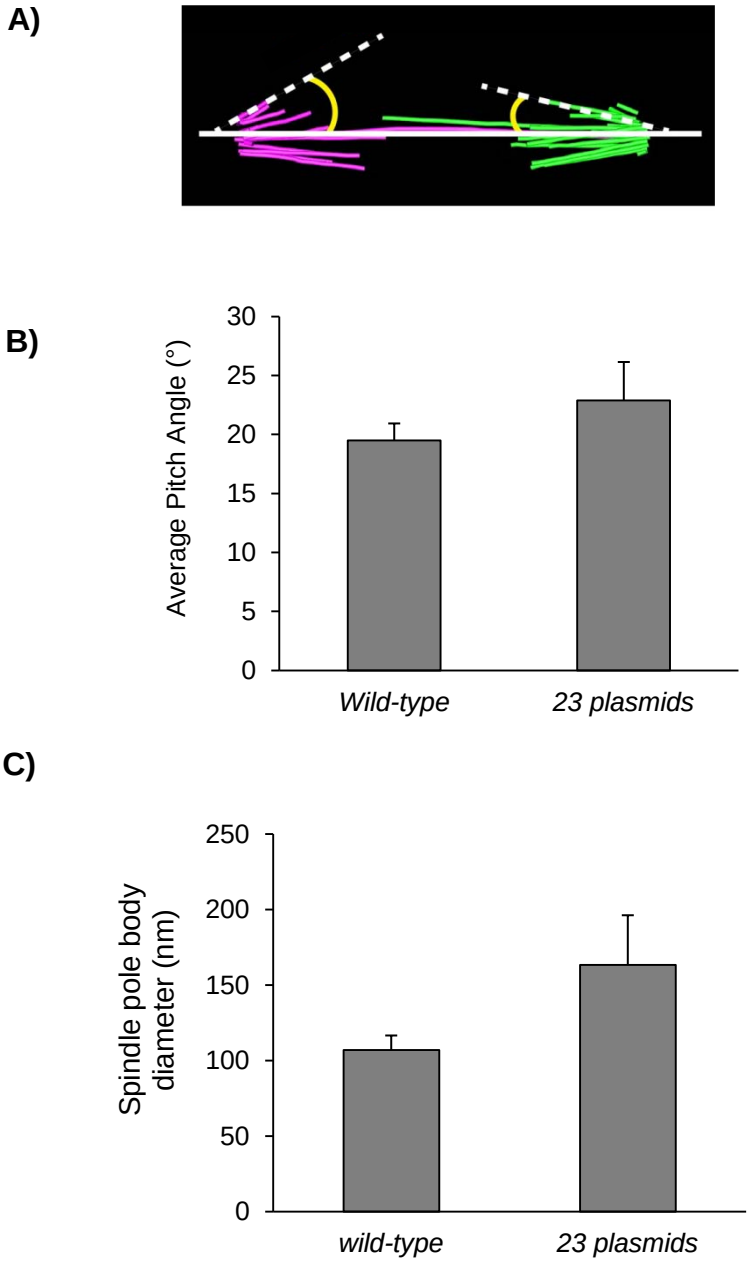

Figure 2-20. Analysis of spindles with extra kinetochores. The "bushy" morphology of plasmid containing spindles can be quantified by measuring the pitch angle of microtubules from the central axis of the spindle (**A**). Average pitch angle of kinetochore microtubules is greater in the four plasmid spindles compared to wild-type (p-value=0.05) Error bars are standard deviation between four spindles (**B**). The size of the spindle pole bodies increased with more microtubules (C). The diameter of the central plaque of the spindle pole body cells with 23 plasmids was greater that the diameter of wild-type spindle pole bodies (p-value =0.001).

DISCUSSION

Spindles are dynamic structures but they achieve similar lengths in every cell division. In this study, we sought to understand the mechanisms that govern spindle length in *S.cerevisiae*, specifically by testing the predictions of the force balance model (**Figure 2-**1). Opposing forces are generated by outward pushing (+) end motors and inward force of chromosomal attachments. Previous studies had shown that deleting these motors shortens the spindle (Saunders et al. 1997; Straight et al. 1998) and removing the linkage between sister chromatids produces longer spindles (Stephens et al. 2011). If spindle length is the steady-state balance of these forces and at least one of the forces is length-dependent, removing chromosomal attachments should elongate the spindle, adding them should shorten it, and varying the number of attachments should cause the spindle to reach equilibrium at different lengths (**Figure 2-1C**).

S.cerevisiae spindle length regulation by balance of length-dependent forces

Removing chromosomal attachments with the *ndc10-1* mutation produced longer metaphase spindles, similar to the elongated spindles seen when chromatids were unlinked from each other by inhibiting cohesin expression (**Figure 2-7; Figure 2-8**). This elongation of the kinetochore-deficient spindle was suppressed when kinesin-5 motor protein Kip1 was deleted (**Figure 2-11**). Other kinetochore mutants (*cft13-30* and *cep3-2*) also had long spindles, although the existence of residual kinetochore function in these mutants makes quantitative interpretation of their phenotypes impossible (**Figure 2-3B; Figure 2-9**). Together these results suggest that chromosomal attachment plays an active role in setting spindle length by providing inward force and restraining spindle elongation. The role of attachments in setting *S.cerevisiae* spindle length is significant because some force-balance models focus on antagonist motors as the source of

opposing forces (Civelekoglu-Scholey et al. 2010; Saunders et al. 1997). Kinesin-14 motors are (-) end directed and generate inward forces; over-expression of the *S.cerevisiae* kinesin-14, Kar3, shortens the spindle (Saunders et al. 1997) and deletion of *S.pombe* kinesin-14, Klp2, elongates the spindle (Troxell et al. 2001). In *Drosophila*, prometaphase spindles are maintained at a steady-state length by a balance of antagonist motors, KLP61 (kinesin-14) and Ncd (kinesin-5) that bind and cross-link anti-parallel microtubules(Sharp et al. 2000). *In vitro* motility assays demonstrated that at certain concentrations of the two motors a "balance point" is achieved with net zero sliding (Tao et al. 2006). Perturbation of either motor changed spindle length (Civelekoglu-Scholey et al. 2010). Antagonistic motor models of force balance posit spindle length is established independently of attachment, perhaps so that spindle integrity is maintained while microtubules seek and capture chromosomes. We find that in *S.cerevisiae* spindle length is dependent on attachment; a possible benefit of an elongated spindle with few attachments is that it may allow spindle pole bodies to explore more nuclear space in search of chromosomes.

Introducing new chromosome attachments to spindles via synthetic kinetochores in *ndc10-1* cells shortened their spindles (**Figure 2-12**). With each additional synthetic kinetochore pair, the spindle shortened a statistically significant amount. It would be interesting to know whether placing synthetic kinetochores on all 16 chromosomes would lead to wild-type spindle length. When additional kinetochore pairs were introduced via centromeric plasmids, spindle length continued to scale with number of attachments (**Figure 2-15; Figure 2-16**). Cells containing high copy numbers of plasmids were still capable of attaching and bi-orienting chromosomes (**Figure 2-17**), and spindles were capable of nucleating enough microtubules to attach these additional kinetochores (**Figure 2-19; Table 2-2**). Electron microscopy showed that in cells with an average of 23 plasmids/cell, spindle pole bodies nucleated 74 ± 7 microtubules, a

dramatic increase compared to wild-type cells. A cell with 23 plasmids would require 78 microtubules (32 for the 16 endogenous chromosomes, 46 for the 23 plasmids plus a few additional interpolar microtubules), which is within the range of total microtubules. These spindles had an average of 63 identified kinetochore microtubules, fewer than the required 78, but it is possible that spindles were imaged of cells that contained fewer than the average 23 plasmids or that some of the microtubules classified as interpolar microtubules were actually attaching to kinetochores. It is also possible that more than one plasmid attached to a microtubule, perhaps with an lateral rather than end-on attachment. Additional microtubules in the plasmid spindles are kinetochore microtubules; the number of interpolar microtubules did not significantly increase in the presence of extra kinetochores.

While we cannot determine the attachment status of all plasmids, the centromere sequences on the plasmids have been shown to be fully capable of directing the segregation of full length chromosomes (Clarke and Carbon 1980). Thus the result that many extra centromeric plasmids did not abolish bi-orientation of endogenous chromosomes, and the spindle pole bodies were able to nucleate sufficient numbers of microtubules, indicating that all kinetochores on both chromosomes and plasmids were attaching to the spindle. This suggests that shortening of the spindle is caused by the increased numbers of microtubules connecting the spindle poles to the chromosomes. The force balance model predicts that chromosomal attachments provide inward force, and the increasing number of inward force generators pushes the equilibrium toward shorter spindle lengths. Our results show that spindle length scales with the number of chromosomal attachments, which supports the presence of length-dependent forces in the spindle.

While our results provide evidence for their role in spindle length regulation, our results do not reveal which forces are length dependent or the molecular mechanism that produces length dependence. Previous studies in *S.cerevisiae* have documented length-dependent activities of motor proteins and their effect on microtubule dynamics in the spindle. *S.cerevisiae* Kip3 is a kinesin-8 (+) end directed motor that depolymerizes microtubules in a length-dependent manner (Varga et al. 2006). *In vitro* assays showed that Kip3 depolymerized longer microtubules faster than shorter microtubules; the authors proposed that this length-dependent depolymerization could function as a length-control mechanism *in vivo* (Varga et al. 2006). Other studies have modeled length-dependent activity of Cin8 on kinetochore microtubules and Kip3 on interpolar microtubules (Gardner et al. 2008). *In vitro* studies on the *S.pombe* protein Ase1 showed that this passive cross-linking molecule infers length-dependent braking of microtubule sliding (Braun et al. 2011). Ase1 accumulates in the overlap region of cross-linked microtubules; as the overlap regions shrinks due to motor-driven microtubule sliding, Ase1 density increases and velocity of sliding drops to zero (Braun et al. 2011). It is possible that Ase1 binds the overlap region of interpolar microtubules in *S.cerevisiae* and decreases the outward pushing force of Cin8 and Kip1 as the spindle lengthens. Another possible mechanism is that fewer molecules of Cin8 and Kip1 are able to bind in the overlap region and thus force drops with lengthening of the spindle. Both of these mechanism are based on a set length of interpolar microtubules which causes a shortening of the overlap region as spindles elongate (see Chapter 4 for more discussion on possible mechanisms).

We sought to test the predictions of a force-balance model based on length-dependent forces (**Figure 2-1C**), and our results support this model of spindle length regulation. Other models of spindle length regulation are based on chemical gradients or molecular rulers. The

goal of our investigation was to test the specific predictions of the force-balance model, and not to rigorously disprove roles for gradients and molecular rulers in *S.cerevisiae* spindle length regulation. However, our results indicate these other sources of regulation may not play a significant role in *S.cerevisiae*. Proposed molecular rulers include the spindle matrix which is thought to provide mechanical restraint on the length of the spindle (Johansen et al. 2011).The equivalent matrix in *S.cerevisiae* is the nuclear envelope; budding yeast cells perform mitosis within their nucleus without breaking down the envelope. In our experiments, the size or elasticity of the nuclear envelope was not directly manipulated. When chromosomal attachments are inhibited, the spindle elongates which argues against physical restraint by the nuclear envelope. Studies by Witkin et al. showed that synthesis of nuclear envelope continues during mitotic delay resulting in excess membrane that is sequestered near the nucleolus (Witkin et al. 2012), thus the *S.cerevisiae* nuclear envelope is not a structure with finite size and unlikely to provide restraint to spindles.

Two types of chemical gradients have been proposed to play a role in spindle length regulation. In *C.elegans*, a gradient of TPXL-1, a protein involved in localizing Aurora kinase A (Özlü et al. 2005), has been shown to emanate from centrosomes (Greenan et al. 2010). Reducing the size of the centrosome by molecular perturbation alters the TPXL-1 gradient and shortens the spindle. However in our cells with larger spindle poles bodies, the spindle was shorter; spindles containing 23 plasmids had on average larger spindle pole body diameter than wild-type (**Figure 2-20C**). The second type of chemical gradient is the RanGTP gradient shown to form around chromatin in *Xenopus* extracts (Bastiaens et al. 2006). Ran's guanine nucleotide exchange factor RCC1 binds chromatin, creating a Ran-GTP around chromatin, which promotes the release of spindle assembly factors and microtubule nucleation around chromosomes

(Carazo-Salas et al. 2001; Wilde et al. 2001). Ran-GTP gradients form around chromatin, and in our experiments detaching chromosomes from the spindle, we did not alter the amount of chromatin present yet spindle elongated. Likewise, in cells with 20 plasmids the chromatin content was only increased by 2.5% but spindle length shortened by 31% (**Figure 2-15**). We cannot rule out regulation of spindle length by gradients emanating from kinetochores, as kinetochore number and function was altered in this study. Eliminating this possibility would require enough knowledge to manipulate molecules that were predicted to create such a gradient. We note that the one known kinetochore-based signaling pathway, the spindle checkpoint, was inactive in the experiments with extra kinetochores arguing that the checkpoint cannot be responsible for alterations in spindle length or microtubule number.

One strength of our investigation is that we were able to measure the effect of chromosomal attachment on spindle length without altering ploidy. Previous studies on *S.cerevisiae* had shown that altering ploidy does not change spindle length; haploid, diploid, triploid and tetraploid cells all had the same spindle length (Lin et al. 2001; Storchová et al. 2006). However, by manipulating number of attachments in a haploid we were able to avoid any possible confounding variables that changing ploidy introduces, such as altering the number of interpolar microtubules, chromatin content, genomic stability, cellular volume (Storchová et al. 2006) or spindle pole body size (Winey and Bloom 2012), and we thus isolated the effect of attachment number on spindle length.

Kinetochores increase microtubule number

During our investigation of spindle length regulation, we generated yeast cells with 30+ plasmids, which after replication presents the cell with 60+ more centromeres than its

endogenous 32 centromeres, tripling the total number of centromeres. Previous studies have shown that as few as five centromeric plasmids can be toxic to cells, causing mitotic delay and cell death (Futcher and Carbon 1986). It has been hypothesized that extra centromeres titrate away limited amounts of kinetochore proteins or microtubules needed for natural chromosomes (Futcher and Carbon 1986; Runge et al. 1991). Wells and Murray (1996), negated this argument by showing that deleting the spindle checkpoint abolished both the cell cycle delay and lethality caused by as many as 8 extra centromeres. Our results extended this conclusion by showing that cells with 30+ plasmids could still bi-orient their endogenous chromosomes and grow normally and produce viable daughters, suggesting that neither kinetochore nor spindle pole body components limit the number of functional kinetochores that a yeast cell can segregate. High-resolution electron tomography showed that haploid yeast spindle pole bodies could increase in size and produce more microtubules to meet this higher demand. The number of microtubules previously observed in yeast spindles has matched the number of chromosomes: a single spindle pole body produces approximately 20 microtubules in haploids (16 chromosomes), 36 in diploids (32 chromosomes), and 65 in tetraploids (64 chromosomes) (Winey et al. 1995; Winey et al. 2005; Storchová et al. 2006). However, these changes in microtubule number were accompanied by changes in ploidy, and it was unclear within a cell of a given ploidy how the number of microtubules is regulated.

In cells arrested in metaphase for four hours by a *cdc20* temperature sensitive mutation, spindles had increased numbers of microtubules (average 81 microtubules in *cdc20* compared to 44 in wild-type) (O'Toole et al. 1997). It was hypothesized that the prolonged mitotic arrest mimicked prolonged activation of the spindle checkpoint, and that mitotic delay led to increased microtubule nucleation, possibly as a mechanism to increase the capture of unattached

kinetochores (Winey and Bloom 2012). Our strains with extra plasmids did not contain a functional spindle checkpoint as deletion of Mad2p was necessary to achieve high plasmid copy number, yet the number of microtubules increased and roughly matched the number of kinetochores (average 74 microtubules for an average of 78 kinetochores). Thus it is unlikely that the spindle checkpoint is solely responsible for regulating microtubule number. Perhaps the yeast spindle pole bodies nucleate many more than the observed numbers of microtubules, but only those attached to kinetochores are stabilized and visualized by electron microscopy. Adding synthetic kinetochores increases the number of microtubules in cells that lack normal kinetochores. *ndc10-1* spindles have reduced numbers of microtubules (**Figure 2-4; Table 2-1**; Romao et al. 2008), but introducing synthetic kinetochores increases microtubule number. These spindles still have defects in spindle integrity (Cell 4 with no interpolar microtuubles and monopolar Cell 2), but when two spindle bodies are found within a spindle, there are more total microtubules and they have a more symmetric distribution. These spindle reconstructions indicate that the both poles are functional and microtubules are stabilized. The number of microtubules is not tightly coupled to number of kinetochores in *ndc10-1* spindles; microtubules are seen from at least one pole even though checkpoint assays suggest there are no functional kinetochores (**Figure 2-3B**). Romao et al showed that in *ndc10-1* spindles, microtubules from the original spindle pole remain stabilized while newly synthesized poles have difficulty producing microtubules (2008). We can account for this difference in two ways. The first is that kinetochores remain intact during DNA replication and the old kinetochore remains attached to the old spindle pole body. The second is that microtubule binding sites on the new spindle pole cannot produce stable microtubules until they have been connected to a kinetochore. We favor the second possibility since the first requires two additional restrictions: previously assembled

kinetochores are not disassembled when *ndc10-1* cells are incubated at 37°C and they are unable to activate the spindle checkpoint. Microtubules nucleated from the old spindle pole body are found throughout the cell cycle and may have other options for stabilization (Winey and O'Toole 2001). It is interesting to note that the *ndc10-1*+ 3 synthetic kinetochore pairs spindles have many more than 3 kinetochore microtubules from the new pole, which is the number expected if each synthetic kinetochore attached to one microtubule. Synthetic kinetochores are constructed from 256 repeat arrays, which allow a maximum of 512 molecules of Ask1-LacI to bind. Quantification of kinetochore proteins suggests that 16-20 molecules of Ask1p are present in a natural yeast kinetochore (Joglekar et al. 2008), so each synthetic kinetochore has sufficient Ask1p to attach many more than one microtubule. It will be interesting to investigate the architecture of the synthetic kinetochore, as it may create a kinetochore similar to species with multiple microtubule attachments per kinetochore. The addition of either normal or synthetic kinetochores specifically increases the number microtubules classified as kinetochore microtubules (**Table 2-1**, **Table 2-2**).

Our studies show that spindle length varies with the number of chromosomal attachments which supports a model of spindle length regulation by a balance of length-dependent forces. Our investigation also revealed that kinetochores increase the number of microtubules in the *S.cerevisiae* spindle. *S.cerevisiae* have very simple spindles with few components compared to the complex spindles of higher eukaryotes. Balance of length-dependent forces may represent the most basic level of spindle length regulation, and higher eukaryotes may have evolved additional layers of length regulation for their complex spindles.

METHODS and MATERIALS

Yeast strains and cell culturing

Strains used in this study are listed in **Table 2-3**. All yeast strains were constructed in W303 background (*ade2-1 his3-11,15 leu2-3,112 trp1-1 ura3-1 can1-100*) and were constructed using standard genetic techniques. High copy centromeric plasmid strains were constructed by transformation of the plasmid, followed by growth in copper sulfate ($CuSO_4$). Growth in successively higher $CuSO_4$ concentration drives up the copy number of the plasmid; cultures began in 0.01mM $CuSO_4$ and were passaged until resistant to 2.0-4.0mM $CuSO_4$. All media were prepared by standard recipes (Sherman et al. 1974), and contained 2% wt/vol of specified sugar. Cells were grown in either YPD (2% glucose) or Synthetic Complete media (2% glucose) without methionine (SC-Met) at 23°C for temperature sensitive strains or 30°C for all others. *GAL-MCD1* cells were grown in SC-Met + 2% galactose. YPD containing 1-(butylcarbamoyl)-2-benzimidazolecarbamate (benomyl) and nocodazole was prepared by heating YPD to 65°C and adding dimethyl sulfoxide (DMSO) 10mg/ml stocks of benomyl dropwise to a final concentration of 30µg/ml; media was cooled to 37°C for dropwise addition of DMSO 10mg/ml stock of nocodazole to a final concentration of 30µg/ml. All drugs and chemicals were purchased from Sigma Aldrich.

Fluorescence microscopy imaging

Images were acquired at room temperature (25°C) using a Nikon Eclipe Ti-E inverted microscope with a 60x Plan Apo VC, 1.4 NA oil objective lens with a Photometrics CoolSNAP HQ camera (Roper Scientific). Metamorph 7.7 (Molecular Devices) was used to acquire z-series image stacks with z-step size of 200nm and 21 total z-planes. Spindle pole bodies were labeled with mCherry (Spc42-mCherry) and chromosomes were labeled with GFP by a 256 lacO repeat

array inserted near the centromere and expression of monomeric yeast optimized GFP fused to lacI. Fixed samples were imaged in 1.2M Sorbitol + 0.1M KH_2PO_4 pH8.5 buffer on Concanavalin A-coated coverslips (VWR) adhered to glass slides (Corning). Exposure times were 10ms for differential interference contrast images and 300ms for fluorescent images.

Electron microscopy and 3-D spindle reconstruction

Strains were prepared for electron microscopy as described in Giddings et al., 2001. Aliquots from liquid cultures were collected onto a 0.45 um milipore filter by vacuum filtration, loaded into freezer hats and frozen using a Wohlwend Compact 02 high pressure freezer. The frozen samples were freeze substituted in 0.25% glutaraldehyde and 0.1% uranyl acetate in acetone for three days at -90°C. The samples were then warmed to -20°C, rinsed in acetone and embedded in Lowicryl HM20 resin. Serial sections (250nm) were collected onto formvar-coated slot grids and post stained using 2% aqueous uranyl acetate followed by lead citrate. Colloidal gold particles (15nm) were affixed to the sections to serve as alignment markers.

Tomography was performed as described in Giddings et al., 2001 and O'Toole et al., 2002. Dual axis tilt series data were collected using a Technai F20 or F30 intermediate electron microscope operating at 200 or 300 kV, respectively. The SerialEM program (Mastronarde 2005) was used to automatically acquire images every one degree over a $\pm$60 degree range. Data was acquired at a pixel size of 1-1.5 nm using a Gatan CCD camera. The tilt series images were aligned and tomograms computed using the IMOD software package (Mastronarde 1997). The mitotic spindles examined spanned 2-5 serial sections. Tomograms were computed from each section and then joined to produce the final volume of the spindle. In total, four wild type, four 23 plasmid, three 11 plasmid, three *ndc10-1*, and three *ndc10-1* + 3 synthetic kinetochore pairs were reconstructed.

Tomograms were displayed and modeled using the 3dmod program in the IMOD software package (Kremer et al. 1996). Spindle microtubules originating from each pole were modeled in the tomographic volume. The core bundle microtubules were identified using the mtpairing program in the IMOD software package and described in Winey et al., 1995). The program, fiberpitch, was used to measure the pitch angle of microtubules from the spindle axis.

Spindle checkpoint activation by benomyl and nocodazole.

Strains were grown in YPD at the permissive temperature of 23°C and maintained in log phase for 24 hours before the experiment. Log phase cells (~$5x10^6$ cells/ml) were arrested in G1 with 10μg/ml α factor (Bio-Synthesis) for 2.5 hours at 23°C, then moved to 37°C for 30 minutes. After confirmation of arrest by light microscopy, cells were washed three times with YPD at 37°C to remove α factor and resuspended in YPD + 30μg/ml benomyl + 30μg/ml nocodazole. Cells were grown for 4 hours at 37°C, sonicated to separate cells, then scored for cell morphology by light microscopy. Large-budded cells are indicative of spindle checkpoint-induced mitotic arrest.

Measuring metaphase spindle length, chromatin stretch and bi-orientation.

Strains were grown to log phase in SC-Met media at either 23°C for experiments with temperature sensitive alleles or 30°C for experiments with centromeric plasmids. For *GAL-MCD1* experiments, cells were grown to log phase in SC-Met + 2% galactose. Log phase cells (~$5x10^6$ cells/ml) were arrested in G1 by α factor treatment (10μg/ml). In *ndc10-1* experiments, cells were arrested at 23°C for 3 hours, methionine was added (500μg/1ml) to induce Cdc20p deletion, then cells were incubated for an additional 1hour at 37°C. Cells were washed three times and at 37°C with YPD + methionine and grown 3 hours in YPD + methionine at 37°C. For experiments with centromeric plasmids and *GAL-MCD1*, strains were arrested with α factor

at 30°C for 3 hours, with methionine addition after 2.5 hours. Cells were washed 3 times and released into YPD + methionine and grown at 30°C for 3 hours. In all experiments, after 3 hour post-release cells were fixed with 10% formalin (final concentration of 1%) for 10 minutes, washed with 0.1M KH_2PO_4 pH8.5, washed with 1.2M Sorbitol + 0.1M KH_2PO_4 pH8.5, resuspended in 1.2M Sorbitol + 0.1M KH_2PO_4 pH8.5, and stored at 4°C.

Samples were imaged as described above. Spindle length was calculated as the three-dimensional distance between mCherry-labeled spindle pole bodies, and chromatin stretch distance was calculated as the three-dimensional distance between GFP- chromatin dots. In brief, we used the MOSAIC 3D Single-Particle Tracking ImageJ software (Sbalzarini and Koumoutsakos 2005) to achieve subpixel and sub z-plane resolution of spindle pole body or chromatid location in x,y,z dimensions. The sub-pixel x and y location of the particle (spindle pole body or chromatid) was determined by fitting the pixel of peak fluorescence intensity and its surrounding pixels with a uniform Gaussian; x and y coordinates were the peak value of the Gaussian. To determine the sub-plane z-position of the particle, a uniform Gaussian was fitted to the peak plane and its surrounding planes (Sbalzarini and Koumoutsakos 2005). Once the x,y, and z coordinates of the particles were determined, a MATLAB (MathWorks) script was used to pair the nearest neighbor particles and calculate distance between the two paired coordinates. Given the average signal-to-noise ratio in our fluorescent images, particle position can theoretically be determined with accuracy to within 1nm (Sbalzarini and Koumoutsakos 2005) however this is under the assumption that the particle is smaller than the resolution of light. **Figure 2-21** shows an example of spindle pole body identification and pairing; spindle pole bodies are labeled with Spc42-mCherry and appear as white dots. The original fluorescent image is shown in **Figure 2-21A**; for simplification, all images in Figure 2-21 are shown as z-

projections of maximum intensity to collapse all z-planes into a single image. However, all z-planes were used for coordinate identification. In **Figure 2-21B**, spindle pole bodies identified by the MOSAIC software are circled in blue. Spindle pole bodies that were paired with another pole by MATLAB are denoted by pink circles, the calculated spindle length is represented by the pink line (**Figure 2-21C**). Green circles are identified poles that were not paired because no pole was found within the designated distance from it. The percentage of bi-orientated chromosomes was calculated as the number of chromosomes with two resolvable GFP dots out of all chromosomes scored.

Qunantifying plasmid copy number

Centromeric plasmid copy was determined by quantitative PCR. Genomic DNA was purified from cells and quantified using Qubit 2.0 Fluorometer (Invitrogen). Quantitative PCR was performed with 0.5ng of template DNA, 0.4mM of forward and reverse primers, and PerfeCta SYBR Green FastMix, Rox mastermix in a 7900 Real-Time PCR machine (Applied Biosystems) with an annealing temperature of 55°C. Control primers (forward: 5'-GTTTAATCCGGGCTGGTTCCAT-3'; reverse: 5'-TAGACCCAGTGGACAGATAGCG-3') amplified a 113bp fragment of gene ALG9 and experimental primers (forward: 5'-GGAAAAAAAGCACTACCTAGGAGCGGCC-3'; reverse: 5'-CTGTGACGATAAAACCGGAAGGAAG-3') amplified 127bp near CEN4, the centromere on the plasmid.

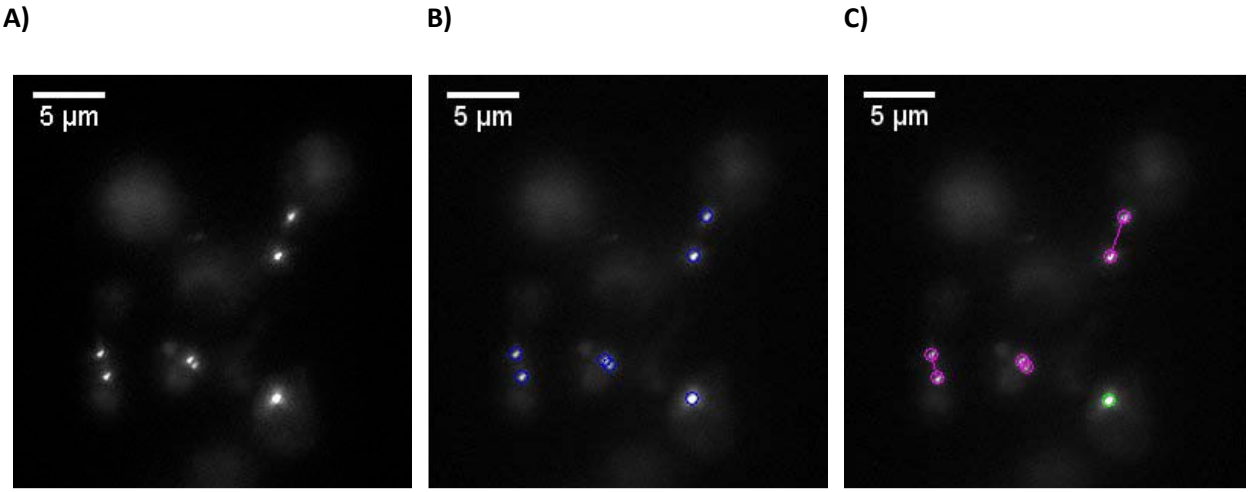

Figure 2-21. Identification and pairing of particles. Spindle pole bodies labeled by Spc42-mCherry and sister chromatids labeled with GFP were identified using the MOSIAC 3D Single-Particle Tracking ImageJ software. The images in (**A**), (**B**) and (**C**) are 2-D maximum intensity projections of all z-planes, but z-plane information was used to determine the z coordinate. The starting image for analysis is shown in (**A**); spindle pole bodies appear as white dots. In (**B**) spindle pole bodies are identified using the algorithm described in the text and in Sbalzarini and Koumoutsakos 2005. The reported x,y,z location of the spindle pole body is at the center of the blue circle. Coordinates were analyzed with MATLAB to find the nearest neighbor particle and calculate the distance between the paired particles (**C**). Spindle pole bodies that were paired are represented by a pink circle; the pink line connecting the two circles is a 2D representation of the calculated spindle length. Green circles represent identified poles that did not have a pairing partner given a distance cut-off for spindle length.

Table 2-3. Strains used in Chapter 2

Strain Name	Genotype
yNJN1	*MATa ade2-1 can1-100 his3-11,15 leu2-3,112 trp1-1 ura3-1* *(all other strains are derivatives of W303with the same auxotrophies)*
yNJN258	*MATa P_{Met}-HA3-Cdc20::TRP1 Spc42-mCherry::HIS3*
yNJN270	*MATa P_{Met}-HA3-Cdc20::TRP1 Spc42-mCherry::HIS3 CEN15::LacO(256)::URA3 Spc42-mCherry::KanMX ctf13-30*
yNJN271	*MATa P_{Met}-HA3-Cdc20::TRP1 CUP1Δ::HIS5sp MAD2Δ::KanMX Spc42-mCherry::HIS3*
yNJN273	*MATa P_{Met}-HA3-Cdc20::TRP1 CUP1Δ::HIS5sp MAD2Δ::KanMX Spc42-mCherry::HIS3 Centromeric plasmid: CEN4 CUP1 LEU2*
yNJN276	*MATa P_{Met}-HA3-Cdc20::TRP1 P_{CUP1}-GFP-$LacI_2$::HIS3 CEN15::LacO(256)::URA3 Spc42-mCherry::HIS3 ndc10-1*
yNJN292	*MATa P_{Met}-HA3-Cdc20::TRP1 P_{CUP1}-GFP-$LacI_2$::HIS3 CEN15::LacO(256)::URA3 CEN3::LacO(256)::LEU2 CEN8::LacO(256)::TRP1 Spc42-mCherry::HIS3 P_{HIS3}-ASK1-$LacI_2$:: ADE2 ndc10-1*
yNJN294	*MATa P_{Met}-HA3-Cdc20::TRP1 Spc42-mCherry::HIS3 cep3-2*
yNJN300	*MATa P_{Met}-HA3-Cdc20::TRP1 P_{CUP1}-GFP-$LacI_2$::HIS3 CEN15::LacO(256)::URA3 Spc42-mCherry::HIS3 P_{HIS3}-ASK1-$LacI_2$:: ADE2 ndc10-1*
yNJN302	*MATa P_{Met}-HA3-Cdc20::TRP1 P_{CUP1}-GFP-$LacI_2$::HIS3 CEN15::LacO(256)::URA3 CEN3::LacO(256)::LEU2 Spc42-mCherry::HIS3 P_{HIS3}-ASK1-$LacI_2$:: ADE2 ndc10-1*
yNJN360	*MATa P_{Met}-HA3-Cdc20::TRP1 Spc42-mCherry::KanMX KIP1Δ::HIS3*
yNJN323	*MATa P_{Met}-HA3-Cdc20::TRP1 Spc42-mCherry::HIS3 CUP1Δ::HIS5sp P_{HIS3}-GFP-$LacI_2$:: ADE2 CEN3::LacO(256)::URA3*
yNJN324	*MATa P_{Met}-HA3-Cdc20::TRP1 Spc42-mCherry::HIS3 CUP1Δ::HIS5sp P_{HIS3}-GFP-$LacI_2$:: ADE2 CEN3::LacO(256)::URA3; Centromeric plasmid: CEN4 CUP1 LEU2*
yNJN417	*MATa P_{Met}-HA3-Cdc20::TRP1 Spc42-mCherry::KanMX P_{TUB1}-GFP-TUB1::URA3 ndc10-1 kip1Δ::Clonat*
yNJN478	*MATa P_{Met}-HA3-Cdc20::TRP1 CEN15::LacO(256)::URA3 P_{CUP1}-GFP-$LacI_2$::HIS3 Spc42-mCherry::KanMX P_{GAL1}-3HA-MCD1::TRP1*

Table 2-3 (continued). Strains used in Chapter 2

Strain Name	Genotype
DLY453	*MATa* P_{Met}*-HA3-Cdc20::TRP1 Spc42-mCherry::KanMX* P_{HIS3}*-GFP-LacI*$_2$*::ADE2 LacO(256)::LEU2* P_{HIS3}*-ASK1-LacI*$_2$*:: HIS3 URA3::ChromIII 116k* P_{GAL1}*-CEN3::TRP1 ctf13-30*
VBI885	*MATa* P_{Met}*-HA3-Cdc20::TRP1 Spc42-mCherry::KanMX* P_{CUP1}*-GFP-LacI*$_2$*::HIS3 CEN15::LacO(256)::URA3 bar1*Δ
SLY237	*MATa mad2*Δ*::KanMX*
SLY840	*MATa ndc10-1*
yBS86	*MATa ndc10-2*
yBS87	*MATα ctf13-30*
yBS89	*MATa cep3-2*
yBS345	*MATa TRP1 scc1-73*

REFERENCES

Bastiaens P. M. Caudron, P. Niethammer, E. Karsenti. 2006. Gradients in the self-organization of the mitotic spindle. *Trends Cell Biol* 16: 125-134.

Bloom K. and A. Joglekar. 2010. Towards building a chromosome-segregation machine. *Nature* 463: 446-456.

Bouck D. and K. Bloom. 2005. The role of centromere-binding factor 3 (CBF3) in spindle stability, cytokinesis, and kinetochore attachment. *Biochem Cell Biol* 83: 696-702.

Braun M., Lansky Z., Fink G., Ruhnow F., Diez S. and M.E. Janson. 2011. Adaptive braking by Ase1 prevents overlapping microtubules from sliding completely apart. *Nat Cell Biol* 13: 1259-1264.

Carazo-Salas R.E., Gruss O.J., Mattaj I.W. and E. Karsenti. 2001. Ran-GTP coordinates regulation of microtubule nucleation and dynamics during mitotic-spindle assembly. *Nat Cell Biol* 3: 228-234.

Caudron M., G. Bunt, P. Bastiaens, E. Karsenti.. 2005. Spatial coordination of spindle asssembly by chromosome-mediated signaling gradients. *Science* 309: 1373-1376.

Civelekoglu-Scholey G., L. Tao, R. Wollman, I. Brust-Mascher, P. Sommi, A. Mogilner, J.M. Scholey. 2010. Prometaphase spindle maintenance by an antagonistic motor-dependent force-balance made robust by a disassembling lamin B envelope. *J Cell Biol* 188: 49-68.

Clarke L. and J. Carbon. 1980. Isolation of a yeast centromere and construction of functional small circular chromosomes. *Nature* 287: 504-509.

Futcher B. and J. Carbon. 1986. Toxic effects of excess cloned centromeres. *Mol Cell Biol* 6: 2213-2222.

Gardner R.D., Poddar A., Yellma C., Tavormina P.A., Monteagudo M.C. and D.J. Burke. 2001. The spindle checkpoint of the yeast *Saccharomyces cerevisiae* requires kinetochore function and maps to the CBF3 domain. *Genetics* 157: 1493-1502.

Gardner M.K., Bouck D.C., Paliulis L.V., Meehl J.B., O'Toole E., Haase J., Soubry A., Joglekar A.P., Winey M., Salmon E.D., Bloom K. and D.J. Odde. 2008. Chromosome congression by kinesin-5 motor-mediated disassembly of longer kinetochore microtubules. *Cell* 135: 894-906.

Goh P.Y. and J.V. Kilmartin. 1993. NDC10: a gene involved in chromosome segregation in *Saccharomyces cerevisiae*. *J Cell Biol* 121: 503-512.

Goshima G and M Yanagida. 2000. Establishing biorientation occurs with precocious separation of the sister kinetochores, but not the arms, in the early spindle of budding yeast. *Cell*, 100: 619-33.

Goshima G., Wollman R., Stuurman N., Scholey J.M. and R.D.Vale. 2005. Length control of the metaphase spindle length. *Curr Biol* 15: 1979-1988.

Goshima G. and J. Scholey. 2010. Control of mitotic spindle length. *Annu Rev Cell Dev Biol* 26: 21-57.

Greenan G. C.P. Brangwynne, S. Jaensch, J. Gharakhani, F. Julicher, A.A. Hyman. 2010. Centrosome size sets mitotic spindle length in *Caenorhabditis elegans* embryos. *Curr Biol* 20: 353-358.

Halpin D., P. Kalab, J. Wang, K. Weis, R. Heald. 2011. Mitotic spindle assembly around RCC1-coated beads in Xenopus egg extracts. *PLoS Biol* 9:

Heald R., Tournebize R., Blank T., Sandaltzopoulos R., Becker P., Hyman A.A. and E., Karsenti. 1996. Self-organization of microtubules into bipolar spindles around artificial chromosomes in *Xenopus* egg extracts. *Nature* 382: 420-425.

Joklekar A.P., Salmon E.D. and K.S. Bloom. 2008. Counting kinetochore protein numbers in budding yeast using genetically encoded fluorescent protesin. *Methods Cell Biol* 85: 127-151.

Johansen, K.M., A. Forger, C. Yao, J. Girton, J. Johansen. 2011. Do nuclear envelope and intranuclear proteins reorganize during mitosis to form an elastic, hydrogel-like spindle matrix? *Chromosome Res*. 19: 345-365.

Kalab P. and R. Heald. 2008. The RanGTP gradient- a GPS for the mitotic spindle. *J Cell Sci* 121: 1577-1586.

Kane R.E. and A. Forer. 1965. The mitotic apparatus. Structural changes after isolation. *J Cell Biol* 25: 31-39.

Karin M., Najarian R., Haslinger A., Valenzuela P., Welch J. and S. Fogel. 1984. Primary structure and transcription of an amplified genetic locus: the CUP1 locus of yeast. *Proc Natl Acad Sci USA* 81: 337-341.

Katsura I. 1987. Determination of bacteriophage lambda tail length by a protein ruler. *Nature* 327: 73-75.

Katsura I. 1990. Mechanism of length determination in bacteriophage lambda tails. *Adv Biophys* 26: 1-18.

Kiermaier E., Woehrer S., Peng Y., Mechtler K. and S. Westermann. 2009. A Dam1-based artificial kinetochore is sufficient to promote chromosome segregation in budding yeast. *Nat Cell Biol* 11: 1109-1115.

Kramer J. and R.S. Hawley. 2003. The spindle-associated transmembrane protein Axs identifies a membranous structure ensheathing the meiotic spindle. *Nat Cell Biol* 5: 261-263.

Kremer J.R., Mastronarde D.N. and J.R. McIntosh. 1996. Computer visualization of three-dimensional image data using IMOD. *J Struct Biol* 116: 71-76.

Lacefield S., Lau D.T.C. and A.W. Murray. 2009. Recruiting a microtubule-binding complex to DNA directs chromosome segregation in budding yeast. *Nat Cell Biol* 11: 1116-1120.

Lin H., Carvalho P., Kho D., Tai C-Y., Pierre P., Fink G.R. and D. Pellman. 2001. Polyploids require Bik1 for kinetochore-microtubule attachment. *J Cell Biol* 155: 1173-1184.

Liu Z. and Y. Zheng. 2009. A requirement for epsin in mitotic membrane and spindle organization. *J Cell Biol* 186: 473-480.

Loughlin R., Wilbur J.D., McNally F.J., Nédélec, and R. Heald. 2011. Katanin contributes to interspecies spindle length scaling in *Xenopus*. *Cell* 147: 1397-1407.

Ma L., M.Y. Tsai, S. Wang, B. Lu, R. Chen R., Yates III J.R., Zhu X. and Y. Zheng. 2009. Requirement for NudeI and dynein for assembly of the lamin B spindle matrix. *Nat Cell Biol* 11: 247-256.

Mastronarde D.N. 1997. Dual-axis tomography: an approach with alignment methods that preserve resolution. *J Struct Biol* 120: 343-352.

Mastronarde D.N. 2005. Automated electron microscope tomography using robust prediction of specimen movements. *J Struct Biol* 152: 36-51.

Muller-Reichert T., Sassoon E., O'Toole E., Romao M., Ashford A.J., Hyman A.A. and C. Antony. 2003. Analysis of the distribution of the kinetochore protein Ndc10p in *Saccharomyces cerevisiae* using 3-D modeling of mitotic spindles. *Chromosoma* 111: 417-428.

O'Toole E.T. Mastonarde D.N., Giddings Jr T.H., Winey M., Burke D.J. and J.R. McIntosh. 1997. Three-dimensional analysis and ultrastructural design of mitotic spindles from the *cdc20* mutant of *Saccharomyces cerevisiae*. *Mol Biol Cell* 8: 1-11.

O'Toole E.T., Winey M., McIntosh J.R., and D.N. Mastronarde. 2002. Electron tomography of yeast cells. *Methods Enzymol* 351: 81-95.

Özlü N., Srayko M., Kinoshita K., Habermann B., O'Toole E., Müller-Reichert T., Schmalz N., Desai A., and A.A. Human. 2005. An essential function of the *C.elegans* ortholog of TPX2 is to localize activated Aurora A kinase to mitotic spindles. *Dev Cell* 9: 237-248.

Rebhun L.I. and R.E. Palazzo. 1988. In vitro reactivation of anaphase B in isolated spindles of sea urchin egg. *Cell Motil Cytoskel* 10: 197-209.

Romao M., Tanaka K., Sibarita J.B., Ly-Hartig N.T., Tanaka T.U. and C. Antony. 2008. Three-dimensional electron microscopy analysis of *ndc10-1* mutant reveals an aberrant organization of the mitotic spindle and spindle pole body defects in *Saccharomyces cerevisiae*. *J Struct Biol* 163: 18-28.

Runge K.W., Wellinger R.J. and V.A. Zakian. 1991. Effects of excess centromeres and excess telomeres on chromosome loss rates. *Mol Cell Biol* 14 8282-8291.

Saunders W.S., Lengyel V. and M.A. Hoyt. 1997. Mitotic spindle function in *Saccharomyces cerevisiae* requires a balance between different types of kinesin-related motors. *Mol Biol Cell* 8: 1025-1033.

Sbalzarini I.F. and P. Koumoutsakos. 2005. Feature point tracking and trajectory analysis for video imaging in cell biology. *J Struct Biol* 151: 182-195.

Sharp D.J., Brown H.M., Kwon M., Rogers G.C., Holland G., and J.M. Scholey. 2000. Functional coordination of three mitotic motors in *Drosophila* embryos. *Mol Biol Cell* 11: 241-253.

Sherman F., Fink G., and C. Lawrence. 1974. Methods in Yeast Genetics. New York: Cold Spring Harbor Laboratory Press.

Stephens A.D., Haase J., Vicci L., Taylor II R.M. and K. Bloom. 2011. Cohesin condensin and the intramolecular centromere loop together generate the mitotic chromatin spring. *J Cell Biol* 193: 1167-1180.

Stephens A.D., Haggerty R.A., Vasquez P.A., Vicci L., Snider C.E., Shi F., Quammen C., Mullins C., Haase J., Taylor R.M. II, Verdaasdonk J.S., Falvo M.R., Jin Y., Forest M.G. and K. Bloom. 2013. Pericentric chromatin loops function as a nonlinear spring in mitotic force balance. *J Cell Biol* 200: 757-772.

Storchová Z., Breneman A., Cande J., Dunn J., Burbank K., O'Toole E. and D. Pellman. 2006. Genome-wide genetic analysis of polyploidy in yeast. *Nature* 443: 541-547.

Straight A.F., Belmont A.S., Robinett C.C. and A.W. Murray 1996. GFP tagging of budding yeast chromosomes reveals that protein-protein interactions can mediate sister chromatid cohesion. *Curr Biol* 6: 1599-15608.

Straight A.F., Marshall W.F., Sedat J.W. and A.W. Murray. 1997. Mitosis in living budding yeast: anaphase A but no metaphase plate. *Science* 277: 574-578.

Straight A.F., Sedat J.W., and A.W. Murray 1998. Time-lapse microscopy reveals unique roles for kinesins during anaphase in budding yeast. *J Cell Biol* 143: 687-694.

Tanaka T. 2008. Bi-orienting chromosomes: acrobatics on the mitotic spindle. *Chromosoma* 117: 521-533.

Tao L., Mogilner A., Civelekoglu-Scholey G., Wollman R., Evans J., Stahlberg H., and J.M. Scholey. 2006. A homotetrameric kinesin-t, KLP61F, bundles microtubules and antagonizes Ncd in motility assays. *Curr Biol*. 16: 2293-22302.

Teste M.A., Duquenne M., François J.M. and J.L. Parrou. 2009. Validation of reference genes for quantitative expression analysis by real-time RT-PCR in *Saccharomyces cerevisiae*. *BMC Mol Biol* 10: 99-114.

Troxell C.L., Sweezy M.A., West R.R., Reed K.D., Carson B.D., Pidoux A.L., Cande W.Z. and J.R. McIntosh. 2001. *pkl1+* and *klp2+* : Two kinesins of the Kar3 subfamily in fission yeast perform different function in both mitosis and meiosis. *Mol Biol Cell* 12: 3476-3488.

Tsai, M.Y., S. Wang, J.M. Heidinger, D.K. Shumaker, S.A. Adam, R.D. Goldman, Y. Zheng. 2006. A Mitotic Lamin B Matrix Induced by RanGTP Required for Spindle Assembly. *Science* 311: 1887-1893.

Varga V., Helenius J., Tanaka K., Hyman A.A., Tanaka T.U. and J. Howard. 2006. Yeast kinesin-8 depolymerizes microtubules in a length-dependent manner. *Nat Cell Biol* 8: 957-962.

Welch J.W., Fogel S., Cathala G., and M. Karin. 1983. Industrial yeasts display tandem gene iteration at the CUP1 region. *Mol Cell Biol* 3: 1353-1361.

Wells W.A. and A.W. Murray. 1996. Aberrantly segreagting centromeres activate the spindle assembly checkpoint in budding yeast. *J Cell Biol* 133: 75-84.

Westermann S., Avila-Sakar A., Wang H.W., Niederstrasser H., Wong J., Drubin D.G., Nogales E., and G. Barnes. 2005. Formation of a dynamic kinetochore-microtubule interface through assembly of the Dam1 ring complex. *Mol Cell* 17: 277-290.

Winey, M. Mamay C.L., O'Toole E.T., Mastronarde D.N. Giddings Jr T.H., McDonald K.L. and J.R. McIntosh. 1995. Three-dimensional ultrastructural analysis of the *Saccharomyces cereivisiae* mitotic spindle. *J Cell Biol* 129: 1601-1615.

Winey M. and E.T. O'Toole. 2001. The spindle cycle in budding yeast. *Nat Cell Biol* 3: E23-27.

Winey M. and K. Bloom. 2012. Mitotic spindle form and function. *Genetics* 190: 1197-1224.

Witkin K.L., Chong Y., Shao S., Webster M.T., Lahiri S., Walters A.D., Lee B., Koh J.L., Prinz W.A., Andrew B.J. and O. Cohen-Fix. The budding yeast nuclear envelope adjacent to the nucleolus serves as a membrane sink during mitotic delay. *Curr Biol* 22: 1128-1133.

Wühr M., Chen Y., Dumont S., Groen A.C., Needleman D.J., Salic A., and T.J. Mitchison. 2008. Evidence for an upper limit to mitotic spindle length. *Curr Biol* 18: 1256-1261.

Yao, C. U. Rath, H. Maiato, D. Sharp, J. Girton, K.M. Johansen and J. Johansen. 2012. A nuclear-derived proteinaceous matrix embeds the microtubules spindle apparatus during mitosis. *Mol Biol Cell*. 18: 3532-3541.

Chapter Three:

The spindle checkpoint does not monitor stretching of pericentric chromatin

ABSTRACT

The spindle checkpoint is a surveillance mechanism that ensures dividing cells receive one copy of each chromosome; it prevents the transition from metaphase to anaphase until all chromosomes are correctly attached to the spindle. The checkpoint monitors both attachment of kinetochores and the tension generated by a correct attachment. Tension is created when sister kinetochores are attached to and pulled toward opposite poles, but are held together by cohesin until anaphase; this forces stretches the chromatin around centromeres and elongates kinetochores. Despite its importance, how and where tension is monitored by the checkpoint is unclear. Inter-kinetochore models predict that the distance between kinetochores caused by chromatin stretching is monitored, while intra-kinetochore models posit that the checkpoint measures separation within the kinetochore. To distinguish between these two models, we inhibited chromatin stretch by tethering sister chromatids together using the cross-linking properties of the tetrameric form of the Lac repressor. Inhibition of chromatin stretch did not activate the spindle checkpoint; cells with inhibited stretch passed through mitosis on the same time scale as control cells that express a dimeric version of the Lac repressor that cannot cross link chromatids and spindle checkpoint deleted cells. The spindle checkpoint remains functional as chromatin stretch-inhibited cells could still arrest in response to microtubule-depolymerizing drugs. Our results indicate that the spindle checkpoint does not measure tension by the separation of kinetochores.

INTRODUCTION

The faithful segregation of genetic material during cell division is essential for an organism's viability. Mistakes in this process can lead to aneuploidy (Siegel and Amon 2012), a hallmark of cancer (Kops et al. 2005) and birth defects (Driscoll and Gross 2009) To ensure proper division of chromosomes, eukaryotes have evolved the spindle assembly checkpoint. The spindle checkpoint operates through the kinetochore, a large multi-protein complex that assembles on centromeres and facilitates microtubule attachment to the chromosomes. In *Saccharomyces cerevisiae*, the kinetochore consists of over 65 proteins that bind the conserved 125bp centromere (Westermann et al. 2007). The spindle checkpoint delays the onset of anaphase until all chromosomes are properly aligned and bi-oriented on the mitotic spindle (Li and Murray 1991; Hoyt et al. 1991). Bi-orientation occurs when sister kinetochores are attached to microtubules emanating from opposite poles. The spindle checkpoint is activated by unattached kinetochores (Li and Murray 1991; Rieder et al. 1995) and lack of tension at the kinetochore (Li and Nicklas 1995; Stern and Murray 2001).

Tension is created across bi-oriented chromosomes as microtubules attempt to pull sister chromatids apart, but are opposed by the cohesin complex that encircles and holds them together. This tension can be visualized by the pre-anaphase splitting of GFP-labeled centromeres (Goshima and Yanagida 2000; He et al. 2000) and by elongation of kinetochores (Maresca and Salmon 2009; Uchida et al 2009; Wan et al. 2009). In *S.cerevisiae*, it was shown that chromatids incapable of generating tension due to inhibition of replication or cohesin activate the spindle checkpoint and arrests cells in mitosis (Stern and Murray 2001). An unpaired, tensionless chromosome in praying mantid spermatocytes delays cell division, and applying tension directly to this chromosome through micromanipulation allows cells to enter anaphase (Li and Nicklas

1995). Checkpoint activation in response to lack of tension is potentiated by the Ipl1/Aurora B kinase (Biggins and Murray 2001).Without Ipl1, *S.cerevisiae* are unable to arrest in the presence of mono-oriented chromosomes and unable to correct these erroneous attachments, leading to severe chromosome mis-segregation (Tanaka et al. 2002; Pinsky et al. 2003, 2006).

Despite its importance for activation of the spindle checkpoint, the mechanism of tension-sensation is not understood. The tension placed on a bi-oriented chromosome could be measured in two locations, either between the two sister kinetochores (inter-kinetochore, L_1 in **Figure 3-1A**) or within an individual kinetochore (intra-kinetochore, L_2 in **Figure 3-1A**). The inter-kinetochore view of tension-sensation proposes that distance between sister kinetochores is monitored, either with stretching pericentric chromatin itself serving as tensiometer to silence the spindle checkpoint (He et al. 2000) or with a protein tensiometer that spans the distance the distance between kinetochores, such as PICH (Tanaka 2008). PICH is a protein that has been visualized spanning the inter-kinetochore distance in HeLa cells (Baumann et al. 2007; Wang et al 2008) (**Figure 3-1B**). The intra-kinetochore stretch model suggests that separation within a kinetochore is monitored, activating the checkpoint when the kinteochore is compressed but silencing it when the kinetochore is elongated by tension (Maresca and Salmon 2009; 2010, Uchida et al. 2009) (**Figure 3-1B**).

We sought to distinguish between these two models of tension-sensation by inhibiting the stretching of pericentric chromatin using the genetically tractable model organism *S.cerevisiae* (**Figure 3-1C**). Inhibition of chromatin stretch should activate the spindle checkpoint if the kinetochore-kinetochore distance is a signal of a tensionless attachment. We introduced 256 tandem repeats of the lactose operator (LacO) into the pericentric chromatin on either side of a centromere and expressed either the wild-type Lac repressor that tetramerizes ($LacI_4$) or a

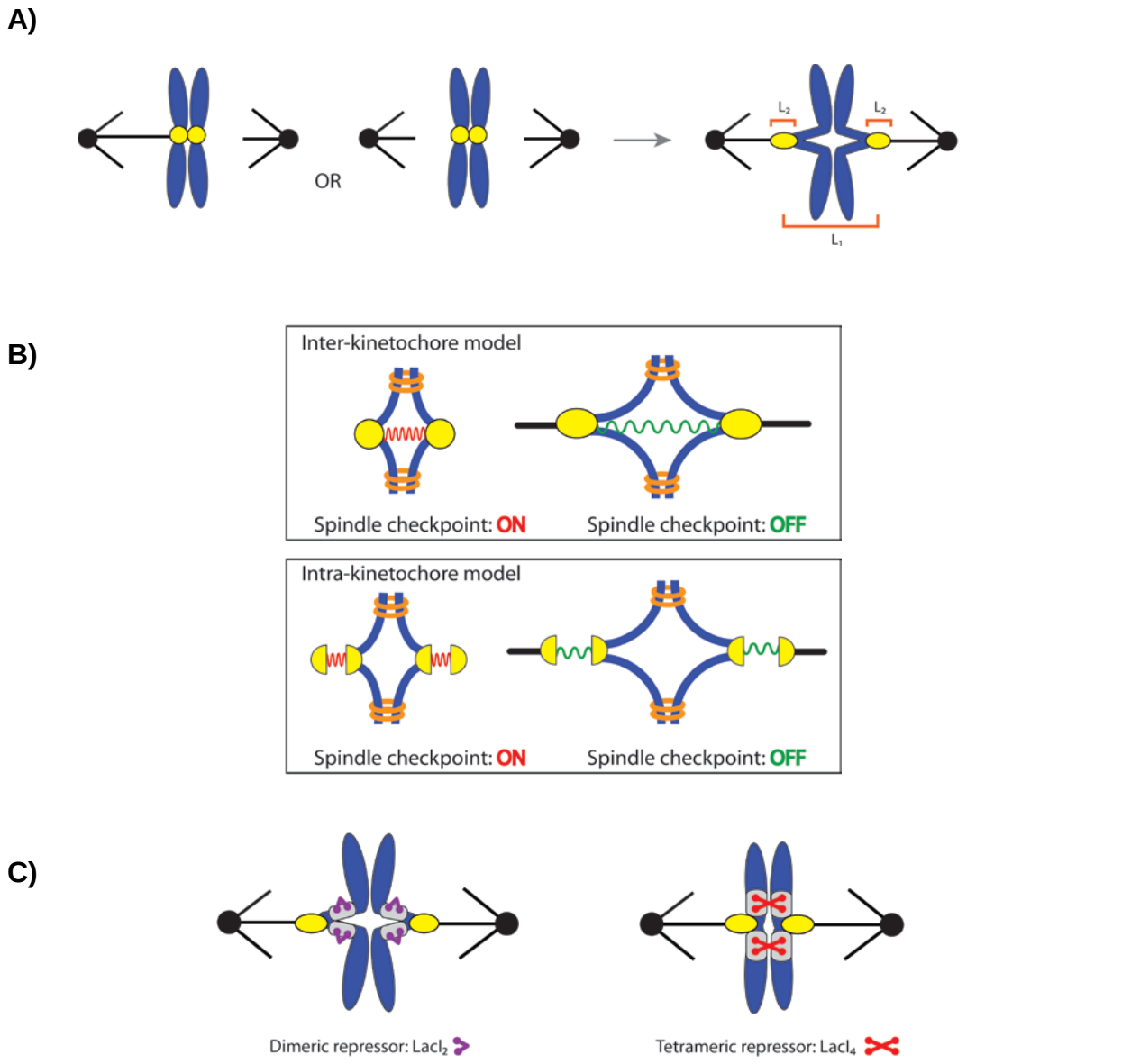

Figure 3-1. The spindle checkpoint is sensitive to tension on bi-oriented chromosomes. Unattached or incorrectly attached chromosomes produce no tension; correct attachments (bi-orientation) occur when sister chromatids (blue) attach to opposite poles (black dot) via kinetochores (yellow dot) **(A).** Tension is generated as microtubules attempt to pull chromatids apart but are resisted by cohesin rings (orange rings). Bi-orientation tension creates separation within the kinetochore (L_1) and separation between kinetochores (L_2) as pericentric chromatin stretches. The spindle checkpoint promotes bi-oriented attachments. Two different models of where the spindle checkpoint monitors tension: between kinetochores (inter-kinetochore) or within kinetochores (intra-kinetochore) **(B).** To distinguish between models, pericentric chromatin stretching and the separation of kinetochores were inhibited by tethering chromatids together with the cross-linking properties of the Lac repressor. Lac operator arrays (gray boxes) are placed on either side of the centromere and either a dimeric repressor (purple) or tetrameric repressor (red) is expressed. The dimeric form of the repressor contains a C-terminal truncation that prevents tethering while the tetrameric form can crosslink two chromatids **(C).**

repressor with a C-terminal truncation that allows dimerization but prevents tetramerization ($LacI_2$) (Chen and Matthews 1994). It has been previously demonstrated that the tetramerization of the Lac repressor can be used to tether sister chromatids together in mitosis (Straight et al. 1996) and homologous chromosomes together in meiosis (Lacefield and Murray 2007). We found that expression of $LacI_4$ inhibited stretching of the pericentric chromatin while expression of the dimer version $LacI_2$ did not. However, synchronous populations of $LacI_2$- and $LacI_4$-expressing cells entered anaphase at the same time indicating that the checkpoint was not activated. These cells were still competent for checkpoint activation as transient treatment with microtubule-depolymerizing drugs delayed anaphase entry. Our results demonstrate that inhibition of inter-kinetochore stretch does not activate the spindle checkpoint. These findings dispute an inter-kinetochore model of tension-sensation, lending support to intra-kinetochore monitoring of tension by the spindle checkpoint.

RESULTS

Tethering chromatids together with tetramerizing Lac repressor inhibits chromatin stretch

Tension on bi-oriented chromosomes helps the spindle checkpoint distinguish between correct and incorrect attachments, but it is unknown where on a bi-oriented chromosome this tension is monitored. Tension generates separation between kinetochores and within kinetochores (**Figure 3-1A**); we sought to determine if the stretching of pericentric chromatin is important for silencing the checkpoint. To tether sister chromatids together (**Figure 3-1C**), two DNA fragments each composed of 256 tandem repeats of the Lac operator (LacO) were placed on Chromosome III, with one on each side of the centromere. One of two forms of the Lac repressor were expressed, either the tetramerizing Lac repressor ($LacI_4$) that can bind simultaneously to two chromatids or the dimeric form of the repressor ($LacI_2$) (Straight et al.

1996). $LacI_2$ served as a control; it binds the lactose operator but cannot link two separate DNA molecules. Both repressors were fused to GFP to aid visualization of chromatin stretching. Stretched chromatin can be visualized as two GFP dots, and one GFP indicates chromatids that are either unstretched or stretched less than the 200nm resolvable by light microscopy (**Figure 3-2A**).

To determine if the tetrameric Lac repressor can inhibit chromatin stretch, cells were synchronized in G1 with alpha factor and released into a metaphase arrest induced by Cdc20-depletion (**Figure 3-3**). Cells expressing GFP-$LacI_2$ or GFP-$LacI_4$ were sampled every 30 minutes for 3 hours, and their chromatids were scored as unstretched (1 GFP dot) or stretched (2 GFP dots) by light microscopy. At 0 and 30 minutes post-G1, control (GFP-$LacI_2$) or tethered (GFP-$LacI_4$) cells were not significantly different, both showed little stretched chromatin (<10% stretched). At these time points cells are in S phase undergoing DNA replication. At 60 minutes post-G1 release, cells are entering mitosis; 50.3 ± 3.0% of control GFP-$LacI_2$ cells (n>100) have a visibly stretched Chromosome III where as only 23.5 ± 1.5% of tethered GFP-$LacI_4$ cells (n>100) are stretched (p-value <0.005) (**Figure 3-2B**). Throughout the continuing time points, approximately 50% of control GFP-$LacI_2$ cells have stretched chromatids, similar to previous studies (He et al. 2000; Goshima and Yanagida 2000). Cells expressing GFP-$LacI_4$ have significantly lower percentage of stretched chromatids at all time points (p-values<0.005), however the percentage stretched increased during the metaphase arrest from 23.5 ± 1.5% at T=60 minutes to 41.9 ± 2.0% at T=180 minutes (p-value<0.005). These results suggest that the tetramerized Lac repressor can inhibit stretching of pericentric chromatin but during a prolonged metaphase arrest, spindle forces are able to overcome the tether, increasing the percentage of stretched chromatids.

A)

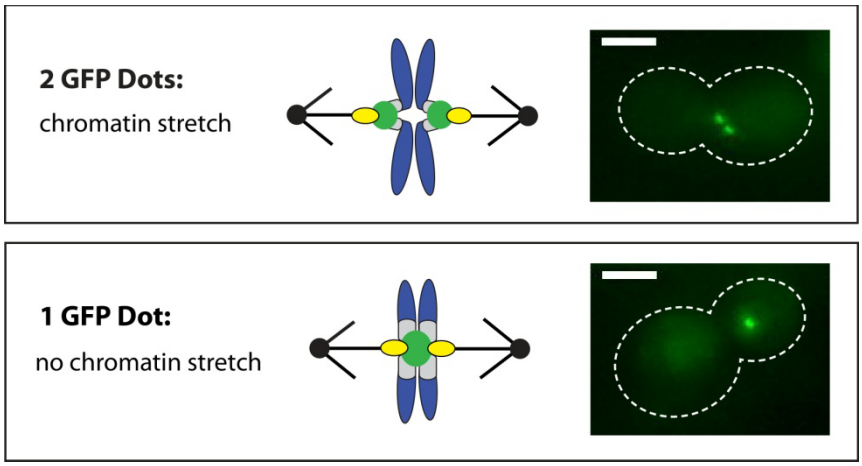

B)

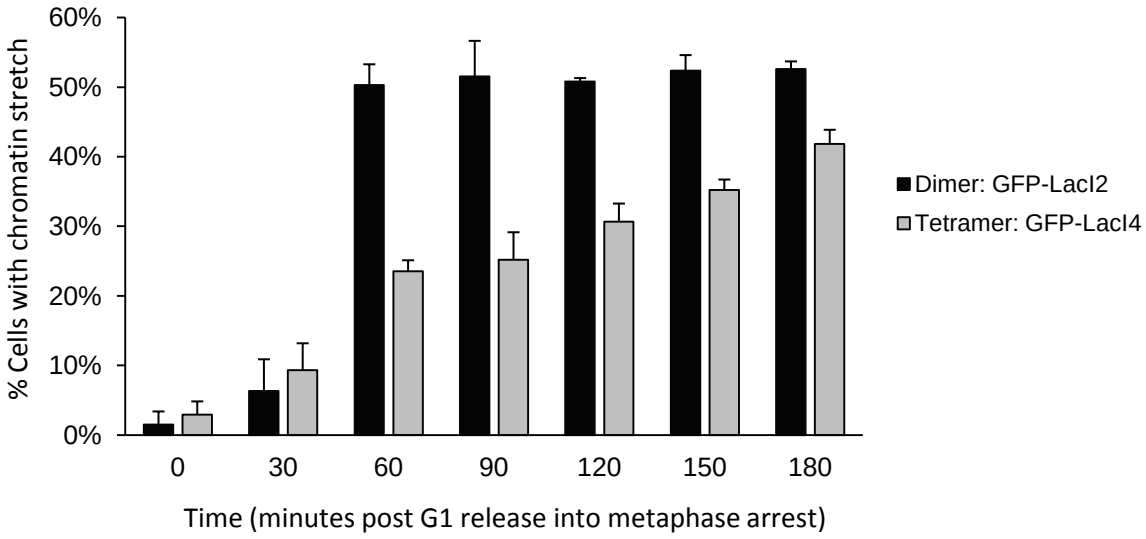

Figure 3-2. Tetrameric Lac repressor inhibits sister chromatids stretching. Both versions of the repressor are fused to GFP to visualize sister chromatids. Stretching chromatids appear as two GFP dots and one GFP dot is categorized as no stretch. Scale bar is 3μm **(A)**. Chromatin stretching is inhibited if the tetrameric form of the Lac repressor (GFP-LacI4) is expressed in cells containing Lac operators flanking the centromere on Chromosome III. Control cells expressing the dimeric repressor (GFP-LacI2) reach percent maximum stretching 60 minutes post-release from G1; the tetrameric strain has fewer visibly stretched cells at all time points in metaphase arrest, but the fraction of stretched cells gradually rises (p-values<0.005). Cells were synchronized in G1 with alpha factor and released into metaphase arrest induced by Cdc20p depletion; samples were taken every 30 minutes and scored for chromatin stretching (n<100). Error bars represent standard deviation across 3 independent trials **(B)**.

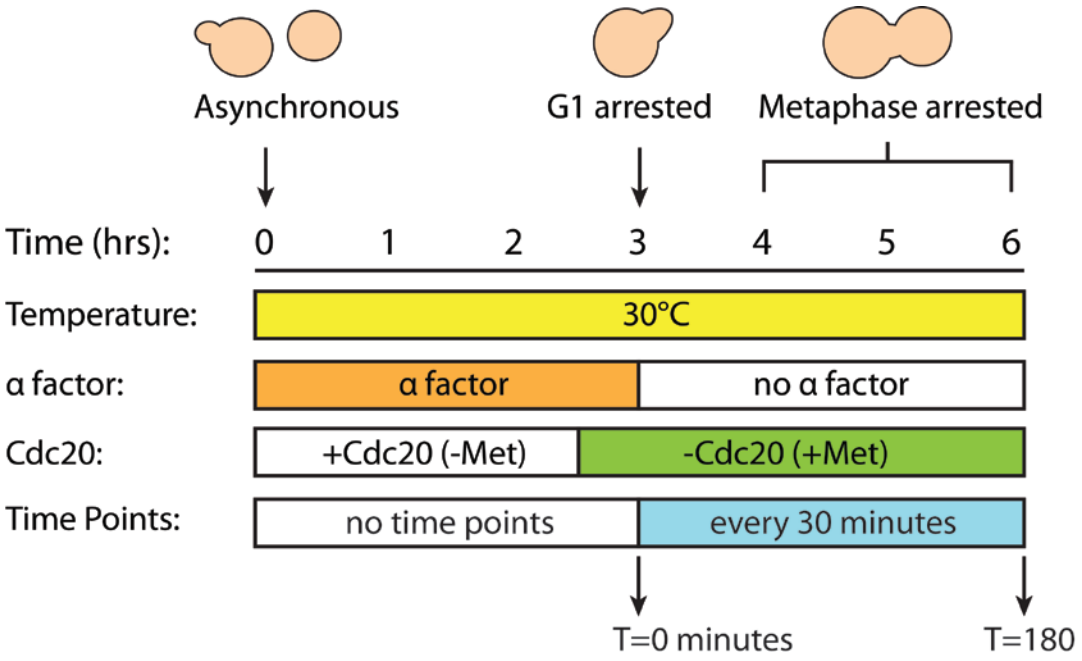

Figure 3-3. Experimental set-up to measure stretching of GFP-labeled chromatids. Cells were grown in log phase for 24 hours; asynchronous populations were treated with α factor for 3 hours to arrest cells in G1. Cells were washed and released from G1 into a metaphase arrest generated by depletion of Cdc20, an essential co-activator of the Anaphase Promoting Complex. Time point samples of cells were collected every 30 minutes post-release from G1; cells were fixed and visualized by fluorescent microscopy. The percentage of 2 GFP-dot cells was scored in all samples from all time points.

Inhibiting chromatin stretch does not activate the spindle checkpoint

Tethering sister chromatids with GFP-$LacI_4$ inhibits stretching, so we next assayed whether this inhibition activated the spindle checkpoint. Cells were synchronized in G1 with alpha factor, washed and released to proceed through the cell cycle. Samples were taken every 10 minutes, fixed, and visualized to score mitotic progression (**Figure 3-4**). Cells were scored for anaphase by the segregation of their GFP-labeled chromosome (**Figure 3-5A, B**). Control cells expressing GFP-$LacI_2$ began to enter anaphase 40-50 minutes post-release from G1 and peaked with approximately 80% of cells in anaphase by 60-70 minutes. By 100 minutes, nearly all cells had existed mitosis (**Figure 3-5C**). Cells expressing GFP- $LacI_4$ showed the same pattern of mitotic progression as control cells; they entered anaphase at the same time (T=40-50 minutes), peaked at the same time (T=60-70 minutes) with ~80% anaphase cells, and had fully exited mitosis by T=100 minutes. At all time points, there was no statistically significant difference between control and tethered cells.

Both dimeric and tetrameric GFP-LacI cells entered and exited mitosis with the same timing, suggesting that inhibition of chromatin does not activate the spindle checkpoint. It is possible however both GFP-$LacI_2$ and GFP-$LacI_4$ cells activated the spindle checkpoint and experience mitotic delay. To rule out this possibility, we knocked out Mad2p, an essential component of the spindle checkpoint, in both dimeric and tetrameric LacI strains. All four strains moved through mitosis on the same time scale. All strains (GFP-$LacI_2$, GFP-$LacI_4$, GFP-$LacI_2$ mad2Δ, and GFP-$LacI_4$ mad2Δ) peaked in anaphase at 60-70 minutes post-G1 release with no statistically significant difference between any of the four strains (**Figure 3-6**). These results suggest that neither the dimeric or tetrameric strains have a delay in mitosis due to activation of the spindle checkpoint.

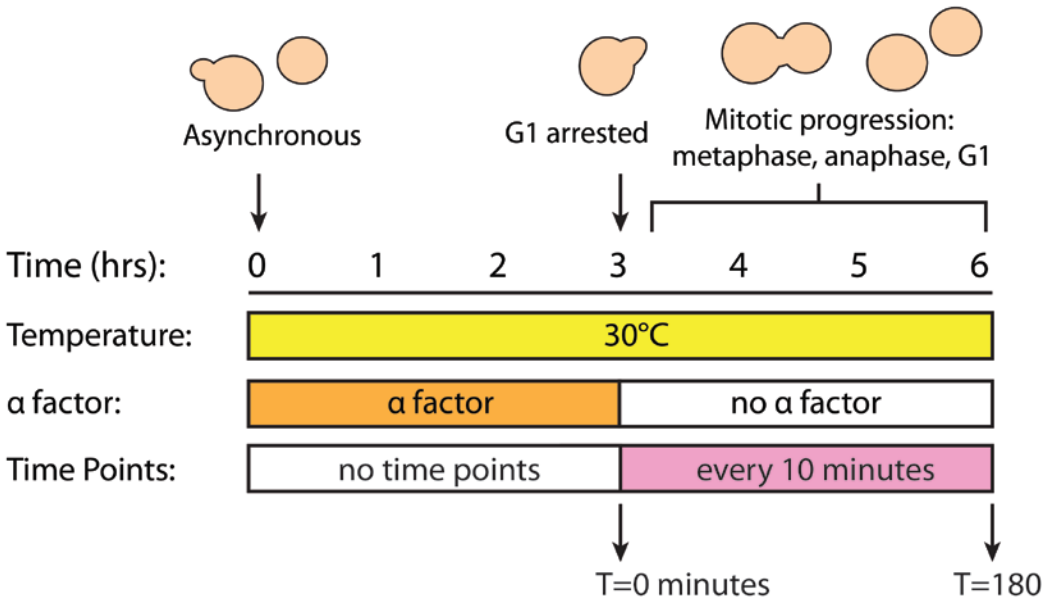

Figure 3-4. Experimental set-up to measure mitotic progression. Cells were grown in log phase for 24 hours; asynchronous populations were treated with α factor for 3 hours to arrest cells in G1. Cells were washed and released from G1 and allowed to proceed through mitosis and into the next cell cycle. Time point samples of cells were collected every 10 minutes post-release from G1; cells were fixed and visualized by fluorescent microscopy. Mitotic progression was scored by the position of GFP-labeled chromosomes (described in Figure 3-5A) in cells at all time points.

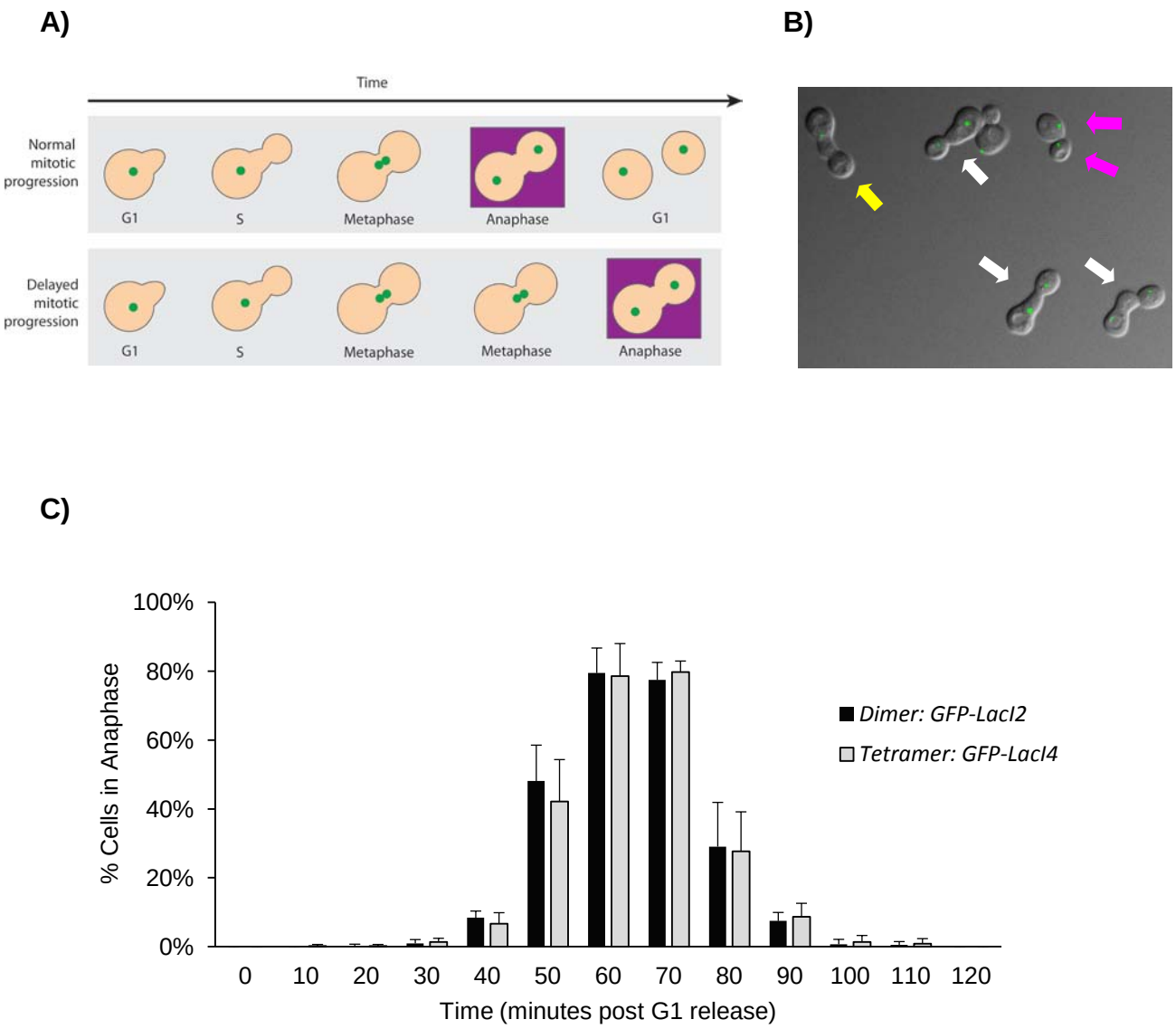

Figure 3-5. Inhibition of chromatin stretch does not delay mitotic progression. Normal mitotic progression passes through all stages of the cell cycle; when the spindle checkpoint is activated, cells arrest in metaphase, delaying anaphase. To observe mitotic progression, cells are synchronized in G1 with alpha factor (produces a "shmoo" projection). The GFP-labeled chromosome is denoted by the green dot; in anaphase chromatids separate into mother and daugther cells. Number of anaphase cells are scored in mitotic progression assays (purple box) **(A)**. Example of cells progressing through mitosis. Image was taken T=70 minutes post release from G1; in addition to pre-anaphase (yellow arrow) and anaphase (white arrows) cells, there are also post-cytokinetic cells (magenta arrows). **(B)**. Cells expressing the tetrameric Lac repressor do not delay mitosis compared to control cells expressing dimeric Lac repressor. Both strains peak in anaphase 60-70 minutes after release from G1. Cells were synchronized in G1 with alpha factor and released at T=0. Samples were taken every 10 minutes, fixed, and scored for anaphase (n>100 cells); error bars represent standard deviation across 4 independent trials **(C)**.

A)

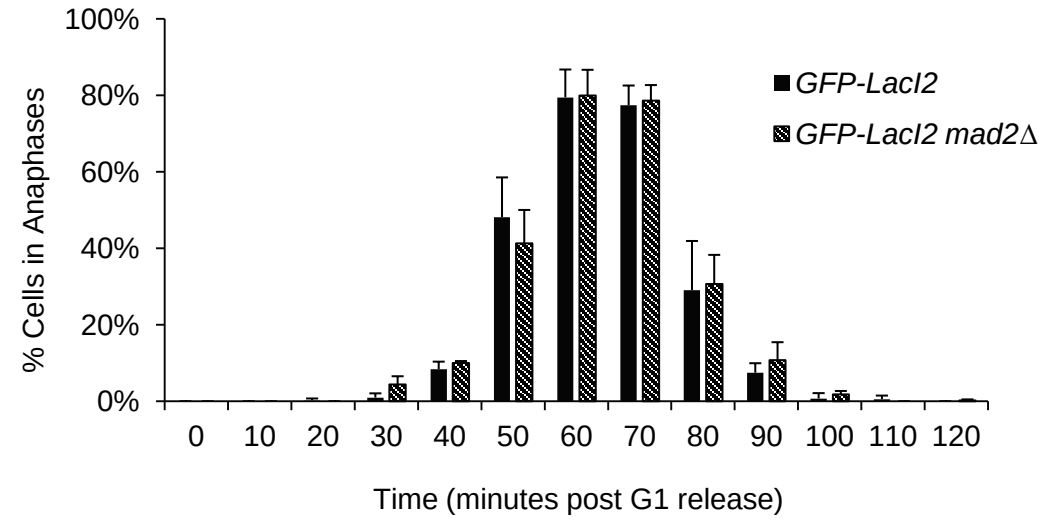

B)

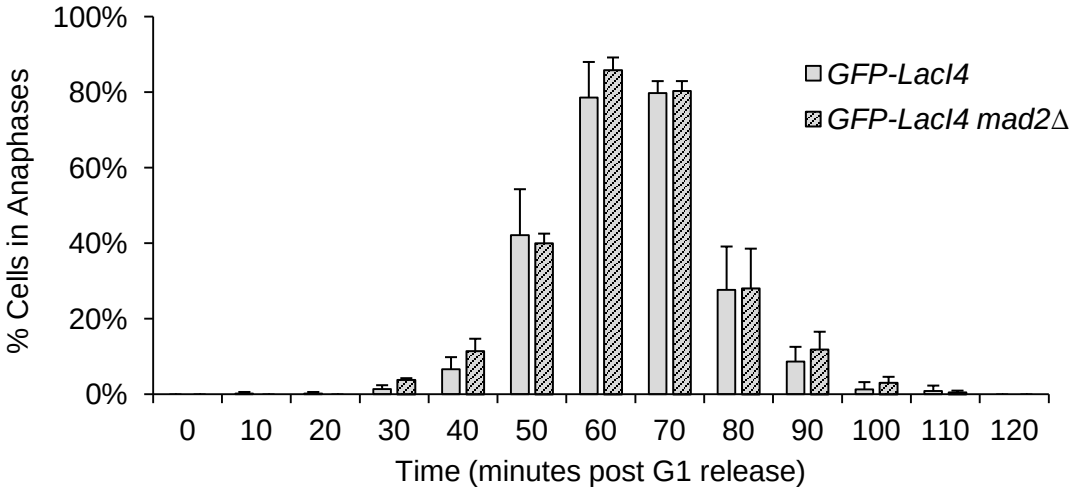

Figure 3-6. Deletion of the spindle checkpoint does not alter mitotic progression. The essential spindle checkpoint component Mad2p was deleted in both control dimeric cells and in stretch-inhibited tetrameric cells. All four strains move through mitosis on the same time scale, peaking at T=60-70 with approximately 80% of cells in anaphase. There was no statisical significance between all four strains (p-values>0.1). Comparison of control dimeric strain with and without Mad2 is shown in (**A**); comparison of stretch-inhibited tetrameric strain with and without Mad2 is shown in (**B**). These results suggest that neither control $LacI_2$ cells nor tethered $LacI_4$ cells are delayed due to checkpoint activation. Cells were synchronized in G1 with alpha factor, washed and released; samples were collected every 10 minutes, sonicated, fixed, and scored for anaphase (n>100 cells). Error bar represent the standard deviation of at least 3 independent trials.

It is possible that introduction of the tethering components (Lac operator and either Lac repressor) disrupted the spindle checkpoint, and these cells may be unable to activate the checkpoint. To confirm that strains expressing either the dimeric or tetrameric from of the Lac repressor can still activate the spindle checkpoint, cells were synchronized in G1 with alpha factor and released into microtubule-depolymerizing drugs benomyl and nocodazole. Treatment with these drugs activates the spindle checkpoint and inhibits progression into anaphase (Li and Murray 1991). No dimeric or tetrameric cells entered anaphase while in the presence of benomyl and nocodazole (0% anaphase cells through T=90), indicating that both strains activated the spindle checkpoint (**Figure 3-7**). After 90 minutes of drug treatment, cells were washed and transferred to drug-free media; a red dot on the x-axis marks drug wash-out. Both dimeric and tetrameric cells recovered from the mitotic arrest and began entering anaphase; by T=150 minutes approximately 30% of both GFP-$LacI_2$ and GFP-$LacI_4$ cells had entered anaphase. This results indicate that both strains have functional spindle checkpoints and are capable of inducing mitotic arrest in response to checkpoint activation.

DISCUSSION

The spindle checkpoint is insensitive to pericentric chromatin stretch

The spindle checkpoint ensures that all chromosomes are properly attached to the spindle; it monitors both the attachment of microtubules to kinetochores and the tension generated by a correct bi-oriented attachment (**Figure 3-1A**). The Ipl1/Aurora B kinase is responsible for sensing this tension; it activates the checkpoint and destabilizes incorrect attachments (Biggins and Murray 2001; Stern and Murray 2001; Pinsky et al. 2006). It is not known how and where the kinase and thus the spindle checkpoint measures tension. Tension across a bi-oriented

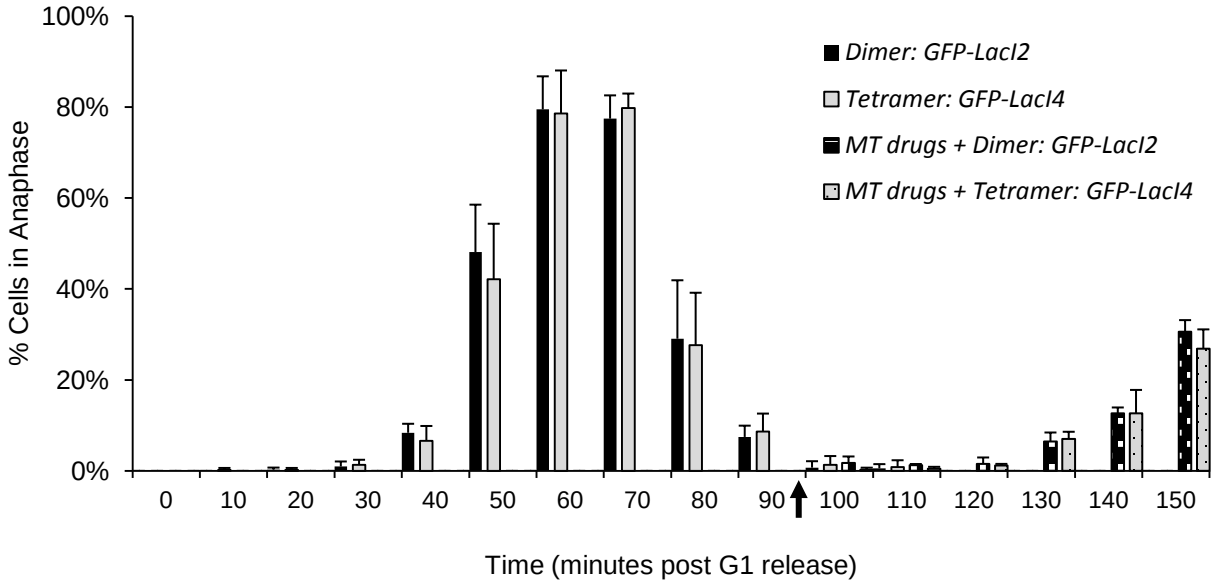

Figure 3-7. Control and tethered cells can activate the spindle checkpoint. It is possible that during the creation of the control and tethered strains, the spindle checkpoint became crippled and was no longer capable of arresting the cell cycle. Dimeric and tetrameric strains were treated with microtubule-depolymerizing drugs benomyl and nocodazole which activates the checkpoint. Both strains arrested in the presence of the drug and did not enter anaphase until the drugs were washed out. Drug wash-out occured after the T=90 time point and is indicated by the black arrow. Cells were synchronized in G1 with alpha factor, washed and released; samples were collected every 10 minutes, sonicated, fixed, and scored for anaphase (n>100 cells). Error bars represent the standard deviation of at least 3 independent trials.

chromosome manifests as separation of sister kientochores by stretching of pericentric chromatin (Goshima and Yanagida 2000; He et al. 2000) and elongation within the kinetochore (Maresca and Salmon 2009; 2010, Uchida et al. 2009).

We used *S.cerevisiae* to determine if the spindle checkpoint monitors the stretching of pericentric chromatin as proposed by inter-kinetochore models of tension-sensation (**Figure 3-1B**) (He et al. 2000; Tanaka 2008). We placed Lac operator arrays on either side of the centromere on Chromosome III and expressed a tetrameric Lac repressor ($LacI_4$) to tether sister chromatids together. Expression of a dimeric form of the repressor ($LacI_2$) was used as a control because this mutant repressor contains a C-terminal trunctation that prevents cross-linking of two DNA molecules (Chen and Matthews 1994).

By 60 minutes post-release from G1, 50% of dimeric control cells (GFP-$LacI_2$) had stretched Chromosome III; this percentage held throughout the metaphase arrest and matched previous observations (Goshima and Yanagida 2000; He et al. 2000) Visualizing approximately half of chromatids stretched in metaphase is expected because stretching is dynamic and chromatids go through cycles of stretching and retracting ("breathing") (He et al. 2000; Tanaka et al. 2000; Indjeian and Murray 2007). The tetrameric repressor (GFP-$LacI_4$) inhibited pericentric chromatin stretching, visualized as a reduction cells with 2 GFP-chromatin dots (**Figure 3-2B**). At 60 minutes post-release only 23% of cells had a stretched Chromosome III; this percentage increased during the metaphase arrest suggesting that over time spindle forces are able to overcome the $LacI_4$-LacO tether.

We then asked whether this inhibition in chromatin stretch activated the spindle checkpoint. Cells were synchronized in G1 and followed as they progress through the cell cycle. Inhibiting chromatin stretch did not cause mitotic delay. Control dimeric cells and tethered

tetrameric cells progessed through mitosis on the same time scale, peaking with 80% cells in anaphase at 60-70 minutes post-release from G1. At 60 minutes, the peak of anaphase, only 23% of tetrameric tethered cells have a stretched Chromosome III, compared to 50% in control cells (**Figure 3-2B**). If the spindle checkpoint is sensitive to chromatin stretch, we expect that half of the tetrameric cells would have delayed entry to anaphase. However, 80% of tetrameric cells were in anaphase at T=60, the same as control dimeric cells (80% anaphase at T=60) (**Figure 3-3C**). Mitotic timing is the same when the spindle checkpoint was deleted (**Figure 3-6**), demonstrating that neither the control ($LacI_2$) nor the chromatin stretch inhibited cells ($LacI_4$) delayed mitosis due to checkpoint activation. Lack of delay was not caused by defective checkpoints. Both strains were able to arrest in response to known checkpoint stimuli; cells only entered anaphase once the microtubule-depolymerizing drugs were washed out (**Figure 3-7**). Together our results indicate that the spindle checkpoint is not sensitive to pericentric chromatin stretching, and it is unlikely that inter-kinetochore distance is measured by the checkpoint.

Intra-kinetochore stretch models for tension-sensation

Our results counter an inter-kinetochore model of tension-sensation and thus lend support to intra-kinetochore models. Intra-kinetochore models suggest that the Ipl1/Aurora B kinase monitors separation within a kinetochore, activating the checkpoint when the kinetochore is not under tension (Marcesca and Salmon 2009, 2010; Uchida et al. 2009). Studies by Maresca and Salmon showed that treating *Drosophila S2* cells with taxol causes a reduction in inter-kinetochore stretch but not intra-kinetochore stretch; these cells did not activate the spindle checkpoint (Maresca and Salmon 2009). Uchida et al. also showed that treating HeLa cells with low amounts of nocodazole leads to a compression of the kinetochore with no effect on inter-

kinetochore stretch; this kinetochore compression led to spindle checkpoint activation (Uchida et al. 2009). Our studies come to the same conclusion that inhibition of chromatin stretch does not activate the checkpoint, but they avoid any potential side effects of altering microtubule dynamics with drugs.

Kinetochores have been shown to elongate under tension (Maresca and Salmon 2009; Uchida et al. 2009; Wan et al. 2009). In *Drosophila* S2 cells, unattached kinetochores measure 65 ± 31nm from the inner centromere protein CENP-A to outer kinetochore protein Ndc80. When attached and bi-oriented, kinetochores elongate to 102 ± 27nm, increasing by an average of 37nm (Maresca and Salmon 2009). How does the kinetochore accommodate this elongation? The composition of the kinetochore changes upon bi-orientation with some proteins becoming enriched and others decreasing (reviewed in Tanaka 2012). Some kinetochore component change conformation when placed under tension. Studies using immunoelectron and fluorescent microscopy showed that inner kinetochore proteins CENP-A, -C, and -R deform under tension, and CENP-T elongates with increased separation of its N and C-termini (Suzuki et al. 2011). The outer kinetochore complex Ndc80 has also been shown to shift 15nm further away from the inner kinetochore upon bi-orientation (Wan et al. 2009). The Ndc80 complex has a long coiled-coil domain broken by a flexible elbow-like hinge that is thought to straighten out under tension (Wang et al. 2008).

There are two different proposed mechanisms for how the Ipl1/Aurora B kinase could make use of this kinetochore elongation to distinguish between correct and incorrect attachment. Under tension, the Ipl1/Aurora B kinase could be deactivated, therefore no longer able to activate the spindle checkpoint or destabilize incorrect attachments, or the kinase maybe spatially separated from its targets. Studies in *S.cerevisiae* show that Bir1p and Sli15p (Survivin and

INCENP in higher eukaryotes), members of the chromosomal passenger complex that localize and activate Ipl1, help link centromeres and microtubules (Sandall et al. 2006, Carmena et al. 2012). Microtubule binding mutants of Sli15 phenocopy the chromosome segregation defects seen Ipl1 activation mutants; the authors propose that Sli15p and Bir1p not only recruit Ipl1 to the kinetochore, but also act as a tensiometer that selectively activates Ipl1p in tensionless kinetochores and deactivates the kinase under tension (Sandall et al. 2006). The other mechanism suggests that Ipl1/Aurora B is constitutively on, capable of activating the checkpoint and destabilizing attachments, but when under tension, the kinase's targets are physically separated from its range of activity. Liu et al. showed that the phosphorylation of an Aurora B target depends on its physical distance from the kinase located in the inner kinetochore (Liu et al. 2009). The authors also demonstrated that repositioning the kinase closer to its targets in the outer kinetochore causes destabilization of the attachment and activation of the checkpoint despite being a bi-oriented attachment. The authors proposed that tension-induced elongation of the kinetochore spatially separates the Ipl1/Aurora B kinase from its targets, preventing it from destabilizing correct attachments and activating the checkpoint.

Our result that the spindle checkpoint is not sensitive to chromatin stretch counters inter-kinetochore stretch models and thus lends support to these intra-kinetochore based models of tension-sensation. Further support for the intra-kinetochore models could be obtained by tethering kinetochores, artificially compressing them even when correctly attached and under tension and determining if the checkpoint is constitutively activated (see Chapter 4 for further discussion of future experiments). Flexible elements in the kinetochore could be stiffened or truncated, and cells could be probed for constitutive checkpoint activity. Likewise, artificially elongating components of the kinetochore should constitutively satisfy the checkpoint. These

experiments would support intra-kinetochore models without altering microtubule dynamics to achieve kinetochore compression.

METHODS and MATERIALS

Yeast strains and culturing

Strains used in this study are listed in Table 3-1; all strains were constructed in W303 background (*ade2-1 his3-11,15 leu2-3,112 trp1-1 ura3-1 can1-100*) using standard genetic techniques. Lactose operator arrays containing 256 repeats of the operator were integrated on either side of the centromere on Chromosome III. Both arrays were approximately 1 kb from the centromere. Dimeric control strains contained a C-terminal truncation mutant of the Lac repressor ($LacI_2$) that cannot cross-link two arrays; experimental cells contained the wild-type version of the Lac repressor capable of tetramerizing and cross-linking two arrays ($LacI_4$). Both versions of the repressor were placed under the *HIS3* promoter and were fused via their N-terminal to monomeric yeast optimized GFP. Cells were either grown in Synthetic Complete media (2% glucose) lacking histidine (SC-HIS) or Synthetic Complete media (2% glucose) lacking histidine and methionine (SC-HIS-MET) at 30°C to promote expression of the Lac repressor under the *HIS3* promoter. YPD containing 1-(butylcarbamoyl)-2-benzimidazolecarbamate (benomyl) and nocodazole was prepared by heating YPD to 65°C and adding dimethyl sulfoxide (DMSO) 10mg/ml stocks of benomyl dropwise to a final concentration of 30µg/ml; media was cooled to 37°C for dropwise addition of DMSO 10mg/ml stock of nocodazole to a final concentration of 30µg/ml. All drugs and chemicals were purchased from Sigma Aldrich.

Chromatin stretch assay

Strains were grown in SC-HIS-MET at 30°C and maintained in log phase for 24 hours before the experiment. Log phase cells (~$5x10^6$ cells/ml) were arrested in G1 with 10µg/ml α

factor (Bio-Synthesis) for 3 hours. After confirmation of arrest by light microscopy, cells were washed three times with YPD to remove α factor and released into SC-HIS media. Media lacking methionine allows cells to grow, but media lacking methionine inhibits expression of Cdc20p from the *MET* promoter and induces metaphase arrest. Cells were grown at 30°C for 3 hours, and samples were collected every 30 minutes. Samples were fixed with formalin (see below) and stored at 4°C for imaging. Using fluorescence microscopy to visualize GFP-tagged chromatids, samples were scored for the presence of one or two GFP dots; two dots indicates stretched chromatids.

Mitotic progression assay

Strains were grown in SC-HIS at 30°C and maintained in log phase for 24 hours before the experiment. Log phase cells (~$5x10^6$ cells/ml) were arrested in G1 with 10μg/ml α factor (Bio-Synthesis) for 3 hours. After confirmation of arrest by light microscopy, cells were washed three times with YPD to remove α factor and released into SC-HIS media. Cells were grown at 30°C for 3 hours, and samples were collected every 10 minutes. Samples were sonicated, fixed with formalin (see below), and stored at 4°C for imaging. After 60 minutes, 10μg/ml α factor was to prevent additional entry into a second mitosis during 3 hour experiment. Samples were scored for mitotic progression by cell morphology and position of GFP-tagged chromatids. Anaphase was scored as large-budded cells with GFP-tagged chromatids separated into mother and daughter cells.

Sample fixation and imaging by fluorescent microscopy

Samples for imaging were fixed with 10% formalin (final concentration of 1%) for 10 minutes, washed with with 0.1M KH_2PO_4 pH 8.5, washed with 1.2M Sorbitol + 0.1M KH_2PO_4 pH 8.5, resuspended in 1.2M Sorbitol + 0.1M KH_2PO_4 pH 8.5, and stored at 4°C. Images were acquired at room temperature (25°C) using a Nikon Eclipe Ti-E inverted microscope with a 60x Plan Apo VC, 1.4 NA oil objective lens with a Photometrics CoolSNAP HQ camera (Roper Scientific). Metamorph 7.7 (Molecular Devices) was software was used to acquire images. Fixed samples were imaged in 1.2M Sorbitol + 0.1M KH_2PO_4 pH8.5 buffer on Concanavalin A-coated coverslips (VWR) adhered to glass slides (Corning). Exposure times were 10ms for differential interference contrast and 300ms for fluorescence.

Table 3-1. Strains used in Chapter 3

Strain Name	Genotype
yNJN175	*MATa, P_{HIS3}-GFP-$LacI_2$::HIS3, LacO(256)::LEU2::1.3kb upstream CEN3, LacO(256)::URA3::1.3kb downstream CEN3*
yNJN176	*MATa , P_{HIS3}-GFP-$LacI_4$::HIS,3 LacO(256)::LEU2::1.3kb upstream CEN3, LacO(256)::URA3::1.3kb downstream CEN3*
yNJN189	*MATa, P_{HIS3}-GFP-$LacI_2$::HIS3, LacO(256)::LEU2::1.3kb upstream CEN3, LacO(256)::URA3::1.3kb downstream CEN3 mad2Δ*
yNJN190	*MATa, P_{HIS3}-GFP-$LacI_4$::HIS3, LacO(256)::LEU2::1.3kb upstream CEN3, LacO(256)::URA3::1.3kb downstream CEN3 mad2Δ*
yNJN210	*MATa, P_{HIS3}-GFP-$LacI_2$::HIS3, LacO(256)::LEU2::1.3kb upstream CEN3, LacO(256)::URA3::1.3kb downstream CEN3, P_{Met}-HA3-Cdc20::TRP1*
yNJN211	*MATa, P_{HIS3}-GFP-$LacI_4$::HIS3, LacO(256)::LEU2::1.3kb upstream CEN3, LacO(256)::URA3::1.3kb downstream CEN3, P_{Met}-HA3-Cdc20::TRP1*

All strains are derivatives of *Saccharomyces cerevisiae* W303 with the following auxotrophic genotypes: *ade2-1 can1-100 his3-11,15 leu2-3,112 trp1-1 ura3-1*

REFERENCES

Baumann C., Kömer R., Hofmann K., and E.A. Nigg. 2007. PICH, a Centromere-Associated SNF2 Family ATPase, Is Regulated by Plk1 and Required for the Spindle Checkpoint. *Cell* 128: 101-114.

Biggins S and AW Murray. (2001). The budding yeast protein kinase Ipl1/Aurora allows the absence of tension to activate the spindle checkpoint. *Genes Dev.* 15: 3118-29.7.

Carmena M., Wheelock M., Funabiki H. and W.C. Earnshaw. 2012. The chromosomal passenger complex (CPC): from easy rider to the godfather of mitosis. *Nat Rev Mol Cell Biol* 13: 789-803.

Chen J. and K.S. Matthews. 1994. Subunit dissociation affects DNA binding in a dimeric lac repressor produced by C-terminal deletion. *Biochemistry* 33: 8728-8735.

Driscoll D.A. and S.G. Gross. 2009. Prenatal screening for aneuploidy. *N Eng J Med* 360: 2556-2562.

Goshima G and M Yanagida. (2000). Establishing Biorientation Occurs with Precocious Separation of the Sister Kinetochores, but Not the Arms, in the Early Spindle of Budding Yeast. *Cell*, 100: 619-33.

Hoyt M.A., Totis L. and B.T. Roberts. 1991. *S.cerevisiae* genes required for cell cycle arrest in response to loss of microtubule function. *Cell* 66: 507-517.

Indjeian V.B. and A.W. Murray. 2007. Budding yeast mitotic chromosomes have an intrinsic bias to biorient on the spindle. *Curr Biol* 17: 1837-1846.

Kops GJ et al. 2005. On the road to cancer: aneuploidy and the mitotic checkpoint. *Nat Rev Cancer*. 5: 773-785.

Lacefield S. and A.W. Murray. 2007. The spindle checkpoint rescues the meiotic segregation of chromosomes whose crossovers are far from the centromere. *Nat Genet* 39: 1273-1277.

Li R. and A.W. Murray. 1991. Feedback control of mitosis in budding yeast. *Cell* 66: 519-531.

Li X. and R.B. Nicklas. 1995. Mitotic forces control a cell-cycle checkpoint. *Nature* 16: 630-632.

Liu D., Vader G., Vromans M.J., Lampson M.A. and S.M. Lens. 2009. Sensing chromosome bi-orientation by spatial separation of aurora B kinase from kinetochore substrates. *Science* 323: 1350-1353.

Maresca T.J. and E.D. Salmon. 2009. Intrakinetochore stretch is associated with changes in kinetochore phosphorylation and spindle assembly checkpoint activity. *J Cell Biol* 184: 373-381.

Maresca T.J. and E.D. Salmon. 2010. Welcome to a new kind of tension: translating kinetochore mechanics into a wait-anaphase signal. *J Cell Sci* 123: 825-835.

Pinsky, B.A., Tatsutani S.Y., Collins K.A. and S. Biggins. 2003. An Mtw1 complex promotes kinetochore biorientation that is monitored by the Ipl1/Aurora protein kinase. *Dev Cell* 5: 735-745.

Pinsky B.A. and S. Biggins. 2005. The spindle checkpoint: tension versus attachment. *Trends Cell Biol* 15: 486-493.

Pinsky, B.A., Kung C., Shokat K.M., and S. Biggins. 2006. The Ipl1-Aurora kinase activates the spindle checkpoint by creating unattached kinetochores. *Nat Cell Biol* 8: 78-83.

Rieder C.L., Cole R.W., Khodjakov A., and G. Sluder. 1995. The checkpoint delaying anaphase in response to chromosome monoorientation is mediated by an inhibitory signal produced by unattached kinetochores. *J Cell Biol* 130: 941-948.

Siegel J.J. and A. Amon. 2012. New insights into the troubles of aneuploidy. *Annu Rev Cell Dev Biol* 28: 189-214.

Straight A.F., Belmont A.S., Robineet C.C. and A.W. Murray . 1996. GFP tagging of budding yeast chromosomes reveals that protein-protein interactions can mediate sister chromatid cohesion. *Curr Biol* 6: 1599-1608.

Suzuki A., Hori T., Nishino T., Usukura J., Miyagi A., Morikawa K. and T. Fukagawa. 2011. Spindle microtubules generate tension-dependent changes in the distribution of inner kinetochore proteins. *J Cell Biol* 193: 125-140.

Tanaka T., Fuchs J., Loidl J. and K. Nasmyth. 2000. Cohesin ensures bipolar attachment of microtubules to sister centromeres and resists their precocious separation. *Nat Cell Biol* 2: 492-499.

Tanaka T., Rachidi N., Janke C., Pereira G., Galova M., Schiebel E., Stark M.J.R., and K. Nasmyth. 2002. Evidence that the Ipl1-Sli15 (Aurora Kinase-INCENP) complex promotes chromosome bi-orientation by altering kinetochore-spindle pole connections. *Cell* 108: 317-329.

Tanaka T. 2008. Bi-orienting chromosomes: acrobatics on the mitotic spindle. *Chromosoma* 117: 521-533.

Tanaka K. 2012. Dynamic regulation of kinetochore-microtubule interaction during mitosis. *J Biochem* 152: 415-424.

Uchida K.S.K., Takagaki K., Kumada K., Hirayama Y., Noda T. and T. Hirota. 2009. Kinetochore stretching inactivates the spindle assembly checkpoint. *J Cell Biol* 184: 383-390.

Wan X. O'Quinn R.P., Pierce H.L., Joglekar A.P., Gall W.E., DeLuca J.G., Carroll C.W., Liu S.T., Yen T.J., McEwen B.F., Stukenberg P.T., Desai A., and E.D. Salmon. 2009. Protein architecture of the human kinetochore microtubule attachment site. *Cell* 137: 672-684.

Wang H.W., Long S., Ciferri C., Westermann S., Drubin D., Barnes G., and E. Nogales. 2008. Architecture and flexibility of the yeast Ndc80 kinetochore complex. *J Mol Biol* 383: 894-903.

Wang L .H., Schwarzbraun T., Speicher M.R., and E.A. Nigg. 2008. Persistence of DNA threads in human anaphase cells suggests late completion of sister chromatid decatenation. *Chromosoma* 117: 123-35.

Westermann S., Drubin D.G, and G. Barnes. 2007. Structures and functions of the yeast kinetochore complexes. *Annu Rev Biochem* 76: 563-559.

Chapter Four:

Discussions, Conclusions and Future Directions

ABSTRACT

Chromosome segregation is an essential process that must occur without mistakes. We sought to better understand two aspects of chromosome segregation; how the length of the spindle is determined, and how the spindle checkpoint measures tension to ensure proper attachment and segregation of chromosomes. We found that spindle length scales with the number of chromosomal attachments, supporting length regulation by a balance of length-dependent forces (Chapter 2). Investigations of the spindle checkpoint revealed that the stretching of pericentric chromatin does not activate the checkpoint (Chapter 3) and the location of the tension-sensing kinase does alter checkpoint activity (Appendix). Our findings negate tension-sensation models based on the stretching of chromatin; instead they lend support to tension-sensing models based on measuring stretch within a kinetochore. This chapter will summarize our findings and discuss questions left unanswered, new questions that arose, and how we may address some of these questions in the future.

INTRODUCTION

The ability to faithfully pass on genetic material is the very essence of life. In order to divide and reproduce, organisms must copy and segregate their chromosomes equally to their progeny, with each daughter cell receiving one copy of every chromosome. The cellular structure responsible for eukaryotic chromosome segregation is the spindle, a dynamic system of microtubules organized around two poles. The spindle attaches to replicated chromosomes and pulls the two sister chromatids apart. To ensure proper chromosome division, eukaryotes utilize the spindle checkpoint. The checkpoint operates through the kinetochore, a large multi-protein complex that assembles on chromosomes at the centromere and facilitates microtubule attachment. The goal of the checkpoint is to delay division until all chromosomes are properly aligned on the spindle with each sister chromatid attached to microtubules from opposite poles. Once the checkpoint is satisfied, mitosis is allowed to proceed from metaphase to anaphase and the chromatids are pulled into the two daughter cells (Musacchio and Salmon 2007; Tanaka 2008).

Using the simple model system *S.cerevisiae*, we have sought to better understand 1) how cells establish the spindle, the machinery that segregates chromosomes (Chapter 2), and 2) how cells ensure chromosomes are correctly attached to the spindle (Chapter 3, Appendix). More specifically, we wanted to understand what regulates the length of the spindle, and we tested several prediction of a force-balance model of regulation (Chapter 2). We found that spindle length scales with the number of chromosomal attachments, which supports the predictions of a force-balance model. In the course of investigating spindle length regulation, we also found that chromosomal attachments regulated the number of microtubules stabilized in the mitotic spindle which had previously thought to be a fixed number.

To understand how chromosomes correctly attached to the spindle, we investigated how the spindle checkpoint uses tension to distinguish between correct and incorrect attachments. Tension is generated when a chromosome bi-orients on the spindle: the two chromatids are attached to microtubules and pulled toward opposite poles but are resisted by cohesin (**Figure 2-1**). The spindle checkpoint is activated by lack of tension sensed by the Ipl1/Aurora B kinase (Pinsky and Biggins 2005). When I began my thesis work, most models of tension-sensation placed the kinase within the inner kinetochore where it was deactivated by tension either between kinetochores (inter-kinetochore models) or within them (intra-kinetochore models) (**Figure 3-1**). In my first thesis project, I investigated a novel mechanism of tension-sensation based on the dynamic localization of a constitutively active kinase. While our model, the Ipl1-cohesin sliding ring model was not supported by our experiments (Appendix), the concept of a constitutively active kinase that is spatially separated from its targets under tension has gained support through studies in higher eukaryotes (Liu et al. 2009; Maresca and Salmon 2009; Uchida et al. 2009; Wan et al. 2009). Our investigations also gathered further support for this intra-kinetochore/ spatial separation model by negating inter-kinetochore stretch models (Chapter 3). We found that inhibiting the stretching of chromatin, thus inhibiting the inter-kinetochore distance, did not activate the spindle checkpoint.

DISCUSSION and FUTURE DIRECTIONS

Chromosomal attachments regulate spindle length and microtubule number

The spindle is an essential component of chromosome segregation; it is the machinery that physically pulls chromosomes apart in anaphase. We wanted to understand how cells set the length of the metaphase spindle. The length of the metaphase spindle is important because it sets the minimum distance chromosome are separated (anaphase A distance) and in many organisms it plays a role in determining where the cleavage furrow forms (Straight and Field 2000). Mouse oocytes that assemble a longer than normal meiosis I spindle have a more symmetric cell division, creating an abnormally large polar body that sequesters important maternal molecules away from the developing egg (Dumont et al. 2007). There are three general proposed models for how cells regulate spindle length: molecular rulers, gradients, and balance of length-dependent forces (**Figure 1-6**). These three types of models were explained in depth in Chapter 1 and Chapter 2. In *S.cerevisiae*, previous work supported a force-balance model, but two key predictions of this general mechanism had not been tested. At its simplest, the force-balance model posits that spindle length is the results of outward pushing forces generated by (+) end motor proteins (Cin8 and Kip1 in *S.cerevisiae* (Hoyt et al. 1992; Saunders and Hoyt 1992)) opposed by forces that pull the kinetochores on sister chromatids towards poles. Since sister chromatids are tethered together, this results in a net inward force (Goshima et al. 2005; Stephens et al. 2013) (**Figure 2-1**).

The model predicts that chromosomal attachments provide inward force to counter the motors, and that at least one force must be length-dependent to allow spindles to reach steady-state lengths (**Figure 2-1**). Previous work had shown that eliminating cohesin, the linkage between sister kinetochores (Stephens et al. 2011), or loosening the tensile properties of

chromatin (Bouck and Bloom 2007) elongated the spindle. We found that eliminating kinetochores (*ndc10-1*) created longer spindles, and this length was similar to spindles in cells without cohesin (*GAL-MCD1*), suggesting that tethered chromatids provide inward force (**Figure 2-7**). To demonstrate that this inward force counters outward force created by (+) end motors, we measured spindle length in *kip1*Δ cells and *ndc10-1 kip1*Δ cells. Spindles were shorter without Kip1 as previously shown (Saunders et al. 1997; Straight et al. 1997) and the double deletion caused spindle length to approach wild-type length. The second prediction is that at least one force in the spindle must length-dependent to allow spindles to reach steady-state equilibriums. If there are length-dependent forces, varying the number of chromosomal attachments should cause the spindle to reach new equilibrium lengths (**Figure 2-1B and C**). We found that the number of chromosomal attachments sets the spindle length; decreasing the number of attachments produced longer spindles and increasing the number of attachments produced shorter spindles (**Figure 2-11, Figure 2-14, Figure 2-15**).

During our investigation we created cells that contained more than 30 plasmids, which presented the cell with twice as many extra centromeres as its endogenous number. Previous studies had shown that as few as 5 centromeric plasmids caused mitotic arrest and cell death (Futcher and Carbon 1986), but despite Wells and Murray's demonstration that deleting the spindle checkpoint abolishes this toxicity, the belief has persisted that multiple centromeric plasmids titrate away essential spindle component such as kinetochore proteins and microtubules from endogenous chromosomes (1996). We have expanded on Wells and Murray's finding; we are able to generate viable, healthy cells carrying more than 30 centromeric plasmids, further negating the limiting components theory of centromeric toxicity. We also demonstrated that these cells carrying 30+ plasmids are still able to attach and bi-orient endogenous chromosomes

(**Figure 2-16**) and the number of microtubules increases in the presence of extra kinetochores (**Figure 2-17**).

Previous electron microscopy on haploid yeast cells had shown that spindles contained 44±8 microtubules; because the number matches cellular needs and because the spindle pole bodies appear to be operating at or near their microtubule nucleation capacity, it is believed that this number of microtubules is fixed unless actively signaled to increase (Winey et al. 1995; Winey and Bloom 2012). The spindle checkpoint has been suggested as a possible signaling mechanism to increase microtubule number, but our strains with extra kinetochores do not contain a functional checkpoint (*mad2*Δ) which argues against checkpoint-based signaling. It is possible that *S.cerevisiae* spindle pole bodies nucleate many more than the observed ~40 microtubules, but only those stabilized by attachment to kinetochores are visualized by electron microscopy. If this is the case, our *ndc10-1* spindles raise questions about how microtubules without kinetochores are stabilized. In both our spindle reconstructions (**Figure 2-4**) and previous studies (Romao et al. 2008), *ndc10-1* spindles have microtubules emanating from the old spindle pole body. Our spindle checkpoint assay and our bi-orientation assay demonstrated that *ndc10-1* cells retain little if any kinetochore function (**Figure 2-3, Figure 2-9**). Introducing synthetic kinetochores allows microtubules from the new spindle pole to be stabilized and visualized by electron microscopy (**Figure 2-4**), so it is unlikely that residual kinetochores are stabilizing microtubules from the original pole. It will be interesting to investigate how these microtubules are stabilized and why the new spindle pole body is unable to make use of these same strategies.

Our investigation of spindle length has yielded results that support a force-balance model of spindle length regulation, but we still do not know how or where length-dependent forces

are generated in the spindle. Length-dependent forces could be generated along kinetochore microtubules or along interpolar microtubules. **Figure 4-1** shows the two different microtubule lengths that could be important for force production, either along the length of the kinetochore microtubules or in the overlap region of cross-linked interpolar microtubules. Previous studies lend some support for an overlap-length based mechanism. Ase1 has been shown to accumulate in the cross-linked region of anti-parallel microtubules, braking the sliding of microtubules to a zero velocity as the overlap region gets shorter (Braun et al. 2011). If the overlap region on interpolar microtubules shortens as spindle elongates, Ase1 could provide length-dependent braking to outward sliding force, increasing braking as the overlap shrinks (**Figure 4-2**). Kip3, a kinesin 8 motor, has been show to provide length-dependent depolymerization of microtubules *in vitro*; it depolymerizes longer microtubules faster than shorter microtubules (Varga et al. 2006). Kip3 could provide the destabilization necessary to keep interpolar microtubules from elongating and thus keep the overlap zone from growing when there are few attachments. Another mechanism based on Cin8 and Kip1 binding the overlap could produce outward length-dependent forces. Both of these (+) end motors crosslink and slide anti-parallel microtubules (Gheber et al. 1999; Kapitein et al. 2005). A shrinking overlap in longer spindles would limit the number of motors able to bind and push outward (**Figure 4-2**). Studies have modeled this potential length-dependent activity and shown that spindle length can reach equilibrium lengths based on the number of Cin8 molecules present in the spindle (Gardner et al. 2008).

In the future, the length of the overlap zone in spindles with varying attachments could be measured to see if it grows and shrinks with attachment number. We were unable to do this in our current study for two reasons: 1) changes in the overlap length are difficult to measure in spindles with extra kinetochores because the overlap already extends nearly the whole length of

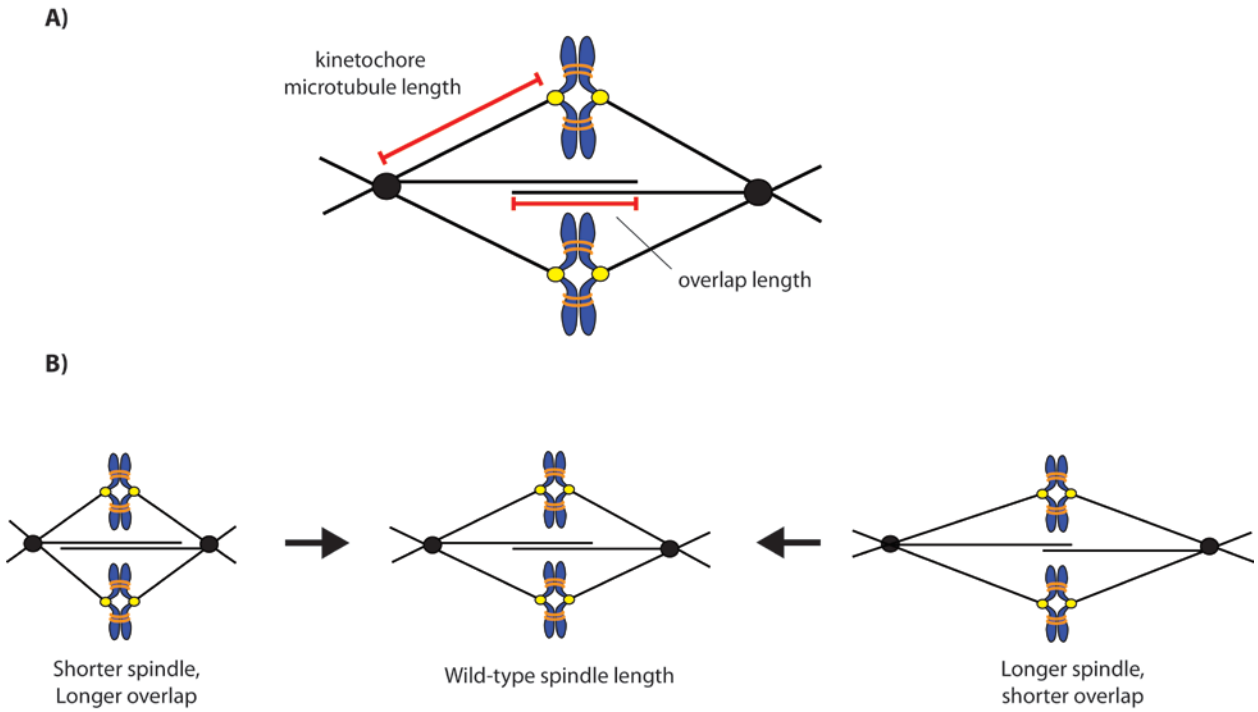

Figure 4-1. Location of length-dependent forces in the spindle. The two microtubule lengths that may generate length-dependent forces are the kinetochore microtubules, or the pole to kinetochore length, and the region of overlapped, crosslinked interpolar microtubules (**A**). *In vitro* studies of crosslinking motors have shown that length-dependent forces can be generated between antiparallel microtubules (see text for references). In order for these mechanisms to operate *in vivo*, the length of the interpolar microtubules must stay constant which will create a longer overlap region in short spindles and a shorter overlap region in long spindles (**B**).

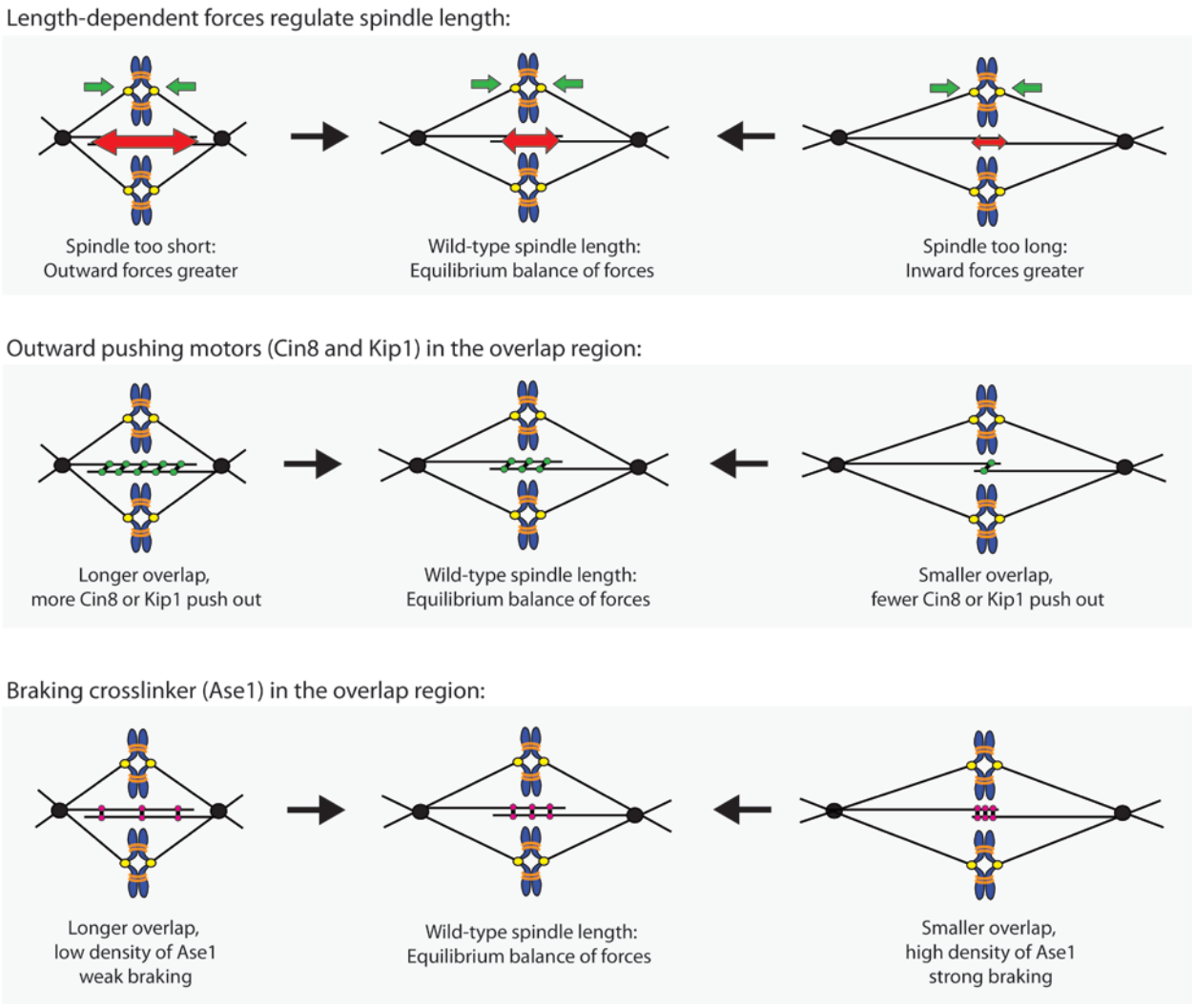

Figure 4-2. Possible mechanisms of length-dependent force generation. We found evidence for length-dependent forces regulating spindle length (Chapter 2). Shorter spindles have larger outward forces (red arrow) that push spindles to a longer length. Elongated spindles have a smaller outward force than inward force (green arrow) which causes the spindle to shorten. Wild-type spindle length is the equilibrium of these pushing and pulling forces. Two possible mechanisms for generating length-dependent forces are based on molecules bound to the overlap region. Outward pushing kinesin 5 motors Cin8 and Kip1 bind in the interpolar microtubule overlap region. A longer overlap region in short spindles could allow more molecules of these (+) end motors to bind and more strongly push outward. Conversely, a smaller overlap region in long spindles could limit the number of motors binding and pushing outward. Another possible mechanism is based on the braking ability of Ase1, a passive cross-linking molecule. Ase1 has been shown to accumulate in shrinking overlap regions and acts as a brake to microtubule sliding. Ase1 braking is stronger with higher densities of the molecule in a small overlap and weaker in a longer overlap region (see text for references).

the spindle in wild-type cells and 2) the overlap zone was compromised in *ndc10-1* spindles. Ndc10p has been shown to localize to the spindle mid-zone as well as kinetochores, and it may play a role in spindle integrity (Goh and Kilmartin 1993; Muller-Reichert et al. 2003; Bouck and Bloom 2007). We attempted eliminate kinetochores through another mechanism to avoid complications with *ndc10-1*; we tried to create a degradable form of Cep3, another CBF3 complex member that binds centromeres and interacts with other kinetochore complexes (Westermann et al. 2006). The temperature sensitive allele of Cep3 (*cep3*-2) activates the spindle checkpoint in response to microtubule depolymerization, suggesting that this allele still retains some kinetochore function (**Figure 3-3**). Previous studies had knocked out Cep3 by tagging it with a heat-inducible N-degron, an unstable protein element fused to the N-terminus of the protein of interest; when exposed to heat it causes the protein to be ubiquitinated and degraded (Gardner et al. 2001). We obtained this Cep3-degron from the authors of this study, but in our hands, it did not fully eliminate kinetochores. When treated with benomyl and nocodazole like in **Figure 2-3**, approximately half of the population arrested in metaphase implying residual kinetochore function (data not shown). We attempted to make our Cep3-degron with an improved version of the heat inducible N-degron tag (Dohmen and Varshavsky 2005) and with a plant hormone (auxin) based inducible degron (Nishimura et al. 2009), but these also activated the spindle checkpoint in response to microtubule depolymerization (data not shown).

If Cep3 or another member of the CBF3 complex not required for synthetic kinetochore function could be fully knocked out, we could investigate the effect of long spindles on the overlap zone. With no kinetochores or a few synthetic kinetochores present, we could perform electron tomography to image the length of interpolar microtubules and the size of their overlapped region. It might also be possible to image the length of the overlap using

fluorescently-tagged Ase1. As mentioned above, Ase1 passively cross-links anti-parallel microtubules and accumulates in regions of overlap *in vitro* (Varga et al. 2006) *In vivo* studies of GFP-Ase1 show that it remains in the shrinking overlap zone during anaphase but during metaphase it is hard to distinguish if it is exclusively located in the overlap region or if it is also localized along uncross-linked microtubules (Schuyler et al. 2003). In a functional Cep3-degron, we could visualize the length of the Ase1-GFP signal and see if its localization length is shorter than microtubules, which would indicate that it is just at the overlap region. Ase1-GFP length could measured in cells with a range of synthetic kinetochores.

Another question surrounding interpolar microtubules is how the cell regulates the number of these microtubules. Based on our results that the number of kinetochore microtubules increases with kinetochores suggesting that the spindle pole bodies may nucleate many microtubules, but only those attaching to kinetochores are stabilized. Interpolar microtubules remain unchanged by our perturbations; as in previous studies, there are ~5-8 interpolar microtubules per spindle (Winey et al. 1995; **Figure 2-17**; **Table 2-2**). Interpolar microtubules play an important role creating the platform for outward forces; if there were too many, outward force would be increased and too few would reduce force. How do cells set the number of interpolar microtubules? Perhaps there are specialized nucleation sites for interpolar microtubules, but this just raises the question of how the number of interpolar nucleation sites are set. The narrow geometry of the *S.cerevisiae* spindle and the crowding of chromosomes into a compact region may only allow a few interpolar microtubules to reach through to the spindle mid-zone. Another possibility is that the number is not regulated or restricted, and if held in metaphase, more interpolar microtubules would be stabilized. Studies in cells held in metaphase for 4 hours by depletion of Cdc20 show that the number of microtubules increases dramatically,

from a mean of 44 microtubules to a mean of 81 microtubules. These spindles are also longer than wild-type metaphase spindles (O'Toole et al. 1997). These electron microscopy studies were performed before the development of methods to distinguish interpolar and kinetochore microtubules, so we do not know if the number of interpolar microtubules increased. However, the elongation of the spindle length suggests that there was an increase in outward force over time, which could be provided by more interpolar microtubules providing a platform for (+) end motors. We too saw an increase in average spindle length as cells were held in a prolonged metaphase arrest (data not shown).

While investigating the increase in microtubule number in cells with centromeric plasmids, we wondered if spindle pole bodies can acutely adapt to an increased kinetochore load. In our studies, the number of centromeric plasmids was driven up over the course of several days. Cells containing the plasmid were grown to saturation in a range of copper sulfate concentrations; cells that grew in the highest concentration of copper sulfate were diluted into a new, higher range of copper sulfate concentrations (**Figure 2-13**). After approximately 4-5 days, we would have cells containing 30+ plasmids. One major question is whether the spindle poles chronically adapted to the increased demand for microtubules, or whether they can acutely nucleate more microtubules in response to extra kinetochores. In order to answer this question, we would need to drive up the copy number of a plasmid with a conditional centromere that is turned off so spindle pole bodies do not encounter the extra kinetochores until the experiment.

We have built a conditional centromere with a galactose promoter in front of the centromere (**Figure 4-3A**). Growing cells in glucose represses the promoter and the plasmid segregates similar to a wild-type centromeric plasmid (**Figure 4-3B**). When grown in galactose, the promoter is active and it is thought that the transcription machinery inhibits the binding of

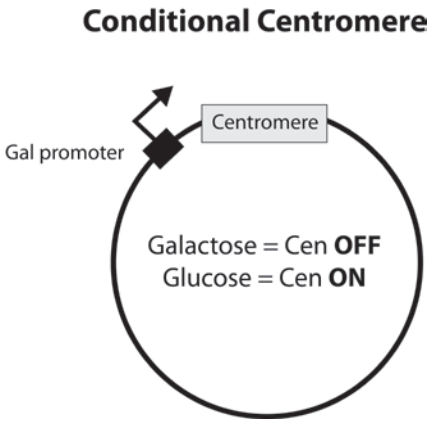

Figure 4-3A. Conditional centromere plasmid. To engineer a conditional centromere, the galactose promoter (GAL1) is placed in front of the centromere sequence. Growing the cells in glucose keeps the galactose promoter transcriptionally silent and the centromere functional. Growing the cells in galactose turns on the promoter; the recruitment of the transcriptional machinery inhibits kinetochores from binding the centromere and the centromere is turned off. This system was developed by Hill and Bloom in 1987.

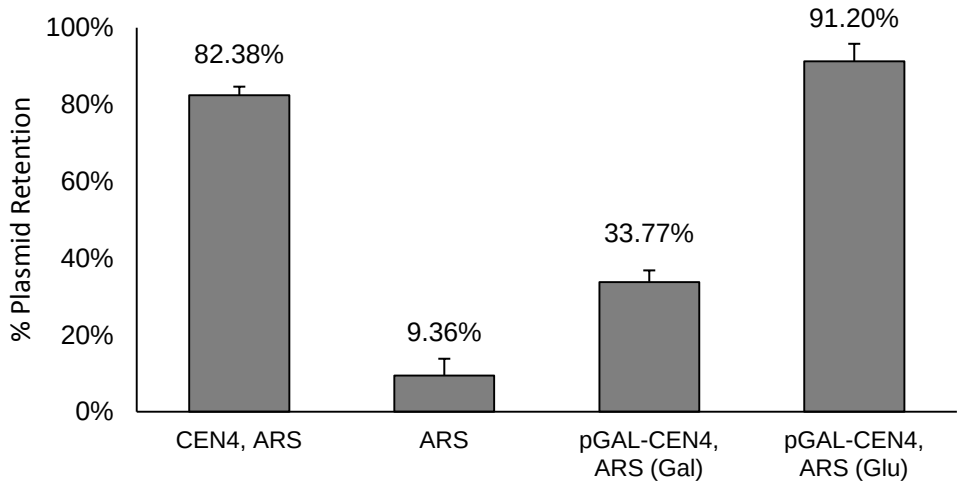

Figure 4-3B. Segregation of the conditional centromere plasmid. Plasmids bearing a centromere (CEN4) are retained by 83% of cells grown in non-selective media for 5 generations; without a centromere, only 9% of cells retain the plasmid (ARS= autonomous replication sequence). When grown in glucose, the conditional centromere plasmid behaves like a regular centromeric plasmid with high retention after 5 divisions; activation of the Gal promoter inhibits centromere function. Only 33% of cells retain the plasmid; this is higher than a non-centromeric plasmid (ARS) so some residual centromere function (p-value=0.002) but retention is significantly reduced compared to when the promoter is off in glucose (p-value=0.002). Retention rates are the average of three independent trials (two for pGAL-CEN4 in glucose); error bars represent standard deviation across trials.

kinetochore proteins (Hill and Bloom 1987). The plasmid segregates poorly in galactose, although better than a plasmid with no centromere suggesting that the centromere is not completely inactivated (p-value=0.003) (**Figure 4-3B**). We would need to drive up copy number in galactose to keep the centromere off and the spindle pole bodies unexposed to the extra kinetochores. One difficulty with these experiments is that ARS plasmids are not equally segregated and are retained in the mother cell (Murray and Szostak 1983). Mother cells would accumulate copies of the plasmid, but they would make up a small fraction of the population. We would need to be able to sort out these mother cells and perform experiments exclusively with them. Sorting could be achieved by FACS if the plasmids carried a unstable fluorescent marker. It would also be interesting to turn the centromeres on and off in a single cell cycle while holding the cells in metaphase. We could observe in real time if spindles shrink with centromeres turned on and elongate with centromeres turned off.

Our electron microscopy collaborators at the University of Colorado, Professor Mark Winey and Dr. Eileen O'Toole, are interested in using the extra centromeric plasmid system to probe when during the cell cycle spindle pole bodies grow and nucleate microtubules. Since the centromeric plasmids may provide a way to stabilize additional microtubules nucleated from the spindle pole body, they are curious if S phase-arrested spindle pole bodies can grown in size and nucleate more microtubules than previously seen (Winey and O'Toole 2001).

We have learned that chromosomal attachments generated through kinetochores set spindle length by providing an inward force that opposes outward forces from motor proteins. When chromosomes come under force, the chromatin around the kinetochore on sister chromatids stretches (Chapter 3; Goshima and Yanagida 2000; He et al. 2000). Pericentric chromatin has been shown to behave like an elastic element with spring-like properties such as

providing a restoring force that bring the centromeres back together when outward force is reduced (Bouck and Bloom 2007). There has been much investigation trying to understand the physical properties of chromatin; chromatin is often modeled as a linear Hookean spring (Goshima et al. 2005; Riberiro et al. 2009; Gay et al. 2012) but recent studies argue that a linear spring model does not explain certain observations (Stephens et al. 2013) such as the asymmetric stretching of the two sister chromatids (Stephens et al. 2011) and the distribution of kinetochore microtubules (Gardner et al. 2005). The new model posits that chromatin is a non-linear spring that has two states, an initial stiff spring that switches to a soft spring (Stephens et al. 2013). This model is based on measurements of chromatin stretch and spindle length when the chromatin spring is loosened by inhibiting pericentric cohesin. Our work in both Chapter 2 and Chapter 3 could provide more experimental conditions to test this model of chromatin properties. Stephens et al. based their model on measurements of looser chromatin springs; our experiments in Chapter 3 tightened the chromatin spring by tethering the two sister together and inhibiting stretch. Our experiments in Chapter 2 added and subtracted chromatin springs from the spindle system.

One complication with using our experimental systems to test the non-linear spring model is that we used synthetic kinetochores to generate a few attachments to kinetochore-inhibited (*ndc10-1*) cells. Synthetic kinetochore differ from natural kinetochores in several ways: they have not been shown to activate the spindle checkpoint, they bypass the need for DNA-binding kinetochore proteins, and they are not as strong as natural kinetochores (Lacefield et al. 2009). Unpublished experiments performed by Soni Lacefield showed that when an unreplicated chromosome containing both a natural kinetochore and a synthetic kinetochore (dicentric chromosome) attaches to opposite poles, the natural kinetochore "wins" the tug of war

(**Figure 4-4**). The whole chromatid is pulled closer to the pole that the natural kinetochore is attached to; if the two types of kinetochore had equal strength, the chromatid would remain in the middle of the dividing cell. Synthetic kinetochores are not as strong as natural kinetochores and may not produce the same amount of inward force, thus it would not be appropriate to calculate chromatin spring properties by quantitatively comparing spindle length in synthetic kinetochore strains to strains with extra natural kinetochores. In order to directly compare these types of spindles, we would need to create either repressible natural kinetochores or a stronger version of the synthetic kinetochore. Natural kinetochores could be inhibited by placing galactose promoters in front of all centromeres (or in front of 14 or 15 centromeres if 1 or 2 natural kinetochores are desired), but expression from the galactose promoter does not fully repress centromeres (**Figure 4-3**).

We considered the second possibility of making a stronger synthetic kinetochore during our investigations. We attempted to create an "orthologous" kinetochore by fusing the protein-interacting domain of *S.cerevisiae* Cep3 to the DNA-binding domain of *Candida glabrata* Cep3 (chimeric Cep3) and introducing a *S.cervisiae- C.glabrata* chimeric centromere (**Figure 4-5A**). Cep3p is the primary, sequence-specific binding protein that recognizes the CDEIII element in the centromere (Purvis and Singleton 2008); this recognition is species-specific. *C.glabrata* is a yeast belonging to the same family as *S.cerevisiae*; while its centromere is structurally similar to *S.cerevisiae* with a CDEI, II, and III element (reviewed in Chapter 1), it is not recognized by *S.cerevisiae* kinetochore proteins (Kitada et al. 1997). Similarly, the *C.glabrata* Cep3 (CgCEP3) does not recognize and bind *S.cerevisiae* centromeres (Stoyan and Carbon 2004). The Cep3 chimera should interact with other *S.cerevisiae* kinetochore proteins, but bind a *C.glabrata-S.cerevisiae* chimeric centromere (*S.cerevisiae* CDEI, II *C.glabrata* CDEIII) that is normally not

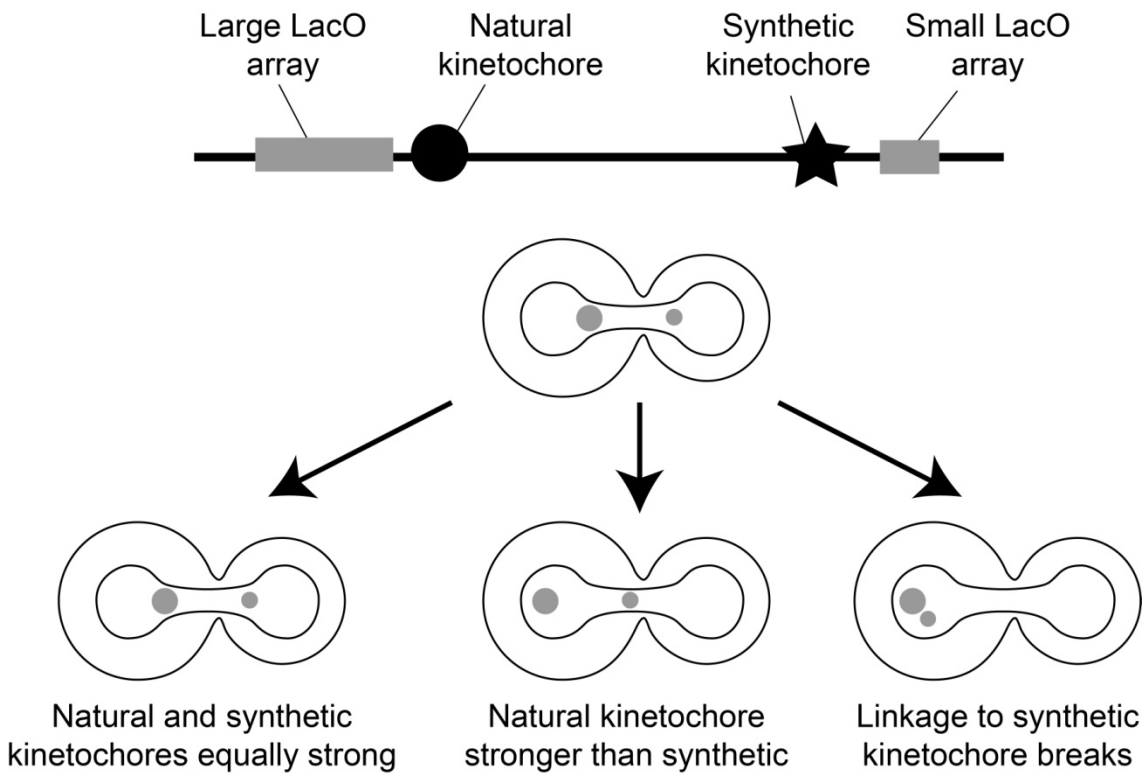

Figure 4-4. Natural kinetochores are stronger than synthetic kinetochores. A dicentric chromatid was created by introducing a synthetic kinetochore on a chromatid with a natural kinetochore. Both structures can attach to microtubules, and if attached to microtubules from opposite poles, the chromatid will be placed in a tug of war situation. A large LacO array is placed near the natural kinetochore end of the chromatid and a small array is placed near the synthetic kinetochore (makes up the synthetic kinetochore). GFP fused to the Lac repressor will label the natural kinetochore end with a large GPF dot and the synthetic kinetochore end with a small GFP dot. In mitosis, if the two dots are held in the middle of the spindle, equidistance from either pole, then the natural and synthetic kinetochores are equally strong. If the distance between the two dots collapses and they appear near each, the linkage to the synthetic kinetochore has been broken, suggesting either the synthetic kinetochore fell apart or the chromatin broke. If the large dot is closer to a pole, this suggests that the natural kinetochore is stronger than the synthetic kinetochore. Microscopy performed by Soni Lacefield found that the larger GFP dot was pulled close to the pole with the smaller dot pulled along, suggesting that the natural kinetochore won the tug of war and is stronger than synthetic kinetochore.

recognized by *S.cerevisiae* (Kitada et al. 1997). In this way, we could introduce *C.glabrata-S.cerevisiae* chimeric centromeres to provide the few chromosomal attachments when natural kinetochores are rendered nonfunctional by turning off or knocking out endogenous Cep3 (**Figure 4-5B**). We engineered the chimeric Cep3 and chimeric centromere, but the placing the chimeric centromere on an acentric plasmid and expressing the chimeric Cep3 did not segregate the plasmid. Other studies on *C.glabrata-S.cerevisiae* hybrid centromeres showed that the 50-75bp directly downstream of the CDEIII element helped stabilize *C.glabrata* Cep3 on CDEIII (Kitada et al. 1997). Our chimeric centromere contained only a *C.glabrata* CDEIII and *C.glabrata* no downstream sequence (*S.cerevisiae* downstream sequence); introduction of the sequence element may help the binding of the chimeric Cep3 and promote segregation of the plasmid.

Our investigation of spindle length raised many other questions surrounding kinetochore attachment to microtubules. Why does the presence of just one plasmid affect the ability of an endogenous chromosome to stretch (**Figure 2-16A**)? Why does the stretching of pericentric chromatin decrease significantly (from 1.2μm to 800nm) in the presence of a single centromeric plasmid? Why does chromatin stretch not drop below 800nm even as the spindle gets shorter and shorter (**Figure 2-16B**)? It would be interesting to investigate how the presence of centromeric plasmids alters the attachment and stretching dynamics of endogenous chromosomes, and if this alteration would activate the spindle checkpoint.

Electron tomography of *ndc10-1+* 3 synthetic kinetochore pairs raised questions about how many microtubules a synthetic kinetochore is capable of attaching. They appear to stabilize many more than 1 microtubule per kinetochore present, and it would be interesting to dissect how they coordinate their attachments to the same pole. Because *S.cerevisiae* have only one

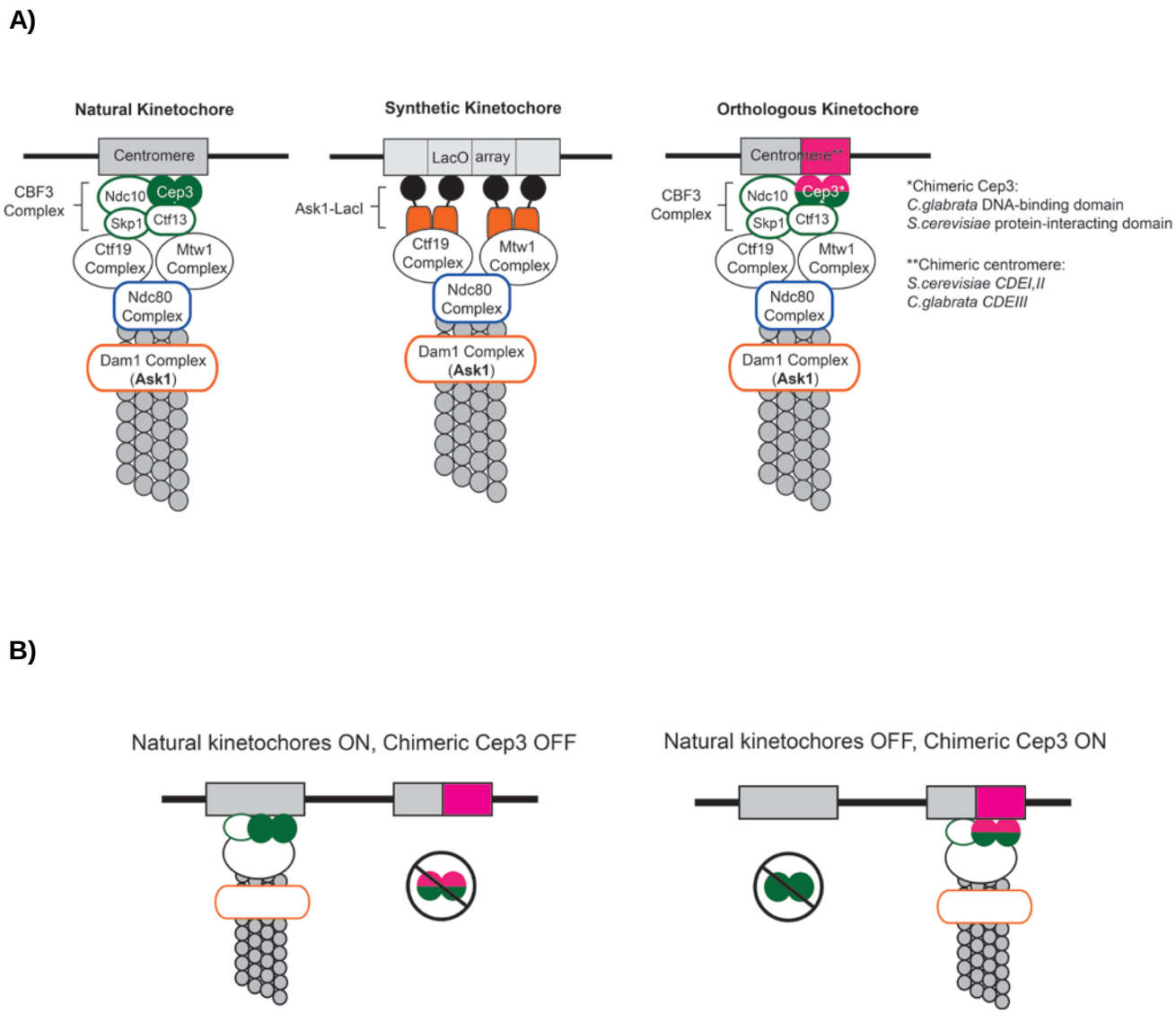

Figure 4-5. Controlling chromosomal attachments with an orthologous kinetochore. A comparison of natural kinetochores, synthetic kinetochores, and orthologous kinetochores is shown in (**A**). In natural kinetochores, Ndc10 and Cep3 are the main DNA-binding proteins. Ndc10 contacts the CDEI and CDEII elements in the centromere, and Cep3 contacts the CDEIII. Synthetic kinetochores bypass the need for the DNA-binding activity of the CBF3 complex by tethering Ask1, a Dam1 complex member, directly to the DNA at LacO arrays (no centromere needed). Orthologous kinetochores should have an architecture closer to that of a natural kinetochore. A chimeric version of Cep3 is expressed that contains the *C.glabrata* DNA-binding domain and the *S.cerevisiae* protein-interacting domain. This chimeric protein should be able to bind a chimeric centromere that has a *S.cerevisiae* CDEI and II for Ndc10 to bind but a *C.glabrata* CDEIII element for the chimeric Cep3. Natural kinetochores with wild-type Cep3 do not recognize chimeric centromeres, and without chimeric Cep3, no kinetochore proteins bind the chimeric centromere (**B**). If wild-type Cep3 is shut off and chimeric Cep3 is expressed, natural kinetochores are nonfunctional as no kinetochore proteins bind the wild-type centromere and chimeric centromeres now aseemble orthologous kinetochores with the chimeric Cep3.

microtubule attachment per kinetochore, they avoid the complications of merotelic attachments, when one kinetochore is attached to microtubules from both poles (**Figure 1-8**). It would be interesting to see how merotelic attachments are avoided or corrected with synthetic kinetochores when *S.cerevisiae* would have never needed to evolve these type of mechanisms.

Tension sensing mechanisms in the spindle checkpoint

The Ipl1/Aurora B kinase senses tension generated on bi-oriented chromosomes to distinguish between correct and incorrect attachments. The kinase activates the spindle checkpoint to arrest cells in metaphase and it destabilizes the incorrect attachment (Musacchio and Salmon 2007). In Chapter 3 and the Appendix we discuss our attempts to understand how and where the Ipl1 kinase senses tension. Tension generates stretch and elongation of pericentric chromatin and kinetochores, thus it is thought that the kinase either measures between kinetochores or within a single kinetochore (**Figure 3-1**). In Chapter 3, we asked if the spindle checkpoint measures stretching of pericentric chromatin. Introduction of lactose operator arrays on either side of the centromere and expression of a tetramerizing version of the Lac repressor inhibited chromatin stretch (**Figure 3-2**). By comparing stretch-inhibited cells to cells that express a dimeric form of the repressor that does not inhibit stretch, we found that both move through mitosis on the same time scale (**Figure 3-3**). Deletion of the spindle checkpoint does not alter this timing (**Figure 3-4**). These results suggest that Ipl1 and the spindle checkpoint does not monitor chromatin stretching and inter-kinetochore distance, which argues against inter-kinetochore models of tension-sensation. The alternative model is that tension is sensed the kinetochore. Support for the intra-kinetochore model has been found in higher eukaryotes where compressing kinetochores but maintaining inter-kinetochore distance leads to constitutive activation of the checkpoint (Uchida et al. 2009; Wan et al. 2009). Additionally, relocating the

kinase closer to the outer kinetochore destabilizes attachments and activates the checkpoint (Liu et al. 2009).

It will be interesting to test the intra-kinetochore model in *S.cerevisiae* because there are some differences in kinetochore scale and size from higher eukaryotes; *S.cerevisiae* kinetochores bind only a single microtubule and form on a short 125bp sequence. They are approximately 25nm wide and are on the order of 80nm thick (Westermann et al. 2006; Wang et al. 2008). The kinetochores of higher eukaryotes such as humans attach 20+ microtubules, span megabases of DNA, and have been measured by electron microscopy to be ~300 nm thick (Liu et al. 2009; Wan et al. 2009). This size differences begs the question of whether higher eukaryotes and *S.cerevisiae* kinetochores utilize the same intra-kinetochore stretch mechanism to separate the activity of the kinase from its targets at the microtubule interface (Liu et al. 2009; Maresca and Salmon 2009; Uchida et al. 2009; Wan et al 2009).

In the future, we could directly test the predictions of the intra-kinetochore model in *S.cerevisiae* by inhibiting stretch within the kinetochore. Both inter- and intra-kinetochore models agree that the microtubule-kinetochore interface must stretch beyond the range of Aurora B/Ipl1 activity, but it is disputed where this range of activity exists and thus where tension is measured (**Figure 4-6A**). In Chapter 3, we discounted the inter-kinetochore stretch model by demonstrating that gluing sister chromatids together and preventing stretch between kinetochores does not constitutively activate the spindle checkpoint. To directly test the predictions of the intra-kinetochore tension model, we could inhibit stretching within the kinetochore. We expect that preventing stretching of the kinetochore will cause the checkpoint to be constitutively activated. Previous studies have shown that kinetochores stretch and elongate under tension (Maresca and Salmon 2009; Uchida et al. 2009; Wan et al. 2009), and the Ndc80 complex is

A)

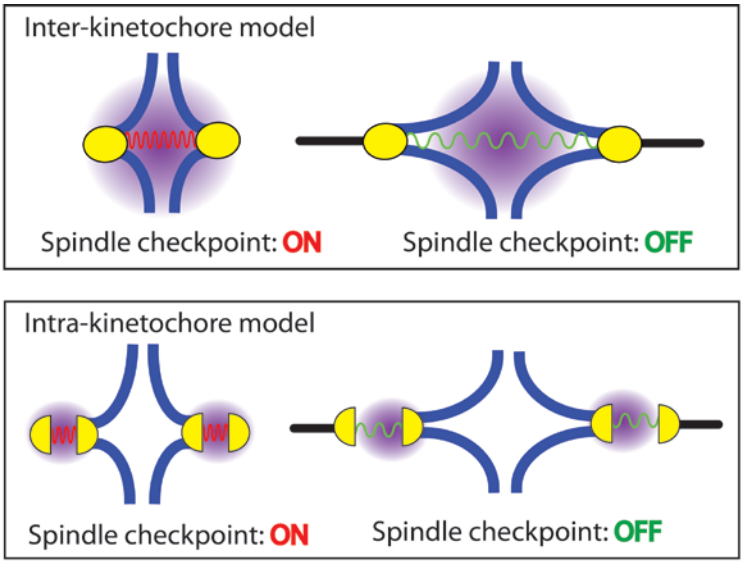

B)

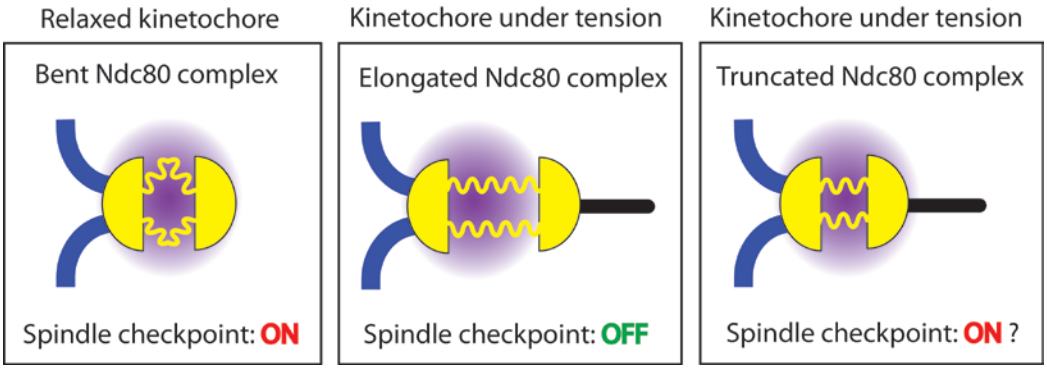

Figure 4-6. Investigation of the intra-kinetochore model in *S.cerevisiae*. Tension on bi-oriented chromosomes (blue) could either be measured in the stretch between kinetochores (inter-kinetochore model) or within a kinetochore (intra-kinetochore model) by the spindle checkpoint. In both models, the kinetochore (yellow circle)-microtubule (black line) interface must stretch beyond the activity of the Ipl1/Aurora B kinase (purple region) in order to silence the checkpoint (**A**). We found evidence against the inter-kinetochore model; when chromatin stretch is inhibited, the spindle checkpoint is not turned on (Chapter 3). Studies in higher eukaryotes have garnered support for the intra-kinetochore model, but no investigation of this model has occurred in *S.cerevisiae* (see text for references); we will do this by inhibiting kinetochore stretch (**B**). The intra-kinetochore model proposes that Ipl1 (purple region) measures stretch on a single chromatid (blue), within its kinetochore (yellow hemispheres and spring). The model predicts that inhibiting the elongation of the Ndc80 complex (yellow spring) will cause activation of the checkpoint even when the kinetochore is correctly attached to a microtubule (black line).

thought to be one of the flexible elements The Ndc80 complex is a long coiled-coil rod that contains a flexible elbow-like hinge that is thought to straighten out under tension (Wang et al. 2008; Wan et al. 2009). When Ndc80 is elongated, it is thought that the microtubule-kinetochore interface is pulled away from Ipl1, which stabilizes the microtubule attachment and turns off the checkpoint. When the kinetochore is relaxed, the kinase can contact the interface, phosphorylate it, and make the kinetochore let go of microtubules (Pinsky et al. 2006). By conditionally expressing truncated versions of the Ndc80 complex, we can determine if the checkpoint is constitutively activated as predicted by the intra-kinetochore model (**Figure 4-6B**). We could make Ndc80 truncations of varying lengths, and we would expect that shorter versions of the complex would more strongly activate the checkpoint. Conditional expression of the truncations would have to be used to avoid lethality of constitutive checkpoint activation.

In Chapter 2, we used small circular centromeric plasmids to introduce extra kinetochores to our spindles. Both in my research and in previous studies, it has been observed that the presence of multiple centromeric plasmids as well as mini-chromosomes activate the spindle checkpoint and delays mitosis (Chapter 2; Wells and Murray 1996). Mini-chromosomes are centromeric DNA elements which are much shorter than the endogenous chromosomes; they are either circular or linear plasmids that contain less than 20kb of DNA. These mini-chromosomes are often mis-segregated and their frequent inability to align correctly on the spindle activates the spindle checkpoint (Byers and Goetsch 1974). Linear mini-chromosome have more severe defects than circular mini-chromosomes, and the defects decrease with increasing length of the linear mini-chromosome (Murray et al. 1986). Why do mini-chromosomes, particularly short linear mini-chromosomes, activate the checkpoint and why do they have difficulty segregating correctly? After replication, sister chromatids are held together by cohesin rings until

segregation. Previous work from our lab suggests that mini-chromosomes may have difficulty staying linked to their sister molecule and that the chance of losing linkage increases as cells spend longer in mitosis (A.Murray personal communication). While these separated mini-chromatids could attach to the spindle, the attachments would not generate tension and Ipl1 would activate the checkpoint.

To investigate checkpoint activation by mini-chromosomes, we will observe their position on the spindle in metaphase. In metaphase, properly attached sister chromatids become stretched under tension but remain tethered to each other by cohesin rings (Goshima and Yanagida 2000; He et al. 2000); if this linkage disappears, the chromatids separate from each other prematurely (Nasymth 2005). We will fluorescently-label both a regular chromosome and a mini-chromosome near the kinetochore, and determine if the mini-sister chromatids are further apart from each other than the sister chromatids of a regular chromosome in metaphase-arrested cells (**Figure 4-7**). We will also ask if the checkpoint can be silenced by tethering mini-chromosomes together using the LacO-LacI system demonstrated in Chapter 3, and conversely, if the checkpoint is activated more strongly in cells that make less cohesin. If mini-chromosomes activate the checkpoint because their sister chromatids cannot generate tension, activation of the checkpoint should depend on Ipl1.

Both the inter-kinetochore and intra-kinetochore models of tension-sensation posit that the Ipl1 kinase is localized to the kinetochore, however in *S.cerevisiae* the location of Ipl1 remains controversial (Kim et al. 1999; Kang et al. 2001; Tanaka et al. 2002; Buvelot et al. 2003; Huh et al. 2003; Makrontoni and Stark 2009; Shimogawa et al. 2009). Determining where the kinase is located is important for understanding the mechanism of tension-sensation. Part of the difficulty surrounding Ipl1-GFP localization is that if the kinase is located in kinetochores, the

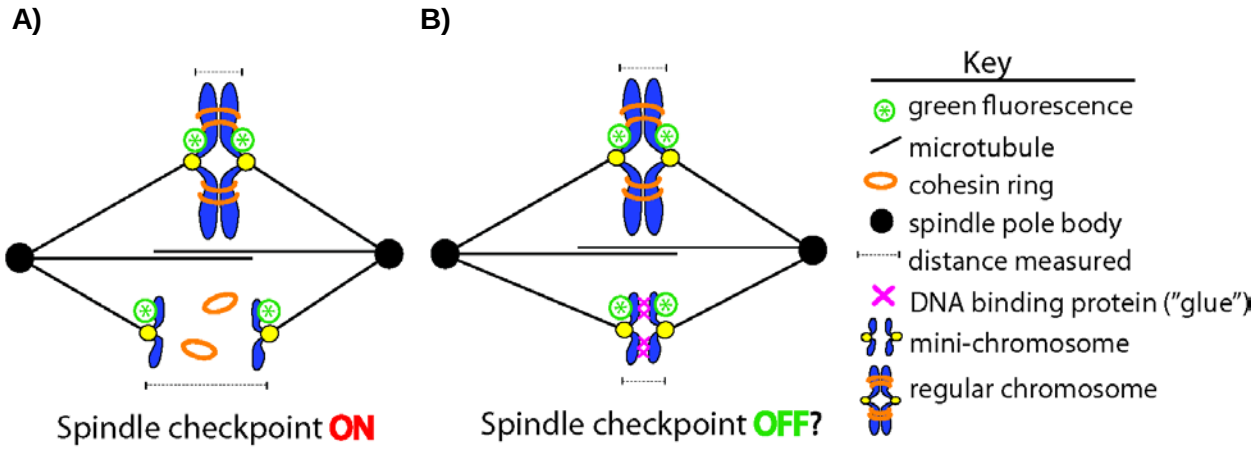

Figure 4-7. Investigation of spindle checkpoint activation by mini-chromosomes. Mini-chromosomes, both circular and linear, activate the spindle checkpoint. In Chapter 2 we used circular mini-chromosomes (centromeric plasmids) to introduce extra kinetochores but we were required to delete the spindle checkpoint in order to drive up copy number. It is believed that mini-chromosomes activate the checkpoint because the mini-sister chromatids become untethered during a prolonged metaphase arrest (**A**). In the case of linear mini-chromosomes, it is possible that cohesin rings slide off the ends of the chromatid. We will compare the distance between the endogenous sister chromatids and the mini-sister chromatids to determine if mini-chromosomes prematurely separate in metaphase. We will also glue mini-chromosomes together and ask if the checkpoint is silenced (**B**). The gluing will be accomplished through the LacI-LacO tethering system used in Chapter 3. Sister chromatids will be labeled with GFP to measure separation.

fluorescent fusion will localize to all kinetochores. In *S.cerevisiae,* kinetochores are small and restrained to the small 2µm spindle, so it is difficult to distinguish the localization pattern of 32 kinetochores from microtubules, chromatin, and spindle pole bodies, the other proposed locations of the kinase (Kim et al. 1999; Kang et al. 2001; Tanaka et al. 2002; Huh et al.2003; Shimogawa et al. 2009). We could use synthetic kinetochores to study the location of Ipl1-GFP; all other natural kinetochores could be rendered non-functional with *ndc10-1* and we could ask if Ipl1-GFP co-localizes with a single synthetic kinetochore. It is possible that Ipl1 is not in the synthetic kinetochore since synthetic kinetochores are different from natural kinetochores in several ways and we do not yet know the architecture of synthetic kinetochores. Orthologous kinetochores, explained above and in **Figure 4-5**, could be useful in this investigation because their architecture may be closer to a natural kinetochore. If Ipl1-GFP does not co-localize with synthetic kinetochores, it will be interesting to investigate if its fellow complex members Sli15 and Bir1 are located in synthetic kinetochores and if they are required for synthetic kinetochore function. Sli15 and Bir1 are important for kinase localization and activity (Kim et al. 1999; Kang et al. 2001; Tanaka et al. 2002; Shimowaga et al. 2009), and these two protein are also important structural components of the kinetochore, without out them the linkage between centromere and microtubules is compromised (Sandall et al. 2006).

Ipl1 and its complex members may not be part of the synthetic kinetochore architecture, which would explain why a single unattached synthetic kinetochore cannot activate the spindle checkpoint (Soni Lacefield and Andrew Murray, personal communication). When all natural kinetochores are knocked out with *ndc10-1,* the presence of a single synthetic kinetochore is insufficient to arrest cells in the presence of benomyl and nocodazole. These results can be interpreted to mean that synthetic kinetochores cannot activate the checkpoint, or that they

activate the checkpoint so weakly that they are unable to arrest cells. We developed a system to drive up plasmid copy number (Chapter 2); we could use this system to distinguish between these two possibilities. We could place a LacO array on a centromeric plasmid bearing *CUP1*; plasmid copy number would be driven up by selection on copper sulfate (**Figure 2-13**). The presence of a centromere on the plasmid is required to ensure a more equal distribution of the plasmid in the population; non-centromeric plasmids only accumulate in mother cells (Murray and Szostak 1983). Ask-LacI would be placed under an inducible promoter, and in a synchronized cell cycle, natural kinetochores could be turned off with *ndc10-1* and synthetic kinetochores turned on (induction of Ask1-LacI). We would assay whether these multiple synthetic kinetochores could arrest the cell cycle in the presence of benomyl and nocodazole. If synthetic kinetochores cannot arrest the checkpoint, it would interesting to see if this function could be engineered by tethering Ipl1 and its activators along with Ask1 to the LacO array.

Closing Remarks

Chromosome segregation is an essential task that must be flawlessly executed. We understand what components and structures are responsible for segregating chromosomes and we know that cells utilize a surveillance mechanism to delay the process in the face of errors. However, we do not fully understand the complex mechanisms that underlie these functions. We have found that kinetochores play an important role regulating the length of the spindle and the number of microtubules in it. Length-dependent forces regulate how long the spindle becomes, but we do not how and where these forces are generated. Spindle forces generate tension on chromatin and kinetochores and this tension is monitored by the spindle checkpoint. While stretching chromatin does not seem to be critical for distinguishing between correct and incorrect attachments, we do not know how tension may be sensed in the kinetochores. We do not know if a certain amount of force and tension is required to deactivate the Ipl1 kinase or if the kinase must simply be held at a distance from its targets. It is yet to be determined how the kinase activates the checkpoint; it may be both activate the checkpoint and destabilize incorrect attachments, or it may activate the checkpoint only indirectly by creating unattached kinetochores. Investigating these unanswered questions is essential; by studying how cells segregate chromosomes, we may shed light on how these processes go awry in cancer and birth defects and how we may prevent or correct segregation errors in the future.

REFERENCES

Braun M., Lansky Z., Fink G., Ruhnow F., Diez S. and M.E. Janson. 2011. Adaptive braking by Ase1 prevents overlapping microtubules from sliding completely apart. *Nat Cell Biol* 13: 1259-1264.

Bouck D.C. and K. Bloom. 2007. Pericentric chromatin is an elastic component of the mitotic spindle. *Curr Biol* 17: 741-748.

Buvelot S., Tatsutani S.Y., Vermaak D., and S. Biggins. 2003. The budding yeast Ipl1/Aurora protein kinase regulates mitotic spindle disassembly. *J Cell Biol* 160: 329-339.

Byers B and Goetsch L. (1974). Duplication of spindle plaques and integration of the yeast cell cycle. *Cold Spinrg Harb Symp Quant Biol* 38: 123-131.

Campbell C.S. and A.Desai. 2013. Tension sensing by Aurora B kinase is independent of survivin-based centromere localization. *Nature*: Epub ahead of print.

Dohmen R.J. and A. Varshavsky. 2005. Heat-inducible degron and the making of conditional mutants. *Methods Enzymol* 399: 799-822.

Dong Y., Vanden Beldt K.J., Meny X., Khodjakov A. and B.F. McEwen. 2007. The outer plate in vertebrate kinetochores is a flexible network with multiple microtubule interactions. *Nat Cell Biol* 9: 516-522.

Dumont J., Petri S., Pellegrin F., Terret M.E., Bohnsack M.T., Rassinier P., Georget V., Kalab P., Gruss O.J., and M.H.Verlhac. 2007. A centriole- and RanGTP-independent spindle assembly pathway in meiosis I of vertebrate oocytes. *J Cell Biol* 176: 295-305.

Futcher B. and J. Carbon. 1986. Toxic effects of excess cloned centromeres. *Mol Cell Biol* 6: 2213-2222.

Gardner R.D., Poddar A., Yellman C., Tavormina P.A., Monteagudo M.C., and D.J. Burke. 2001. The spindle checkpoint of the yeast *Saccharomyces cerevisiae* requires kinetochore function and maps to the CBF3 domain. *Genetics* 157: 1493-1502.

Gardner M.K., Pearson B.L., Sprague T.R., Zarzar T.R., Bloom K., Salmon E.D. and D.J. Odde. 2005. Tension-dependent regulation of microtubule dynamics at kinetochores can explain metaphase congression in yeast. *Mol Biol Cell* 16: 3764-3775.

Gay G., Courtheoux T., Reyes C., Tournier S. and Y. Gachet. 2012. A stochastic model of kinetochore-microtubule attachment accurately describes fission yeast chromosome segregation. *J Cell Biol* 196: 757-774.

Gheber L., Kuo S.C., and M.A. Hoyt. 1999. Motile properties of the kinesin-related Cin8p spindle motor extracted from *Saccharomyces cerevisiae* cells. *J Biol Chem* 274: 9564-9572.

Goh P.Y. and J.V. Kilmartin. 1993. NDC10: a gene involved in chromosome segregation in *Saccharomyces cerevisiae*. *J Cell Biol* 121: 503-512.

Goshima G and M Yanagida. 2000. Establishing biorientation occurs with precocious separation of the sister kinetochores, but not the arms, in the early spindle of budding yeast. *Cell*, 100: 619-33.

Goshima G., Wollman R., Stuurman N., Scholey J.M. and R.D. Vale. 2005. Length control of the metaphase spindle. *Curr Biol* 15: 1979-1988.

He X, Asthana S and PK Sorger. 2000. Transient sister chromatid separation and elastic deformation of chromosomes during mitosis in budding yeast. *Cell*, 101: 763-775.

Hill A. and K. Bloom. 1987. Genetic manipulation of centromere function. *Mol Cell Biol* 7: 2397-2405.

Hoyt M.A., He L., Loo K.K., and W.S. Saunders. 1992. Two *Saccharomyces cerevisiae* kinesin-related gene products required for mitotic spindle assembly. *J Cell Biol* 118: 109-120.

Kang J., Cheeseman I.M., Kallstrom G., Velmurugan S., Barnes G. and C.S.M. Chan. 2001. Functional cooperation of Dam1, Ipl1, and the inner centromere protein (INCENP)-related protein Sli15 during chromosome segregation. *J Cell Biol* 155: 763-774.

Kapitein L.C., Peterman E.J., Kwok B.H., Kim J.H., Kapoor T.M. and C.F. Schmidt. 2005. The bipolar mitotic kinesin Eg5 moves on both microtubules that it crosslinks. *Nature* 435: 114-118.

Kim J.H., Kang J.S. and C.S.M. Chan. 1999. Sli15 associates with the Ipl1 protein kinase to promote proper chromosome segregation in *Saccharomycs cerevisiae*. *J Cell Biol* 145: 1381-1394.

Kitada K., Yamaguchi E., Hamada K. and M. Arisawa. 1997. Structural analysis of a *Candida glabrata* centromere and its functional homology to the *Saccharomyces cerevisiae* centromere. *Curr Genet* 31: 122-127.

Lacefield S., Lau D.T.C. and A.W. Murray. 2009. Recruiting a microtubule-binding complex to DNA directs chromosome segregation in budding yeast. *Nat Cell Biol* 11: 1116-1120.

Liu D., Vader G., Vromans M.J., Lampson M.A. and S.M. Lens. 2009. Sensing chromsome bi-orientation by spatial separation of aurora B kinase from kinetochore substrates. *Science* 323: 1350-1353.

Maiato H., DeLuca J., Salmon E.D. and W.C. Earnshaw. 2004. The dynamic kinetochore-microtubule interface. *J Cell Sci* 117: 5461-5477.

Makrantoni V. and M.J.R. Stark. 2009. Efficient chromosome biorientation and the tension checkpoint in *Saccharomycs cerevisiae* both require Bir1. *Mol Cell Biol* 29: 455-4562.

Maresca T.J. and E.D. Salmon. 2009. Intrakinetochore stretch is associated with changes in kinetochore phosphorylation and spindle assembly checkpoint activity. *J Cell Biol* 184: 373-381.

Muller-Reichert T., Sassoon E., O'Toole E., Romao M., Ashford A.J., Hyman A.A. and C. Antony. 2003. Analysis of the distribution of the kinetochore protein Ndc10p in *Saccharomyces cerevisiae* using 3-D modeling of mitotic spindles. *Chromosoma* 111: 417-428.

Murray A.W. and J.W. Szostak. 1983. Pedigree analysis of plasmid segregation in yeast. *Cell* 34: 961-970.

Murray A.W., Schultes N.P. and J.W. Szostak.1986. Chromosome length controls mitotic chromosome segregation in yeast. *Cell* 45: 529-536.

Musacchio A. and E.D. Salmon. 2007. The spindle-assembly checkpoint in space and time. *Nat Rev* 8: 379-393.

Nasmyth K. 2005. How might cohesin hold sister chromatids together? *Phil Trans R Soc B* 360: 483-496.

Nishimura K., Fukagawa T., Takisawa H., Kakimoto T. and M. Kanemaki. 2009. An auxin-based degron system for the rapid depletion of proteins in nonplant cells. *Nat Methods* 6: 917-922.

O'Toole E.T. Mastonarde D.N., Giddings Jr T.H., Winey M., Burke D.J. and J.R. McIntosh. 1997. Three-dimensional analysis and ultrastructural design of mitotic spindles from the *cdc20* mutant of *Saccharomyces cerevisiae*. *Mol Biol Cell* 8: 1-11.

Pinsky B.A. and S. Biggins. 2005. The spindle checkpoint: tension versus attachment. *Trends Cell Biol* 15: 486-493.

Pinsky, B.A., Kung C., Shokat K.M., and S. Biggins. 2006. The Ipl1-Aurora kinase activates the spindle checkpoint by creating unattached kinetochores. *Nat Cell Biol* 8: 78-83.

Purvis A. and M.R. Singleton. 2008. Insights into kinetochore-DNA interactions from the structure of Cep3Δ. *EMBO Reports* 9: 56-62.

Ribeiro S.A., Gatlin J.C., Dong Y., Joglekar A., Cameron L., Hudson D.F., Farr C.J., McEwen B.F., Salmon E.D., Earnshaw W.C. and P. Vagnarelli. 2009. Condensin regulates the stiffness of vertebrate centromeres. *Mol Biol Cell* 20: 2371-2380.

Romao M., Tanaka K., Sibarita J.B., Ly-Hartig N.T., Tanaka T.U. and C. Antony. 2008. Three-dimensional electron microscopy analysis of *ndc10-1* mutant reveals an aberrant organization of the mitotic spindle and spindle pole body defects in *Saccharomyces cerevisiae*. *J Struct Biol* 163: 18-28.

Saunders W.S. and Hoyt M.A. 1992. Kinesin-related proteins required for structural integrity of the mitotic spindle. *Cell* 70: 451-458.

Schuyler S.C., Liu J.Y. and D. Pellman. 2003. The molecular function of Ase1p: evidence for a MAP-dependent midzone-specific spindle matrix. *J Cell Biol* 17: 517-528.

Shimogawa M.M., Widlund P.O., Riffle M., Ess M., and T.N. Davis. 2009. Bir1 is required for the tension checkpoint. *Mol Biol Cell* 20: 915-923.

Stephens A.D., Haase J., Vicci L., Taylor II R.M. and K. Bloom. 2011. Cohesin condensin and the intramolecular centromere loop together generate the mitotic chromatin spring. *J Cell Biol* 193: 1167-1180.

Stephens A.D., Haggerty R.A., Vasquez P.A., Vicci L., Snider C.E., Shi F., Quammen C., Mullins C., Haase J., Taylor R.M. II, Verdaasdonk J.S., Falvo M.R., Jin Y., Forest M.G. and K. Bloom. 2013. Pericentric chromatin loops function as a nonlinear spring in mitotic force balance. *J Cell Biol* 200: 757-772.

Stoyan T and J Carbon. (2004). Inner kinetochore of the pathogenic yeast *Candida glabrata*. *Eukaryot Cell* 3(5): 1154-63.

Straight A.F., Marshall W.F., Sedat J.W. and A.W. Murray. 1997. Mitosis in living budding yeast: anaphase A but no metaphase plate. *Science* 277: 574-578.

Straight A.F. and C.M. Field. 2000. Microtubules, membranes and cytokinesis. *Curr Biol* 19: R760- 770.

Tanaka T., Rachidi N., Janke C., Pereira G., Galova M., Schiebel E., Stark M.J.R., and K. Nasmyth. 2002. Evidence that the Ipl1-Sli15 (Aurora Kinase-INCENP) complex promotes chromosome bi-orientation by altering kinetochore-spindle pole connections. *Cell* 108: 317-329

Tanaka T. 2008. Bi-orienting chromosomes: acrobatics on the mitotic spindle. *Chromosoma* 117: 521-533.

Uchida K.S.K., Takagaki K., Kumada K., Hirayama Y., Noda T. and T. Hirota. 2009. Kinetochore stretching inactivates the spindle assembly checkpoint. *J Cell Biol* 184: 383-390.

Wan X. O'Quinn R.P., Pierce H.L., Joglekar A.P., Gall W.E., DeLuca J.G., Carroll C.W., Liu S.T., Yen T.J., McEwen B.F., Stukenberg P.T., Desai A., and E.D. Salmon. 2009. Protein architecture of the human kinetochore microtubule attachment site. *Cell* 137: 672-684.

Wang H.W., Long S., Ciferri C., Westermann S., Drubin D., Barnes G., and E. Nogales. 2008. Architecture and flexibility of the yeast Ndc80 kinetochore complex. *J Mol Biol* 383: 894-903.

Wells W.A. and A.W. Murray. 1996. Aberrantly segreagting centromeres activate the spindle assembly checkpoint in budding yeast. *J Cell Biol* 133: 75-84.

Westermann. S, Wang H.W., Avila-Sakar A., Drubin D.G., Nogales E., and G. Barnes. 2006. The Dam1 kinetochore ring complex moves processively on depolymerizing microtubule ends. *Nature* 440: 565-569.

Varga V., Helenius J., Tanaka K., Hyman A.A., Tanaka T.U. and J. Howard. 2006. Yeast kinesin-8 depolymerizes microtubules in a length-dependent manner. *Nat Cell Biol* 8: 957-962.

Winey, M. Mamay C.L., O'Toole E.T., Mastronarde D.N. Giddings Jr T.H., McDonald K.L. and J.R. McIntosh. 1995. Three-dimensional ultrastructural analysis of the *Saccharomyces cereivisiae* mitotic spindle. *J Cell Biol* 129: 1601-1615.

Winey M. and E.T. O'Toole. 2001. The spindle cycle in budding yeast. *Nat Cell Biol* 3: E23-27.

Winey M. and K. Bloom. 2012. Mitotic spindle form and function. *Genetics* 190: 1197-1224.

Appendix:

Investigation of a tension-sensing mechanism in the spindle checkpoint: the Ipl1-Cohesin sliding ring model

ABSTRACT

Cells utilize the spindle checkpoint to ensure that their progeny receive exactly one copy of each chromosome. In addition to monitoring the attachment of microtubules to kinetochores, the spindle checkpoint also monitors tension on chromosomes. Correctly attached or bi-oriented chromosomes experience tension as the two sister chromatids are pulled toward opposite poles but are resisted by cohesin rings that hold them together. The Ipl1/Aurora B kinase is responsible for activating the checkpoint in response to lack of tension, but it is not known how the kinase senses tension. Two current models of tension-sensation (discussed in Chapter 2) are based on a kinetochore localization of the kinase which then measures distance within the kinetochore (intra-kinetochore stretch models) or between the kinetochores (inter-kinetochore stretch models). We proposed a novel mechanism of tension-sensation in *S.cerevisiae* based on Ipl1p localization on cohesin rings. On a bi-oriented chromosome, pericentric chromatin becomes stretched as kinetochores are pulled apart and cohesin-Ipl1 slides away, unable to reach its phosphorylation targets. To test this model, we investigated whether the artificial localization of the kinase next to the kinetochore induced constitutive spindle checkpoint activation and chromosome detachment. Initially we found promising support for the model, strains with the kinase artificially tethered close to the kinetochore displayed growth defects, but further studies revealed this to be a non-related mutation. Cells with the Ipl1 kinase tethered near the kinetochore did not have growth defects, did not delay or arrest in mitosis, and did not lose centromeric plasmids at an increased rate. Our results did not support the sliding ring model of tension-sensation.

INTRODUCTION

Cells must replicate and divide their genetic material between their progeny in order to reproduce. Organisms have evolved the ability to package their genetic material into chromosomes and segregate these chromosomes equally between their daughter cells during cell division. Each replicated chromosome consists of two identical sister chromatids that must be attached to the spindle via the kinetochore (Westermann et al. 2006). To avoid mis-segregation, the kinetochores on sister chromatids must attach to microtubules from opposite spindle poles. Eukaryotes use a surveillance mechanism called the spindle checkpoint to halt the cell cycle in mitosis until all sister chromatids are properly aligned on the spindle (Musacchio and Salmon 2007). The spindle checkpoint controls the transition from metaphase to anaphase, delaying anaphase until all chromosomes are properly attached (**Figure 1-9**).

The spindle checkpoint monitors attachment of chromosomes to the spindles; it activates in response to incorrect or mono-oriented attachments such as an unattached kinetochore or both kinetochores attached to the same pole. Bi-oriented attachments with chromatids attached to opposite poles satisfy the spindle checkpoint (Li and Murray 1991; Rieder et al. 1995; Li and Nicklas 1995). The microtubules exert a force on the chromatids as they try to pull them apart, but the chromatids are held together by cohesin rings until anaphase (Nasymth 2005) . These opposing forces create tension on properly attached sister chromatids, and in the absence of tension, the Ipl1/Aurora B kinase activates the checkpoint (Biggins and Murray 2001; Stern and Murray 2001) and destabilizes the incorrect attachment (Tanaka et al 2002; Pinsky et al. 2006). Once all chromatids are bi-oriented and under tension, the checkpoint satisfied, and the cell is allowed to enter anaphase (Musacchio and Salmon 2007).

The Ipl1/Aurora B kinase selectively destabilizes incorrect attachments and activates the checkpoint, either directly activating the checkpoint or indirectly by creating unattached kinetochores (Pinsky et al. 2006). The kinase targets components of the outer kinetochore that bind microtubules (Akiyoshi et al. 2009; Cheeseman et al 2002); Ndc80 is a well-studied target of the kinase. Phosphorylation of Ndc80's basic unstructured N-terminal reduces the protein's affinity for the acidic surface of microtubules and causes the kinetochore to turn over the incorrect attachment (Ciferri et al. 2008; Wei et al. 2007; Cheeseman et al. 2006).

It is not understood how or where the spindle checkpoint and the Ipl1/Aurora B kinase sense tension. In Chapter 3, I discussed the inter-kinetochore and intra-kinetochore models of tension-sensation that propose tension is understood by the distance it creates between kinetochores (inter-kinetochore) or within a kinetochore (intra-kinetochore) (**Figure 3-1** for models). Both of these models assume that the Ipl1/Aurora B kinase is localized to the inner kinetochore, and information about these stretching distances are relayed to it (Sandall et al. 2006; Tanaka 2008; Liu et al. 2009; Maresca and Salmon 2010). Before we gathered evidence that the spindle checkpoint is not sensitive to chromatin stretch (Chapter 3), we developed a third model different from either inter- or intra-kinetochore stretch. Our model, called the Ipl1-cohesin sliding ring model, was based on a different localization of the kinase (**Figure A-1**). We predicted that the kinase was tethered to cohesin rings; without tension the cohesin and kinase slide close to the kinetochores, allowing the kinase to reach and phosphorylate its targets like Ndc80. When tension is applied, chromatin stretches causing cohesin and Ipl1 to slide away from the kinetochore, physically separating the kinase from its targets and preventing phosphorylation.

Evidence for our sliding ring model included the inconsistencies surrounding Ipl1 localization, stretching of pericentric chromatin, and the tension-dependent localization of

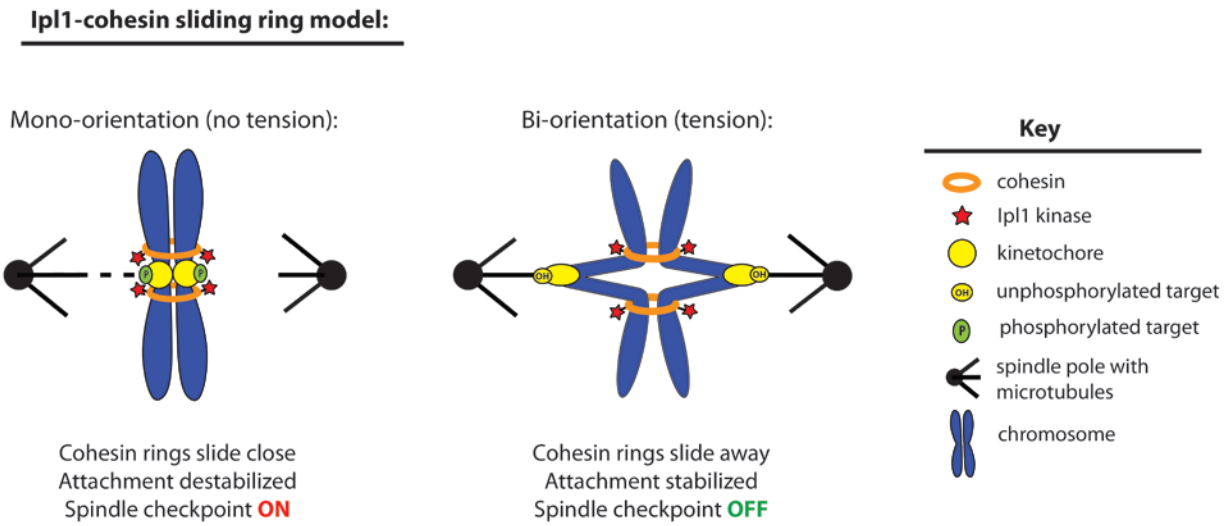

Figure A-1. Ipl1-Cohesin sliding ring model of tension-sensation. Current models of tension-sensation (inter-kinetochore and intra-kinetochore, see Chapter 3 for more on these models) posit that the tension-sensing kinase Ipl1 is statically located within kinetochores. We developed a novel mechanism of tension-sensation based on the dynamic localization of Ipl1 with cohesin rings that can slide along sister chromatids. When chromosomes make a mono-oriented attachment (does not generate tension), the cohesin rings with the associated kinase are able to slide close to the kinetochore, phosphorylate its targets and activate the checkpoint. In a correct bi-oriented attachment, the geometry of stretch chromatin forces cohesin and the kinase to slide away from the kinetochore.

cohesin around centromeres. Ipl1p localization in *S.cerevisiae* is controversial; separate studies have shown that Ipl1-GFP localizes between stretched kinetochores (Shimogawa et al. 2009), on the spindle and at spindle pole bodies (Kang et al. 2001; Kim et al. 1999; Huh et al. 2003), at the kinetochores (Makrontoni and Stark 2009), diffusely around the whole spindle region (Tanaka et al. 2002), or that it has heterogeneous localization depending on the cell (Buvelot et al. 2003). Thus the exact location of the Ipl1 kinase in *S.cerevisiae* is still unclear.

Pericentric chromatin stretches up to 800nm apart which equates to approximately 20kb of chromatin surrounding the centromere stretching to the beads-on-a-string conformation (Goshima and Yanagida 2000; He et al. 2000). Cohesin rings have a diameter of 35nm which makes them large enough to concatenate and slide on two histone-wrapped DNA strands (Nasmyth 2005; Haering et al. 2008), and it has been shown that cohesin can load at one location and translocate to another (Ciosk et al. 2000). Cohesin located along silent genes moves to sites of transcriptional convergence within 30 minutes of gene activation (Lengronne et al. 2004). The 20kb of chromatin (10kb on either side of the centromere) thought to stretch under tension is enriched for cohesin when there is no tension such as before replication or in the presence of microtubule-depolymerizing drugs (Ocampo-Hafalla et al. 2007). When chromosomes become bi-oriented, cohesin disappears in this 20kb region but cohesin levels are unchanged out on chromosome arms (Ocampo-Hafalla et al. 2007). Similarly, kinetochore mutants that disrupt microtubule attachment and weaken bi-oriented attachments cause enrichment of cohesin around the centromere (Eckert et al. 2007). Studies also showed that delocalizing cohesin from the centromere with insulator sequences that repel cohesin by static charge causes significant chromosome mis-segregation (Eckert et al. 2007). The authors argued that cohesin plays a more significant role in mediating correct chromosome attachment than simply holding chromatids

together and stabilizing kinetochore attachments because cohesin present on arms could provide this function (Eckert et al. 2007). Thus there is strong evidence for tension-dependent localization of cohesin near the centromere without tension and disappearance of cohesin on the chromatin that stretches in bi-orientation.

If our sliding ring model is correct and Ipl1 localizes on cohesin, it is removed from the centromere region and held away from its targets at the kinetochore during bi-orientation (Figure **A-1**). We sought to test our model by artificially positioning the kinase near the kineochore regardless of tension (**Figure A-2**). We fused the Ipl1 kinase to Lac repressor (LacI) and introduced a Lac operator (LacO) array near the centromere; Ipl1-LacI binds LacO and the kinase is constitutively localized to the centromere. Preliminary data supported our model; strains with the kinase tethered near the centromere exhibited growth defects but further investigation revealed this growth defect was not related to the spindle checkpoint. We expected that artificial localization of the kinase near the kinetochore would constitutively activate the spindle checkpoint and destabilize kinetochore-microtubule attachments. However, we found that tethering the kinase did not create growth defects, induce mitotic delay or arrest, or increase loss rate of centromeric plasmids. We also found that inhibiting chromatin stretch does not activate the spindle checkpoint (Chapter 3), which argues against the sliding ring model and support an intra-kinetochore model of tension-sensation (**Figure 3-3**). Ultimately our results did not support the sliding ring model.

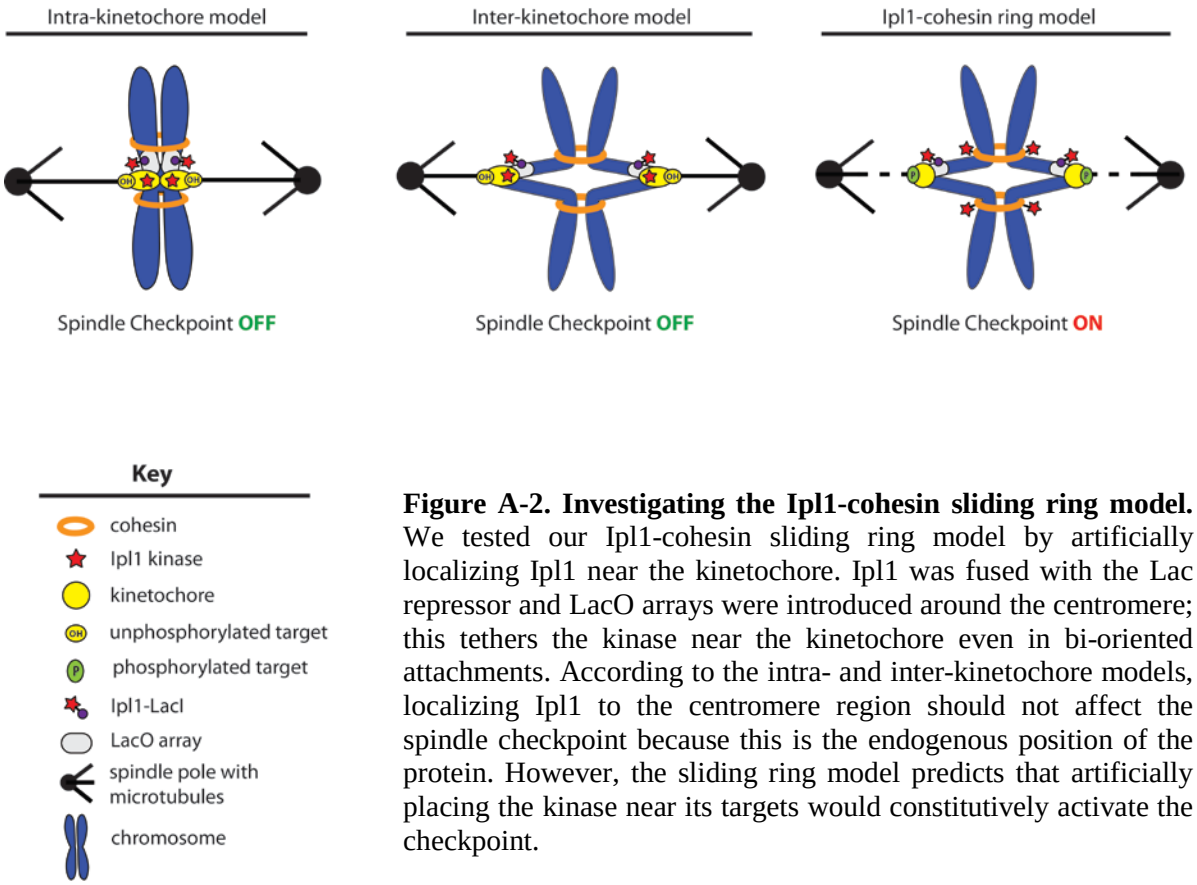

Figure A-2. Investigating the Ipl1-cohesin sliding ring model. We tested our Ipl1-cohesin sliding ring model by artificially localizing Ipl1 near the kinetochore. Ipl1 was fused with the Lac repressor and LacO arrays were introduced around the centromere; this tethers the kinase near the kinetochore even in bi-oriented attachments. According to the intra- and inter-kinetochore models, localizing Ipl1 to the centromere region should not affect the spindle checkpoint because this is the endogenous position of the protein. However, the sliding ring model predicts that artificially placing the kinase near its targets would constitutively activate the checkpoint.

RESULTS

Our model predicts that the position of the kinase is dynamic during the attachment of microtubules, while the other models (inter- and intra-kinetochore stretch, Chapter 3, **Figure 3-1**) predict that it is statically located at the kinetochore. To distinguish between the models, Ipl1 was artificially placed at varying distances from the centromere by LacI-LacO tethering. We predicted that the kinase would continually phosphorylate its targets even in bi-orientation, leading to constitutive microtubule detachment and mitotic delay or arrest. Growth rates, mitotic arrest, and plasmid loss frequency were assayed to investigate this potential phenotype. All assays compared an Ipl1-LacI tethered strain to a GFP-LacI tethered control strain.

Tethering Ipl1p near the centromere does not inhibit growth

The growth rates were measured in strains that contained Ipl1-LacI under the *HIS3* promoter or as a control, GFP-LacI under the HIS3 promoter. Functionality of the P_{HIS3}-*IPL1-LacI* fusion construct was confirmed by its ability to rescue inviable *ipl1*Δ spores. Strains also contained the LacO array integrated near the centromere on Chromosome III (1kb away from CEN3) or further away (5.6kb). We expected that tethering the kinase, and not GFP, 1kb away from the centromere could activate the checkpoint and inhibit growth, and this phenotype would disappear as the kinase was tethered further away (5.6kb).

Growth of all four strains (Ipl1 tethered 1kb away, GFP tethered 1 kb away, Ipl1 tethered 5.6kb away, and GFP tethered 5.6kb away) was measured; all grew similarly except Ipl1 tethered 1kb away which was 6 hours delayed for log phase entry compared to the other strains (**Figure A-3**).

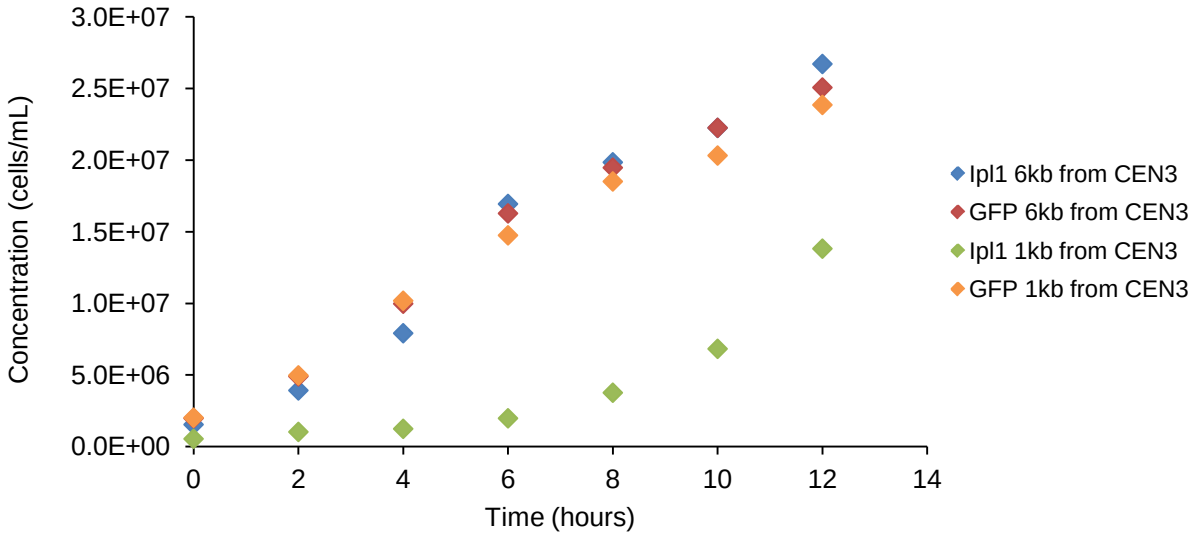

Figure A-3. Strains with Ipl1 tethered near the centromere have a growth defect. Ipl1-LacI or GFP-LacI was tethered to a LacO array near the centromere (1kb) or further away (6kb). Tethering GFP at either location and Ipl1 tethered 6kb all had similar growth curves. Strains with Ipl1 tethered 1kb away from CEN3 showed impaired growth. Cells were grown overnight in SC-HIS+ 10mM 3'aminotriazole and back-diluted to a starting density around $1x10^6$ cells/mL. Culture density was measured every two hours for twelve hours.

These growth curves were performed in synthetic complete media lacking histidine (SC-HIS) with 10mM 3'aminotriazole to induce expression of the *HIS3* promoter, and thus Ipl1-LacI and GFP-LacI. Growing cells in SC-HIS + 3'aminotriazole induces moderate expression while growing them in histidine containing media allows only low levels of expression (Struhl and Hill 1987; Straight et al. 1996). We grew our strains in YPD (containing histidine) and assayed growth to determine if the growth defect would persist with reduced levels of the kinase. The growth pattern was similar, strains containing Ipl1-LacI tethered 1kb away from the centromere showed a growth defect compared to the other strains (**Figure A-4**). This pattern held when we reduced the size of the Lac operator. The array used throughout these studies contained 256 repeats and can therefore tether up to 512 molecules; we reduced to the number of repeats to 32, allowing only a maximum of 64 molecules to be tethered and we still saw the growth defect in strains with Ipl1 tethered near the centromere (**Figure A-5**).

During the course of experimentation, the Ipl1-LacI strain was remade to confirm that the phenotype was due to kinase tethering. We found that the growth defect of the original Ipl1-LacI strain did not depend on tethering as expected; cells without a LacO array still exhibited the growth defect (**Figure A-6**). When the strain was remade, the new Ipl1-LacI did not display the growth defect when tethered 1 kb from the centromere (**Figure A-7**). The growth defect seen in the original Ipl1-LacI strain was not spindle checkpoint dependent. Deletion of Mad2 did not suppress the growth phenotype, thus the growth defect was not due to activation of the checkpoint and most likely due to a non-related mutation (**Figure A-8**). We remade the strain several times to confirm, and found with each strain that tethering the Ipl1 kinase near the centromere did not cause growth defects (data not shown).

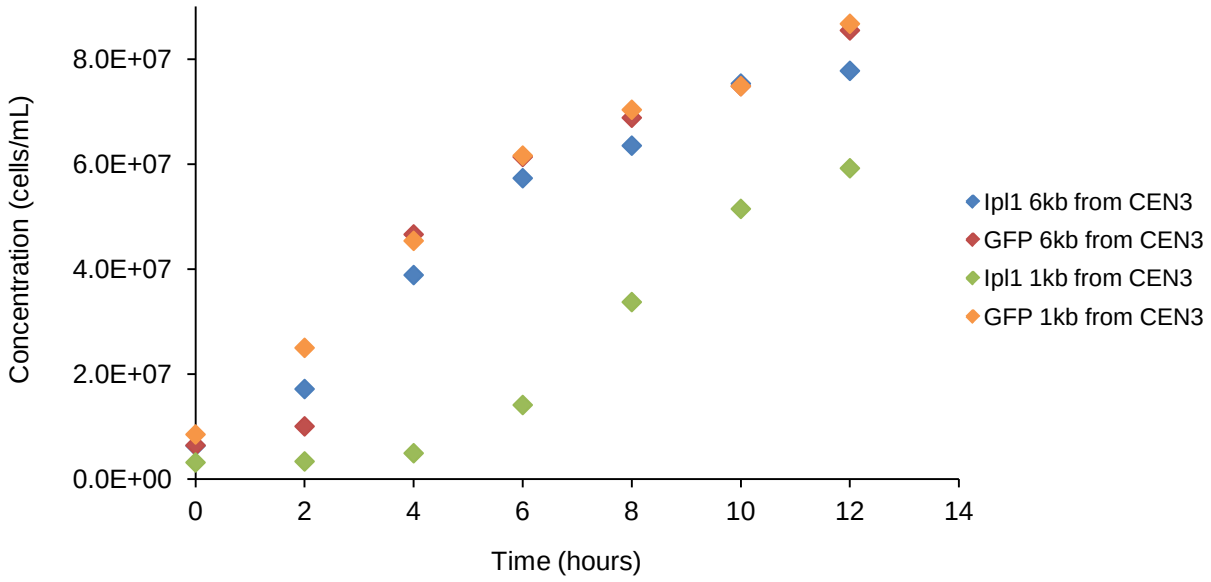

Figure A-4. Ipl1 growth defect present in media that reduces expression of the fusio protein. Ipl1-LacI or GFP-LacI was tethered to a LacO array near the centromere (1kb) or further away (6kb). Tethering GFP at either location and Ipl1 tethered 6kb all had similar growth curves. Strains with Ipl1 tethered 1kb away from CEN3 showed impaired growth, even in YPD media that only allows basal expression of the fusion proteins. Cells were grown overnight in YPD and back-diluted to a starting density around $1x10^6$ cells/mL. Culture density was measured every two hours for twelve hours.

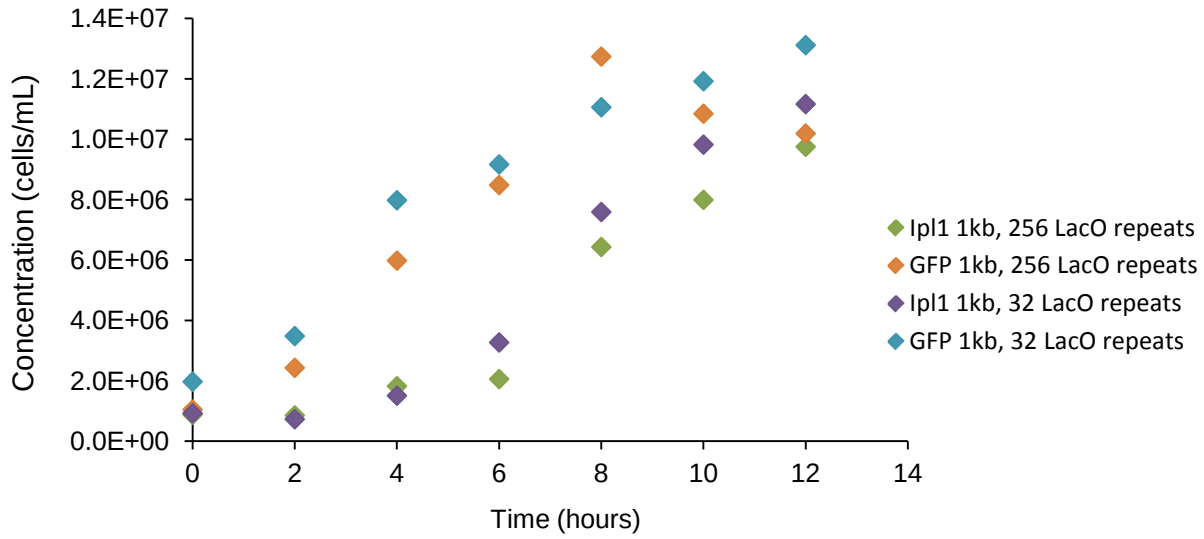

Figure A-5. The amount of kinase tethered near the centromere does not affect the growth defect defect. The 256 LacO array can maximally bind and tether 512 molecules of Ipl1-LacI; we reduced the number of tethered molecules by replacing the 256 repeat array with a 32 repeat array, allowing only a maximum of 64 Ipl1-LacI (or GFP-LacI) molecules to bind. The growth defect was still present in the strain that could only bind 64 molecules of Ipl1-LacI. . Cells were grown overnight in YPD and back-diluted to a starting density around $1x10^6$ cells/mL. Culture density was measured every two hours for twelve hours.

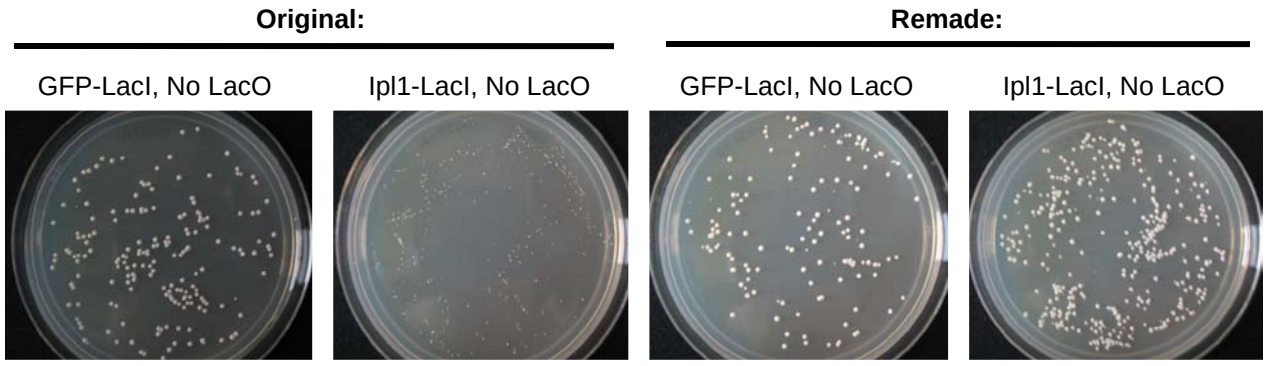

Figure A-6. Ipl1 growth defect is not reproducible or dependent on tethering. The observed growth defect is strain specific, appearing only in the original strain but not in the remade strain. The defect seen in the original strain is not specific to tethering of the kinase near the centromere; the defect is present in strains without the LacO array.

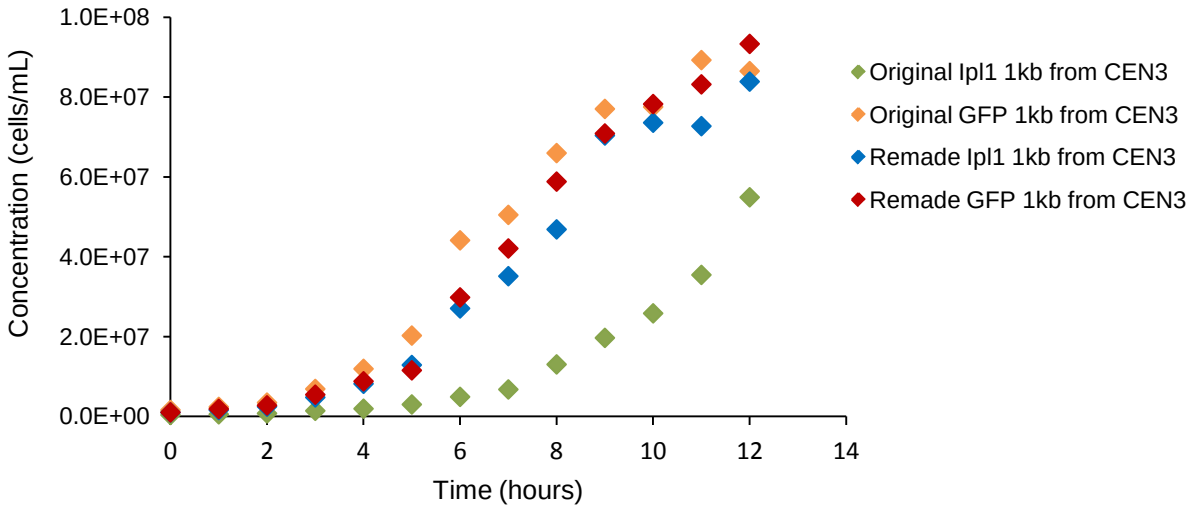

Figure A-7. The Ipl1-tethered growth defect is not reproducible. All strains were remade; genotypically identical strains produced different growth rates. The original Ipl1-tethered strain (green diamond) displayed the growth defect, but a remade version of the Ipl1-strain (blue diamond) did not have a growth defect. Three additional independently made Ipl1-LacI strains did not show a growth defect (data not shown). Cells were grown overnight in YPD and back-diluted to a starting density around $1x10^6$ cells/mL. Culture density was measured every two hours for twelve hours.

Figure A-8. Ipl1 growth defect is not dependent on the spindle checkpoint. The growth defect seen in the original Ipl1-tethered strain was not due to checkpoint activation; knocking out Mad2 did not restore normal growth.

Tethering Ipl1p kinase near the centromere does not delay mitotic progression

It is possible that tethering Ipl1 near the centromere causes only a transient activation of the spindle checkpoint, thus creating a minor delay in mitotic progression that would not be captured by measuring gross growth rates in an asynchronous population. To probe for mitotic delay, cells containing GFP-LacI or Ipl1-LacI (remade) and a LacO array 1kb from the centromere were grown to log phase and synchronized in G1 with alpha factor. Cells were washed and released into a synchronized cell cycle; samples were collected every 30 minutes and scored for cell morphology. As cells progress through the cell cycle, they produce a daughter bud cell that grows in size until it breaks away from the mother at cytokinesis. Cells that delay or arrest in metaphase appear as large-budded cells that persist in the population (**Figure A-9A**). For example, when cells are treated with microtubule-depolymerizing drugs, the spindle checkpoint is activated and 90% of wild-type cells are still large-budded 240 minutes post-release from G1 (**Figure 2-3B**). Both Ipl1- and GFP-tethered cells peaked in metaphase at 90 minutes post-release with approximately 50% large-budded cells (**Figure A-9B**). Tethering did not appear to cause mitotic delay because at T=120 minutes the percent of large budded Ipl1-tethered cells had dropped to approximately 30%, same as the control GFP-tethered cells. There was no statistical difference between Ipl1 and control GFP cells at all time points.

Tethering Ipl1p kinase near the centromere does not increase plasmid loss frequency

The growth curves and mitotic progression assays demonstrated that tethering Ipl1 near the centromere does not cause a delay in mitosis, suggesting that the kinase is not activating the checkpoint. In addition to its role in checkpoint activation, Ipl1 also destabilizes incorrect attachments, so we investigated the effect of tethering the kinase on the transmissibility of a

A)

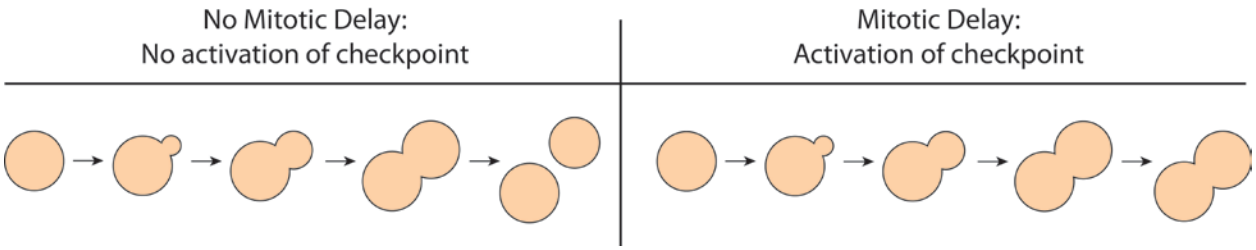

B)

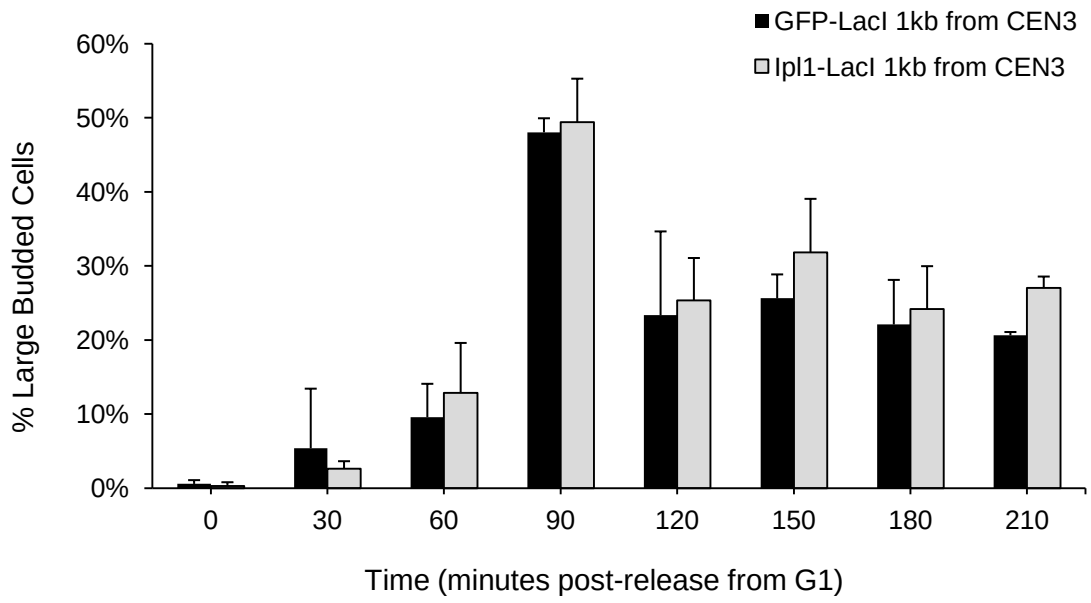

Figure A-9 Tethering Ipl1 near the centromere does not delay mitosis. Transient activation of the spindle checkpoint can cause minor delays in mitosis not seen by gross population growth measurements. Ipl1- and GFP-tethered strains were synchronized and released from G1 into the cell cycle. Samples were taken every 30 minutes and cells were scored for mitotic progression. Delays in metaphase result in a persistence of large-budded cells (**A**). Tethering Ipl1 near the centromere does not cause a persistence of large-budded cells (**B**); both GFP- and Ipl1-tethered cells peak in metaphase at T=90 minutes with 50% large budded and then drop to 30% large-budded for the remaining time points. There is no statistical difference between GFP- and Ipl1-tethered samples (p-values>0.25). Reported values are the average of 3 independent trials with n>100 cells for each trial; error bars represent standard deviation across the trials.

centromeric plasmid. In previous experiments, Ipl1 or GFP was tethered 1kb away from the centromere which if the chromatin was maximally stretched to beads on a string conformation would place the kinase approximately 40nm from the kinetochore. We predicted that this close tethering distance in combination with the dynamic stretching of chromatin that occurs on bi-oriented chromosomes (He et al. 2000; Indjein and Murray 2007) should bring the kinase into contact with the kinetochore. In case the 40nm distance is too far away for the kinase to reach its targets at the kinetochore, we conducted the final set of experiments with Ipl1 tethered 3nm (75bp) from the kinetochore. Technical issues associated with inserting the large LacO array (13kb) next to the chromosomal centromere prevented us from tethering the kinase this closely in previous experiments. Centromeric plasmids were constructed with the LacO array 75bp from the centromere sequence, and either GFP- (control), Ipl1-LacI, Sli15-LacI, or both Ipl1-LacI and Sli15-LacI were tethered on the plasmid. Sli15 (INCENP in higher eukaryotes) is an activator of the Ipl1 kinase, and previous experiments had shown that localizing INCENP at various places within the kinetochore recruits and activates the kinase (Liu et al. 2009; Carmena et al. 2012; Campbell et al. 2013). It possible that tethering Sli15 will recruit and activate the kinase, destabilizing the segregation of the plasmid. Likewise, tethering both Ipl1 and Sli15 could activate the kinase and destabilize the plasmid.

Cells containing the LacO-centromeric plasmid and tethered protein were grown in media selective for the plasmid (synthetic complete media lacking leucine or SC-LEU), then diluted into non-selective media and grown for 9 hours or approximately 5 divisions. The percentage of cells that retained the plasmid was obtained by plating cells on selective and non-selective plate and dividing growth on selective plates by growth on non-selective plates (Lacefield et al. 2009). In all four strains (GFP-, Ipl1-, Sli15-, Ipl1 and Sli15-LacI), approximately 85% of cells retained

the centromeric plasmid (**Figure A-10**). There was no statistical difference between the experimental (Ipl1-, Sli15-, Ipl1 and Sli15-LacI) and control (GFP-LacI) cells. These results indicated that tethering Ipl1, its activator Sli15, or both together next to the centromere does not destabilize plasmid segregation, suggesting that the microtubule-kinetochore attachment is not compromised. We also investigated chromosome loss rates on chromosomes with the kinase tethered near the centromere. Tethering the kinase did significantly increase chromosome loss rates compared to the control (data not shown).

DISCUSSION

The Ipl1/Aurora B kinase is essential for sensing tension on bi-oriented chromosomes and relaying this information to the spindle checkpoint. The kinase activates the checkpoint in response to tensionless attachments and destabilizes the kinetochore-microtubule interaction, allowing cells an opportunity to make a correct attachment (Musacchio and Salmon 2007). Models of tension-sensation posit that the kinase is located within the kinetochore and senses either stretch between the kinetochores (inter-kinetochore models) or within the kinetochore (intra-kinetochore models) (described in more depth in Chapter 3) (Sandall et al. 2006; Tanaka 2008; Liu et al. 2009; Maresca and Salmon 2010). Based on conflicting reports of Ipl1 localization and the tension-dependent localization of cohesin near the centromere, we put forth a novel mechanism in which the kinase is located on cohesin. When chromosomes are mono-oriented, the cohesin rings with the attached kinase are free to slide along the chromatids, allowing Ipl1 to interact with the kinetochores, phosphorylate critical substrates, and destabilize microtubules. However, in a bi-oriented state, the stretched centromeres create a geometry in

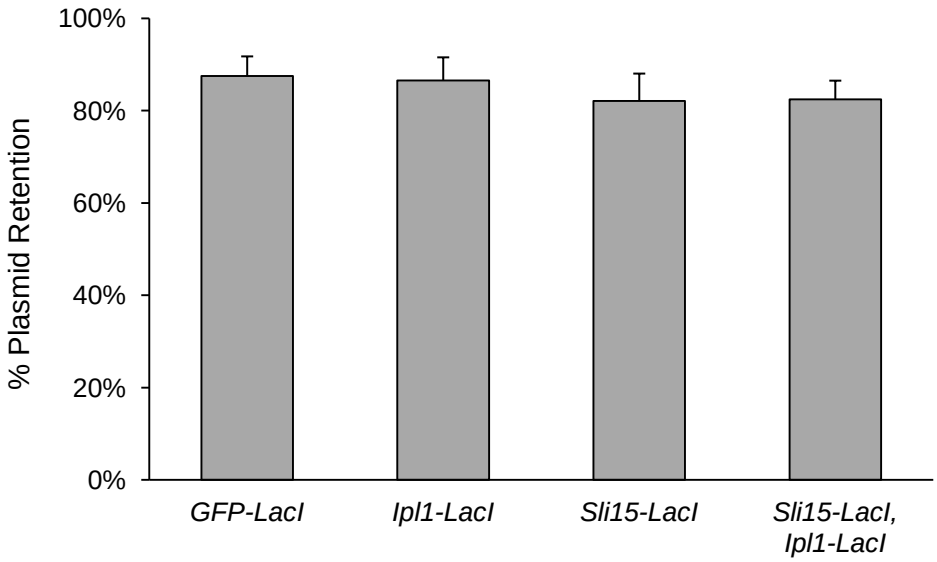

Figure A-10. Tethering Ipl1, Sli15, or both proteins does not destabilize the segregation of a centromeric plasmid. Proteins (GFP, Ipl1, Sli15 or Ipl1 and Sli15) were tethered 73bp from the centromere on a plasmid. Cells were assayed for the ability to retain the plasmid after approximately 6 cell divisions in non-selective media. Tethering the Ipl1 kinase, its activator Sli15, or both together did not affect the segregation of the plasmid. Plasmid retention rates were not statistically different from tethering control GFP near the centromere (p-values>0.2). Reported values are the average of 3 independent trials with n>300 cells counted in each trial; error bar represent the standard deviation across the three trials.

which the cohesin rings are unable to slide near the kinetochore and thus Ipl1 would be inhibited from acting on the microtubule attachment (**Figure A-1**).

We tested our proposed model by tethering the kinase near the centromere using the LacI-LacO system (Lacefield et al. 2009; Lau and Murray 2012). The other models suggest that the kinase is located in the kinetochore, so tethering extra kinase should not affect these mechanisms. Our model however argues that artificially holding the kinase near the centromere should constitutively activate the checkpoint and destabilize kinetochore-microtubule interactions. We found that tethering the kinase near the centromere did not cause growth defects (despite initial findings that later shown to be a strain-dependent phenomenon), did not induce mitotic delay, and did not increase the loss rate of plasmids or chromosomes. In an attempt to test our model, we also tethered sister chromatids together to inhibit chromatin stretching (Chapter 3). According to our model, inhibiting chromatin stretch would allow cohesin to slide close to the kinetochore similar to a tensionless attachment and activate the checkpoint. We found instead that the checkpoint is not sensitive to chromatin stretch; inhibiting stretch does not induce a mitotic delay (**Figure 3-2 and Figure 3-3**).

Our findings do not support our sliding ring model, and based on our chromatin stretch results and similar findings by others (Uchida et al. 2009; Maresca and Salmon 2009; Wan et al. 2009), an intra-kinetochore model of tension-sensation is the most likely mechanism employed by the kinase. Two aspects of our model that may still play a role in tension-sensing are the constitutive activity of the kinase and its physical separation from its targets in bi-orientation. Different intra-kinetochore models have suggested that the kinase is either selectively activated by loss of tension (Sandall et al. 2006; Tanaka 2008) or it is always activate but is spatially separated from its targets under tension (Liu et al. 2009; Maresca and Salmon 2010). Liu et al.

have made a compelling argument for the spatial separation of a constitutively kinase; they demonstrated that the phosphorylation of an Aurora B target depends on how far it is from the kinase, not on the tension state of the kinetochore. When the target is placed closer to the inner kinetochore, it becomes phosphorylated even on bi-oriented chromosomes. Additionally, artificially localizing the kinase further out in the kinetochore, closer to the microtubule interface, causes constitutive activation of the checkpoint and turnover of microtubule attachment. These studies were conducted in HeLa that have much larger kinetochores and centromeres than yeast; the kinase was repositioned 0.5-1µm closer to the outer kinetochore to induce constitutive checkpoint activation. The entire yeast spindle is only 1.5-2.0µm, so it will be interesting to see if the intra-kinetochore spatial separation model holds true in the small kinetochores of *S.cerevisiae.*

METHODS and MATERIALS

Strains and media

Strains used in this study are listed in Table A-1; all strains were constructed in W303 background (*ade2-1 his3-11,15 leu2-3,112 trp1-1 ura3-1 can1-100*) using standard genetic techniques. Lactose operator arrays containing 256 or 32 repeats of the operator were integrated either 5.6kb or 1.3kb from the centromere on Chromosome III. Ipl1- and Sli15-LacI fusion constructs contained a 78bp serine-glycine linker between the two protein domains; without the linker, the fusions were not functional. Unless otherwise noted, cells were grown in YPD (2% glucose) at 30°C. For high induction of constructs under the HIS3 promoter (P_{HIS3}-GFP-LacI and P_{HIS3}-Ipl1-LacI), cells were grown in Synthetic Complete media (2% glucose) lacking histidine (SC-HIS) with 10mM 3'aminotriazole. All chemicals were purchased from Sigma Aldrich.

Growth curves

Cells were grown overnight at 30°C in log phase and back-diluted to a concentration of $1x10^6$ cells/mL (early log phase). Cultures were grown at 30°C for 12 hours; samples were taken every 2 hours, sonicated, and measured for density using a Beckman-Coulter counter. Growth curves were performed in YPD (2% glucose) for low induction of the fusion proteins and in SC-HIS + 3'aminotriazole for high induction (Struhl and Hill 1987; Straight et al. 1996).

Plasmid Loss/Retention Assay

Cells were grown overnight in synthetic complete media lacking leucine and histidine (SC -LEU-HIS). Plasmids carried the *LEU2* gene, so lack of leucine selected for retention of the

plasmid; lack of histidine promotes expression of Ipl-LacI and GFP-LacI. Cells were diluted 1:50 and grown non-selectively for 9 hours in SC-HIS. Approximately 500 cells were plated on SC-HIS and 500 cells were plated on SC-HIS-LEU. The number of cells were counted on all plates and plasmid retention was calculated by dividing the number of cells on SC-HIS-LEU by the number on SC-HIS. Three technical replicate plates were counted and averaged for each trial, 3 independent trials were performed (Lacefield et al. 2009).

Mitotic Progression Assay

Strains used in this assay had both GFP-LacI and Ipl1-LacI under control of the *GAL1* promoter to prevent expression until release in the synchronized cell cycle. Cells were grown overnight in YEP+2% raffinose; Log phase cells (~$5x10^6$ cells/ml) were arrested in G1 with 10μg/ml α factor (Bio-Synthesis) for 3 hours. After confirmation of arrest by light microscopy, cells were washed three times with YEP (no sugar) to remove α factor and released into YEP+2% galactose to induce expression of Ipl1-LacI and GFP-LacI. Cultures were grown for 210 minutes at 30°C and samples were collected every 30 minutes. Samples were scored for mitotic progression by cell morphology (large-budded) using light microscopy.

Table A-1. Strains used in Appendix Chapter.

Strain Name	Genotype
yNJN11	*MATa, P_{HIS3}-GFP-$LacI_2$::HIS3*
yNJN12	*MATa, P_{HIS3}-IPL1-$LacI_4$::HIS3 **growth defect***
yNJN25	*MATa, P_{HIS3}-GFP-$LacI_2$::HIS3 **remade version of yNJN11***
yNJN24	*MATx, P_{HIS3}-IPL1-$LacI_4$::HIS3 **remade version of yNJN12, no growth defect***
yNJN30	*MATa, P_{HIS3}-IPL1-$LacI_4$::HIS3 **remade version of yNJN12, no growth defect***
yNJN31	*MATx, P_{HIS3}-IPL1-$LacI_4$::HIS3 **remade version of yNJN12, no growth defect***
yNJN40	*MATa/x, P_{HIS3}-IPL1-SG-$LacI_4$::HIS3, LacO(256)::LEU2::5.6kb upstream CEN3, URA3:ChromIII 124-124k, TRP1: ChromIII 78-79k*
yNJN41	*MATa/x, P_{HIS3}-GFP-$LacI_2$::HIS3, LacO(256)::LEU2::5.6kb upstream CEN3, URA3:ChromIII 124-124k, TRP1: ChromIII 78-79k*
yNJN42	*MATa/x, P_{HIS3}-IPL1-SG-$LacI_4$::HIS3, LacO(256)::LEU2::1.3kb upstream CEN3, URA3:ChromIII 124-124k, TRP1: ChromIII 78-79k*
yNJN43	*MATa/x, P_{HIS3}-GFP-$LacI_2$::HIS3, LacO(256)::LEU2::1.3kb upstream CEN3, URA3:ChromIII 124-124k, TRP1: ChromIII 78-79k*
yNJN44	*MATa/x, P_{HIS3}-IPL1-SG-$LacI_4$::HIS3, LacO(32)::LEU2::5.6kb upstream CEN3, URA3:ChromIII 124-124k, TRP1: ChromIII 78-79k*
yNJN45	*MATa/x, P_{HIS3}-GFP-$LacI_2$::HIS3, LacO(32)::LEU2::5.6kb upstream CEN3, URA3:ChromIII 124-124k, TRP1: ChromIII 78-79k*
yNJN86	*MATa, P_{HIS3}-IPL1-$LacI_4$::HIS3, mad2Δ::KanMX*
yNJN87	*MATa, P_{HIS3}-GFP-$LacI_2$::HIS3, mad2Δ::KanMX*
yNJN112	*MATa/x, P_{HIS3}-GFP-$LacI_2$::HIS3, LacO(256)::LEU2::1.3kb upstream CEN3, URA3:ChromIII 124-124k, TRP1: ChromIII 78-79k **remade***
yNJN130	*MATa/x, P_{HIS3}-IPL1-SG-$LacI_4$::HIS3, LacO(256)::LEU2::1.3kb upstream CEN3, URA3:ChromIII 124-124k, TRP1: ChromIII 78-79k**remade***
yNJN133	*MATa/x, P_{HIS3}-IPL1-SG-$LacI_4$::HIS3, LacO(256)::LEU2::1.3kb upstream CEN3, URA3:ChromIII 124-124k, TRP1: ChromIII 78-79k**remade***
yNJN134	*MATa/x, P_{HIS3}-IPL1-SG-$LacI_4$::HIS3, LacO(256)::LEU2::1.3kb upstream CEN3, URA3:ChromIII 124-124k, TRP1: ChromIII 78-79k**remade***

Table A-1. Strains used in Appendix Chapter.

Strain Name	Genotype
yNJN140	*MATa/x, P_{HIS3}-IPL1-SG-$LacI_4$::HIS3, LacO(256)::LEU2::1.3kb upstream CEN3, URA3:ChromIII 124-124k, TRP1: ChromIII 78-79k**remade***
yNJN168	*MATa, P_{HIS3}-GFP-$LacI_2$::HIS3, mad2Δ::KanMX*
yNJN169	*MATa, P_{HIS3}-IPL1-SG-$LacI_4$::HIS3, mad2Δ::KanMX*
yNJN171	*MATa, P_{GAL1}-IPL1-SG-$LacI_4$::HIS3, LacO(256)::LEU2::1.3kb downstream CEN3*
yNJN172	*MATa, P_{GAL1}-GFP-$LacI_2$::HIS3, LacO(256)::LEU2::1.3kb downstream CEN3*
yNJN181	*MATa, P_{HIS3}-IPL1-SG-$LacI_4$::HIS3, pNJN112 plasmid: LEU2, ARS1, CEN3, LacO(256):73bp from CEN3*
yNJN182	*MATa, P_{HIS3}-GFP-$LacI_2$::HIS3, pNJN112 plasmid: LEU2, ARS1, CEN3, LacO(256):73bp from CEN3*
yNJN194	*MATa, P_{HIS3}-SLI15-SG-$LacI_4$::TRP1, pNJN112 plasmid: LEU2, ARS1, CEN3, LacO(256):73bp from CEN3*
yNJN196	*MATa, P_{HIS3}-IPL1-SG-$LacI_4$::HIS3, P_{HIS3}-SLI15-SG-$LacI_4$::TRP1, pNJN112 plasmid: LEU2, ARS1, CEN3, LacO(256):73bp from CEN3*

All strains are derivatives of *Saccharomyces cerevisiae* W303 with the following auxotrophic genotypes: *ade2-1 can1-100 his3-11,15 leu2-3,112 trp1-1 ura3-1*

REFERENCES

Akiyoshi B., Nelson C.R., Ranish J.A., and S. Biggins. 2009. Analysis of Ipl1-mediated phosphorylation of the Ndc80 kinetochore protein in *Saccharomyces cerevisiae*. *Genet* 183: 1591-1595.

Biggins S. and A.W. Murray. 2001. The budding yeast protein kinase Ipl1/Aurora allows the absence of tension to activate the spindle checkpoint. *Genes Dev.* 15: 3118-29.

Buvelot S., Tatsutani S.Y., Vermaak D., and S. Biggins. 2003. The budding yeast Ipl1/Aurora protein kinase regulates mitotic spindle disassembly. *J Cell Biol* 160: 329-339.

Carmena M., Wheelock M., Funabiki H. and W.C. Earnshaw. 2012. The chromosomal passenger complex (CPC): from easy rider to the godfather of mitosis. *Nat Rev Mol Cell Biol* 13: 789-803.

Cheeseman I.M., Anderson S., Jwa M., Green E.M., Kang J.S., Yates J.R. III, Chan C.S., Drubin D.G. and G. Barnes. 2002. Phospho-regulation of kinetochore-microtubule attachments by the Aurora kinase Ipl1p. *Cell* 111: 163-172.

Cheeseman I.M., Chappie J.S., Wilson-Kubalek E.M., and A. Desai. 2006. The conserved KMN network constitutes the core microtubule-binding site of the kinetochore. *Cell* 127: 983-997.

Ciferri, C., Pasqualato S., Screpanti E., Varetti G., Santaguida S., Dos Reis G., Maiolica A., Polka J., De Luca J.G., De Wulf P., Salek M., Rappsilber J., Moores C.A., Salmon E.D., and A. Musacchio. 2008. Implications for kinetochore-microtubule attachment from the structure of an engineered Ndc80 complex. *Cell* 133: 427-439.

Ciosk R., Shirayama M., Shevchenko A., Tanaka T., Toth A., Shevchenko A., and K. Nasmyth. 2000. Cohesin's binding to chromosomes depends on a separate complex consisting of Scc2 and Scc4 proteins. *Mol Cell* 5: 243-254.

Eckert C.A., Gravdahl D.J., and P.C. Megee. 2007. The enhancement of pericentromeric cohesin association by conserved kinetochore components promotes high-fidelity chromosome segregation and is sensitive to microtubule-based tension. *Genes & Dev* 21: 278-291.

Goshima G and M Yanagida. 2000. Establishing biorientation occurs with precocious separation of the sister kinetochores, but not the arms, in the early spindle of budding yeast. *Cell*, 100: 619-33.

Haering C.H., Farcas A.M., Arumugam P., Metson J., and K. Nasmyth. 2008. The cohesin ring concatenates sister DNA molecules. *Nature* 454: 297-301.

He X, Asthana S and PK Sorger. 2000. Transient sister chromatid separation and elastic deformation of chromosomes during mitosis in budding yeast. *Cell*, 101: 763-775.

Huh W.-K., Falvo J.V., Gerke L.C., Carroll A.S., Howson R.W., Weissam J.S. and E.K. O'Shea. 2003. Global analysis of protein localization in budding yeast. *Nature* 425: 686-691.

Indjeian V.B. and A.W. Murray. 2007. Budding yeast mitotic chromosomes have an intrinsic bias to biorient on the spindle. *Curr Biol* 17: 1837-1846.

Kang J., Cheeseman I.M., Kallstrom G., Velmurugan S., Barnes G. and C.S.M. Chan. 2001. Functional cooperation of Dam1, Ipl1, and the inner centromere protein (INCENP)-related protein Sli15 during chromosome segregation. *J Cell Biol* 155: 763-774.

Kim J.H., Kang J.S. and C.S.M. Chan. 1999. Sli15 associates with the Ipl1 protein kinase to promote proper chromosome segregation in *Saccharomycs cerevisiae*. *J Cell Biol* 145: 1381-1394.

Lacefield S., Lau D.T.C. and A.W. Murray. 2009. Recruiting a microtubule-binding complex to DNA directs chromosome segregation in budding yeast. *Nat Cell Biol* 11: 1116-1120.

Lau D.T. and A.W. Murray. 2012. Mad2 and Mad3 cooperate to arrest budding yeast in mitosis. *Curr Biol* 22: 180-190.

Li R. and A.W. Murray. 1991. Feedback control of mitosis in budding yeast. *Cell* 66: 519-531.

Li X. and R.B. Nicklas. 1995. Mitotic forces control a cell-cycle checkpoint. *Nature* 16: 630-632.

Liu D., Vader G., Vromans M.J., Lampson M.A. and S.M. Lens. 2009. Sensing chromosome bi-orientation by spatial separation of aurora B kinase from kinetochore substrates. *Science* 323: 1350-1353.

Makrantoni V. and M.J.R. Stark. 2009. Efficient chromosome biorientation and the tension checkpoint in *Saccharomycs cerevisiae* both require Bir1. *Mol Cell Biol* 29: 455-4562.

Maresca T.J. and E.D. Salmon. 2009. Intrakinetochore stretch is associated with changes in kinetochore phosphorylation and spindle assembly checkpoint activity. *J Cell Biol* 184: 373-381.

Maresca T.J. and E.D. Salmon. 2010. Welcome to a new kind of tension: translating kinetochore mechanics into a wait-anaphase signal. *J Cell Sci* 123: 825-835.

Musacchio A. and E.D. Salmon. 2007. The spindle-assembly checkpoint in space and time. *Nat Rev Mol Cell Biol* 8: 379-393.

Nasmyth K. 2005. How might cohesin hold sister chromatids together? *Phil Trans R Soc B* 360: 483-496.

Ocampo-Hafalla M.T., Katou Y., Shirhige K. and F. Uhlmann. 2007. Displacement and re-accumulation of centromeric cohesin during transient pre-anaphase centromere splitting. *Chromosoma* 116: 531-544.

Pinsky, B.A., Kung C., Shokat K.M., and S. Biggins. 2006. The Ipl1-Aurora kinase activates the spindle checkpoint by creating unattached kinetochores. *Nat Cell Biol* 8: 78-83.

Rieder C.L., Cole R.W., Khodjakov A., and G. Sluder. 1995. The checkpoint delaying anaphase in response to chromosome monoorientation is mediated by an inhibitory signal produced by unattached kinetochores. *J Cell Biol* 130: 941-948.

Sandall S., Severin F., McLeod I.X., Yates J.R. III, Oegema K., Hyman A. and A. Desai. 2006. A complex of Bir1-Sli15 (Survivin-INCENP) connects centromeres to microtubules and is the likely tension sensor controlling Aurora B activation. *Cell* 127: 1179-1191.

Shimogawa M.M., Widlund P.O., Riffle M., Ess M., and T.N. Davis. 2009. Bir1 is required for the tension checkpoint. *Mol Biol Cell* 20: 915-923.

Stern B. and A.W. Murray. 2001. Lack of tension at kinetochores activates the spindle checkpoint in budding yeast. *Curr Biol* 11: 1462-1467.

Straight A.F., Belmont A.S., Robinett C.C. and A.W. Murray. 1996. GFP tagging of budding yeast chromosomes reveal that protein-protein interactions can mediate sister chromatid cohesion. *Curr Biol* 6: 1599-1608.

Struhl K. and D.E. Hill. 1987. Two related regulatory sequences are required for maximal induction of *Saccharomyces cerevisiae* HIS3 transcription. *Mol Cell Biol* 7: 104-110.

Tanaka T., Rachidi N., Janke C., Pereira G., Galova M., Schiebel E., Stark M.J.R., and K. Nasmyth. 2002. Evidence that the Ipl1-Sli15 (Aurora Kinase-INCENP) complex promotes chromosome bi-orientation by altering kinetochore-spindle pole connections. *Cell* 108: 317-329.

Tanaka T. 2008. Bi-orienting chromosomes: acrobatics on the mitotic spindle. *Chromosoma* 117: 521-533.

Wan X. O'Quinn R.P., Pierce H.L., Joglekar A.P., Gall W.E., DeLuca J.G., Carroll C.W., Liu S.T., Yen T.J., McEwen B.F., Stukenberg P.T., Desai A., and E.D. Salmon. 2009. Protein architecture of the human kinetochore microtubule attachment site. *Cell* 137: 672-684.

Wei R.R., Al-Bassam J., and S.C. Harrison. 2007. The Ndc80/HEC1 complex is a contact point for kinetochore-microtubule attachment. *Nat Struct Mol Biol* 14: 54-59.

Westermann S., Drubin D.G, and G. Barnes. 2007. Structures and functions of the yeast kinetochore complexes. *Annu Rev Biochem* 76: 563-559.